1-1-1979

Calorimetric studies of polymer blend systems/

Charles Luce Ryan

University of Massachusetts Amherst

Follow this and additional works at: https://scholarworks.umass.edu/dissertations_1

CALORIMETRIC STUDIES OF POLYMER BLEND SYSTEMS

A Dissertation Presented

By

CHARLES LUCE RYAN, JR.

Submitted to the Graduate School of the
University of Massachusetts in partial fulfillment
of the requirements for the degree of

DOCTOR OF PHILOSOPHY

September   1979

Polymer Science and Engineering

CALORIMETRIC STUDIES OF POLYMER BLEND SYSTEMS
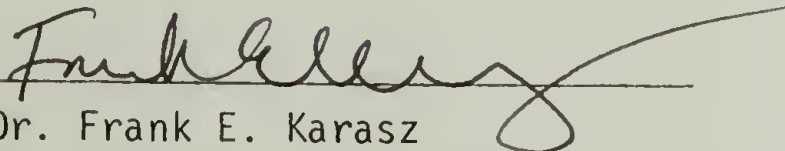
A Dissertation Presented

By
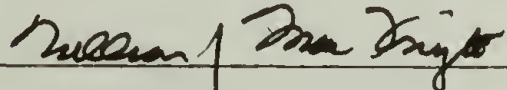
CHARLES LUCE RYAN, JR.

Approved as to style and content by:

_____

Dr. Frank E. Karasz
Cochairperson of Committee

_____

Dr. William J. MacKnight
Cochairperson of Committee

_____

Dr. Richard S. Stein, Member

_____

Dr. William J. MacKnight
Department Head
Polymer Science and Engineering

iii

To my wife, Nancy, as we grow

together professionally and emotionally,

secure in the knowledge that our

love transcends all.

ACKNOWLEDGMENTS

This page would appear to be a directory of faculty, staff and students, past and present, if thanks were extended to all who have helped me in this endeavor. However, a few do stand out in their graciousness. Each of my committee members was quite willing to act as a sounding board for my thoughts, both scientific and non-scientific. Professor Vogl was also very helpful with his timely advice. I would also like to extend my heartfelt thanks to Prof. Peter Couchman for teaching me how to think scientifically and with whom I hope to continue future collaboration. Dr. Peter Alexandrovich was also very helpful in his discussions about this work and early guidance in the proper direction this project should take.

Experimentally, I would like to thank Mark Sine and Gary Miller for their synthesis and characterization of the bromo-substituted polystyrenes. Without their assistance, this section of the thesis work would not have been completed.

Finally, this acknowledgment would not be complete if thanks were not extended to the late Prof. Fraser Price. As my first faculty advisor, Prof. Price was instrumental in my early graduate training. For his advice and friendship, I forever will be indebted.
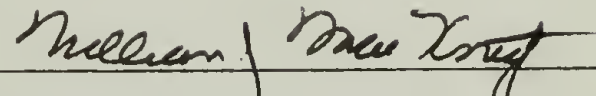
ABSTRACT

Calorimetric Studies of Polymer Blend Systems

(September 1979)

Charles Luce Ryan, Jr.

B.S., Virginia Polytechnic Institute and State University
M.S., Ph.D., University of Massachusetts

Directed by: Professors Frank E. Karasz and William J. MacKnight

Several polymer blend systems were studied utilizing Tian-
Calvet microcalorimetry and differential scanning calorimetry. The
model system for this study was polystyrene/poly(2,6-dimethyl-1,4-
phenylene oxide), well known for its compatibility. Different sub-
stituents were added to the polystyrene chain and noted for the effect
on the compatibility with PPO. Substituents included fluorine,
chlorine, bromine and methyl in both the 2- and 4- position on the
polystyrene phenyl group.

The thermodynamics of mixing was observed utilizing Hess's law
to measure the polymer-polymer heat of mixing. Blends of polystyrene
and PPO yielded negative ΔH_m values, varying smoothly with composi-
tion. This was consistent with the well-established compatibility of
the pair. Copolymers of styrene and 4-chlorostyrene were synthesized
by free-radical polymerization to note the effect of chlorine substitu-
tion in the 4-position. The lower critical solution temperature
dropped sharply in the copolymer composition range of 60-75 mole

percent 4-ClS blended with PPO. Values of ΔH_m also dropped from negative towards zero as the copolymer composition was increased. An anomalous high negative value for p(4-ClS(.759)-S)/PPO blends was found. This blend was only partially miscible. However, the overall behavior of ΔH_m could be explained by postulation of an upper critical solution temperature.

Positive values of ΔH_m were found for blends of polystyrene and poly(2-chlorostyrene). Positive values for ΔH_m are a sufficient condition for phase separation at the experimental temperature. The phase behavior of PS/p(2-ClS) blends changed significantly as the polystyrene molecular weight was changed. However, ΔH_m changed very little as a function of molecular weight. Given this finding, non-combinatorial entropies of mixing were postulated to be the controlling factor in phase separation for PS/p(2-ClS) blends.

Previous studies had shown that although both p(4-FlS) and p(2-FlS) were incompatible with PPO, certain copolymers of the two were compatible with PPO in a certain temperature range. The behavior of ΔH_m as a function of copolymer composition followed an erratic curve. However, the values of ΔH_m could be qualitatively explained allowing for the existence of a polymer-polymer UCST. Whereas the values for ΔH_m were small for PS/p(2-ClS), large positive ΔH_m values for the fluorinated copolymer blends were found. This was striking evidence pointing to a polymer-polymer UCST.

Previous studies in this laboratory have followed the effect of fluoro- and chloro- substitution on polystyrene blended with both

PPO and PS. Extension to the brominated and methylated polystyrenes
was the natural course of this work. From the comparison of styrene
copolymers with halogenated styrene blended with PPO, a ranking of the
power of the polystyrene phenyl substituent to induce incompatibility
with PPO was found to be

$$2\text{-Br} > 4\text{-Fl} \cong 4\text{-Br} > 2\text{-Cl} \cong 4\text{-Cl} > 2\text{-Fl} > 2\text{-Me} \; .$$
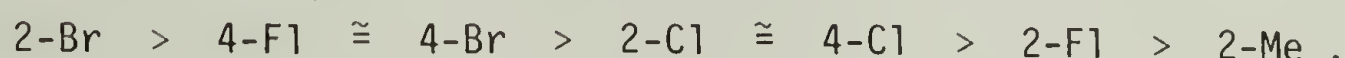
In all cases, the halogenated polystyrene homopolymer was incompatible
with PPO. However, past work has shown that certain copolymers of
either the 2-chlorostyrene with 4-chlorostyrene or of 2-fluorostyrene
with 4-fluorostyrene were compatible with PPO over a certain tempera-
ture range. The analogous brominated situation yielded incompatible
blends over the entire copolymer composition range. The compatibility
of certain copolymers with PPO could be explained due to a fortuitous
matching of a critical physical property, e.g., thermal expansion co-
efficient, solubility parameter or critical temperature. These criti-
cal values for the copolymers were postulated to deviate from a simple
arithmetic average of the pure components. This deviation would be
sufficient to produce compatibility with PPO. All the results for the
halogenated polystyrene copolymers could be explained using the above
postulation.

Equilibrium states below Tg were explored using Tian-Calvet
microcalorimetry coupled with Hess's law. This method allows the loca-
tion of both the binodal and spinodal phase boundaries in the glassy
state and the establishment of an UCST. The contours of the free

energy-composition diagram could also be explicitly examined. This situation is unique to polymer-polymer systems since thermodynamically unstable states can be maintained for finite periods of time.

TABLE OF CONTENTS

LIST OF TABLES

LIST OF FIGURES

C H A P T E R   I

INTRODUCTION

Polymer science is playing an increasing role in the develop-
ment of new materials useful for a variety of applications. Initially,
the thrust of polymer research was the synthesis of new polymers from a
seemingly infinite choice of monomers. Copolymerization was then used
successfully in order to produce material with the desired physical
properties. Recently, polymer blending has been gaining promise as a
useful means of attaining materials suitable for a myriad of applica-
tions.

Polymer blending has several distinct advantages over the con-
ventional synthesis techniques. One is economics. Two relatively inex-
pensive homopolymers can be blended to produce a material with the de-
sirable properties of a more expensive material. Flexibility is another
advantage. Blending different proportions of polymers together allows
a whole range of physical properties to be traversed. Polymer blends
are also easy to process, enabling the use of existing engineering
techniques.

Several different polymer blend systems have been used in com-
mercial products. Examples include the Noryl type resins marketed by
General Electric that are based on polystyrene-poly(2,6-dimethyl-1,4-
phenylene oxide) blends.[1,2] Other industrial blends include PVF_2 mixed
with PMMA and PEMA along with rubber blends that are used in the tire

1

industry. Many more examples of the applications of blends have been recently compiled by Paul.[3]

The thrust of this thesis work was to study the thermodynamics of polymer-polymer systems. Most of the studied blends were based on the highly compatible PS/PPO system. Chemical modifications, via the application of copolymerization, were examined for the effect of substituent type and placement on the phase stability of the blend. The thermodynamics of the changing systems were followed through measurements of the enthalpy of mixing. Phase stability above the glass transition temperature was established using differential scanning calorimetry.

The purpose of this chapter is to present a background to the principles underlying polymer mixing. Included are both early and more recent theories formulated for predicting polymer compatibility. Also, a short review on other blend systems will be presented.

A. Thermodynamics of Polymer Blends

The stability of any binary system requires that the Gibb's free energy,

$$\Delta G_m = \Delta H_m - T\Delta S_m \tag{1.1}$$

be negative. A negative ΔG_m is a necessary, although not sufficient, condition for the stability of the mixture. Thermodynamic stability for a one phase system exists when

$$\frac{\partial^2 G_m}{\partial x_i^2}\Bigg)_{T,P} > 0 \qquad\qquad (1.2)$$

where x_i is some compositional variable. Graphically, the above conditions are shown in Figure 1.1. The restriction of Eqn. (1.2) requires that the free energy-composition diagram be concave downward. For a system that is miscible over the entire composition range at that temperature, a curve similar to Figure 1.1a would be followed. A partially miscible system would include some compositions that were incompatible. Several interesting features of the phase diagram can be derived from Figure 1.1b. Between the composition C and the pure component 1 and composition D to pure component 2, the behavior of ΔG_m with composition obeys Eqn. (1.2). However, phase separation to two phases denoted by A and B would lower the free energy from G' to G". The binary compositions between A and C, D and B exist in a metastable state; stable to small perturbations in the system but unstable to large disturbances. The boundary between the stable region and the metastable region (points A and B) is termed the binodal. Compositions between C and D do not satisfy the restriction of Eqn. (1.2) and are unstable. The boundary between the unstable and metastable state (points C and D) is called the spinodal.

The locus of the spinodal is in principle easy to calculate. The spinodal boundary is simply the inflection points of the free energy-composition diagram given as

$$\frac{\partial^2 \Delta G_m}{\partial x_i^2}\Bigg)_{P,T} = 0 \; . \qquad\qquad (1.3)$$
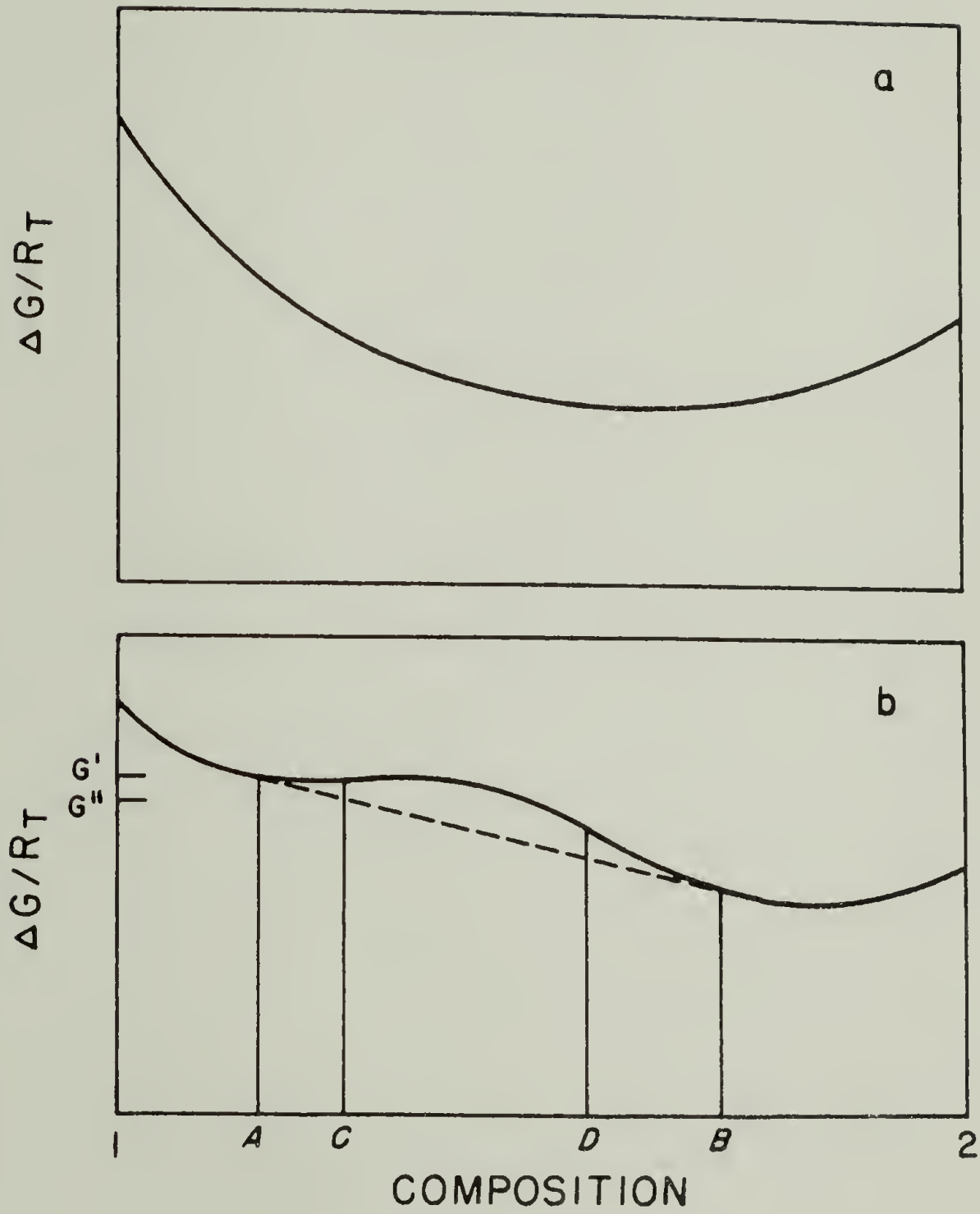
Figure 1.1. Free energy versus blend composition for (a) miscible, and (b) partly miscible polymer blends.

The binodal is much more difficult to calculate since the boundary does not necessarily concur with any critical points on the free energy-composition diagram. The locus of the binodal is found by setting the chemical potentials of both homopolymers equal in the two co-existing phases. Graphically this means the binodal is found by drawing a common tangent between the two concave sections of the free energy diagram (dashed line in Figure 1.1b).

Figure 1.1 is for a single temperature. As the temperature is changed, so does the free energy plot. Upon an increase in temperature, the binary system can phase separate. The temperature at which phase separation first appears is called the lower critical solution temperature (LCST). Analogously, phase separation upon a decrease in temperature is indicative of the existence of an upper critical solution temperature (UCST). The position of the critical solution temperatures can be calculated by

$$\left.\frac{\partial^2 \Delta G_m}{\partial x_i^2}\right)_{P,T} = \frac{\partial^3 \Delta G_m}{\partial x_i^3} = 0 . \tag{1.4}$$

Figure 1.2 illustrates a phase diagram for a binary system with both an LCST and an UCST. The solid line is the binodal and the dashed line indicates the spinodal.

The position of the LCST relative to the UCST is rather confusing. The respective designations refer only to the position of the CST relative to that phase diagram.

Low molecular weight solutions rarely display LCST behavior although the existence of an UCST is fairly common.[9] Polymer-solvent
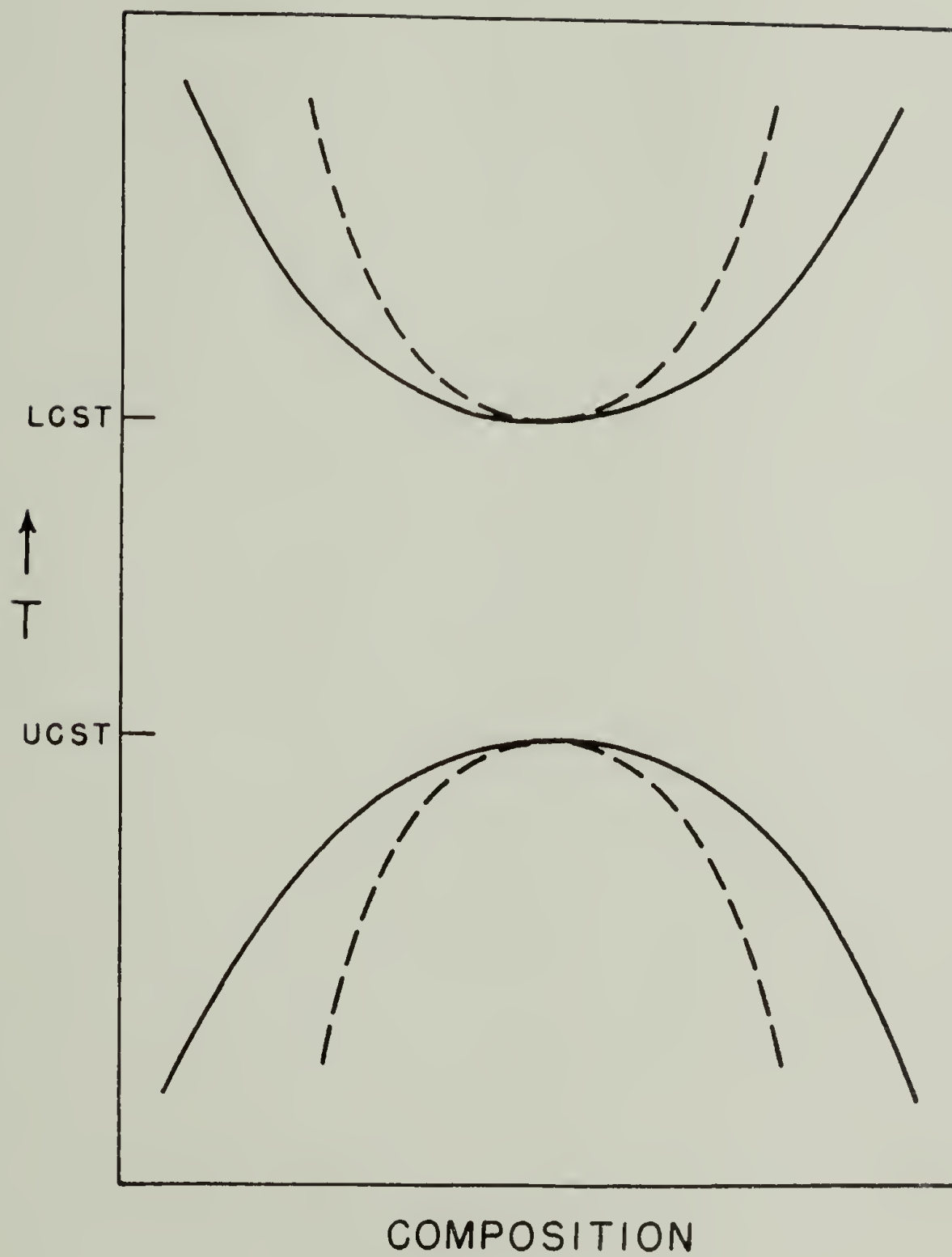
Figure 1.2. Phase diagram showing binodal (solid line) and spinodal (dashed line) phase boundary.

systems have been found to display both regions of phase separation.
Saeki studied polystyrene solutions that displayed both the LCST and
UCST.[4-8] Cowie also found the existence of an LCST and UCST for poly-
styrene in the cosolvent methylcyclohexane-diethyl ether. In some of
the 90 solvents tested, Izumi and Mikaka[11] found that poly(4-chloro-
styrene) solutions showed both sets of phase diagrams.

Polymer-polymer systems have been found to display LCST
behavior. Alexandrovich[12,13] discovered that chlorinated styrene co-
polymers blended with PPO reversibly phase separated at higher tempera-
tures. Vukovic found similar results for PPO blends with fluorinated
styrene copolymers.[14-16] Other systems which have been reported to
exhibit LCST behavior include PS-poly(vinyl methyl ether),[17]
poly(methyl methacrylate)-poly(styrene-co-acrylonitrile)[18] and poly-
caprolactone-poly(styrene-co-acrylonitrile).[19]

The existence of a polymer-polymer UCST has been predicted,
but convincing evidence has not been found. Koningsveld[20] reported
that blends of SBR and natural rubber exhibited UCST behavior. He
based this conclusion on the appearance of two mechanical loss peaks
below 0°C. The system PS-PVME has also been postulated to phase
separate at lower temperatures.[21] Experiments performed in this the-
sis work have uncovered more systems displaying LCST behavior. Evi-
dence has also been presented on the existence of a polymer-polymer
UCST concurrent with the LCST. It is believed this is the first re-
ported coexistence of both phase separation regions in a polymer-
polymer system.

B. Kinetics of Phase Separation

Polymers are unique in that their large size enables them to exist for finite periods of time in unstable conformations. In polymer blends, the mixture can subsist inside the spinodal below Tg and remain in a one phase system.

The kinetics of phase separation are different inside the spinodal as opposed to the metastable region. Between the spinodal and binodal, the system is stable to small compositional fluctuations whereas inside the spinodal, any change in composition results in a large decrease in free energy, favoring phase separation. Two different mechanisms of phase separation have been proposed to explain the kinetics in the two regions.

Inside the spinodal, there is no thermodynamic barrier to phase separation and the process should be spontaneous until separation is complete. The formation of a heterogeneous solution from a homogeneous one-phase system requires diffusion against the concentration gradient, i.e., a negative diffusion coefficient or so-called "uphill" diffusion. Phase separation by this process is called spinodal decomposition and has been treated theoretically by Cahn.[22,23] Since the spinodal decomposition mechanism is spontaneous and continuous, the morphology is characterized by interconnected phases.

In the metastable region, the diffusion coefficient becomes positive and phase separation is by nucleation and growth. A nucleus is formed from a large fluctuation in composition and once established, grows by normal diffusion processes. The work required to form a

nucleus depends on the metastability of the system, vanishing to zero at the spinodal.[24] In the nucleation and growth mechanism, composition of the growing phases remains constant. A good review on the kinetics of phase separation is given by Kwei and Wang.[25]

C. Polymer Mixture Theories

A brief chronology of polymer mixture theories is presented here for background into some of the later discussion. Many reviews of polymer solution thermodynamics have been published.[26-35] The first attempt at a description of polymer solution thermodynamics was performed by Flory[36-38] and Huggins[39-41] (F-H theory). Deviations of polymer solutions from Raoult's law arise largely from the small entropies of mixing. The expression derived by Flory and Huggins contained a combinatorial entropy of mixing term due to the length and volume of the polymer in solution. A van Laar type enthalpy of mixing was also added to obtain the free energy of mixing. Although the F-H theory was useful as a first approximation, it was unable to predict the details of polymer solution behavior.

Extension of F-H theory to polymer-polymer systems was done by Scott[42] and Tompa.[43] The expression for the free energy of mixing two polymers derived by Scott was[32]

$$\Delta G_m = \frac{RTV}{V_R} \left[\frac{v_1}{x_1} \ln v_1 + \frac{v_2}{x_2} \ln v_2 + \chi_{12} v_1 v_2 \right] \tag{1.5}$$

where V is total mixture volume, V_R the reference volume which equals the molar "mer" volume, v_i the volume fractions, x_i the polymer chain

lengths and x_{12} is the polymer-polymer interaction parameter. The terms
containing x_i are entropic and as x_i increases, these terms go to zero.
In other words, the entropy of mixing polymers goes to zero at high
molecular weights. Given the above situation, ΔG_m can only be nega-
tive if the enthalpic term is negative, i.e., negative x_{12}. The in-
teraction parameter reflects the strength of interpolymeric contacts.

Calculations based on Flory-Huggins theory can account for the
existence of an UCST, but not for the LCST. The inclusion of volume
is used in the newer theories to predict LCST behavior. The extension
of F-H theory to include free volume effects was done by Prigogine[44]
and Flory.[28] McMaster[45] applied the Prigogine-Flory theory to polymer-
polymer systems. Although the equations McMaster derived were very com-
plex, several important conclusions were reached. The existence of
a polymer-polymer LCST was predicted and thought to be common. More-
over, the thermal expansion coefficient was the most important param-
eter for polymer blend systems. Small differences in the thermal ex-
pansion coefficient of the pure components was the cause for LCST be-
havior.

Patterson and Robard[35] offered a simpler form of the Prigogine-
Flory theory as applied to polymer-polymer systems. In their treat-
ment, they concluded that the primary cause of LCST behavior was not
unfavorable free volume effects, as McMaster implied, but instead on
the favorable polymer-polymer interactions at low temperatures which
decrease with temperature. However, the predictions of McMaster and
Patterson are similar.

A more recent equation of state theory of polymer fluids and

mixtures has been formulated by Sanchez.[9,46-49] Sanchez theory has

been characterized as a lattice fluid theory and differs from the cor-

responding states theories of Prigogine and Flory. Whereas both

theories require three equation of state parameters, Flory theory re-

quires a separation of the internal and external degrees of freedom.

These quantities are implicit in the lattice fluid theory. From the

lattice fluid theory, an equation of state was derived for the pure

components,

$$\tilde{\rho}^2 + \tilde{P} + \tilde{T}\left[\ln(1 - \tilde{\rho}) + (1 - \frac{1}{r})\tilde{\rho}\right] = 0 \tag{1.6}$$

where ρ, P and T are the reduced density, pressure and temperature and

"r" the number of mers. Utilizing a set of combining rules based on

close-packed volume additivity and pair interactions, an equation of

state formally identical to Eqn. (1.6) could be derived for polymer

mixtures. The only parameter used that characterizes a binary mixture

is the mer-mer interaction energy. All other quantities were derived

from the pure components.

The phase stability of the polymer mixtures could be inferred

by studying the spinodal. The condition for phase stability, upon sim-

plification, was derived as

$$\tilde{\rho}(2\chi + \tilde{T}\psi^2 P^*\beta) < \frac{1}{r_1\phi_1} + \frac{1}{r_2\phi_2} \tag{1.7}$$

where χ is the polymer-polymer interaction parameter, P* the charac-

teristic temperature, β the isothermal compressibility, ψ a term con-

taining volume parameters and ϕ_i the volume fractions. By analysis of

the temperature dependence of the terms of Eqn. (1.7), the general features of the phase diagram could be ascertained. The application of lattice fluid theory to binary polymer systems is discussed in detail in Chapter V in the study of PS-p(2-ClS) blends.

Several conclusions of the phase behavior of blends could be reached using lattice fluid theory. In all cases, LCST behavior was predicted. The situation for most polymer blends is an hourglass-shaped phase diagram, where the UCST is greater than the LCST. An increase in molecular weight of one of the components serves to decrease the LCST and increase the UCST. The pressure dependence of the CST's predicts a larger change in the LCST than the UCST. Pressure should generally increase the CST although a change in sign of the pressure coefficient is possible. Finally, very few polymer pairs would be expected to be miscible.

The problem with the equation of state theories is that very accurate P-V-T data is needed in order to calculate the phase diagram. Very small errors in the thermal expansion coefficient could change the calculated values of the phase separation temperature by tens of degrees. However, the approach used by Sanchez is a useful tool for understanding the mechanisms of polymer-polymer phase behavior.

D. Empirical Approach at Predicting Compatibility: Solubility Parameters

According to the solubility parameter approach at predicting compatibility, two polymers mix if the difference in the pure component solubility parameter is small, typically 1.7-2.0. In low molecular weight materials, the solubility parameter, δ, can be calculated as the

square root of the energy of vaporization per unit volume.[50] For poly-
mer molecules, the solubility parameter is best calculated using tables
of molar attraction coefficients, E, and the equation

$$\delta \;=\; e\, \Sigma\, E/M \qquad\qquad\qquad (1.8)$$

where E is summed over the structural units of the polymer, M the
"mer" molecular weight and e is the density.[51] Tables of calculated
δ have been published.[52]

The solubility parameter approach has been used extensively in
the coatings industry. Hansen[53] introduced the concept that the
solubility parameter is vector composed of hydrogen bonding, polar in-
teractions and dispersion forces, aptly called the three-dimensional
solubility parameter. This enabled the interactions of molecules to
be specifically taken into account in the calculation of δ.

Although the solubility parameter approach is not rigorous,
it allows a useful first approximation to polymer solubility. The dif-
ferent temperature coefficient for the pure component solubility param-
eters has even been suggested as the reason for high temperature phase
separation.[33]

Sanchez[49] compared the predictions of polymer-polymer compati-
bility from the equation of state theories and the solubility parameter
method. The results suggested that the solubility parameter method
was better than Flory theory for predicting polymer mixing. However,
Sanchez recommended all three methods be utilized to determine the pos-
sibility of compatibility.

E. Experimental Determination of Polymer Compatibility

Krause has indexed the phase behavior of a large number of polymer-polymer systems.[32,54] Evident from the listing, and as often pointed out, the occurrence of compatible polymer blend systems is rare. There exists a variety of experimental methods for determining polymer miscibility. Films of miscible polymer blends are optically clear whereas incompatible blends are usually opaque. However, optical clarity is not a sufficient criterion for assessing polymer compatibility. Two incompatible polymer blends with matching refractive indices also would appear clear. One example found in this work, blends of PS/p(2-ClS), remained clear although the blend was phase separated.

Blends of compatible polymers also exhibit good mechanical properties that reflect the properties of the pure components. Kleiner[55] found that the modulus and tensile strength of compatible PS/PPO blends was enhanced from a simple weighted average of pure components.

One of the most commonly used criteria for polymer compatibility is the existence of a single glass transition temperature intermediate the pure component Tg's. Many techniques exist for determining the glass transition temperature. Differential scanning calorimetry (DSC) reflects the glass transition temperature as being a second-order phase transition, observed as a discontinuity in the heat capacity-temperature curve. DSC study of polymer blends is particularly useful due to the speed and ease of measurement of Tg. Incompatible blends reveal two Tg's whereas compatible blends show only the single Tg.

Other methods useful for studying polymer miscibility includes dynamic mechanical and dielectric measurements of the blend alpha relaxation as a function of polymer compatibility. A good review on the methods for the determination of solid state transitions of blends has been published recently by MacKnight, Karasz and Fried.[56]

REFERENCES

1. A.S. Hay, Polym. Eng. Sci. $\underline{16}$, 1 (1976).

2. M. Kramer, J. Appl. Polym. Sci., Appl. Polym. Sym. $\underline{15}$, 227 (1970).

3. D.R. Paul, ed., Polymer Blends, Vol. II, Academic Press, N.Y., 1978.

4. S. Saeki, N. Kuwahara, M. Kaneko, Macrom. $\underline{9}$(1), 101 (1976).

5. S. Saeki, N. Kuwahara, S. Konno, M. Kaneko, Macrom. $\underline{6}$(4), 589 (1973).

6. S. Saeki, S. Konno, N. Kuwahara, M. Nakata, S. Kaneko, Macrom. $\underline{7}$(4), 521 (1974).

7. S. Saeki, N. Kuwahara, S. Konno, M. Kaneko, Macrom. $\underline{6}$(2), 246 (1973).

8. S. Konno, S. Saeki, N. Kuwahara, M. Nakata, M. Kaneko, Macrom. $\underline{8}$(6), 799 (1975).

9. R.H. Lacombe, I.C. Sanchez, J. Phys. Chem. $\underline{80}$(23), 2568 (1976).

10. J.M.G. Cowie, I.J. McEwen, Macrom. $\underline{7}$(3), 291 (1974).

11. Y. Izumi, Y. Mikake, Polym. J. $\underline{3}$, 647 (1972).

12. P.R. Alexandrovich, Ph.D. Dissertation, Univ. of Mass., 1978.

13. P.R. Alexandrovich, F.E. Karasz, W.J. MacKnight, Polymer $\underline{18}$, 1022 (1977).

14. R. Vukovic, F.E. Karasz, W.J. MacKnight, to be published.

15. R. Vukovic, F.E. Karasz, W.J. MacKnight, to be published.

16. R. Vukovic, F.E. Karasz, W.J. MacKnight, to be published.

17. M. Bank, J. Leffingwell, C. Thies, J. Polym. Sci. A-2 $\underline{10}$, 1097 (1972).

18. L.P. McMaster, Adv. Chem. Series #142, 43 (1975).

19.   L.P. McMaster, Macrom. $\underline{6}$, 760 (1973).

20.   R. Koningsveld, L.A. Kleintjens, H.M. Schoeffeleers, Pure Appl. Chem. $\underline{39}$, 1 (1974).

21.   T. Nishi, T.K. Kwei, Polymer $\underline{16}$, 285 (1975).

22.   J.W. Cahn, J. Chem. Phys. $\underline{42}$(1), 93 (1965).

23.   J.W. Cahn, Acta Metal. $\underline{9}$, 795 (1961).

24.   J.W. Cahn, J.E. Hilliard, J. Chem. Phys. $\underline{31}$, 688 (1959).

25.   T.K. Kwei, T.T. Wang, in Polymer Blends, D.R. Paul, ed., Academic Press, N.Y., 1978.

26.   D. Patterson, Rubber Chem. Tech. $\underline{40}$, 1 (1967).

27.   D. Patterson, Macrom. $\underline{2}$(6), 672 (1969).

28.   P.J. Flory, Disc. Farad. Soc. $\underline{49}$, 7 (1970).

29.   E.F. Casassa, J. Polym. Sci.: Symp. #54, $\underline{53}$ (1976).

30.   R.F. Blanks, Polym.-Plast. Tech. Eng. $\underline{8}$(1), 13 (1977).

31.   D.R. Paul, ed., Polymer Blends, Vol. I, Academic Press, N.Y., 1978.

32.   S. Krause, J. Macrom. Sci.-Revs. Macrom. Chem. $\underline{C7}$(2), 251 (1972).

33.   R. Caspar, L. Morbitzer, Angew. Makrom. Chem. $\underline{58/59}$(859), 1 (1977).

34.   B. Schneier, J. Appl. Polym. Sci. $\underline{17}$, 3175 (1973).

35.   D. Patterson, A. Robard, Macrom. $\underline{11}$(4), 690 (1978).

36.   P.J. Flory, Principles of Polymer Chemistry, Cornell Univ. Press, Ithaca, N.Y., 1953.

37.   P.J. Flory, J. Chem. Phys. $\underline{9}$, 660 (1941).

38.   P.J. Flory, J. Chem. Phys. $\underline{10}$, 51 (1942).

39.   M.L. Huggins, J. Chem. Phys. $\underline{9}$, 440 (1941).

40.   M.L. Huggins, J. Phys. Chem. $\underline{46}$, 151 (1942).

41.   M.L. Huggins, J.A.C.S. $\underline{64}$, 1712 (1942).

42.   R.L. Scott, J. Chem. Phys. $\underline{17}$, 279 (1949).

43. H. Tompa, Trans. Farad. Soc. 45, 1142 (1949).

44. I. Prigogine, The Molecular Theory of Solutions, Interscience, N.Y., 1957.

45. L.P. McMaster, Macrom. 6, 760 (1973).

46. I.C. Sanchez, R.H. Lacombe, J. Phys. Chem. 80, 2352 (1976).

47. I.C. Sanchez, J. Polym. Sci.: Polym. Lett. Ed. 15, 71 (1977).

48. I.C. Sanchez, R.H. Lacombe, Nature (London) 252, 381 (1974).

49. I.C. Sanchez, in Polymer Blends, Vol. I, D.R. Paul, ed., Academic Press, N.Y., 1978.

50. J.H. Hildebrand, R.L. Scott, Regular Solutions, Prentice-Hall, Englewood Cliffs, N.J., 1962.

51. F.W. Billmeyer, Textbook of Polymer Science, Wiley-Interscience, N.Y., 1971.

52. K.L. Hoy, J. Paint Tech. 42, 76 (1970).

53. C.M. Hansen, J. Paint Tech. 39, 104 (1967).

54. S. Krause, in Polymer Blends, Vol. I, D.R. Paul, ed., Academic Press, N.Y., 1978.

55. L.W. Kleiner, Ph.D. Dissertation, Univ. of Mass., 1978.

56. W.J. MacKnight, F.E. Karasz, J.R. Fried, in Polymer Blends, Vol. I, D.R. Paul, ed., Academic Press, N.Y., 1978.

C H A P T E R   I I

ENTHALPY OF MIXING OF POLYMER-POLYMER BLENDS--

BACKGROUND

The thrust of this work was to measure the enthalpy of mixing*

(heat of mixing) of several polymer-polymer systems. As was pointed

out in Chapter I, thermodynamic stability requires that the second

derivative of the Gibb's free energy with respect to composition be

positive. A necessary, although not sufficient condition, is that the

free energy of mixing be negative.[1] The molar Gibb's free energy can

be broken down into the enthalpy and entropy components.

$$\Delta g_m \; = \; \Delta h_m \; - \; T\Delta s_m \; . \tag{2.1}$$

Polymers and their blends have such large viscosities that experiments

normally used for the determination of the Gibb's free energy of low

molecular weight substances are no longer applicable. However, in

polymer systems, the entropic term is 2-4 orders of magnitude lower

than the enthalpic term.[2-4] Therefore, if experiments could be devised

for measuring ΔH_m, compatibility could be predicted for polymer-polymer

systems.

Several approaches have been used to calculate ΔH_m. These

include (1) the equation of state approach; (2) calculations from

_____

*The terms enthalpy of mixing and heat of mixing are used in-
terchangeably.

cohesive energy densities; (3) calculation of a polymer-polymer inter-
action parameter; and (4) application of Hess's law to heats of solu-
tion measurements. The final approach was the course followed by this
work. The other methods will be briefly touched on for completeness.

A. Equation of State Approach

Recent theories have been formulated to predict polymer-polymer
compatibility from the polymer equations of state[27-35] (see Chapter I).
Sanchez,[31-34] from lattice fluid theory, derived the following relation
for the heat of mixing:

$$\Delta H_m = rNkT\left[\tilde{\rho}\phi_1\phi_2 + (\tilde{\rho}_1\phi_1{}^\circ - \tilde{\rho}\phi_1)/\tilde{T}_1 + (\tilde{\rho}_2\phi_2{}^\circ - \tilde{\rho}\phi_1)/\tilde{T}_2\right]$$

$$+ p\Delta V_m \qquad (2.2)$$

where each term is explained sufficiently by Sanchez.[34] In order to
evaluate the terms of Eqn. (2.2), very precise values of the equation
of state parameters are warranted. However, it is possible, in prin-
ciple, to predict the heats of mixing of polymer blends from the lat-
tice fluid theory without the use of any adjustable parameters.

B. Heats of Mixing from Cohesive Energy Densities

For non-polar molecules in the absence of hydrogen bonding,
Hildebrand and Scott[36] derived the following expression for the heat
of mixing of small molecules:

$$\Delta H_m = V_m(\delta_1 - \delta_2)^2\phi_1\phi_2 \qquad (2.3)$$

where V_m was the mixture volume, ϕ_i the volume fraction and δ_i the Hildebrand solubility parameter. The quantity δ^2 is known as the cohesive energy density which for small molecules is equal to the energy of vaporization per unit volume of liquid.[37]

The solubility parameter approach is a useful first approximation for predicting polymer-solvent compatibility. If the difference, $\delta_1 - \delta_2$, is less than 1.7-2.0, solubility might be expected.[38] For polymers, values of δ can be calculated from molar attraction constants, E, using[17]

$$\delta_i = \rho \Sigma E/m \qquad (2.4)$$

where m is the "mer" molecular weight and ρ the density. However, values for δ_i have been tabulated.[39,40]

Values for ΔH_m calculated from Eqn. (2.3) cannot be negative since each term is positive. Therefore, qualitative agreement between calculated and experimental values of ΔH_m would not be satisfactory. However, the solubility parameter approach is a useful starting point for predicting polymer-polymer compatibility as shown by Sanchez.[34]

C. Polymer-Polymer Interaction Parameter

The polymer-polymer interaction parameter, usually denoted as χ, is contained in most theories of polymer-polymer systems (see Chapter I). The χ parameter reflects the strength of polymer intermolecular contacts and therefore parallels the heat of mixing. The heat of mixing relies on both the number and the strength of polymer-polymer contacts. However, the calculation of the χ parameter follows the

assumptions set forth by the individual theories and cannot be compared directly to experimental values of ΔH_m. Often, the χ parameter also contains an entropic component in addition to an enthalpic contribution.

D. Hess's Law Approach

One method for measuring experimentally the enthalpies of mixing for polymer blends utilizes Hess's law. Hess's law states that for a given overall reaction, the change in the state function, e.g., enthalpy, will be the same regardless of the path taken from initial to final products. The reaction of interest was

$$\text{polymer A} + \text{polymer B} \xrightarrow{\Delta H_m} \text{polymer solution AB}.$$
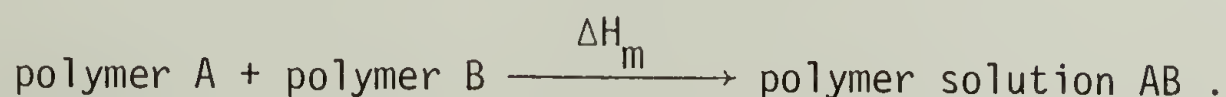
Since the direct combination of polymers A and B with measurement of the corresponding enthalpy change could not be performed experimentally, an indirect procedure was used as outlined in Figure 2.1.

From Hess's law,

$$\Delta H_m + \Delta H_{bl}^S = \Delta H_a^S + \Delta H_b^S + \Delta H_{soln}^S. \tag{2.5}$$

If the final concentration of polymer is very small, $\Delta H_{soln}^S = 0$, and

$$\Delta H_m = \Delta H_a^S + \Delta H_b^S - \Delta H_{bl}^S \tag{2.6}$$

which generalizes to

$$\Delta H_m = a\Delta H_a^S + b\Delta H_b^S - \Delta H_{bl}^S \tag{2.7}$$

POLYMER A + SOLVENT $\xrightarrow{\Delta H_A^s}$ SOLUTION A

\+

POLYMER B + SOLVENT $\xrightarrow{\Delta H_B^s}$ SOLUTION B

$\Big\downarrow \Delta H_M$ $\Big\downarrow \Delta H_S^s$

BLEND AB + SOLVENT $\xrightarrow{\Delta H_{AB}^s}$ SOLUTION A&B

$$\Delta H_A^s + \Delta H_B^s + \Delta H_S^s = \Delta H_M + \Delta H_{AB}^s$$

$$\Delta H_M = a\Delta H_A^s + b\Delta H_B^s - \Delta H_{AB}^s$$
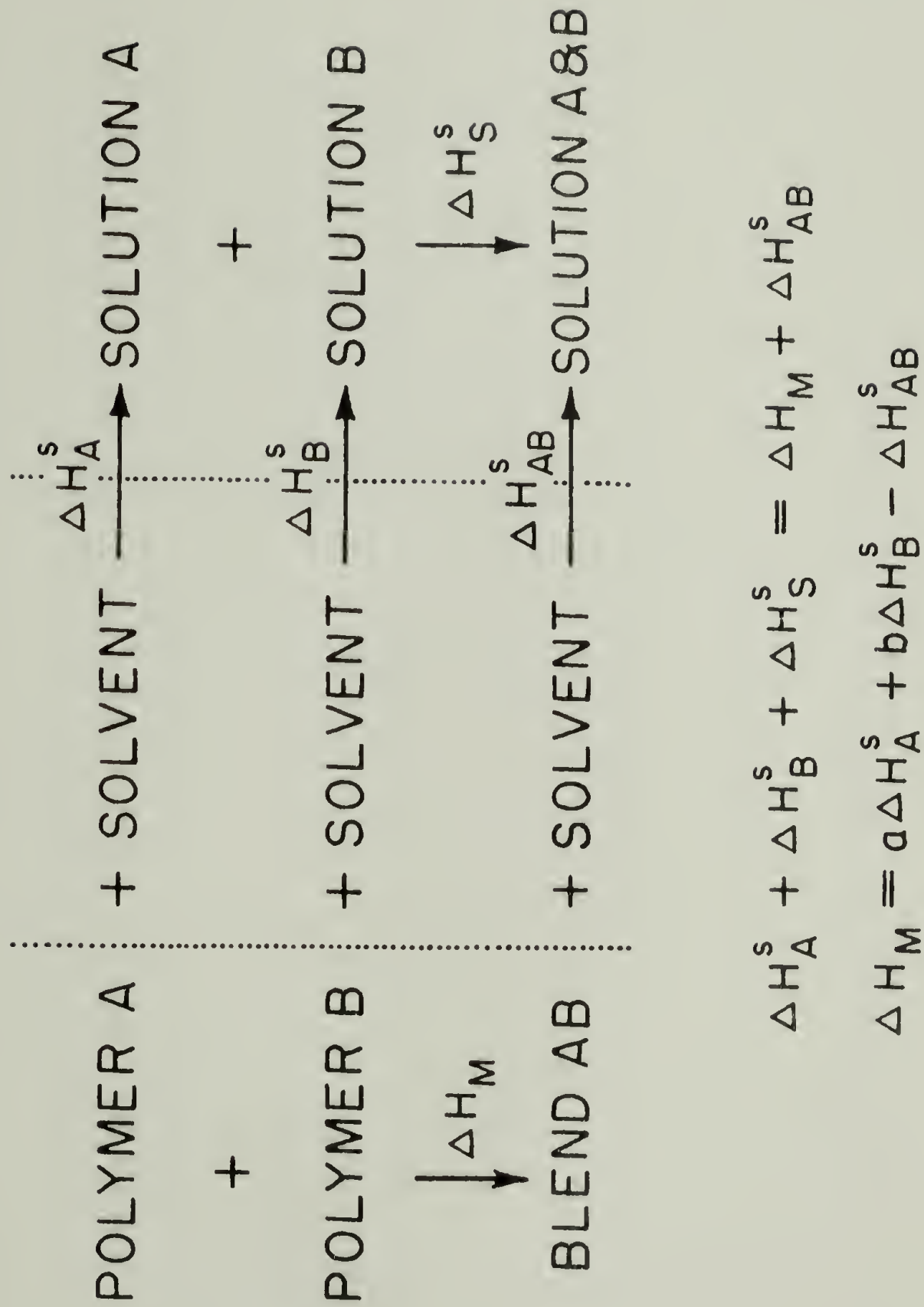
Figure 2.1. Hess's law cycle.

where a and b correspond to weight fractions of polymers A and B in blend AB and ΔH_i^S are the heats of solution in units of energy per gram. Hence, by measuring the heats of solution of the homopolymers A and B and the polymer blend with different compositions of A:B, ΔH_m could be determined. Tian-Calvet microcalorimetry is stable and sensitive enough to measure the small heats evolved upon dissolution of a polymer in a solvent.

The Hess's law approach has been used to measure ΔH_m for several polymer-polymer systems. Zverev et al.[7] studied mixtures of fluorine-containing polymers. They found that poly(vinyl fluoride) was compatible with poly(vinylidene fluoride) as reflected in a favorable heat of mixing for each composition studied. The same was true for blends of poly(vinylidene fluoride) with copolymers of tetrafluoroethylene and vinylidene fluoride. However, the copolymer was deemed incompatible with poly(vinyl fluoride) since the heat of mixing was zero for each composition studied.

The heats of mixing poly(vinyl chloride) (PVC) with poly(methyl methacrylate) (PMMA) was determined by Tager and Bessonov.[8] They found that in the range 0-45 weight percent PVC, ΔH_m was negative where ΔH_m became positive for the remaining compositions. In the mid-composition region, ΔH_m varied linearly with composition changing sign. Tager maintained this linear dependence was due to phase separation in that region. Their explanation followed a complicated phase diagram involving the formation of a transitional layer in the zone of contact of the two polymers. Other studies on the stability of PVC-PMMA blends have been ambiguous. Some workers[9] had found a single blend Tg in

certain composition regions whereas others[4,9-11] showed the existence of two Tg's.[9,12]

Tager[8] also established the compatibility of poly(vinyl acetate) with cellulose nitrate where ΔH_m was negative for all compositions studied. Moreover, the variation of ΔH_m with composition was concave downwards, indicative of the second derivative of the free energy with respect to composition being positive (thermodynamic stability).

Ichihara, Komatsu and Hata determined the heats of mixing of PMMA with poly(vinyl acetate) (PVAc).[13] Negative values of ΔH_m were determined for each composition. The second derivative of the free energy was also positive and DSC showed a single blend Tg intermediate between the pure component Tg's. However, they wrongly considered the negative value to mean incompatibility of the two polymers. Other studies have found PVAc to be miscible with PMMA.[14,15]

Early work in this laboratory involved the measurement of ΔH_m for mixtures of polystyrene and poly(2,6-dimethyl-1,4-phenylene oxide) (PPO). Weeks, Karasz and MacKnight[16] found a smooth variation of ΔH_m with composition as shown in Figure 2.2. They were also the first to consider the effect of the excess enthalpy due to the glassy state of the polymers and blends.

The dissolution of a polymer in a solvent can be thought to occur in two stages. First, the solvent swells the polymer, allowing greater mobility of the individual polymer molecules while maintaining the inter-molecular polymer contacts. In effect, the solvent serves to lower the Tg of the polymer to below the experimental temperature. The "melting" of the glassy initial state was exothermic as shown in
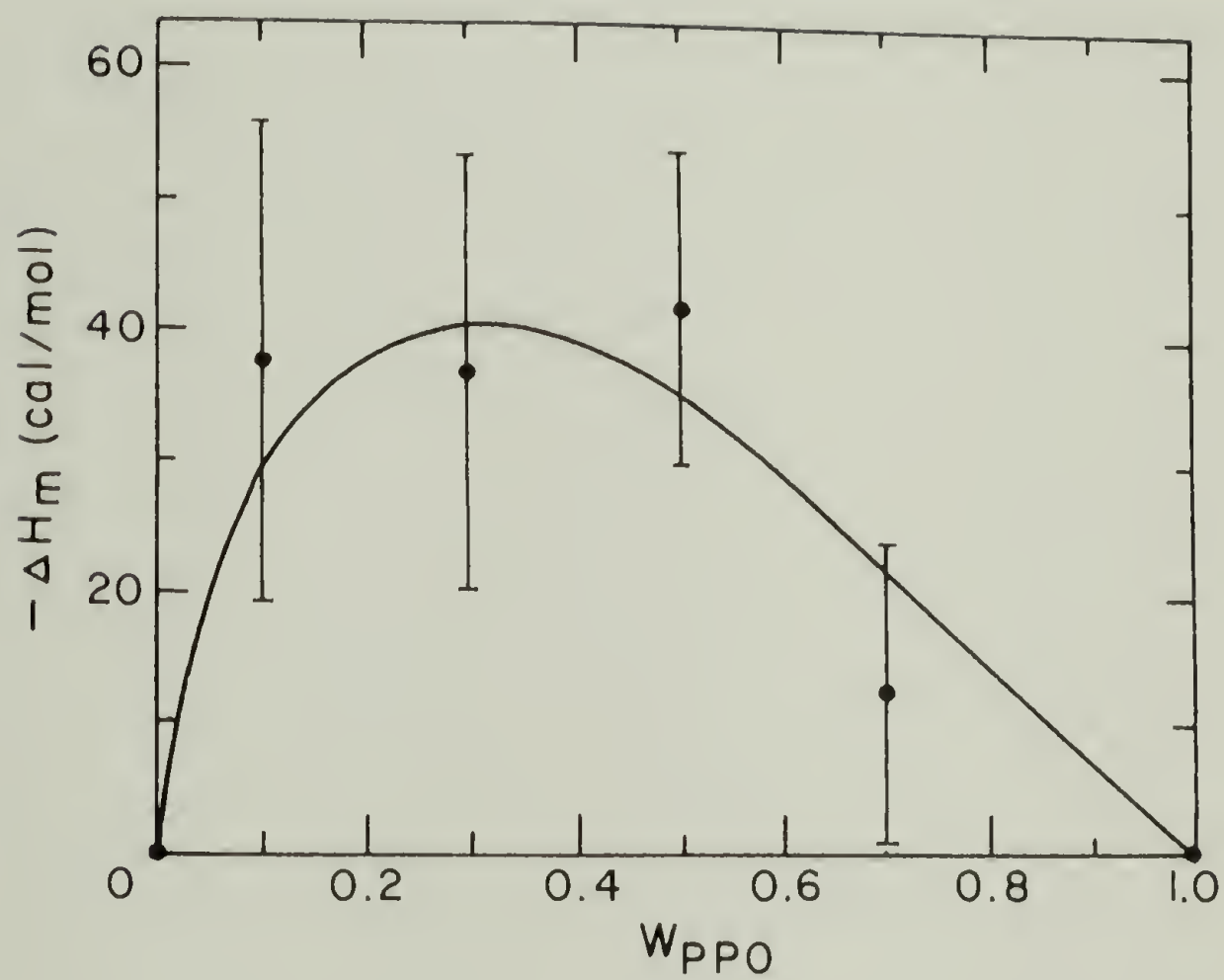
Figure 2.2. $-\Delta H_m$ for PS/PPO blends [from Weeks[16]].

Figure 2.3. The amount of heat given off was ΔH_{xs}. Once the polymer has swelled, the solvent molecules break the polymer-polymer interactions to form polymer-solvent interactions resulting in a true dilute homogeneous solution. If the polymer-polymer interactions are stronger than the polymer-solvent interactions, the solution process would stop at the swollen gel.[17]

In order to obtain a meaningful value for ΔH_m at the experimental temperature, the excess glassy heat, ΔH_{xs}, must be subtracted from the experimental values for the heats of solution. Noticing the enthalpy can be given as:

$$\overline{H} = \int_0^{\overline{T}} C_p dT \tag{2.8}$$

the excess glass enthalpy could be calculated as

$$\Delta H_{xs}(T) = \overline{H}_g(T) - \overline{H}_l(T) \tag{2.9}$$

where T is the experimental temperature, g and l refer to the glassy and liquidus states, respectively. Since,

$$H_i(T) = \int_0^T Cp_i dT \tag{2.10}$$

then

$$H_{xs}(T) = \int_0^T Cp_g dT - \int_0^T Cp_l dT . \tag{2.11}$$
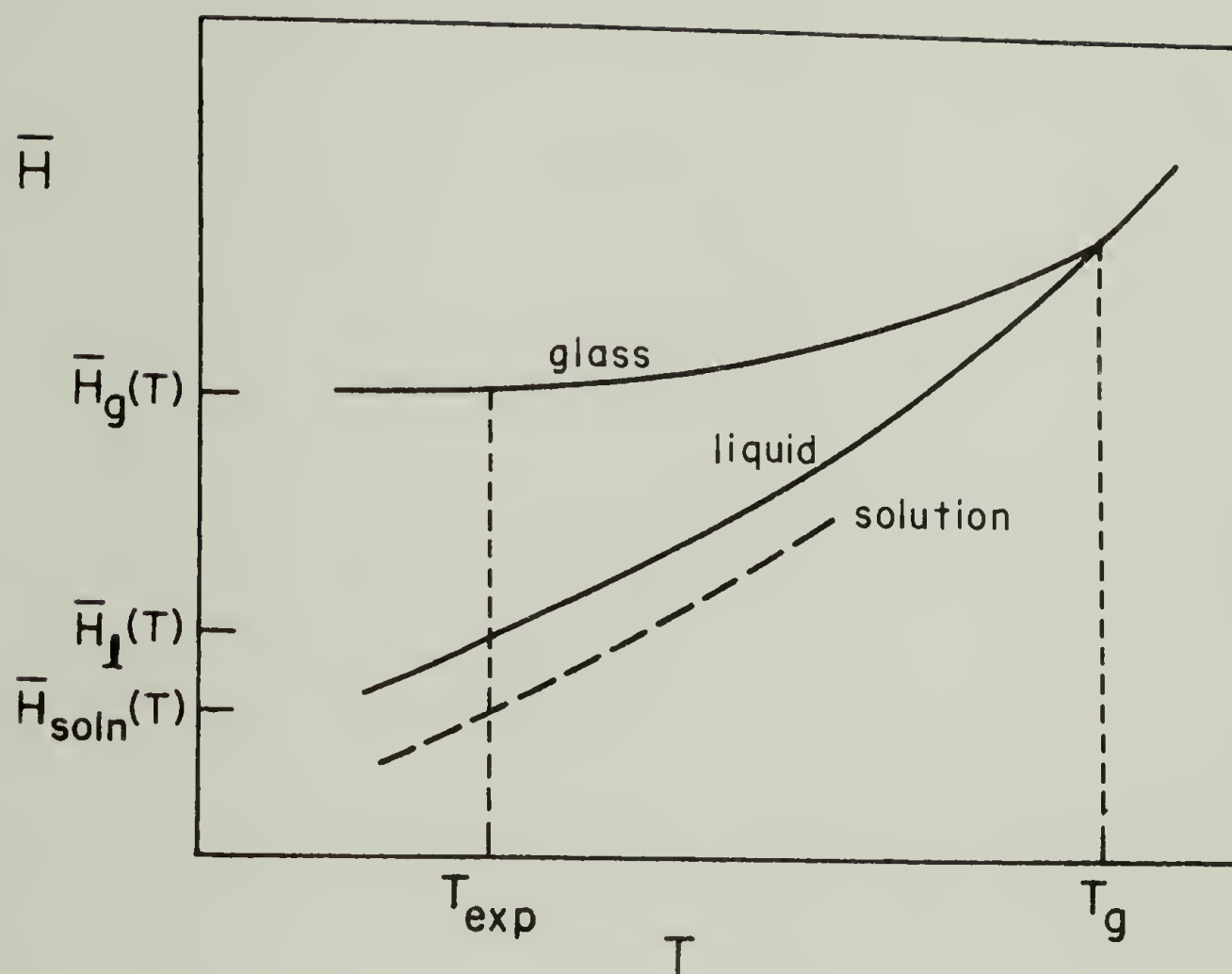
Figure 2.3. Enthalpy-temperature curve.

At the glass transition temperature, the glass and liquid enthalpies are equal (see Figure 2.3). Eqn. (2.11) could then be rewritten as

$$H_{xs}(T) = H_g^o - \int_T^{Tg} Cp_g dT - H_l^o + \int_T^{Tg} Cp_l dT$$

$$= \int_T^{Tg} Cp_l dT - \int_T^{Tg} Cp_g dT .$$ (2.12)

Using DSC, a binomial equation could be calculated for both Cp_l and Cp_g, and integrated according to Eqn. (2.12). However, an accurate determination of the variation of Cp with temperature was difficult. Coupled with this fact, the experimental temperature was typically 35°C whereas the Tg for PPO was 217°C. Any error in the Cp measurement was magnified over an extrapolated temperature range of 180°C.

An approximation was made to Eqn. (2.12) to simplify the calculation of ΔH_{xs}. The assumption that the specific heat was independent of temperature, removed Cp from the integral to give

$$\Delta H_{xs}(T) = Cp_l(T) \int_T^{Tg} dT - Cp_g(T) \int_T^{Tg} dT$$

$$= [Cp_l(Tg) - Cp_g(Tg)](Tg - T)$$

$$= -\Delta Cp \Delta T$$ (2.13)

where ΔCp was the change in specific heat at Tg and ΔT the difference between Tg and the experimental temperature.

It was very important to keep the sign convention consistent. The heat of solution was actually the difference

$$\Delta H_s = \overline{H}_{soln} - \overline{H}_g \qquad\qquad (2.14)$$

as shown in Figure 2.3. The value of interest was the difference

$$\Delta H'_s = \overline{H}_{soln} - \overline{H}_l . \qquad\qquad (2.15)$$

Therefore, the excess glass heat needed to be subtracted from ΔH_s was $\overline{H}_l - \overline{H}_g$. In this convention, ΔH_{xs}, equal to $\Delta Cp\Delta T$, was always exothermic and served to reduce the exothermic value of ΔH_s. In fact, in some cases, subtraction of $\Delta Cp\Delta T$ from ΔH_s yielded a positive value for $\Delta H'_s$.

Others have also taken into account the excess glass energy, although not in heats of mixing measurements. Bianchi treated the effect of the higher energy content of the glass in studies of the conformational energy of amorphous polymers at various temperatures.[18-21] Maron and Daniels used measurements of the heats of solution to determine the energy of polystyrene glass.[22] Their values of -33.6 J/gm were quite large compared to the value of -23.5 J/gm calculated from Eqn. (2.13). However, the solvents used by Maron were not athermal solvents, i.e., the heat of solution was not entirely due to the glassy excess energy. Filisko also observed the excess glass enthalpy which he termed "residual heat."[23-25] They studied the effect of temperature on the heat of solution and found a linear dependence. However, no attempt was made to calculate the excess glass enthalpy.

Morimoto did calculate the excess glassy heat in a manner simi-
lar to Eqns. (2.8)-(2.13).[26] He used the correction applied to the
measurement of the heats of solution of various molecular weight poly-
styrenes.

E. Presentation of ΔH_m Data

For polymer-polymer systems, the familiar Flory-Huggins ex-
pression for the free energy of mixing can be written in its simplest
form as[42]

$$\Delta G_m/RT = \frac{\phi_1}{r_1} \ln \phi_1 + \frac{\phi_2}{r_2} \ln \phi_2 + \phi_1 \phi_2 \chi \tag{2.16}$$

where r_i is the polymer chain lengths, ϕ_i the composition fraction and
χ the polymer-polymer interaction parameter. The first two terms of
Eqn. (2.16) are entropic in nature and as r_i becomes large, the en-
tropic term approaches zero. The enthalpic term can then be expressed
as

$$\Delta H_m/RT = \chi \phi_1 \phi_2 \ . \tag{2.17}$$

Eqn. (2.17) is not a definition; χ is a strong function of temperature.
However, for purposes of illustration, the treatment here considers a
temperature independent χ.

From Eqn. (2.17), the interaction parameter can then be ap-
proximated by $\Delta H_m/R\phi_1\phi_2$ which resembles a van Laar energy interaction
term.[1,41] The heat of mixing can be normalized to constant number of
interpolymeric contacts and as such reflect the strength of the

polymer-polymer interaction.

Cooper and Booth[42] used the above approach in their study of the mixing of ethylene oxide and propylene oxide oligomers. However, most workers presented heats of mixing data in units of energy per gram or per mole of mers, i.e., normalized to the total number of polymer molecules. The results of this work will be presented in both forms discussed above.

REFERENCES

1. R. Koningsveld, L.A. Kleintjens, H.M. Schoffeleers, Pure Appl. Chem. 39, 1 (1974).

2. P.R. Couchman, Macrom. 11, 1156 (1978).

3. T. Pazonyi, M. Dimitrov, Rubber Chem. Tech. 40(4), 1119 (1967).

4. A.A. Tager, T.I. Scholokhovich, Yu. S. Bessonov, Europ. Polym. J. 11, 321 (1975).

5. P.J. Flory, J.L. Ellenson, B.E. Eichinger, Macrom. 1(3), 279 (1968).

6. P.J. Flory, B.E. Eichinger, R.A. Orwoll, Macrom. 1(3), 287 (1968).

7. M.P. Zverev, L.A. Polovikhina, A.N. Barash, L.P. Mal'kova, G.D. Litovchenko, Vysok. Soyed. A16(8), 1813 (1974).

8. A.A. Tager, Yu. S. Bessonov, Vysok. Soyed. A17(11), 2383 (1975).

9. I.N. Razinskaya, L.I. Vidyakina, T.I. Radbil, B.P. Shtarkman, Vysok. Soyed. A14, 968 (1972).

10. R.J. Kern, J. Polym. Sci. 33, 524 (1958).

11. K. Kosai, T. Higashino, Nippon Setchaku Kyokai Shi 11, 2 (1975).

12. J.W. Schurer, A. DeBoer, G. Challo, Polymer 16, 201 (1975).

13. S. Ichihara, A. Komatsu, T. Hata, Polym. J. 2(5), 640 (1971).

14. F. Friese, Plaste. Kaut. 15, 646 (1968).

15. R.J. Peterson, R.D. Corneliussen, L.T. Rozelle, Polym. Prep. A.C.S. 10, 385 (1969).

16. N.E. Weeks, F.E. Karasz, W.J. MacKnight, J. Appl. Phys. 48(10), 4068 (1977).

17. F.W. Billmeyer, Textbook of Polymer Science, Wiley-Interscience, N.Y., 1971.

18. U. Bianchi, E. Pedemonte, M.L. Giudice, Rend. Chim. 8(5), 3 (1965).

19. U. Bianchi, C. Cuniberti, E. Pedemonte, C. Rossi, J. Polym. Sci.: A-2 $\underline{5}$, 743 (1967).

20. U. Bianchi, C. Cuniberti, E. Pedemonte, C. Rossi, J. Polym. Sci.: A-2 $\underline{7}$, 845 (1969).

21. U. Bianchi, C. Cuniberti, E. Pedemonte, C. Rossi, J. Polym. Sci.: A-2 $\underline{7}$, 855 (1969).

22. S.H. Maron, C.A. Daniels, J. Macrom. Sci.-Phys. $\underline{B2}$(4), 769 (1968).

23. F.E. Filisko, R.S. Raghava, G.S.Y. Yeh, J. Macrom. Sci.-Phys. $\underline{B10}$(3), 371 (1974).

24. F.E. Filisko, R.S. Raghava, J. Appl. Phys. $\underline{45}$(10), 4151 (1974).

25. F.E. Filisko, R.S. Raghava, J. Macrom. Sci.-Phys. $\underline{B12}$(3), 317 (1974).

26. S. Morimoto, Bull. Chem. Soc. Japan $\underline{44}$, 879 (1971).

27. P.J. Flory, R.A. Orwoll, A. Vrij, J.A.C.S. $\underline{86}$, 3515 (1964).

28. P.J. Flory, J.A.C.S. $\underline{87}$, 1833 (1965).

29. B.E. Eichinger, P.J. Flory, Trans. Fara. Soc. $\underline{64}$, 2035 (1968).

30. P.J. Flory, Discuss. Fara. Soc. $\underline{49}$, 7 (1970).

31. I.C. Sanchez, R.H. Lacombe, J. Phys. Chem. $\underline{80}$, 2352 (1976).

32. I.C. Sanchez, R.H. Lacombe, J. Polym. Sci. Polym. Lett. Ed. $\underline{15}$, 71 (1977).

33. R.H. Lacombe, I.C. Sanchez, J. Phys. Chem. $\underline{80}$, 2568 (1976).

34. I.C. Sanchez, "Statistical Thermodynamics of Polymer Blends," in Polymer Blends, Vol. I, D.R. Paul, ed., Academic Press, N.Y., 1978.

35. L.P. McMaster, Macrom. $\underline{6}$(5), 760 (1973).

36. J.H. Hildebrand, R.L. Scott, The Solubility of Nonelectrolytes, 3rd edition, Reinhold Publishing Corp., N.Y., 1950.

37. H. Morawetz, Macromolecules in Solution, 2nd edition, Wiley, N.Y., 1974.

38. H. Burrell, Official Digest $\underline{27}$, 726 (1955).

39. H. Burrell, B. Immergut, in Polymer Handbook, J. Brandrup and
     B. Immergut, eds., Interscience, N.Y., 1966.

40. K.L. Hoy, J. Paint Tech. 42, 76 (1970).

41. H.C. Van Ness, Classical Thermodynamics of Non-Electrolyte
     Solutions, The MacMillan Co., N.Y., 1964, p. 125ff.

42. D.R. Cooper, C. Booth, Polymer 18, 164 (1977).

CHAPTER III

EXPERIMENTAL

The purpose of this chapter is to discuss the procedures used
for the synthesis, characterization and calorimetric study of the poly-
mers and blends central to this thesis. Synthesis and characteriza-
tion performed and reported by Fried[8] and Alexandrovich will not be
reiterated.

A. Calorimetric Studies

Since the bulk of this thesis work was concerned with the
calorimetric study of polymer-polymer systems, a short background on
calorimetry will be presented here. Two types of calorimetry were
used for studying polymer-polymer systems: Tian-Calvet microcalorimetry
and differential scanning calorimetry.

1. <u>Tian-Calvet microcalorimetry</u>. Tian-Calvet microcalorimetry evolved
from the early work of Tian[1] in the 1920s and expanded upon by Calvet.[2]
Microcalorimetry is capable of measuring very small heats, on the order
of a millicalorie. It does this not by measuring the amount of heat
produced, i.e., temperature change, rather it records the rate of heat
production, heat flux, of the process being studied. This is done
utilizing banks of thermocouples from the reaction cells to a heat
sink. All heat produced in the reaction cells flows through the

thermocouple wires resulting in an e.m.f. which can be measured. The larger the heat flow through the thermopiles, the larger the e.m.f. produced. Details of the theory and operation of the Tian-Calvet micro-calorimeter have appeared in the literature.[2-4]

The instrument used in this study included the Tian-Calvet microcalorimeter, a Setaram temperature controller, a Keithly model 148 nanovoltmeter-amplifier circuit and Cole-Parmer model 8384-32 single channel integrating recorder. Calibration of the instrument was done using the calibration circuit supplied by IMASS, Inc. and calibration cells supplied with the instrument. Calibration was done by Joule heating utilizing the relation

$$P = I^2R \qquad\qquad (3.1)$$

where I = calibration current and R = heating wire resistance. Since the resistance R was constant (1000 ohms), the power varied as the current was changed. The power (i.e., energy) results in a peak due to the e.m.f. produced by the thermocouples. Calibration of the cells was done by changing the energy produced in the cells and measuring the resulting peak area. Figure 3.1 is a plot of peak area (in counts) versus energy. A least squares fit of the line yielded values for the slope and intercept as given in Table 3.1. The calibration current was accurately measured by connecting a multimeter in series with the calibration cell. The current was quite stable over the usual 15 minutes it was flowing with fluctuations of the order of only .001 milli-amps.

Reaction cell design is important. A variety of cell designs
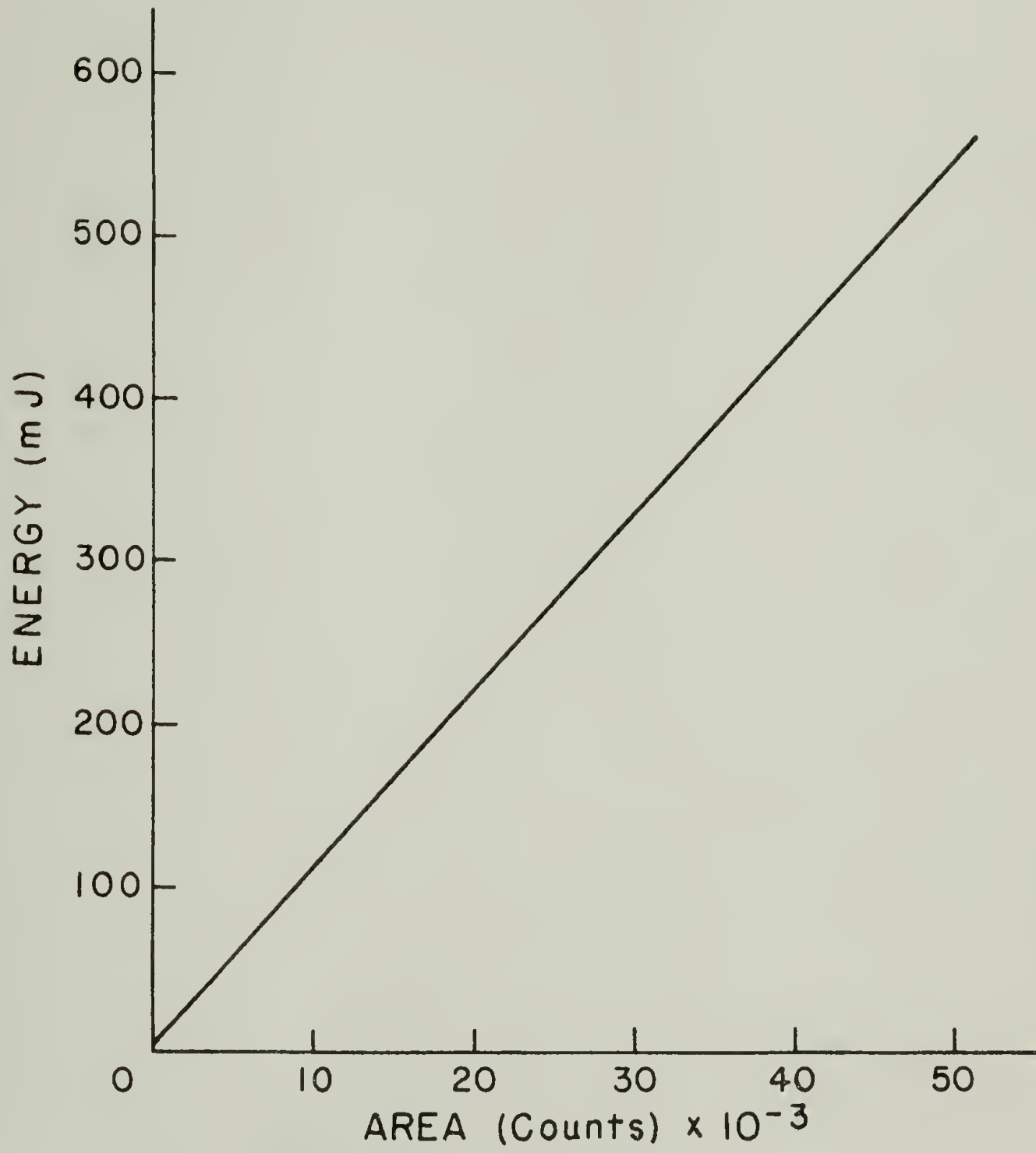
Figure 3.1.   Calibration curve for Tian-Calvet microcalorimeter.

Table 3.1. Calibration Constants for Calorimeter Cells.

Temperature	Slope	Intercept	Cells	Range	Integrater
34.77°C	1.0984E-02	1.052	1,3,5	30 μV	3000 c/min
	1.0870E-02	4.776	2,4,6	30 μV	3000 c/min
101.40°C	1.7793E-03	.8594	1,3,5	10 μV	6000 c/min
	1.7511E-03	.4213	2,4,6	10 μV	6000 c/min

have been tried and reported to fit a myriad of tasks.[2-7] In the present work, several different cell designs were tried, particularly with reference to higher temperature work. Initial work here used the two and three tube setup described in detail by Filisko.[3,5] There are several important requirements to consider in cell design. The liquid-vapor interface must not move. If the vapor space in the cell is changed, the baseline will drift and an exotherm or endotherm will result depending on whether the vapor space is increased or decreased. It must be kept in mind when designing the cell that the effects to be studied produce approximately 400 mJ of heat, equivalent to about 10^{-2} ml of solvent evaporating. The sample must be isolated from the solvent until thermal equilibrium is obtained. Since the flow of heat is measured only on the bottom and sides, any heat flow through the top should be minimized. Finally, ease of handling needs to be taken into account.

Most of the cell designs used in this work were based on the designs of Filisko[3,5] with minor adjustments. For ductile polymers below Tg, a small glass rod (2 mm o.d.) was used to simply spear the polymer (see Figure 3.2). The polymer was immersed in the mercury, thermal equilibrium reached, followed by the rod being raised to introduce the polymer into the solvent. This cell design worked very well for polystyrene, PPO and blends thereof. However, most of the samples studied were very brittle and the spearing techniques simply did not work. Some sort of container was needed for the polymer samples. Since there was a problem with trapped air in the Filisko cell designs, a teflon "cage" was made to hold the samples. (see Figure 3.2a).
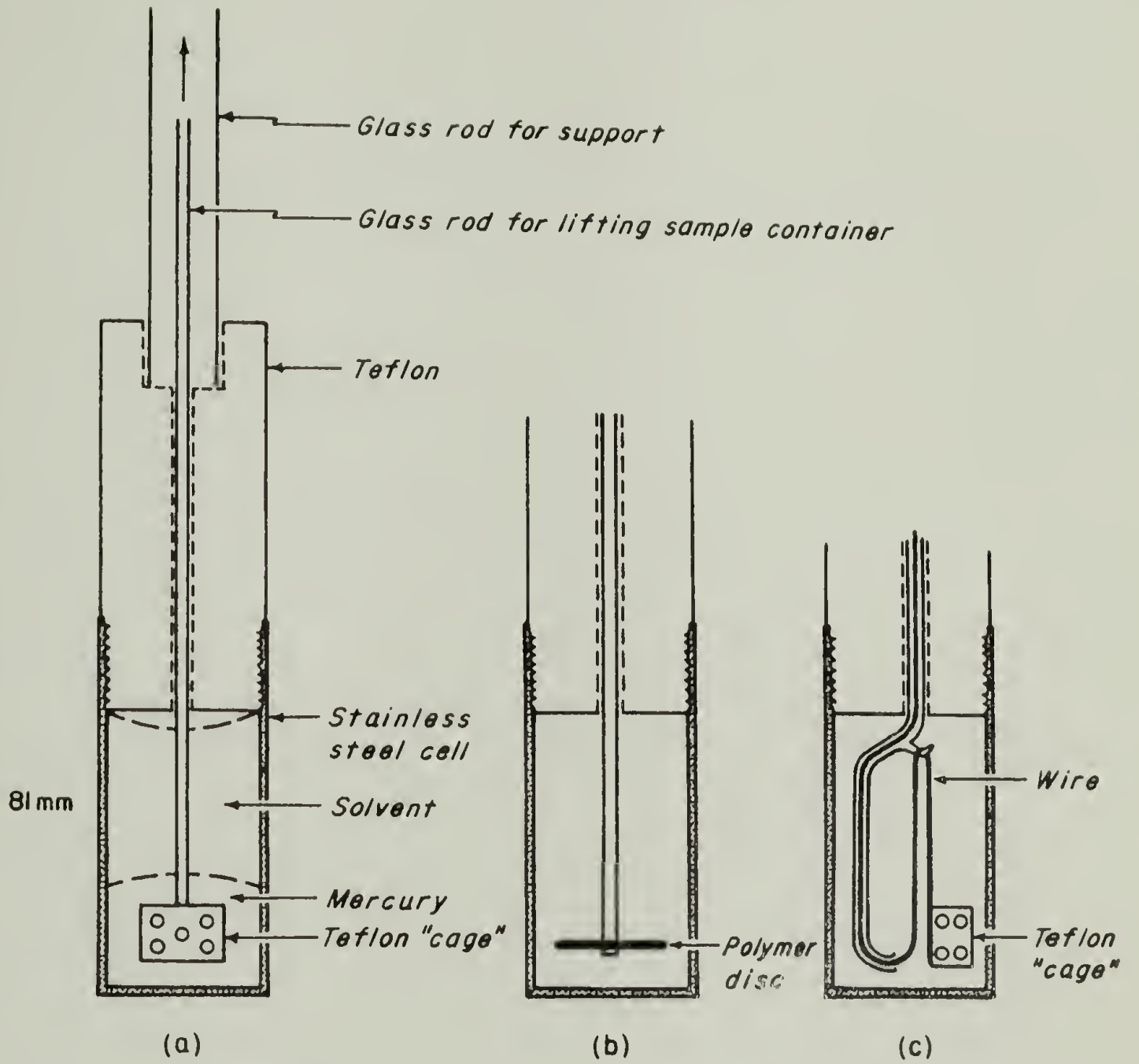
Figure 3.2.   Experimental setup.

This cage was attached to a glass lifting rod and also had many small holes drilled into the sides, top and bottom. The polymer samples, which could be any irregular form, were put inside the cage, and when immersed underneath the mercury, the mercury would flow in through the holes and displace most of the air. Following equilibration, the cage was lifted by means of the attached glass rod, into the solvent which would diffuse into the holes and dissolve the polymer. At temperatures above Tg, polymer surface tension was sufficient to disallow polymer flow through the holes. Therefore, this cell design appeared to be suitable for high temperature work. However, at 111°C, there were other problems. Whenever the teflon cage was pulled through the mercury interface, a large endotherm was produced due to a redistribution of heat. This endotherm was irreproducible and varied quite widely. Any future high temperature (greater than about 90°C) work needs a radical design change.

For completeness, two different cell designs were attempted and failed. Figure 3.2c illustrates one of these designs. In what can be termed the "flagpole" design, two thin teflon coated wires were fed through a small glass rod bent as shown in Figure 3.2c. The wire was looped around a glass hook near the top of the cell and the teflon cage tied into the wire. By pulling on one or the other wire, the teflon cage could be lowered or raised at will similar to raising a flag. However, this design failed because the actual process of raising the cage resulted in a large amount of frictional heat. The design offered promise, however, since the system was closed to solvent. As the temperature was raised, only the mercury level changed and solvent

evaporation was nil. Since the rod vented to atmospheric pressure, no pressure effects were felt. One drawback, however, was the vaporization of the mercury out of the cell which over a certain amount of time could be hazardous.

Two different methods could be used for measuring the heats involved. Weeks[24] used the differential method. In the sample cell, the polymer blend was dissolved against the two pure components in the reference cell. The net heat evolved was the heat of mixing of the polymers. Care must be taken to match the weights of all components. This involved knowing the calibration constants of each cell very accurately in order to match the heats evolved from each cell. One advantage of this method was increased sensitivity due to the compensation of heats. Also, since the same procedure was used to introduce the samples into the solvent, any heat due merely to the mechanical motion would cancel.

In spite of these advantages, the method of choice for this work was the absolute method. Polymers and blends were run singularly against each other using the opposite cell as the reference. This method gave values for the heats of solution of polymers and polymer blends in the solvent (1,2-dichlorobenzene). Although sensitivity was lost due to this method, other advantages far outweighed the differential method. The sample preparation was much simpler. There was no need for matching weights. Data collection was much faster. In the differential method, one run would take four hours from initial equilibration to final dissolution. In that same four hour period, two runs could be made by the absolute method. In the differential

method, the shapes of the curves were not consistent. Therefore, any abnormalities in the run would go unnoticed. Also, since the peaks occurred both above and below the baseline, an integrating recorder would not work since the negative peak would go unreported. In the absolute method, peak shape was consistent and always in one direction, allowing the use of an integrating recorder. The amount of heat evolved from the mechanical process of raising the sample into the solvent was insignificant below 70°C. The extra sensitivity advantage of the differential method was superfluous. The errors in the calibration constants outweighed any lessening of error due to the higher sensitivity.

In this study, heats of solution were measured at two separate temperatures (35°C, 67°C) and attempted at a third (111°C). The procedure for changing and measuring the temperature of the microcalorimeter was discussed in detail by McKnight[6] and will not be explored further here.

2. Differential scanning calorimetry (DSC). Differential Scanning Calorimetry was used extensively in this work both for characterization of the polymers and to study the phase separation above Tg. A Perkin-Elmer DSC-2 with scanning autozero attachment was used for most of this work. However, some work done at Bell Laboratory also utilized a Tektronix Calculator interfaced with the DSC-2. DSC measures the power needed to keep a sample and a reference holder at the same temperature.[10] An endothermic process requires more power to be fed to the sample container which results in a deflection on the chart recorder.

Since DSC results in plots of heat capacity versus either temperature or time, it is very well suited for studying first and second order phase transitions.

Typical sample sizes were 10 mg discs. For a sample of this size, a totally amorphous polymer showed a large step in the specific heat at Tg with a range setting of 2 mcal/sec full scale. Heating rates of 20°C/minute with chart speeds of 40 mm/minute were suitable for studying most polymer glass transition temperatures. Tg was taken as ½ΔCp with an error approximated to be ±2°C. Values for ΔCp and Cp(glass) and Cp(liquid) were determined two ways. The DSC work at Bell Laboratory utilized the Tektronix calculator and gave data already converted to Joules/degree-gram. A more tedious method employed was outlined by Fried.[8,9] Fortunately, the Perkin-Elmer Scanning Auto-zero attachment simplified the technique. A blank baseline was calibrated in and run. Using the same sample pan, the polymer sample was then superimposed on the previous baseline. Calibration of recorder output was done by a sapphire standard. Point-by-point subtraction of baseline from sample run was done using an accurate millimeter scale. Points were taken every 2.5°C in the linear portion of the thermogram 50-100°C above and below Tg. A computer program was used to convert the points into least square fits of Cp(J/°C-gm) versus temperature. Values of ΔCp were then simply Cp(liquid) - Cp(glass) at Tg.

In order to study phase separation above Tg, annealing of the sample was performed in the DSC. Since a phase separated polymer-polymer system exhibited two distinct glass transition temperatures,

annealing studies yielded phase diagrams above Tg and established the existence of a lower critical solution temperature.[15] The polymer blend was scanned, held at a certain temperature for various amounts of time depending on temperature and sample, quenched in the DSC and rescanned. The second scanning was indicative of the equilibrium phase diagram at the annealing temperature. By annealing at different temperatures a complete phase diagram could be derived for temperatures between Tg and degradation temperatures. Phase separation was also reversible for some systems by annealing the sample below the LCST and following the reemergence of one glass transition temperature.

3. Thermomechanical analyzer (TMS-1). A Perkin-Elmer TMS-1 was used to measure the linear thermal expansion coefficient of several of the polymers. The TMS unit was connected to a DSC-1b temperature program-mer and a standard aluminum rod was used to calibrate the instrument. It was necessary to stack 3 to 4 pieces of polymer films in order to measure the linear expansion coefficient since the quantity $\Delta L/L_o$ is needed where L is length. Also, it was necessary to trim the diameter of the polymer rod to be less than the probe in order to keep the probe from penetrating the polymer as Tg was passed. The procedure for determining the linear expansion coefficient was outlined by the instruction manual.[11]

B. Synthesis and Characterization

The model polymer-polymer systems for this work were blends of polystyrene with poly(2,6-dimethyl-1,4-phenylene oxide). Synthesis of

the halogenated and substituted polystyrene homopolymers and copolymers was by free radical mechanism. Table 3.2 lists all the materials studied in this thesis. The only polymers/copolymers unique to this work were the brominated styrene polymers and the methylated styrene polymers. For detailed descriptions of polymerization techniques and copolymer characterization for those polymers other than the above, column 3 in Table 3.2 lists the original references where this data may be obtained. Figure 3.3 shows the basic polymer repeat unit structure of PPO and substituted polystyrenes.

1. <u>Poly(phenylene oxide)</u>. The PPO used throughout this study was poly(2,6-dimethyl-1,4-phenylene oxide). It was obtained from the General Electric Company in powder form. The synthesis of PPO has been amply reviewed by Hay[16] and will not be detailed here. Also, the PPO used in this work was identical to that used previously by Tkacik,[17] Fried,[8] Kleiner,[18] and Alexandrovich[15] in their thesis work at the University of Massachusetts. Each of the above references details the chemistry and physical properties of PPO. Purification of PPO consisted of the following technique. The polymer was dissolved in toluene to give approximately 4% polymer solutions. Upon complete dissolution, the solution was added dropwise from a separatory funnel into methanol. The methanol was stirred vigorously and the polymer solutions were drained into the vortex of the methanol. Final ratio of methanol:toluene was approximately 10:1. After allowing the white precipitant to settle, the solution was then filtered using a Buchner funnel, and the fluffy white precipitant was collected, washed with

Table 3.2. Materials List and Nomenclature.

Polymer	Nomenclature	References
poly(2,6-dimethy-1,4-phenylene oxide)	PPO	
a-polystyrene	PS(HH101), PS	
polystyrene $\overline{M}n$ = 50,000 $\overline{M}n$ = 37,000 $\overline{M}n$ = 32,000 $\overline{M}n$ = 20,400 $\overline{M}n$ = 17,000 $\overline{M}n$ = 9,000	 PS(50) PS(37) PS(32) PS(20.4) PS(17) PS(9)	
poly(2-fluorostyrene)	p(2-F1S)	12-14
poly(2-fluorostyrene-co-styrene)	p(2-F1S(.xxx)-S)$^+$	12-14
poly(4-fluorostyrene)	p(4-F1S)	12-14
poly(4-fluorostyrene-co-styrene)	p(4-F1S(.xxx)-S)$^+$	12-14
poly(4-fluorostyrene-co-2-fluorostyrene)	p(4-F1S(.xxx)-2-F1S)$^+$	12-14
poly(2-chlorostyrene)	p(2-C1S)	8,9,15
poly(2-chlorostyrene-co-styrene)	p(2-C1S(.xxx)-S)$^+$	8,9,15
poly(4-chlorostyrene)	p(4-C1S)	8,9,15
poly(4-chlorostyrene-co-styrene)	p(4-C1S(.xxx)-S)	8,9,15
poly(4-chlorostyrene-co-2-chlorostyrene)	p(4-C1S(.xxx)-2-C1S)$^+$	8,9,15
poly(2-bromostyrene)	p(2-BrS)	
poly(2-bromostyrene-co-styrene)	p(2-BrS(.xxx)-S)$^+$	
poly(4-bromostyrene)	p(4-BrS)	
poly(4-bromostyrene-co-styrene)	p(4-BrS(.xxx)-S)$^+$	

Table 3.2--Continued.

Polymer	Nomenclature	References
poly(4-bromostyrene-co- 2-bromostyrene)	p(4-BrS(.xxx)-2-BrS)[+]	
poly(4-methyl styrene)	p(4-MeS)	

[+]The quantity (·xxx) represents mole fraction of constituent 1 in the copolymer.
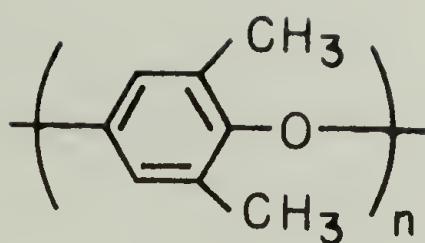
Poly(2,6-dimethyl-l,4-phenylene oxide)
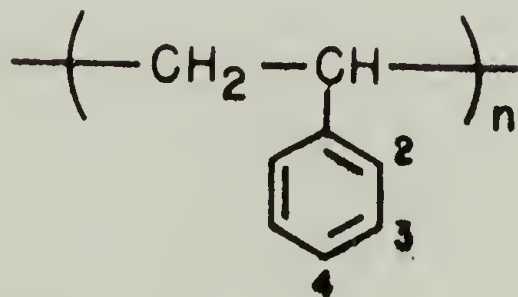
Polystyrene and substitution sites

Figure 3.3. Structures of PPO and PS.

methanol and finally dried in a vacuum oven for 3-4 days at about 80°C.

2. Polystyrene. As can be seen in Table 3.2, many different samples of polystyrene were used in this work. Except for the study of blends of polystyrene with poly(2-chlorostyrene) as a function of polystyrene molecular weight, the polystyrene used was a commercial product obtained from the Monsanto Chemical Company designated as HH101. Purification was as outlined for PPO. Throughout this thesis, unless it is otherwise stated, PS implies PS(HH101).

The monodispersed polystyrene samples used in the PS/P(2-ClS) blends were obtained from the Pressure Chemical Company. Monodispersed polystyrene is synthesized by an anionic polymerization technique. Molecular weights were obtained from the company and also were checked by gel permeation chromatography (GPC). Each of these polystyrene samples was used without further purification.

3. Polymerization techniques. Each of the polymers and copolymers was synthesized by free radical polymerization techniques. The basic technique was the same with minor adjustments in polymerization time and temperature.

The basic polymerization technique was as follows. Monomers were distilled under vacuum to remove the polymerization inhibitor 3,5-di-tert-butyl catechol. The monomer or monomers were weighed into the polymerization flask, typically a 250 ml erlenmeyer flask. Toluene (Burdick and Johnson, glass distilled) was used as the solvent and added to the polymerization flask to give approximately 40 mole percent toluene solutions. Azobisisobutyronitrile (AIBN) was used as the

initiating species and added to the solutions to give 0.5 mole percent AIBN relative to monomer concentration. Dry nitrogen gas was then bubbled through the reaction mixture to remove traces of oxygen which act as a polymerization inhibitor. The flasks were stoppered and sealed with parafilm. Polymerizations were carried out at around 60°C in an oscillating water bath. Reaction times were of the order of 10-12 hours. Following polymerization, the reaction mixture was diluted with distilled toluene to approximately 4% polymer solutions and purified and collected as outlined for PPO. Final polymer conversion was usually near 50%.

4. Brominated polystyrenes. Brominated polystyrene homopolymers and copolymers (see Table 3.2) were prepared following the technique outlined above with minor alterations. The brominated styrene monomers were not vacuum distilled before use because they would polymerize by bulk thermal methods inside the distillation apparatus. Therefore, they were used as received. Conversions were higher for the brominated styrenes which were offset by using a polymerization temperature of 50°C and polymerization time of 8-10 hours. It is especially important to maintain low conversions in copolymers in order to minimize copolymer composition drifting. Copolymer composition was determined by bromine elemental analysis for copolymers with styrene. The analysis was performed at the University of Massachusetts Microanalytical Laboratory. Halogen analysis included burning a 5 mg sample in an oxygen atmosphere containing a solution of potassium hydroxide. After the solution was neutralized, a potentiometric titration was performed

to give weight percent halogen. The claimed accuracy was ±1%.

Copolymer composition for the poly(4-BrS-co-2-BrS) copolymers was obtained using ^{13}C NMR. Approximately 50 weight percent copolymer solutions in deuterated chloroform were analyzed using a Varian CFT-20 ^{13}C NMR. Spectra were obtained after runs of approximately 8 hours. Copolymer composition was calculated from the ratio of normalized peak heights in the 2600 Hz range. Figure 3.8 shows the NMR peaks for p(4-BrS), p(2-BrS), and p(4-BrS(.453)-2-BrS).

a. Reactivity ratios. The reactivity ratios of the brominated systems were determined from a least squares fit of the Fineman-Ross equation for instantaneous copolymerization.[19] A form of the equation[20] is

$$
\frac{f_1}{f_2}\left(\frac{1 - 2F_1}{F_1}\right) = \frac{f_1^2}{f_2^2}\left(\frac{F_1 - 1}{F_1}\right)r_1 + r_2 \tag{3.2}
$$

where f_i = monomer feed fractions, F_i = copolymer composition, and r_i = reactivity ratios. Therefore, a plot of the left-hand side of Eqn. (3.2) as a function of the right-hand side yields a straight line with slope r_1 and intercept r_2. Figures 3.4, 3.5, and 3.6 are plots of copolymer composition versus monomer feed composition for the copolymers listed in the figures. Figure 3.7 is the plot of the Fineman-Ross equation to determine r_1 and r_2 for the copolymer p(4-BrS-co-2-BrS). Table 3.3 lists the values obtained for the reactivity ratios. When $r_1 = r_2 = 1.0$, the copolymer is known to be randomly placed with respect to comonomer.[21] Therefore, it was assumed that each of the brominated copolymers included random placement of the monomer units.
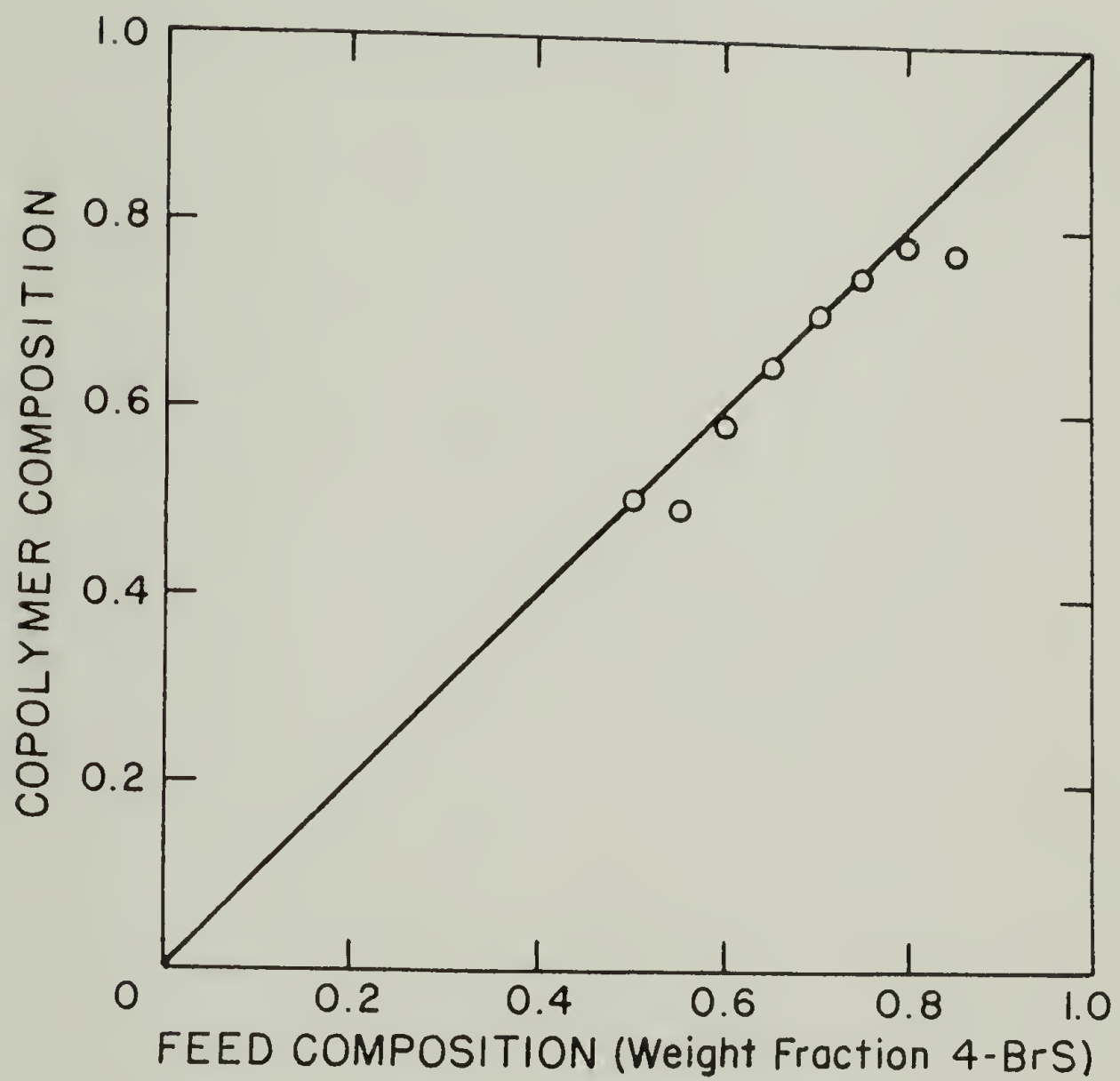
Figure 3.4. p(4-BrS-co-S) copolymer versus feed composition.
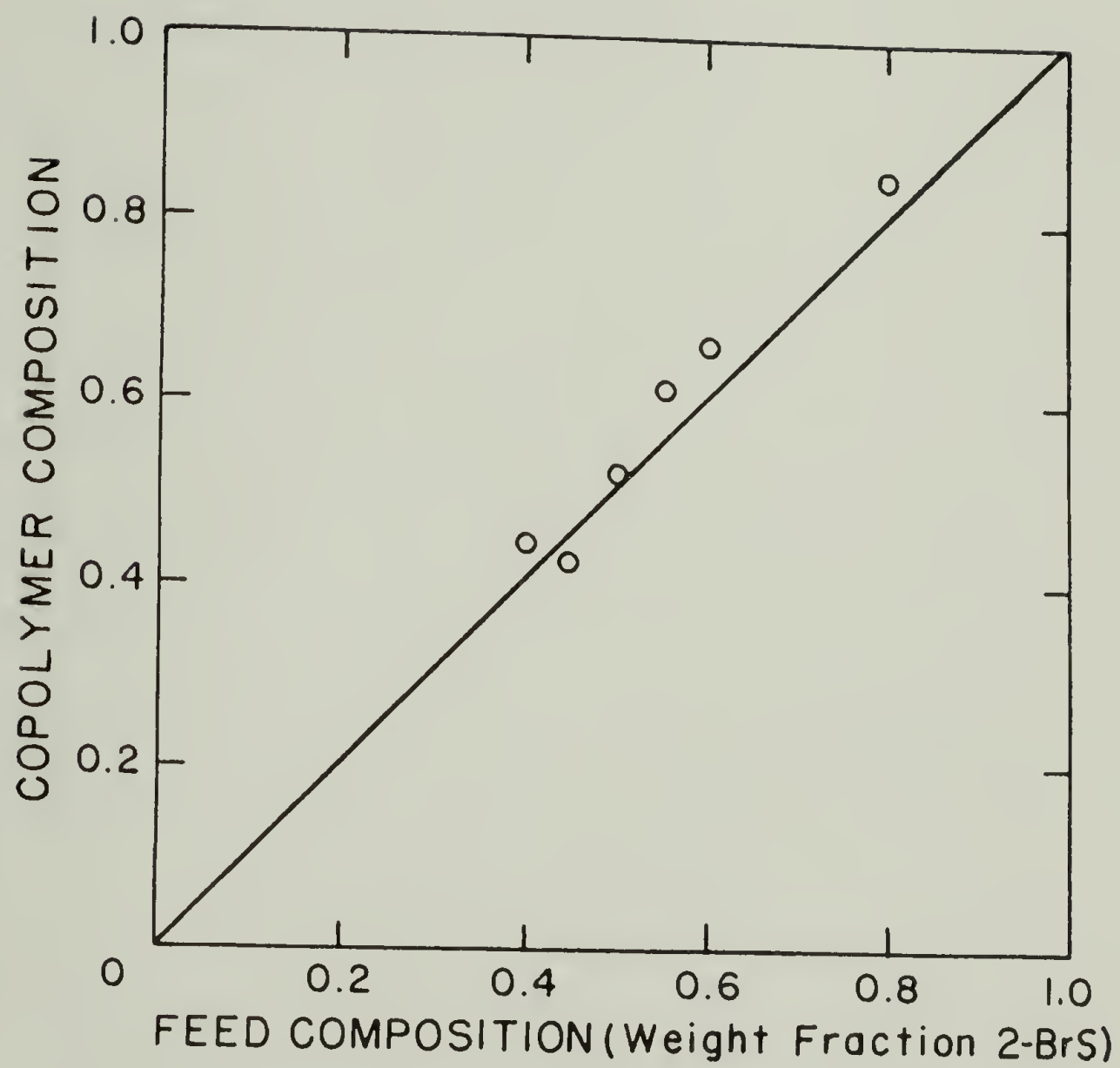
Figure 3.5.   p(2-BrS-co-S) copolymer versus feed composition.
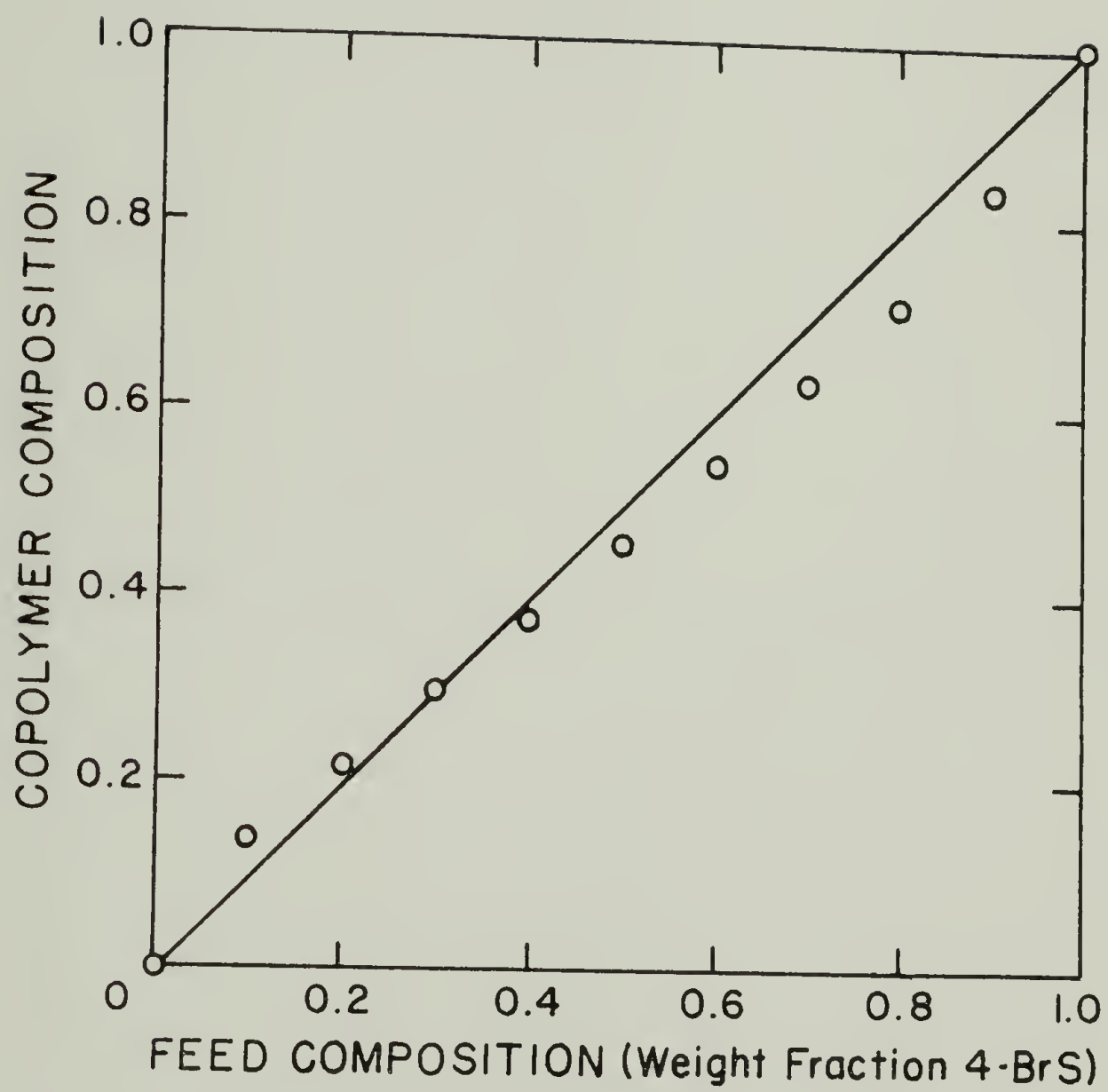
Figure 3.6. p(4-BrS-co-2-BrS) copolymer versus feed composition.
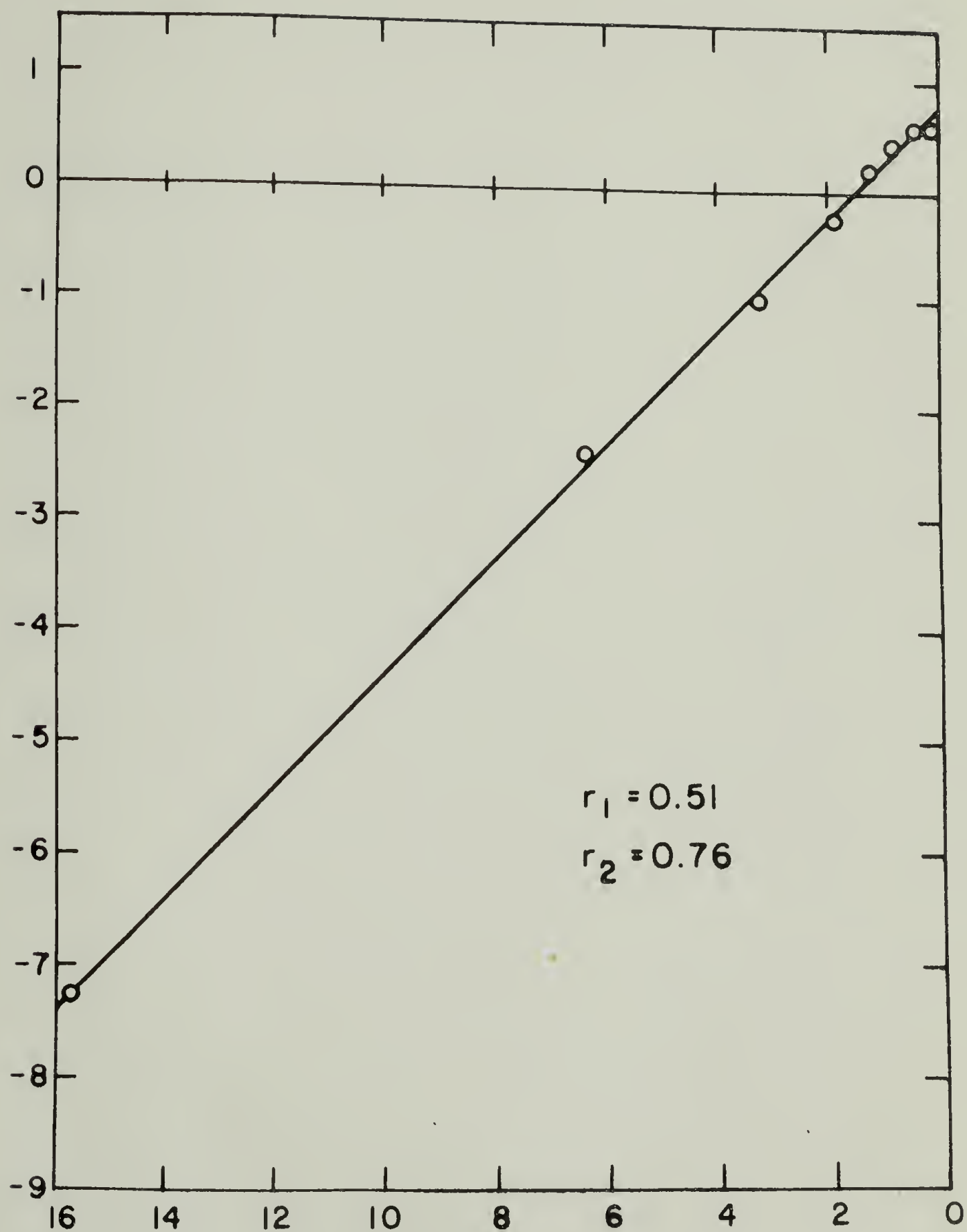
Figure 3.7. Fineman-Ross plot for determination of reactivity ratios for p(4-BrS-co-2-BrS).
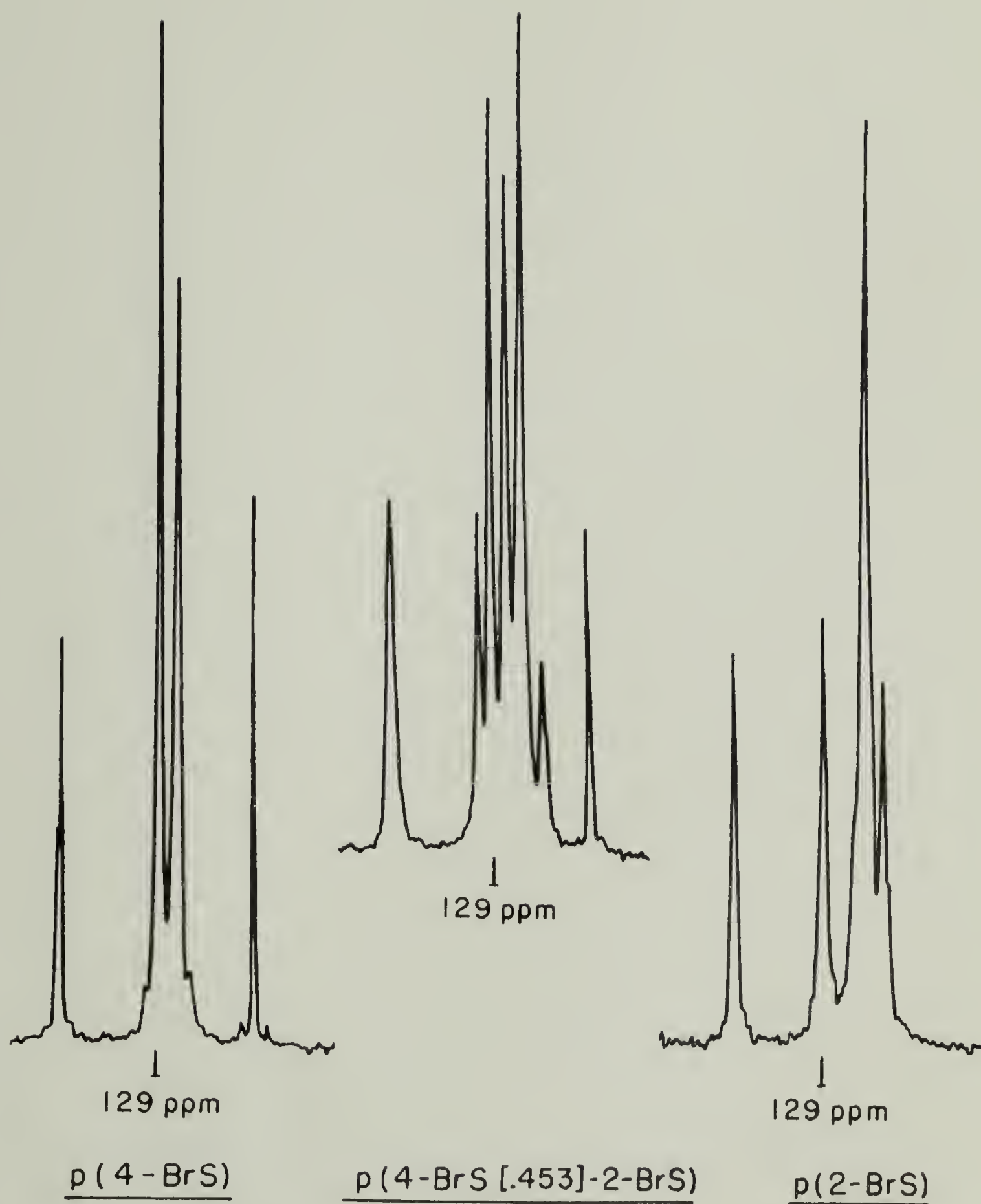
Figure 3.8. ^{13}C NMR spectra for the polybromostyrenes.

Table 3.3. Reactivity Ratios for Brominated Polystyrene Copolymers.

Copolymer	r_1	r_2
p(2-BrS-co-S)	1.74	1.32
p(4-BrS-co-S)	.85	.74
p(4-BrS-co-2-BrS)	.51	.76

Table 3.4 includes each of the comonomer feed ratios, copolymer composi-
tions and nomenclature for the brominated copolymers.

4. Polymer characterization. The characterization of the polymer sam-
ples included determination of molecular weight and glass transition
temperature. The glass transition temperatures will be treated in
greater detail in the next chapter. Molecular weight determination
was by GPC. Two different instruments were used, one being a Waters
model 200 GPC with refractive index indicator; the other a Water
Associates model 201 high pressure unit with a differential refraction
indicator. Each of the GPC's was calibrated using known monodispersed
polystyrene samples. Therefore, most molecular weights given are in
the form of "polystyrene equivalent" molecular weights. However, since
each of the polymers are substituted polystyrenes true molecular
weights are very close to the "polystyrene equivalent" molecular
weights. Detailed analysis of the GPC method is given by
Alexandrovich.[15] Table 3.5 lists each of the polymers used in this
work with values for the number-average molecular weight, $\overline{M}_n$, weight-
average molecular weight, $\overline{M}_w$, and the ratio $\overline{M}_w/\overline{M}_n$ which is a measure
of polydispersity. The data for the chlorinated polystyrenes was
taken directly from Alexandrovich,[15] whereas that for the fluorinated
polystyrenes was from the work of Vukovic.[22]

5. Preparation of polymer-polymer blends. Unless otherwise stated,
all blends in this work were prepared by freeze-drying techniques.
Freeze-drying of polymer blends is known to produce intimately mixed
polymer systems.[23] The freeze-drying technique employed here worked

Table 3.4. Brominated Copolymers.

p(2-BrS-co-S) Copolymers

Comonomer Feed Mole Fraction 2-BrS	Copolymer Composition Mole Fraction 2-BrS	Nomenclature
.275	.313	p(2-BrS(.313)-S)
.318	.297	p(2-BrS(.313)-S)
.362	.405	p(2-BrS(.405)-S)
.410	.482	p(2-BrS(.482)-S)
.460	.530	p(2-BrS(.530)-S)
.695	.774	p(2-BrS(.774)-S)

p(4-BrS-co-S) Copolymers

Comonomer Feed Mole Fraction 2-BrS	Copolymer Composition Mole Fraction 4-BrS	Nomenclature
.362	.373	p(4-BrS(.373)-S)
.410	.357	p(4-BrS(.357)-S)
.460	.446	p(4-BrS(.446)-S)
.514	.520	p(4-BrS(.520)-S)
.570	.576	p(4-BrS(.576)-S)
.630	.622	p(4-BrS(.622)-S)
.695	.675	p(4-BrS(.675)-S)
.763	.663	p(4-BrS(.663)-S)

p(4-BrS-co-2-BrS) Copolymers

Comonomer Feed Mole Fraction 4-BrS	Copolymer Composition Mole Fraction 4-BrS	Nomenclature
.10	.135	p(4-BrS(.135)-2-BrS)
.20	.217	p(4-BrS(.217)-2-BrS)
.30	.302	p(4-BrS(.302)-2-BrS)
.40	.371	p(4-BrS(.371)-2-BrS)
.50	.453	p(4-BrS(.453)-2-BrS)
.60	.542	p(4-BrS(.542)-2-BrS)
.70	.631	p(4-BrS(.681)-2-BrS)
.80	.714	p(4-BrS(.714)-2-BrS)
.90	.838	p(4-BrS(.838)-2-BrS)

Table 3.5. Polymer Molecular Weights.

Polymer	$\overline{M}_n$ $(\times\ 10^{-5})$	$\overline{M}_w$ $(\times\ 10^{-5})$	$\dfrac{\overline{M}_w}{\overline{M}_n}$
PPO	.16	.37	2.3
PS(HH101)	1.2	2.8	2.4
p(2-F1S)	.63	1.21	1.9
p(2-F1S(.0805)-S)	.52	.98	1.9
p(2-F1S(.176)-S)	.53	.95	1.8
p(2-F1S(.286)-S)	.57	1.10	1.9
p(2-F1S(.400)-S)	.65	1.24	1.9
p(2-F1S(.494)-S)	.59	1.14	1.9
p(2-F1S(.585)-S)	.69	1.34	2.0
p(2-F1S(.679)-S)	.68	1.35	2.0
p(2-F1S(.804)-S)	.71	1.39	2.0
p(2-F1S(.843)-S)	.79	1.52	1.8
p(2-F1S(.905)-S)	.72	1.45	2.0
p(4-F1S)	.67	1.27	1.9
p(4-F1S(.077)-S)	.54	.97	1.8
p(4-F1S(.157)-S)	.56	.99	2.0
p(4-F1S(.253)-S)	.51	.97	1.9
p(4-F1S(.357)-S)	.49	.96	2.0
p(4-F1S(.462)-S)	.52	1.00	1.9
p(4-F1S(.483)-S)	.51	.95	1.9
p(4-F1S(.554)-S)	.51	1.04	1.95
p(4-F1S(.671)-S)	.53	1.04	2.0
p(4-F1S(.775)-S)	.50	1.00	2.0
p(4-F1S(.052)-2-F1S)	.63	1.20	1.9
p(4-F1S(.101)-2-F1S)	.65	1.31	2.0
p(4-F1S(.146)-2-F1S)	.58	1.13	2.0
p(4-F1S(.162)-2-F1S)	.91	1.68	1.8
p(4-F1S(.228)-2-F1S)	.86	1.62	1.9
p(4-F1S(.285)-2-F1S)	.91	1.68	1.8

Table 3.5--Continued.

Polymer	$\overline{M}_n$ (x 10^{-5})	$\overline{M}_w$ (x 10^{-5})	$\dfrac{\overline{M}_w}{\overline{M}_n}$
p(4-F1S(.375)-2-F1S)	.80	1.60	2.0
p(4-F1S(.428)-2-F1S)	.83	1.63	2.0
p(4-F1S(.456)-2-F1S)	.88	1.65	1.9
p(4-F1S(.562)-2-F1S)	.86	1.62	1.9
p(4-F1S(.662)-2-F1S)	.77	1.52	2.0
p(4-F1S(.710)-2-F1S)	.70	1.34	1.9
p(4-F1S(.811)-2-F1S)	.74	1.37	1.9
p(2-C1S)	.58	1.2	2.1
p(2-C1S(.151)-S)	.33	.68	2.1
p(2-C1S(.274)-S)	.35	.72	2.1
p(2-C1S(.406)-S)	.39	.82	2.1
p(2-C1S(.562)-S)	.46	.94	2.0
p(2-C1S(.719)-S)	.46	1.10	2.4
p(2-C1S(.872)-S)	.60	1.30	2.2
p(2-C1S(.65)-S)	.36	.99	2.7
p(2-C1S(.51)-S)	.43	.81	1.9
p(2-C1S(.27)-S)	.14	.37	2.6
p(4-C1S)	.64	1.3	2.0
p(4-C1S(.075)-S)	.34	.68	2.0
p(4-C1S(.160)-S)	.35	.71	2.0
p(4-C1S(.245)-S)	.37	.77	2.1
p(4-C1S(.379)-S)	.45	.89	2.0
p(4-C1S(.462)-S)	.34	.70	2.1
p(4-C1S(.50)-S)	.50	1.5	3.0
p(4-C1S(.511)-S)	.49	1.0	2.1
p(4-C1S(.594)-S)	.52	1.1	2.1
p(4-C1S(.652)-S)	.54	1.1	2.0
p(4-C1S(.661)-S)	.55	1.1	2.1
p(4-C1S(.670)-S)	.57	1.2	2.0
p(4-C1S(.679)-S)	.57	1.2	2.0

Table 3.5--Continued.

Polymer	$\overline{M}_n$ (x 10^{-5})	$\overline{M}_w$ (x 10^{-5})	$\dfrac{\overline{M}_w}{\overline{M}_n}$
p(4-ClS(.759)-S)	.58	1.2	2.0
p(4-ClS(.08)-2-ClS)	.81	1.6	2.0
p(4-ClS(.17)-2-ClS)	.79	1.7	2.1
p(4-ClS(.23)-2-ClS)	.82	1.7	2.1
p(4-ClS(.27)-2-ClS)	.77	1.6	2.1
p(4-ClS(.31)-2-ClS)	.68	1.4	2.1
p(4-ClS(.36)-2-ClS)	.70	1.5	2.1
p(4-ClS(.38)-2-ClS)	1.5	4.4	2.9
p(4-ClS(.40)-2-ClS)	.72	1.5	2.1
p(4-ClS(.43)-2-ClS)	.75	1.6	2.1
p(4-ClS(.47)-2-ClS)	.78	1.6	2.0
p(4-ClS(.57)-2-ClS)	.70	1.4	2.0
p(4-ClS(.62)-2-ClS)	.42	1.4	3.4
p(4-ClS(.64)-2-ClS)	.66	1.4	2.1
p(4-ClS(.65)-2-ClS)	.38	1.1	2.8
p(2-BrS)	.26	.74	2.9
p(2-BrS(.313)-S)			
p(2-BrS(.297)-S)	.44	.85	1.9
p(2-BrS(.405)-S)			
p(2-BrS(.482)-S)	.57	1.10	1.9
p(2-BrS(.530)-S)	.79	1.53	1.9
p(2-BrS(.774)-S)	--	3.25	--
p(4-BrS)	.45	1.18	2.6
p(4-BrS(.373)-S)	.34	.64	1.9
p(4-BrS(.357)-S)	.24	.44	1.8
p(4-BrS(.446)-S)	.37	.71	1.9
p(4-BrS(.520)-S)	.29	.53	1.8
p(4-BrS(.576)-S)	.36	.68	1.9
p(4-BrS(.622)-S)			
p(4-BrS(.675)-S)			

Table 3.5--Continued.

Polymer	$\overline{M}_n$ (x 10^{-5})	$\overline{M}_w$ (x 10^{-5})	$\dfrac{\overline{M}_w}{\overline{M}_n}$
p(4-BrS(.663)-S)			
p(4-BrS(.135)-2-BrS)	.36	.80	2.2
p(4-BrS(.217)-2-BrS)	.41	.98	2.4
p(4-BrS(.302)-2-BrS)	.53	1.09	2.1
p(4-BrS(.371)-2-BrS)	.59	1.18	2.0
p(4-BrS(.453)-2-BrS)	.66	1.43	2.2
p(4-BrS(.542)-2-BrS)	.25	.94	3.7
p(4-BrS(.631)-2-BrS)	.38	.92	2.4
p(4-BrS(.714)-2-BrS)	.15	.43	2.9
p(4-BrS(.838)-2-BrS)	.14	.36	2.5
p(4-MeS)	.14	.30	2.1
p(2-ClS)polym. 3/9/79	.02	.05	2.7

as follows. The desired quantities of each polymer were weighed into a large-mouth 2 oz. bottle. Benzene was used as the solvent with approximately 2-4% solutions being prepared. Typical quantities were 1 gram total polymer and 25 ml benzene. If larger quantities were employed, the freeze-drying apparatus frequently plugged up requiring another attempt. Once the polymers had dissolved, the solutions were transferred to freeze-drying flasks. Four blends could be prepared at once. The solutions were then rotated at an angle in liquid nitrogen until the sides of the flask were coated about halfway up with polymer frozen in a benzene matrix. After the flasks were attached to the central apparatus, they were evacuated under high vacuum. The flasks were covered with ice. Liquid nitrogen was used in the vacuum trap to collect the benzene sublimed off. Sublimation of benzene is an endothermic process and the benzene carries heat off as it sublimes. The ice was used to warm the flasks. After a minimum of 3 hours, the flasks could be taken off the vacuum and the polymer blend collected. The polymer blend appeared as a fluff coating the inside of the flasks. Frequently it was highly static due to its dryness to water and therefore very difficult to collect. Once collected, the polymer blend was dried at approximately 80°C for 3-4 days to rid excess solvent.

Blends throughout this work were prepared by weight. Therefore, the designation PS/PPO 70/30 is indicative of a polymer blend of PS with PPO containing by weight 70% polystyrene and 30% PPO.

6. Preparation of polymer films. Films of polymers and polymer blends were prepared by compression molding. Polymers were pressed between

6 inch square steel platens (10 mil thick) using brass shims of 10 mil
thickness with a 1½ inch square cut in the middle. Aluminum foil was
placed around the shim and rubbed to form the impression of the square
hole. Polymer powder or "fluff" was heaped in the middle of the
square impression, covered with another sheet of foil and placed be-
tween the two steel platens. Under pressure and temperature, the
polymer flowed to fill the impression resulting in a polymer film en-
cased between two sheets of aluminum foil. Pressures were cycled ini-
tially to remove air bubbles, then held at high pressures (20,000 lbs.)
to form a uniform film. Compression temperatures were sample depen-
dent. However, a safe rule of thumb was to press about 40°C above the
expected glass transition temperature. Care must be exercised in film
preparation since too high a temperature might result in polymer-polymer
phase separation whereas too low a temperature produces very poor films.

REFERENCES

1. A. Tian, Bull. Soc. Chim. Fr. $\underline{33}$(4), 427 (1923).

2. E. Calvet, H. Prat, <u>Recent Progress in Microcalorimetry</u>, The MacMillan Co., N.Y., 1963.

3. S. Maron, F. Filisko, J. Macrom. Sci.-Phys. $\underline{B6}$(1), 57 (1972).

4. Tian-Calvet Microcalorimeter Instruction Manual.

5. F.E. Filisko, Ph.D. Dissertation, Case Western Reserve University, 1969.

6. R.P. McKnight, Ph.D. Dissertation, University of Massachusetts, 1975.

7. G. Delmas, D. Patterson, T. Somcynsky, J. Polym. Sci. $\underline{57}$, 79 (1962).

8. J.R. Fried, Ph.D. Dissertation, University of Massachusetts, 1976.

9. J.R. Fried, F.E. Karasz, W.J. MacKnight, Macrom. $\underline{11}$(1), 151 (1978).

10. Perkin-Elmer DSC-2 Instruction Manual.

11. Perkin-Elmer TMS-1 Instruction Manual.

12. R. Vukovic, F.E. Karasz, W.J. MacKnight, to be published.

13. R. Vukovic, F.E. Karasz, W.J. MacKnight, to be published.

14. R. Vukovic, F.E. Karasz, W.J. MacKnight, to be published.

15. P.S. Alexandrovich, Ph.D. Dissertation, University of Massachusetts, 1978.

16. A.S. Hay, Polym. Eng. Sci. $\underline{16}$, 1 (1976).

17. J.J. Tkacik, Ph.D. Dissertation, University of Massachusetts, 1976.

18. L.W. Kleiner, Ph.D. Dissertation, University of Massachusetts, 1979.

19. M. Fineman, S.D. Ross, J. Polym. Sci. $\underline{5}$(2), 259 (1959).

20. E.L. McCaffery, <u>Laboratory Preparation for Macromolecular Chemistry</u>, McGraw-Hill, N.Y., 1970.

21. R.W. Lenz, <u>Organic Chemistry of Synthetic High Polymers</u>, Interscience, N.Y., 1967.

22. R. Vukovic, unpublished data.

23. A.R. Shultz, G.I. Mankin, J. Polym. Sci.: Symp. #54, 341 (1976).

24. N.E. Weeks, F.E. Karasz, W.J. MacKnight, J. Appl. Phys. $\underline{48}$, 4068 (1977).

C H A P T E R   I V
GLASS TRANSITIONS OF POLYMERS AND BLENDS

Many substances, notably polymers, undergo a phase change from a liquid or rubbery state to glassy state as the temperature is lowered. Rubbery polymers become stiff and brittle below this glass transition temperature, Tg. Most polymer physical properties, such as brittleness, modulus and heat capacity, undergo a marked change as the Tg is traversed.

On a molecular scale, the glass transition signals the beginning of large scale molecular motion. Below Tg, the molecules are confined to vibrate in a localized lattice, although there is no large scale molecular order. Many theories have been proposed to explain the glass transition phenomenon. An excellent review is that of Shen and Eisenberg.[1]

The glass transition appears to be a thermodynamic effect superimposed on a kinetic effect. Therefore, Tg is often referred to as a pseudo-second order phase transition since the glassy state is a quasi-equilibrium state. In the glassy state, the polymer molecules are stable in terms of short range molecular motion whereas they are unstable with respect to long range motion.

Of particular interest to this work was the effect of composition on the glass transition temperatures of polymer-polymer systems. Miscible polymer-polymer systems exhibited a single glass transition

70

temperature intermediate between the two pure component Tg's. Immis-
cible polymer blends showed two distinct Tg's corresponding to the
pure component glass transition temperatures.[2-4] Many attempts have
been made to predict the Tg for compatible polymer blends. Most of
these treatments have been empirical in nature. In the simplest treat-
ments, the blend Tg was an appropriately weighted average of the pure
component Tg's. For example, Kelley and Bueche,[5] using a free volume
approach, obtained

$$Tg = (Tg_1 + (kTg_2 - Tg_1)v_2)/(1 + (k - 1)v_2) \qquad (4.1)$$

where k is an adjustable parameter approximately equal to $\Delta\alpha_2/\Delta\alpha_1$,
α being the thermal expansion coefficient and v_i is the volume frac-
tion. In actuality, Eqn. (4.1) was derived for polymer-diluent sys-
tems, but extension to polymer-polymer systems is straightforward.
Other theoretical approaches have yielded the empirical relation of
Wood.[16]

$$Tg = (Tg_1 + (kTg_2 - Tg_1)W_2)/(1 - (1 - k)W_2) \qquad (4.2)$$

where again k is an empirical constant and W_i is the weight fraction of
component i. The Wood equation is essentially identical to the Kelley-
Bueche relation. A rearrangement of Eqn. (4.2) with $k = Tg_1/Tg_2$ pro-
duces an empirical form first set forth by Fox.[7]

$$1/Tg = W_1/Tg_1 + W_2/Tg_2 . \qquad (4.3)$$

Each of the above equations is based on empirical fits of Tg versus

composition for mixed polymer systems, either copolymers, diluents or blends.

Recently, a variety of relations has been derived to predict the Tg of compatible polymer blends from the Tg's of the pure components. Pochan, Beatty and Hinman[8] derived an empirical relationship of the form

$$\ln Tg = W_1 \ln Tg_1 + W_2 \ln Tg_2 . \tag{4.4}$$

Gordon et al.[9] approached the problem from the configurational entropy theory of Tg first set forth by Gibbs and DiMarzio.[10,11] The difficulty in this approach is the need to fit Cp data with third-order polynomials as a function of temperature and a knowledge of the fusion entropy. A more useful approach has been that of Couchman.[12-14] The Couchman relations are based on the continuity, at the glass transition temperature, of the extensive thermodynamic variables such as entropy. The glass transition is treated as an Ehrenfest second-order transition. The relations derived provide a prediction for compatible blend Tg's solely in terms of pure component glass transition properties. Figure 4.1 is a summary of the Couchman relations.[15] The degree of approximation increases from top to bottom.

The general equation derived by Couchman

$$\ln Tg = \frac{\sum_i W_i \Delta Cp_i \ln Tg_i}{\sum_i W_i \Delta Cp_i} \tag{4.5}$$

can be reduced by a series of approximations to the empirical relations given earlier. For example, Eqn. (4.9) is derived from Eqn. (4.5)

Figure 4.1. Summary of Couchman Relations.
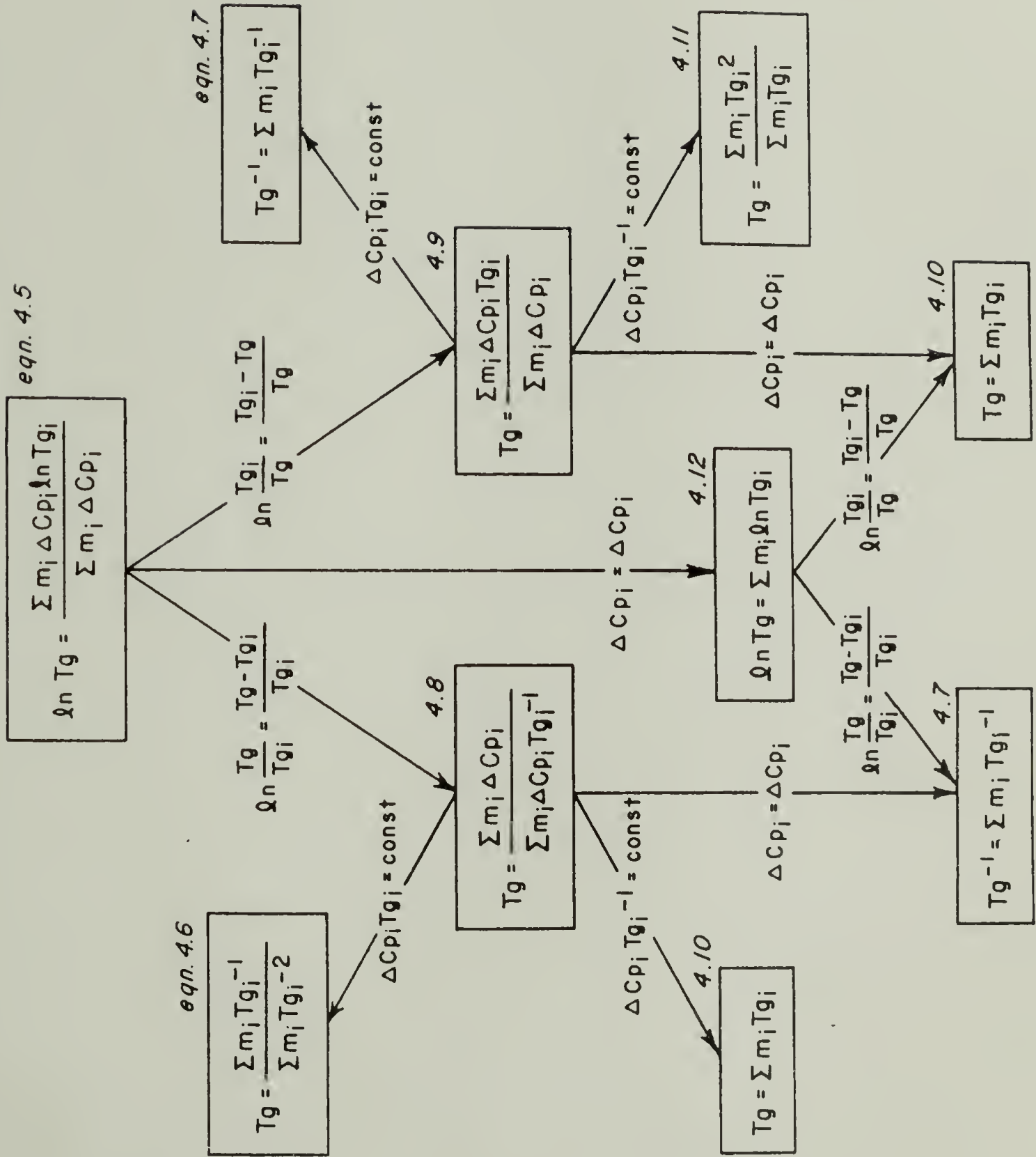
using the logarithmic approximation

$$\ln (Tg/Tg_i) = (Tg - Tg_i)/Tg_i .$$
(4.13)

Eqn. (4.9) is identical in form to the empirical equation derived by Wood,[16] but does not contain any adjustable parameters. The above approximation coupled with an equality of ΔCp_i's yields the Fox equation. The Pochan, Beatty, Hinman relationship (Eqn. (4.4)) is obtained from Eqn. (4.5) with the approximation of the equality of ΔCp's. Thus, the beauty of the Couchman relations is that from one basic expression, several simplifying approximations can be used to produce the empirical relations derived by others.

Tables 4.1 through 4.5 list the predicted values for the blend Tg's for the systems listed in each table. Figures 4.2 through 4.5 are plots of Tg versus weight percent polymer for the blends listed. The solid lines are the Tg's calculated from Eqn. (4.5). For PS/PPO blends, the fit of Eqn. (4.5) with the experimental data was quite good, which was shown by Couchman.[13] Figures 4.3 and 4.4 also show the remarkable agreement between theory and experiment. The difference in molecular weight of the polystyrene had little effect on the predictive power of Eqn. (4.5) although ΔCp was taken to be the same in both cases.

It appeared that one case in which the predictions of the Couchman relations broke down was when ΔCp was smaller for the pure component with the lowest Tg. This is illustrated in Figure 4.5 for blends of p(4-F1S(.285)-2-F1S) with PPO. The fluorinated copolymers blended with PPO all showed this discrepancy between theory and

Table 4.1. Calculated Tg's for PS/PPO Blends.

m_1	m_2	Eqn. 4.5	Eqn. 4.8	Eqn. 4.6	Eqn. 4.10	Eqn. 4.7	Eqn. 4.9	Eqn. 4.11	Eqn. 4.12
.10	.90	384.30	383.42	383.47	387.80	385.40	385.33	390.76	386.51
.20	.80	392.67	390.96	391.06	399.10	394.72	394.60	404.22	396.79
.30	.70	401.65	399.21	399.36	410.40	404.51	404.34	416.93	407.34
.40	.60	411.33	408.27	408.46	421.70	414.80	414.60	428.97	418.18
.50	.50	421.79	418.29	418.50	433.00	425.63	425.40	440.37	429.30
.60	.40	433.11	429.40	429.63	444.30	437.03	436.80	451.20	440.71
.70	.30	445.40	441.80	442.03	455.60	449.07	448.85	461.49	452.44
.80	.20	458.79	455.74	455.93	466.90	461.78	461.61	471.28	464.47
.90	.10	473.44	471.51	471.63	478.20	475.24	475.13	480.60	476.82

$\Delta Cp(PPO) = .222$ J/$^\circ$-gm $\Delta Cp(PS) = .291$ J/$^\circ$-gm

Tg(PPO) = 489.5°K   Tg(PS) = 376.5°K

Table 4.2. Calculated Tg's for PS(50)/p(2-ClS) Blends.

m_1	m_2	Eqn. 4.5	Eqn. 4.8	Eqn. 4.6	Eqn. 4.10	Eqn. 4.7	Eqn. 4.9	Eqn. 4.11	Eqn. 4.12
.10	.90	402.36	402.24	402.69	403.10	402.90	402.47	403.29	403.00
.20	.80	398.91	398.71	399.48	400.20	399.85	399.11	400.54	400.03
.30	.70	395.66	395.41	396.37	397.30	396.84	395.90	397.74	397.07
.40	.60	392.57	392.30	393.35	394.40	393.88	392.84	394.91	394.14
.50	.50	389.64	389.38	390.43	391.50	390.96	389.91	392.04	391.23
.60	.40	386.86	386.62	387.59	388.60	388.09	387.11	389.12	388.34
.70	.30	384.22	384.02	384.82	385.70	385.26	384.42	386.16	385.48
.80	.20	381.70	381.55	382.14	382.80	382.46	381.84	383.15	382.63
.90	.10	379.29	379.22	379.54	379.90	379.71	379.37	380.10	379.80

$\Delta Cp(PS) = .273$ J/°-gm $\Delta Cp(p(2-ClS)) = .219$ J/°-gm

Tg(PS) = 377°K   Tg(p(2-ClS) = 406°K

Table 4.3.   Calculated Tg's for PS(32)/p(2-ClS) Blends.

m_1	m_2	Eqn. 4.5	Eqn. 4.8	Eqn. 4.6	Eqn. 4.10	Eqn. 4.7	Eqn. 4.9	Eqn. 4.11	Eqn. 4.12
.10	.90	401.77	401.61	402.09	402.65	402.38	401.92	402.90	402.52
.20	.80	397.78	397.51	398.33	399.30	398.83	398.04	399.75	399.07
.30	.70	394.01	393.67	394.70	395.95	395.33	394.33	396.55	395.65
.40	.60	390.44	390.08	391.19	392.60	391.90	390.80	393.29	392.25
.50	.50	387.06	386.70	387.81	389.25	388.53	387.41	389.97	388.89
.60	.40	383.85	383.53	384.54	385.90	385.21	384.17	386.60	385.55
.70	.30	380.80	380.53	381.38	382.55	381.95	381.07	383.17	382.25
.80	.20	377.90	377.71	378.32	379.20	378.75	378.10	379.67	378.97
.90	.10	375.13	375.03	375.37	375.85	375.60	375.24	376.12	375.72

$\Delta Cp(PS) = .273$ J/°-gm $\Delta Cp(p(2-ClS)) = .217$ J/°-gm

$Tg(PS) = 372.5°K$ $Tg(p(2-ClS)) = 406°K$

78

Table 4.4. Calculated Tg's for PS(17.5)/p(2-ClS) Blends.

m_1	m_2	Eqn. 4.5	Eqn. 4.8	Eqn. 4.6	Eqn. 4.10	Eqn. 4.7	Eqn. 4.9	Eqn. 4.11	Eqn. 4.12
.10	.90	401.51	401.32	401.82	402.45	402.15	401.68	402.73	402.30
.20	.80	397.27	396.96	397.80	398.90	398.37	397.57	399.41	398.64
.30	.70	393.27	392.89	393.94	395.35	394.66	393.64	396.02	395.01
.40	.60	389.48	389.08	390.22	391.80	391.01	389.89	392.57	391.41
.50	.50	385.90	385.50	386.63	388.25	387.44	386.30	389.06	387.84
.60	.40	382.50	382.14	383.17	384.70	383.93	382.87	385.49	384.31
.70	.30	379.28	378.98	379.84	381.15	380.48	379.58	381.84	380.81
.80	.20	376.21	375.99	376.62	377.60	377.09	376.43	378.13	377.34
.90	.10	373.28	373.17	373.51	374.05	373.77	373.41	374.35	373.91

$\Delta Cp(PS) = .273$ J/°-gm $\Delta Cp(p(2-ClS)) = .219$ J/°-gm

$Tg(PS) = 370.5°K$ $Tg(p(2-ClS)) = 406°K$

Table 4.5.   Calculated Tg's for p(4-FlS(.285)-2-FlS)/PPO Blends.

m_1	m_2	Eqn. 4.5	Eqn. 4.8	Eqn. 4.6	Eqn. 4.10	Eqn. 4.7	Eqn. 4.9	Eqn. 4.11	Eqn. 4.12
.10	.90	476.40	474.86	469.66	476.63	473.49	477.74	479.16	475.17
.20	.80	464.65	461.97	453.44	465.06	459.65	467.05	469.67	462.49
.30	.70	452.94	449.50	439.14	453.49	446.59	456.13	459.69	450.15
.40	.60	441.27	437.44	426.44	441.92	434.25	444.97	449.19	438.14
.50	.50	429.66	425.75	415.07	430.35	422.57	433.56	438.13	426.44
.60	.40	418.10	414.44	404.85	418.78	411.51	421.90	426.45	415.06
.70	.30	406.60	403.47	395.60	407.21	401.01	409.97	414.11	403.99
.80	.20	395.17	392.83	387.20	395.64	391.03	397.77	401.05	393.21
.90	.10	383.80	382.51	379.53	384.07	381.54	385.28	387.21	382.71

$\Delta Cp(copolymer) = .204$ J/°-gm $\Delta Cp(PPO) = .228$ J/°-gm

Tg(copolymer) = 372.5°K   Tg(PPO) = 488.2°K
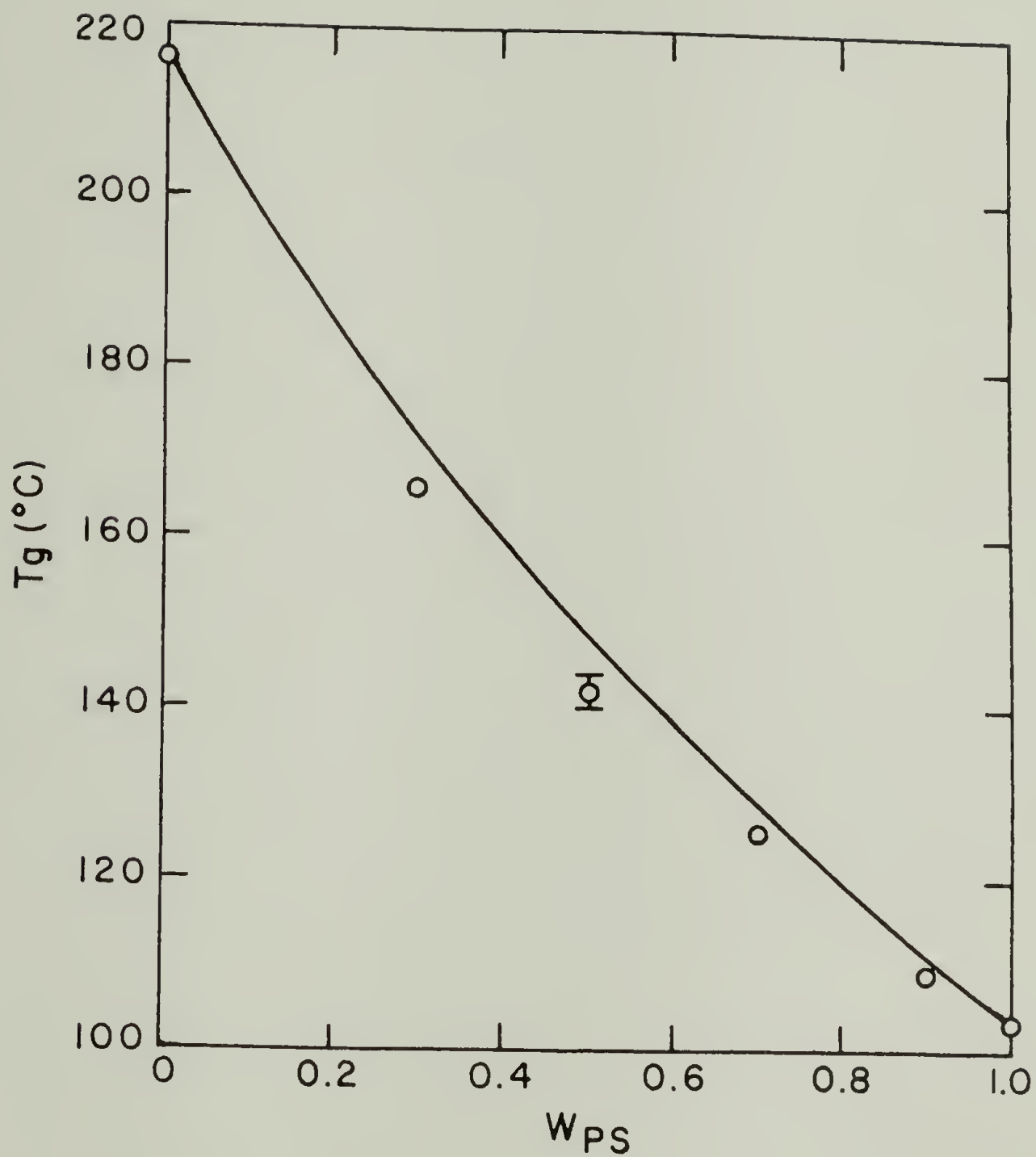
Figure 4.2. Tg vs. W_{PS} for PS/PPO blends [solid line from Eqn. (4.5)].
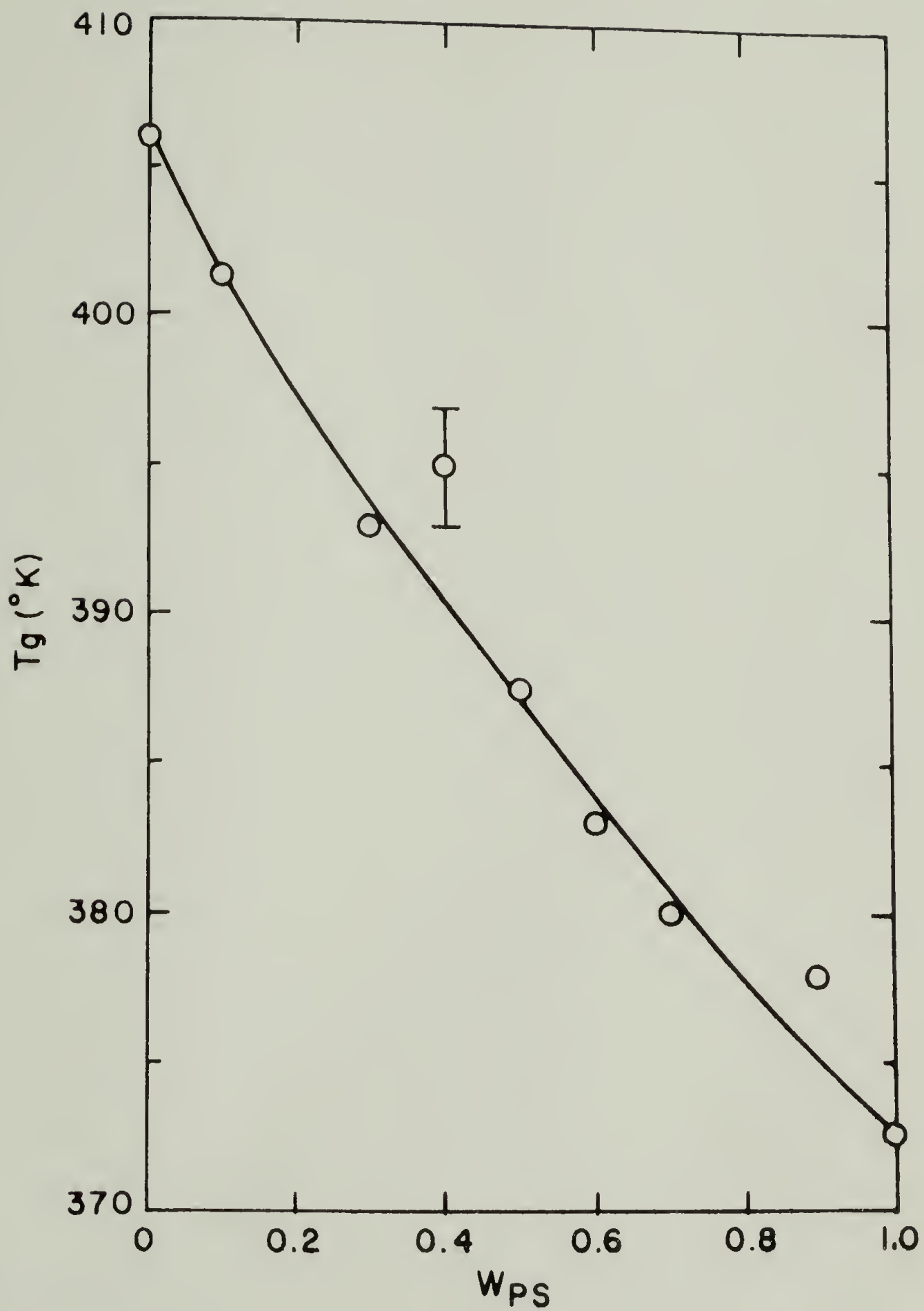
Figure 4.3. Tg vs. W_{PS} for PS(32)/p(2-ClS) blends.
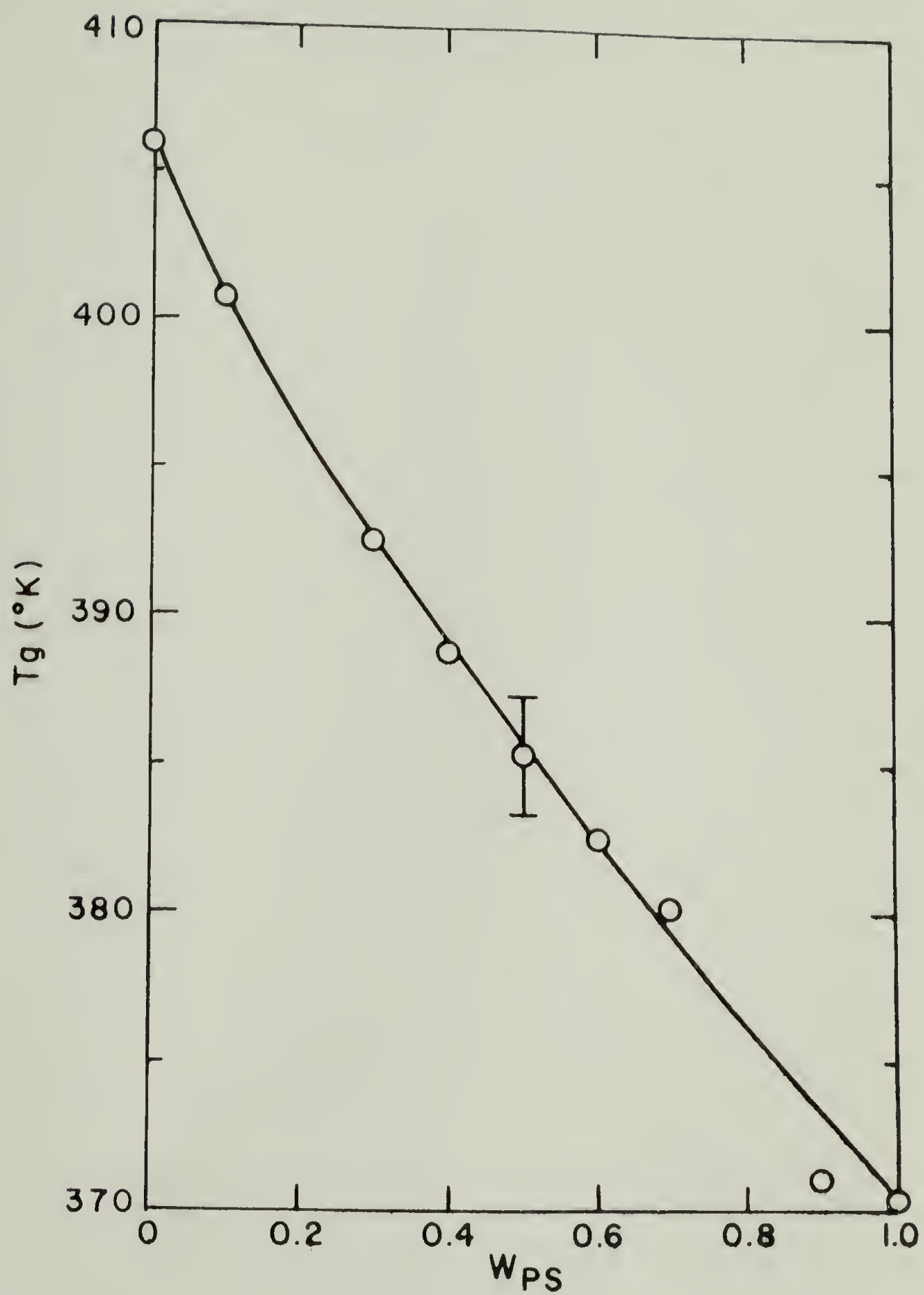
Figure 4.4.   Tg vs. W_{PS} for PS(17.5)/p(2-ClS) blends.
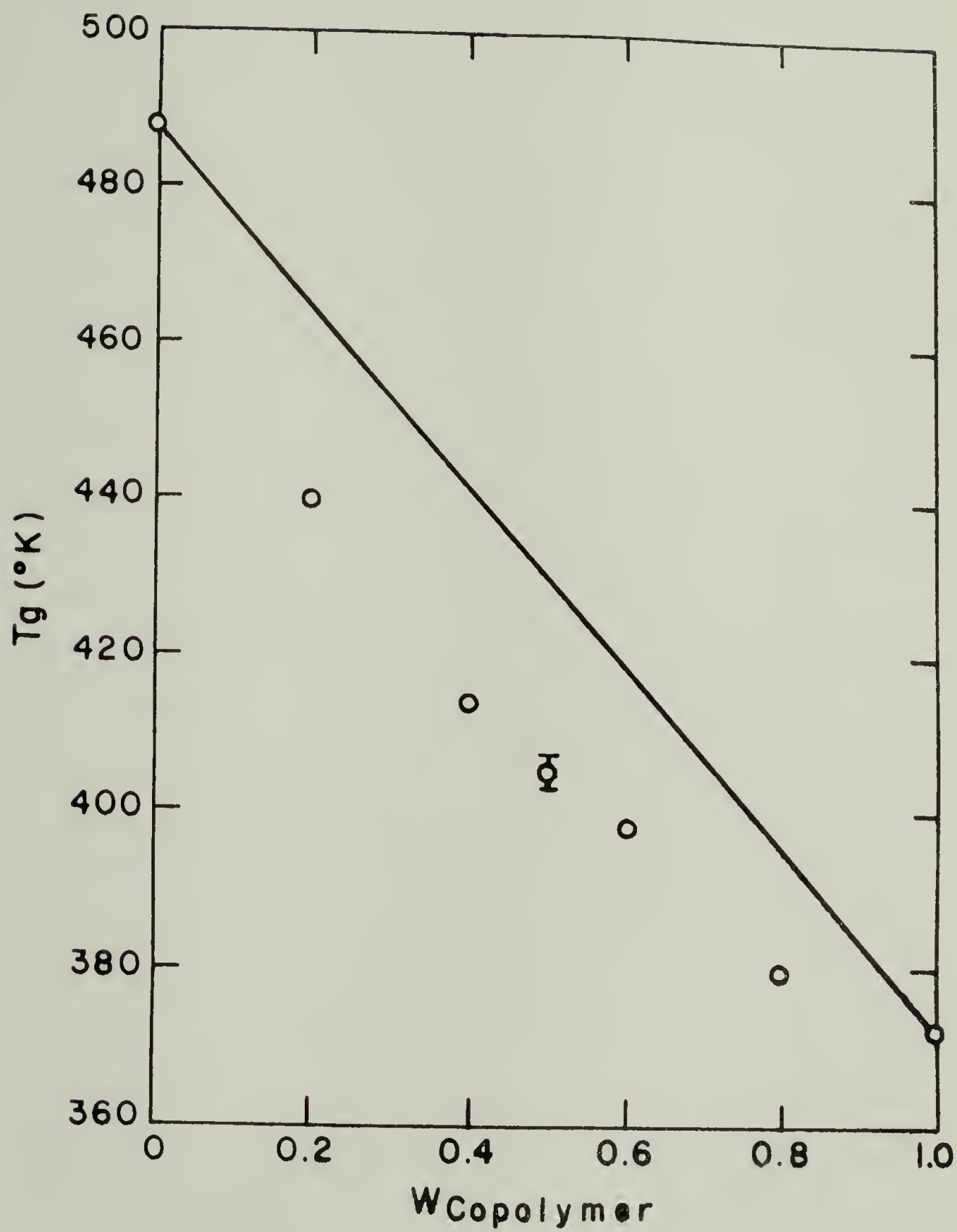
Figure 4.5. Tg vs. $W_{copolymer}$ for p(4-F1S(.285)-2-F1S)/PPO blends.

experiment. However, for the case where $\Delta Cp_1 > \Delta Cp_2$ and $Tg_1 < Tg_2$, the Couchman relations are a powerful tool for predicting blend Tg.

The variation of polymer glass transition temperatures with molecular weight has also been the subject of many empirical theories. Fox and Flory[17,18] concluded that the variation of Tg with molecular weight was

$$Tg = Tg^0 - K/M \tag{4.14}$$

where Tg^0 is the Tg of infinite molecular weight polymer and K is a constant. However, it had been shown that K was only constant for higher molecular weights and higher Tg's.[19-22] Boyer[23] established a totally empirical relation between Tg^0 and K which permitted curve fitting of Eqn. (4.14).

Recently, Couchman[24] has derived a relation between Tg and molecular weight based on the thermodynamic theory of the compositional variation of Tg discussed earlier. Couchman treated the polymer as a mixture of chain ends with middles. The chain middles have properties indicative of infinite molecular weight polymers, whereas the chain ends have quite different properties. Therefore, the polymer can be thought of as a compatible blend of polymer ends with middles. Using this approach, the following relationship was derived,

$$\ln Tg = \frac{(n-m)\Delta Cp^0 \ln Tg^0 + m\Delta Cp^m \ln Tg^m}{(n-m)\Delta Cp^0 + m\Delta Cp^m} \tag{4.15}$$

where ΔCp^0, Tg^0 are for infinite molecular weight; ΔCp^m, Tg^m are for the m-mer; n = degree of polymerization of the polymer; and m = degree

of polymerization of the m-mer. Again, a series of approximations was made to reduce Eqn. (4.15) to the empirical relations of Fox and Flory and others.

For polystyrene, the smallest m-mer studied has been a hexamer (m=6), with Tg = 243°K. Couchman used the ratio of $\Delta Cp^6/\Delta Cp^0$ = 1.35. Figure 4.6 shows the agreement between the Couchman equation and experimental values for polystyrene Tg as a function of molecular weight as found in this work. The variables in Eqn. (4.15) were set as

$$\Delta Cp^6 = 0.375 \text{ J/°K-gm}$$

$$Tg^6 = 243°K$$

$$\Delta Cp^0 = 0.273 \text{ J/°K-gm}$$

$$Tg^0 = 376.5°K .$$

The use of the absolute prediction of Tg from the above treatment was superior to the empirical theories developed previously.

A parameter vital to this thesis work was the change in heat capacity, ΔCp, at Tg. Values for ΔCp were determined by DSC as outlined in Chapter III. The values for ΔCp for the compatible blends could be calculated from the weighted averages of the pure components ΔCp,

$$\Delta Cp_{bl} = W_1 \Delta Cp_1 + W_2 \Delta Cp_2 \tag{4.16}$$

where W_i is weight fraction. Fried[3] found Eqn. (4.16) to be true, within experimental error, for each of the compatible blends he
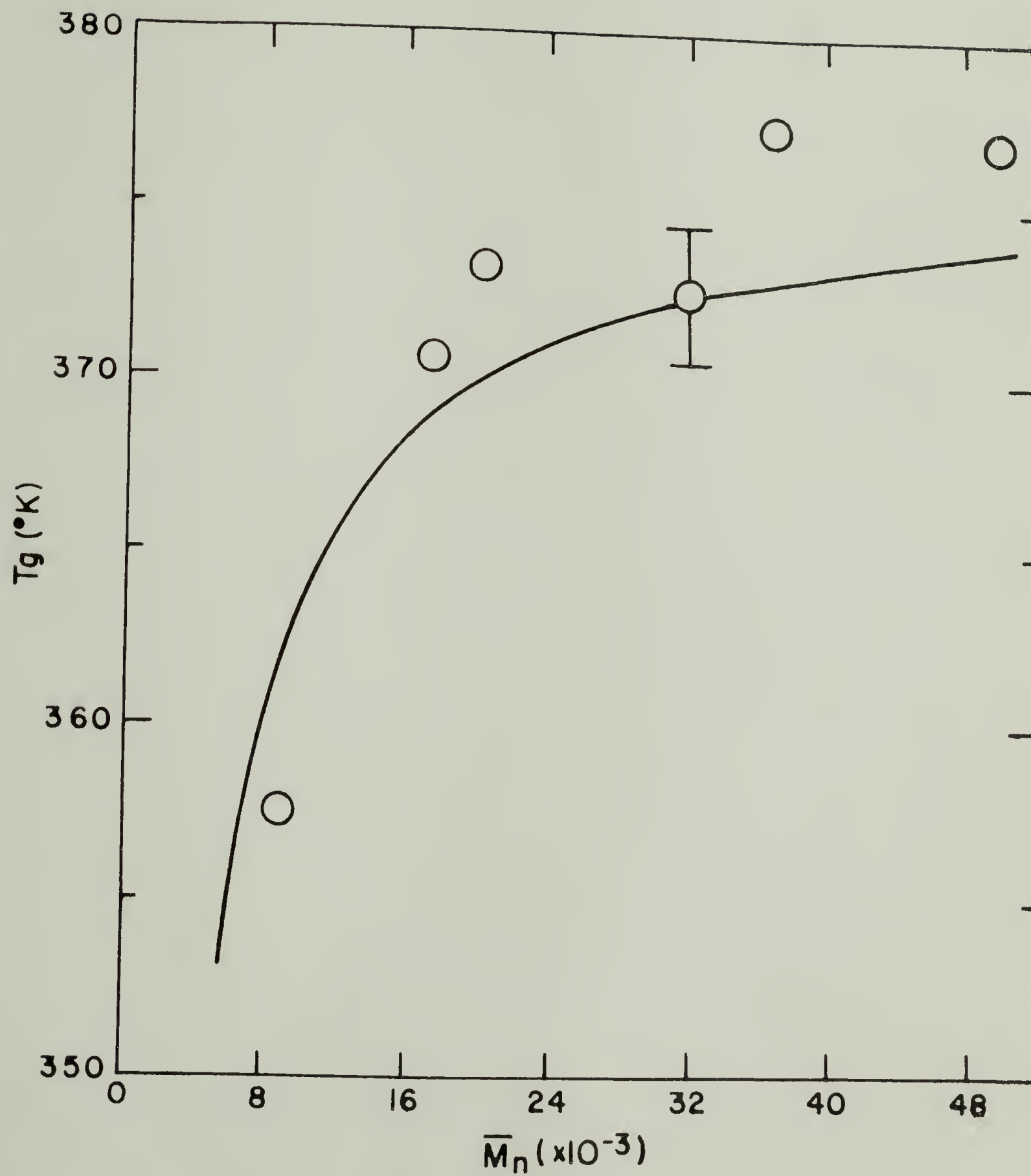
Figure 4.6. Tg vs. MW for polystyrene.

studied. Figure 4.7 shows the effect of composition on the heat
capacities at Tg for blends of PS(MW)/p(2-ClS). Values of ΔCp were
independent of polystyrene molecular weight for the range of weights
studied. The ΔCp for the blends fell on a straight line between pure
components as Eqn. (4.16) suggests. The same relationship was found
true for random copolymers. Figure 4.8 shows the effect of copolymer
composition on ΔCp for copolymers of p(4-FlS-co-2-FlS). Appendix II
is a compendium of all the values for Cp and Tg measured during the
course of this work. Values for Cp were least squares fits of straight
line portions below and above Tg. The data gathered at Bell Labora-
tories appeared to give consistently high Tg's and may be due to in-
correct temperature calibration. The values of Cp determined from the
point-by-point subtraction method were also believed to reflect an
incorrect temperature calibration.

The calibration of the temperature on the DSC for most of these
Cp determinations involved putting indium on the reference side and
lead on the sample side. Melting temperatures were determined for both
without need to change samples. However, it was later determined that
the sample and reference sides were not necessarily at the same tem-
perature. In one extreme case, indium melted at 429.8°K on the sample
side whereas it melted at 423.5°K on the reference side. Therefore,
the variation of Tg per sample might be a reflection of the improper
temperature calibration of the DSC. Proper calibration involves only
melting the standards on the sample side. In one set of experiments,
each of the polymer and blends Tg's was determined to be used in all
subsequent calculations. The final column in Appendix II lists the
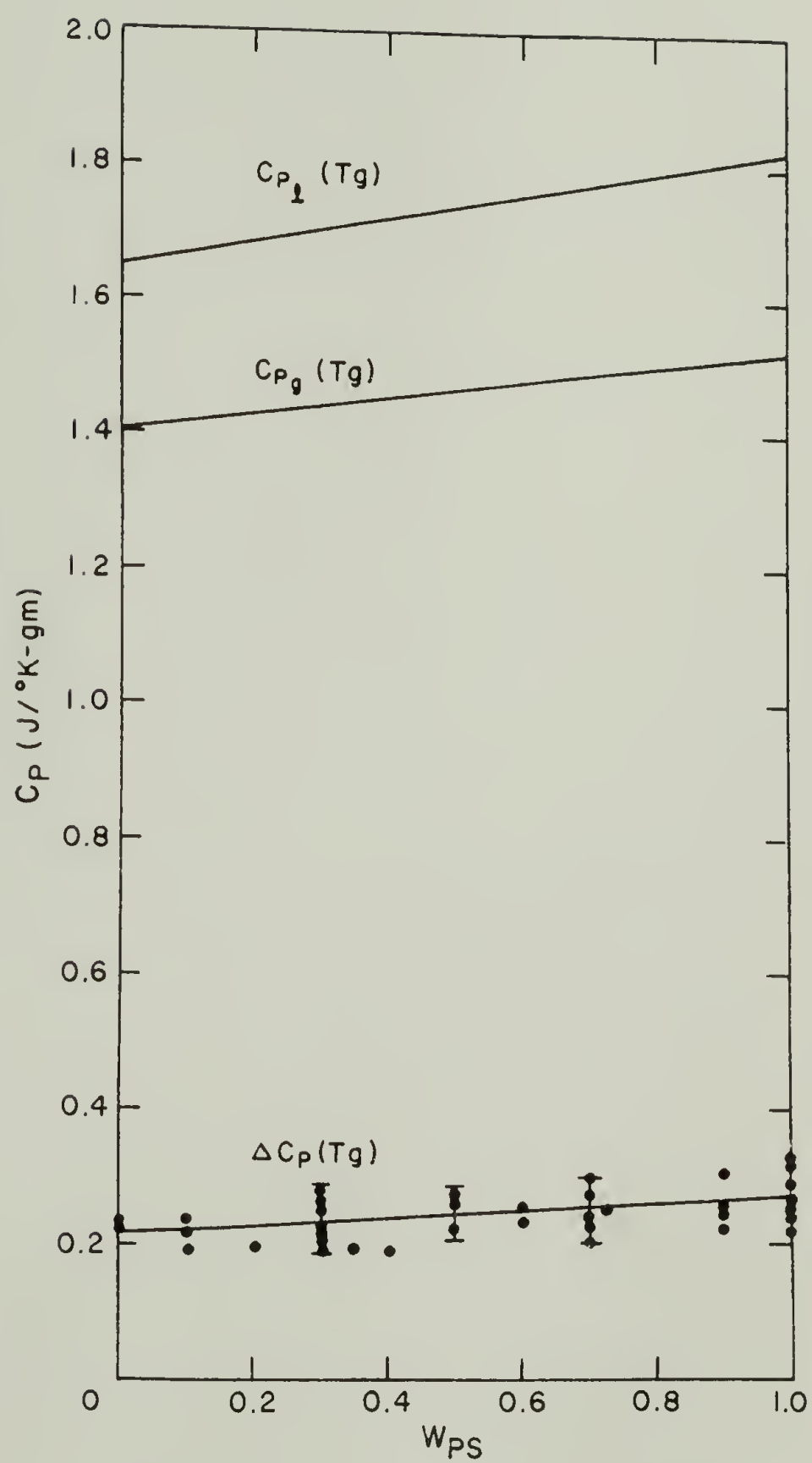
Figure 4.7. ΔCp vs. composition for PS/p(2-ClS) blends.
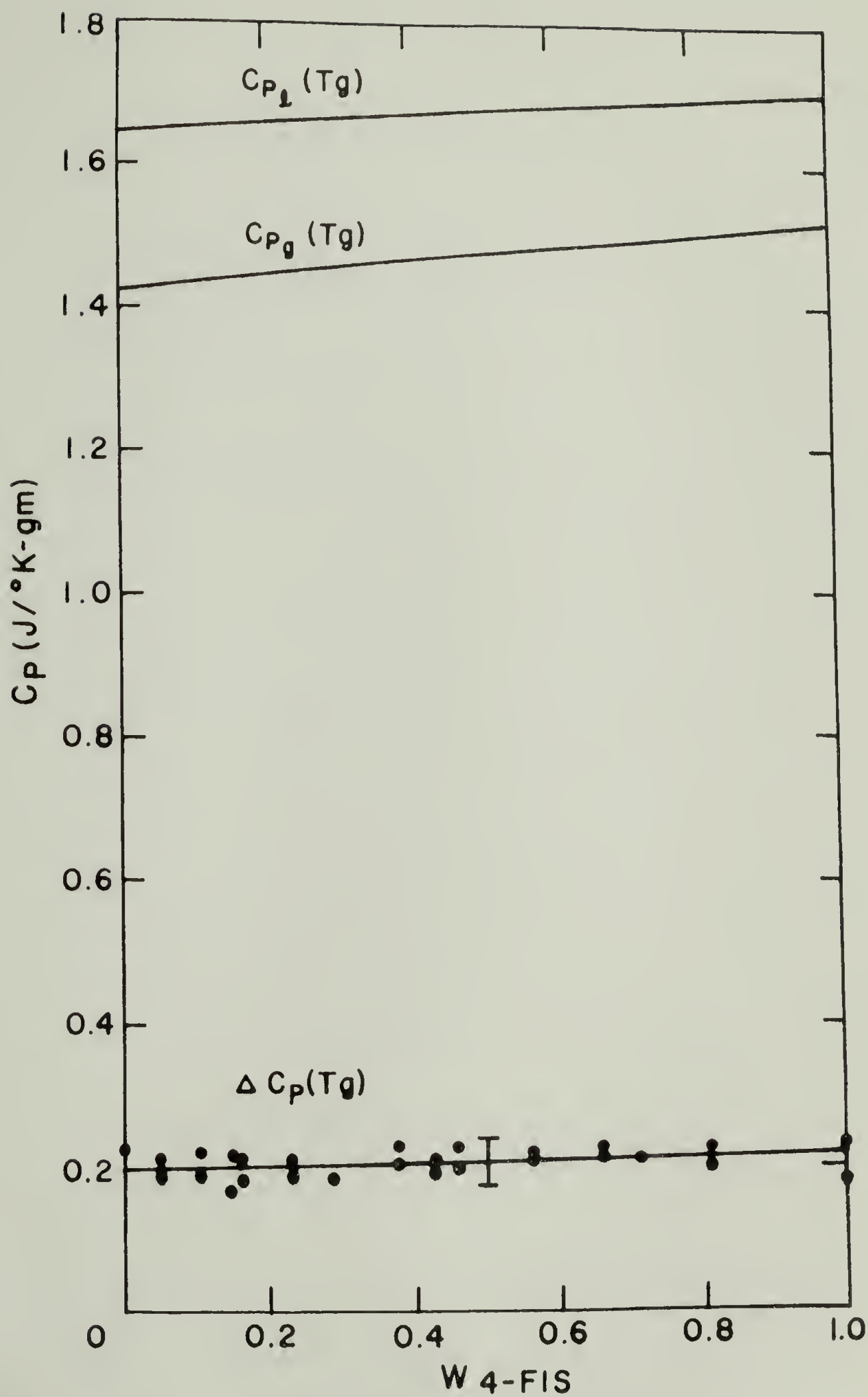
Figure 4.8. ΔCp as function of copolymer composition for p(4-FlS)-co-2-FlS).

values of Tg as determined above.

Experimental values of ΔCp and Tg correlated well with the values determined by Fried.[3] Table 4.6 compares values of ΔCp and Tg for polymers common to both works.

Table 4.6. Comparison of ΔCp, Tg Data with Data from Fried.

System	Tg (°K)		ΔCp (J/°-gm)	
	This Work	Fried	This Work	Fried
PPO	488.2	489.0	.228	.221
PS	378.0	378.0	.273	.280
p(2-ClS)	406.0	408.0	.219	.221
p(4-ClS)	405.0	405.0	.225	.242

REFERENCES

1. M.C. Shen, A. Eisenberg, Progress in Solid State Chem. $\underline{3}$, 407 (1967).

2. W.J. MacKnight, F.E. Karasz, J.R. Fried, "Solid State Transition Behavior of Blends," in Polymer Blends, Vol. I, D.R. Paul, ed., Academic Press, N.Y., 1978.

3. J.R. Fried, Ph.D. Dissertation, University of Massachusetts, 1976.

4. P.S. Alexandrovich, Ph.D. Dissertation, University of Massachusetts, 1978.

5. F.N. Kelley, F. Bueche, J. Polym. Sci. $\underline{50}$, 549 (1961).

6. M. Gordon, J.S. Taylor, J. Appl. Chem. $\underline{2}$, 493 (1952).

7. T.G. Fox, Bull. Amer. Phys. Soc. $\underline{1}$, 123 (1956).

8. J.M. Pochan, C.L. Beatty, D.F. Hinman, submitted to Macromolecules.

9. J.M. Gordon, G.B. Rouse, J.H. Gibbs, W.M. Risen, J. Chem. Phys. $\underline{66}$(11), 4971 (1977).

10. J.H. Gibbs, E.A. DiMarzio, J. Chem. Phys. $\underline{28}$, 373 (1958).

11. E.A. DiMarzio, J.H. Gibbs, J. Chem. Phys. $\underline{28}$, 807 (1958).

12. P.R. Couchman, F.E. Karasz, Macrom. $\underline{11}$(1), 117 (1978).

13. P.R. Couchman, Macrom. $\underline{11}$, 1156 (1978).

14. P.R. Couchman, submitted to Physics Letters.

15. P.R. Couchman, private communication.

16. L.A. Wood, J. Polym. Sci. $\underline{28}$, 319 (1958).

17. T.G. Fox, P.J. Flory, J. Appl. Phys. $\underline{21}$, 581 (1950).

18. T.G. Fox, P.J. Flory, J. Polym. Sci. $\underline{14}$, 315 (1954).

19. R. Ueberreiter, G. Kanig, Z. Naturforsch $\underline{6A}$, 551 (1951).

20. J.M.G. Cowie, P.M. Toporowski, Eur. Polym. J. $\underline{4}$, 621 (1968).

21. G. Pezzin, F. Fillio-Grandi, P. Sanmartin, Eur. Polym. J. $\underline{6}$, 1053 (1970).

22. R.B. Beevers, E.F.T. White, Trans. Farad. Soc. $\underline{56}$, 744 (1960).

23. R.F. Boyer, Macrom. $\underline{7}$(1), 142 (1974).

24. P.R. Couchman, to be published.

C H A P T E R   V

CALORIMETRIC STUDIES OF POLYMER SYSTEMS:
RESULTS AND DISCUSSION

The purpose of this chapter is to present the results obtained throughout the course of this work. The presentation is roughly in chronological order and degree of complexity. Included is a study of the enthalpy relaxation of polystyrene, DSC determination of polymer compatibility and measurements of the heats of mixing of several polymer systems as a function of both copolymer and blend composition. The polymers involved were halogenated polystyrene homopolymers and copolymers blended with PPO and with polystyrene. Each of these systems was studied in an attempt to correlate substituent effect on polymer compatibility. All data for ΔCp, Tg and ΔH_s is contained in Appendix II.

A. Enthalpy Relaxation of Polystyrene

The effect of thermal history on the heat of solution of atactic polystyrene was explored in this study. Samples of PS(HH101) were held at various temperatures, both above and below Tg, for different time periods. All polystyrene films were held at 113°C in a fluidized sand bath for ten minutes whereupon they were quenched in ice water. Following this initial heat treatment, the films were then annealed in the fluidized bath for from 0-512 hours and four separate

93

temperatures below Tg. Tables 5.1-5.5 list the values for the heats of solution for each annealing temperature. Figure 5.1 shows the effect of annealing temperature above Tg on the heat of solution. The effect is so slight as to be insubstantial.

The effect of annealing time at temperatures below Tg is illustrated in Figure 5.2. Several workers have measured the enthalpy relaxation of amorphous polymers below the Tg.[1-5] Differential scanning calorimetry was used in all cases. If the polymer was heated through Tg faster than it was quenched, a peak was superimposed upon the step change in specific heat at Tg. The peak area had been frequently used as a measure of enthalpy relaxation.[1-5] However, Richardson and Savill[6] pointed out that the peak area actually was unrelated to the enthalpy relaxation. Since the glass was in a non-equilibrium state, Tg was sensitive to rate effects. DSC is a dynamic technique, therefore Tg as derived from DSC was very much a function of experimental conditions. Although the peak area parallels the degree of enthalpy relaxation, it was not a quantitative measure.

Figure 5.3 illustrates the DSC traces for polystyrene annealed at 94.8°C for the times indicated. The so-called enthalpy relaxation peak increased markedly with time followed with an increase in the apparent glass transition temperature. Richardson and Savill[6,7] claimed that the Tg of polymers could not be obtained directly from DSC curves because of kinetic effects. This was especially true for samples showing large enthalpy relaxation peaks. They maintained that the correct way to calculate Tg from DSC measurements involved derivation of the enthalpy lines for the glassy and liquid states. The Tg would then

Table 5.1. ΔH_S as a Function of Annealing Temperature above Tg.

T_{anneal}	$-\Delta H_S$ (J/gram)
113.0°C	29.10
117.6	29.15
138.0	29.53
144.8	29.70

Table 5.2. Enthalpy Relaxation of Polystyrene, T_{anneal} = 92°C.

Time Annealed (hrs)	$-\Delta H_S$ (J/gram)	$\Delta(\Delta H_S)$ (J/gram)
0	27.09	0
.5	26.36	.73
1	26.06	1.03
2	25.74	1.35
4	25.53	1.56
10	25.12	1.97
24	25.90	1.19
72	25.26	1.83

Table 5.3. Enthalpy Relaxation of Polystyrene, T_{anneal} = 96°C.

Time Annealed (hrs)	$-\Delta H_s$ (J/gram)	$\Delta(\Delta H_s)$ (J/gram)
0	29.12	0
.5	28.07	1.05
1	27.82	1.30
2	27.36	1.76
4	27.32	1.80
26	26.94	2.18
512	27.74	1.38

Table 5.4. Enthalpy Relaxation of Polystyrene, T_{anneal} = 94.8°C.

Time Annealed (hrs)	$-\Delta H_s$ (J/gram)	$\Delta(\Delta H_s)$ (J/gram)
0	29.12	0
.5	27.65	1.47
1	28.26	.86
2	27.55	1.57
4	27.22	1.90
26	28.12	1.00
458	27.27	1.85

Table 5.5. Enthalpy Relaxation of Polystyrene, T_{anneal} = 81.3°C.

Time Annealed (hrs)	$-\Delta H_s$ (J/gram)	$\Delta(\Delta H_s)$ (J/gram)
0	29.12	0
.5	27.84	1.28
1	28.13	.99
2	28.13	.99
4	27.88	1.24
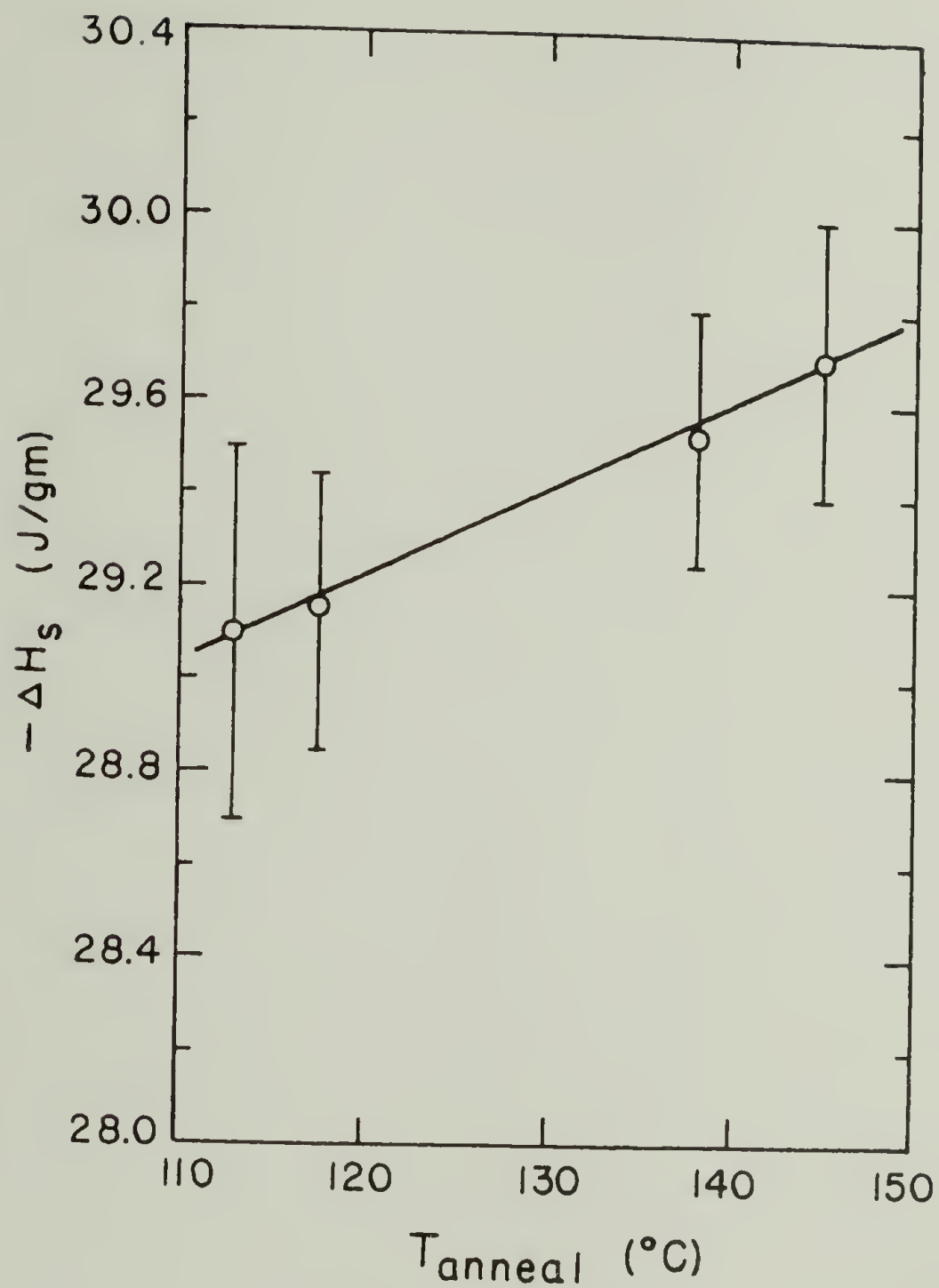
Figure 5.1. Heat of solution for PS(HH101) as a function of annealing temperature above Tg.
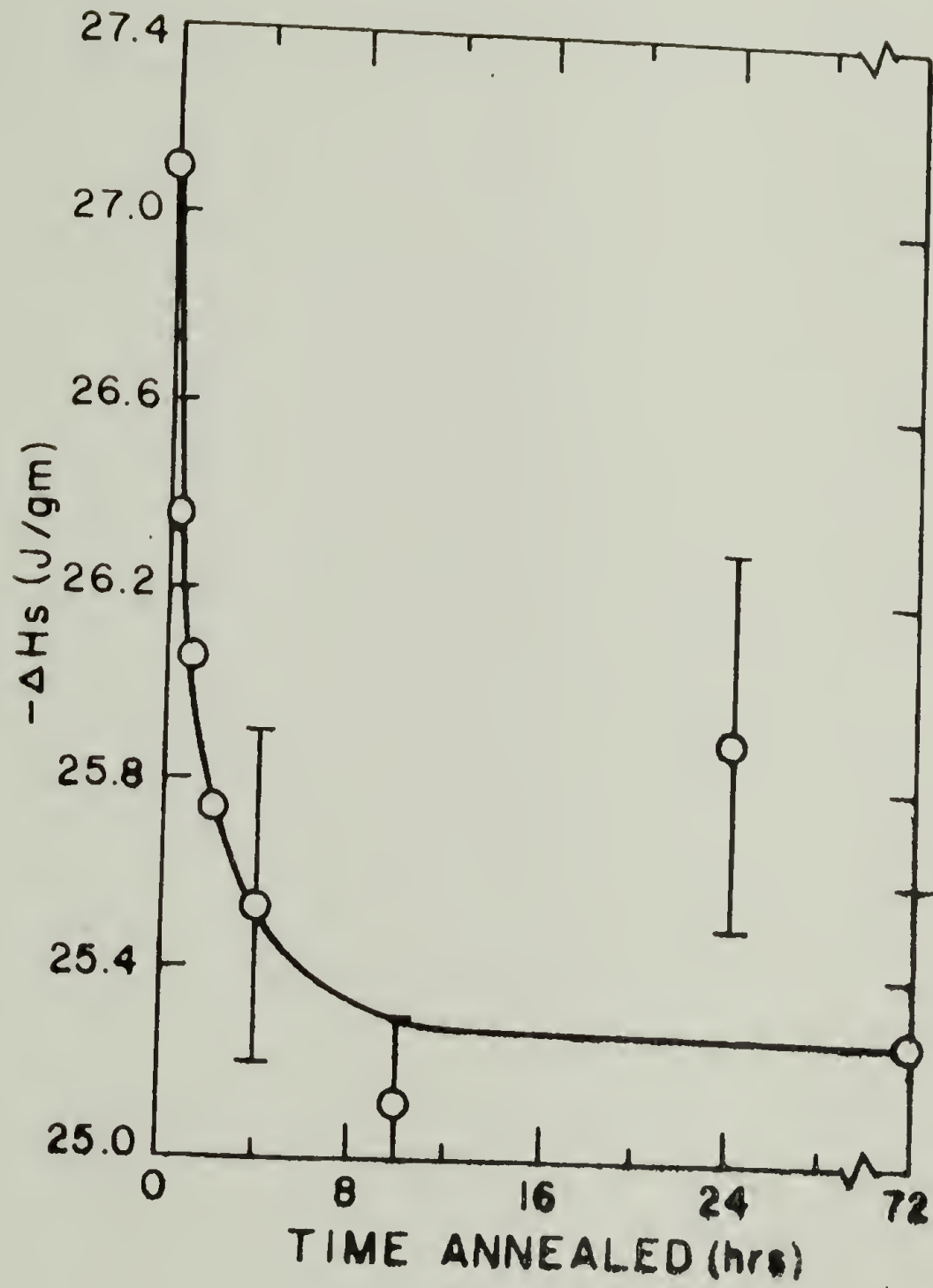
Figure 5.2. ΔH_s for PS(HH101) as a function of annealing temperature below Tg.
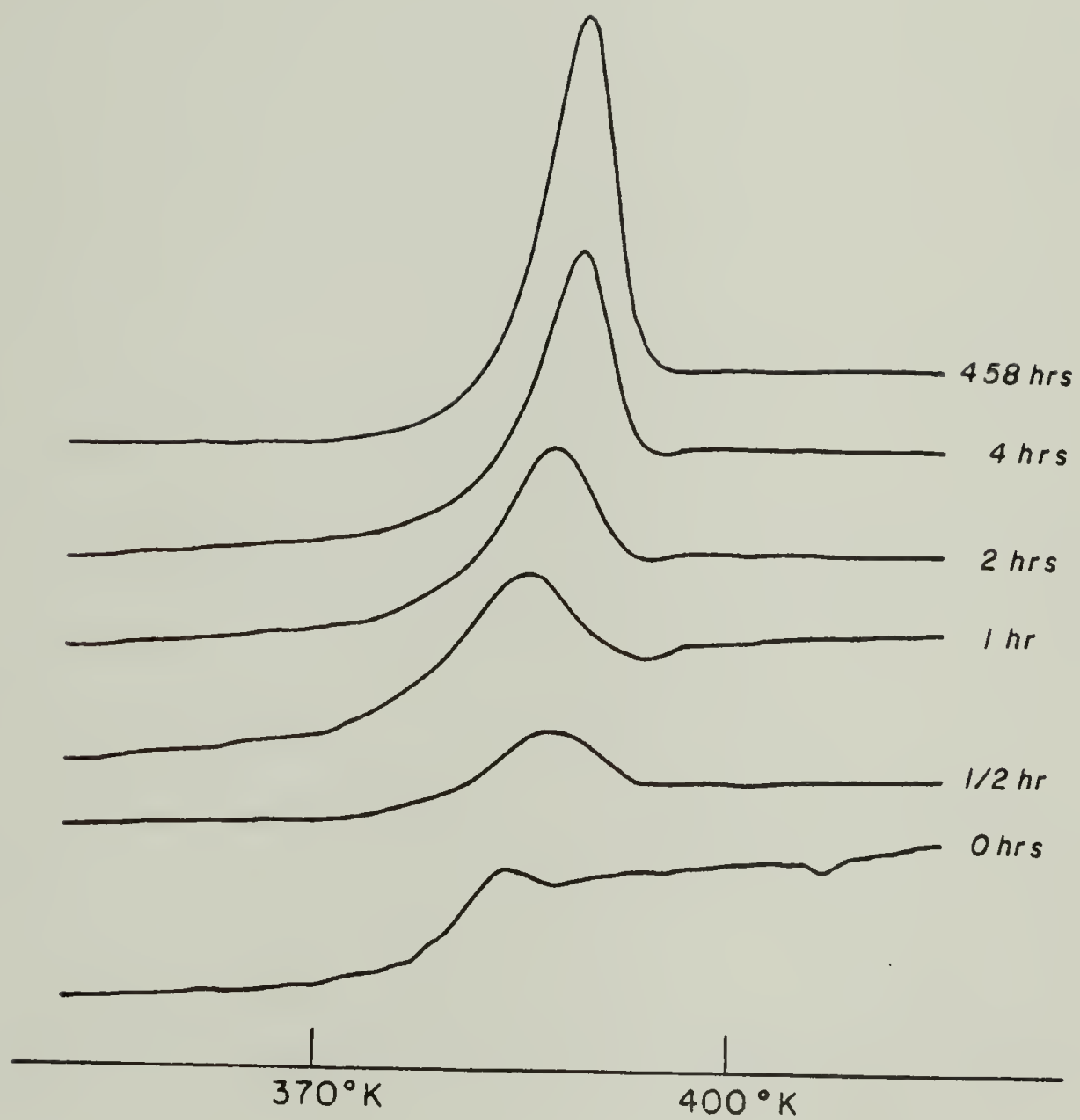
Figure 5.3. DSC thermograms for PS annealed at 94.8°C for indicated times.

be defined as the point of intersection of the enthalpy curves. Using this method, Tg typically laid below the step change in specific heat associated with the glass-liquid transition. However, this experimental determination of Tg was quite tedious and relied on accurate calibration of the enthalpy.

Table 5.6 gives the values for Tg measured as a function of annealing time at 94.8°C. The increase of Tg with annealing time was also found by Petrie for polystyrene.[1] However, a decrease in enthalpy of the glassy state should have been followed by a decrease in Tg. This conclusion could be reached by following the enthalpy-temperature curve of Figure 2.2 and the definition of Tg as being the intersection of the enthalpy lines of the glassy and liquidus states. Therefore, a correlation could not be made between the enthalpy relaxation as determined by heats of solution measurements and those said to be determined by DSC.

Figure 5.4 shows the values for the enthalpy relaxation of polystyrene as a function of annealing time and temperature. The enthalpy relaxation is denoted as $\Delta(\Delta H_s)$ and was the difference in ΔH_s for the annealed sample as opposed to the quenched sample. Values of $\Delta(\Delta H_s)$ are given in the last column of Tables 5.2-5.5.

From these studies, it could be shown that the value of ΔH_s varied greatly with annealing temperatures below Tg but did not change significantly for annealing temperatures above Tg. Moreover, since different polymers probably have varying rates and degrees of enthalpy relaxation, it was concluded that the most reproducible method for heat treatment was to quench from temperatures above Tg. Therefore,

Table 5.6. Tg as a Function of Annealing Time at 94.8°C.

Time Annealed (hrs)	Tg (°K)	Tg (°C)
0	373.6	100.4
.5	373.8	100.6
1	373.0	99.8
2	374.0	100.8
4	375.3	102.1
26	374.5	101.3
458	377.2	104.0
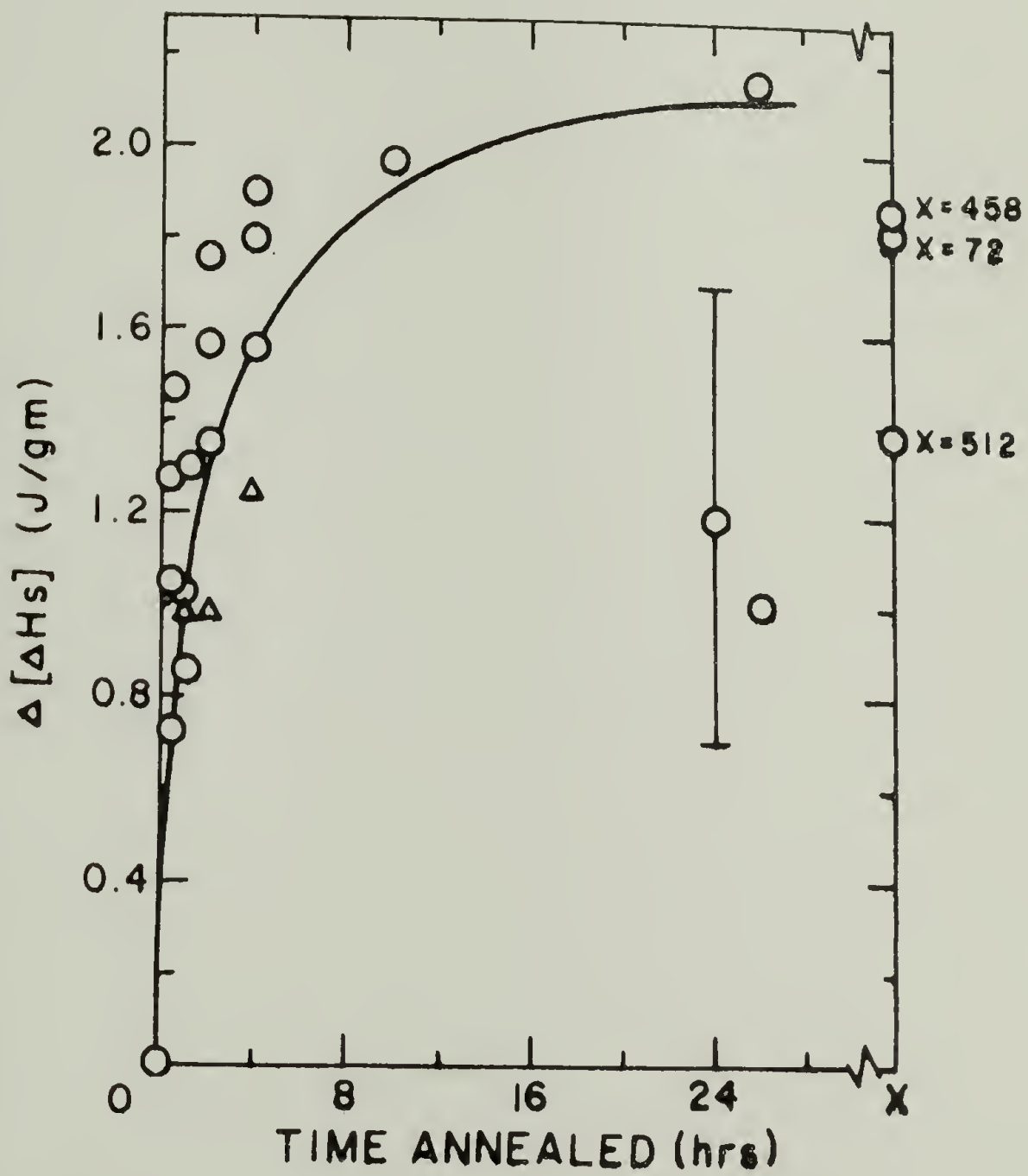
Figure 5.4.   Enthalpy relaxation of polystyrene.

unless otherwise indicated, the thermal history for all polymers and blends studied involved quenching from above Tg.

B. Polystyrene-poly(2,6-dimethyl-1,4-phenylene oxide) Blends

All blend systems in this work were based on the model system polystyrene-poly(2,6-dimethyl-1,4-phenylene oxide) PS/PPO. Previous work on this project was performed in this laboratory by Weeks.[8] Their work was repeated in order to corroborate and improve upon the work of Weeks by utilizing a slightly different approach. The data of Weeks was given in Chapter II.

Figure 5.5 shows the magnitude of the heats evolved for the determination of the heat of mixing via Hess's law. The heats of solution, ΔH_s, were determined using Tian-Calvet microcalorimetry. As derived in Chapter II, $\Delta Cp\Delta T$ was the approximation to the excess glass enthalpy due to the "melting" of the glassy state. Hess's law could then be applied to the extrapolated "liquid" heat of solution, $\Delta H_s - \Delta Cp\Delta T$, to determine the heat of mixing at the experimental temperature. Notice that all heats evolved were exothermic, including ΔH_m. Figure 5.6 is a plot of ΔH_m as a function of composition where the heat is given in units of joules per gram. The function is smoothly negative over the entire composition range with the second derivative of the free energy being positive, indicative of polymer thermodynamic stability.

The system, PS/PPO, was known to be a stable polymer blend over the entire composition range as well as stable to temperatures up
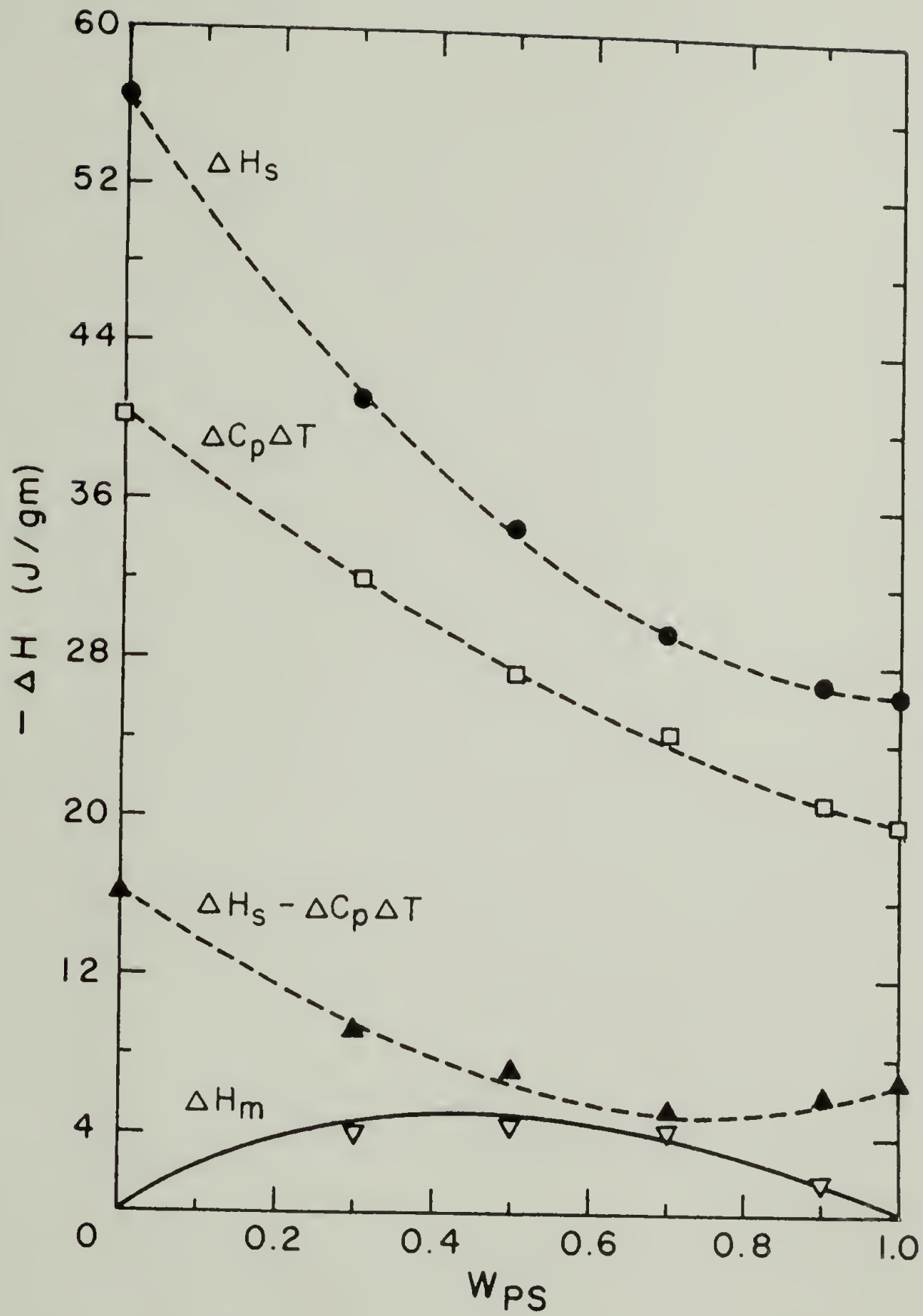
Figure 5.5. Measured and calculated heats involved in the calculation of ΔH_m for PS(HH101)/PPO blends.
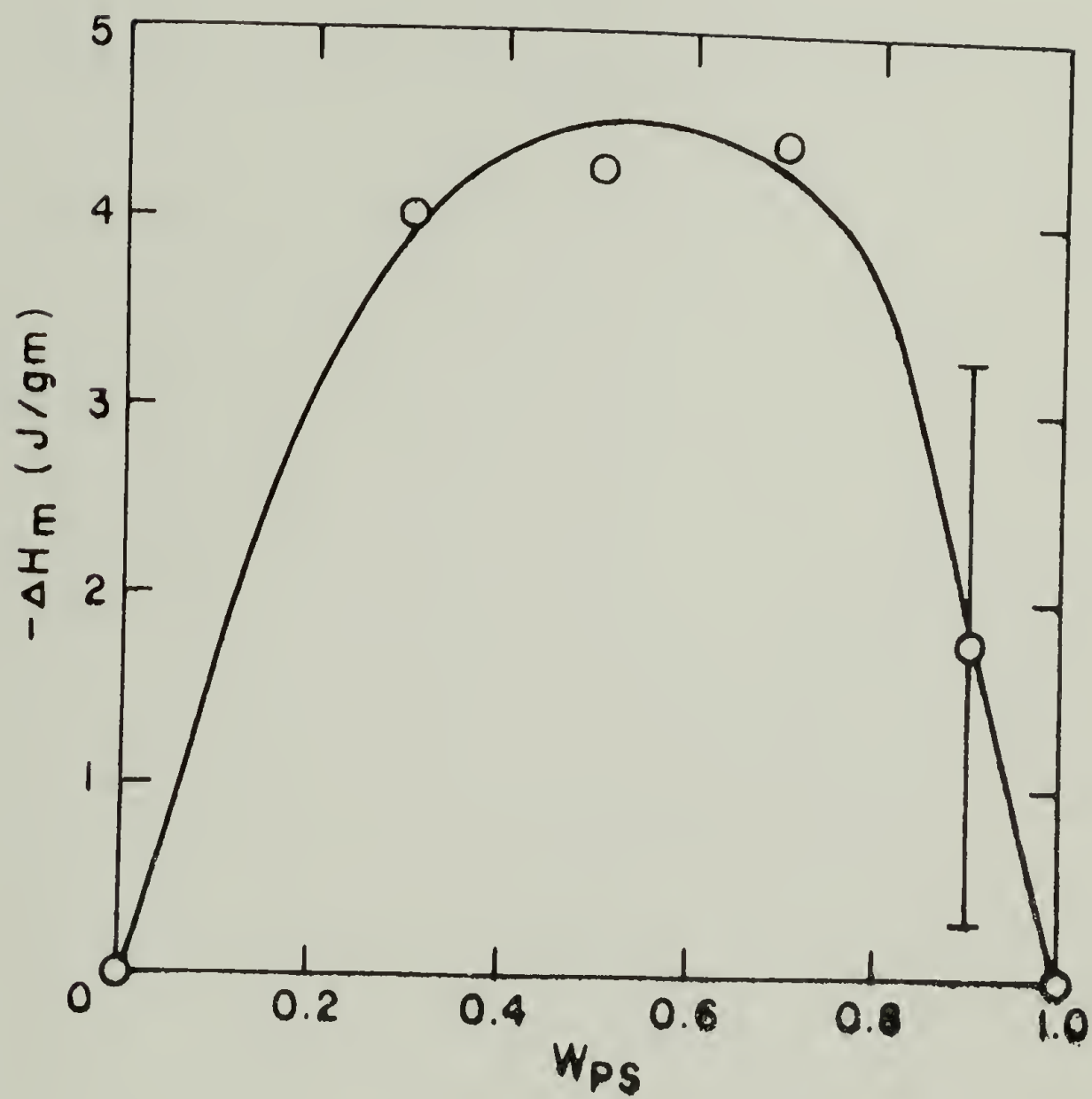
Figure 5.6. ΔH_m vs. composition for PS/PPO blends.

until degradation. Films of the blends were optically clear and displayed one Tg intermediate the pure component Tg (see Figure 4.2). Dynamic mechanical measurements of the PS/PPO blend had also established compatibility.[9] The determination of a favorable, negative heat of mixing over the entire composition range was consistent with the established compatibility of PS with PPO.

Since PS and PPO had both been thoroughly studied, it was a good system in which to determine the severity of the approximation that the excess glassy enthalpy be given as $\Delta Cp\Delta T$. Karasz, Bair and O'Reilly[10,11] determined Cp as a function of temperature for PS and PPO using adiabatic calorimetry. As pointed out in Chapter II, the excess glass enthalpy could be calculated as

$$\Delta H_{xs} = \int_{T}^{Tg} Cp_1 dT - \int_{T}^{Tg} Cp_g dT . \qquad (5.1)$$

Least squares lines were fitted to the data of Karasz for Cp above and below Tg and ΔH_{xs} calculated. Values for ΔH_{xs} were also calculated from Cp lines determined from DSC. For blends of PS and PPO, Cp was determined from an assumed arithmetic average of the pure component properties. Table 5.7 lists the values for ΔH_{xs} as determined from $\Delta Cp\Delta T$, the data of Karasz and from Cp lines calculated from DSC. The discrepancy was quite large, upwards to over 100%. However, the quantity of interest was the contribution of the excess glass enthalpy to the heat of mixing. Applying Hess's law to the quantities in Table 5.7 yielded the correction to ΔH_m due to ΔH_{xs} given in Table 5.8.

Table 5.7. ΔH_{xs} Determined from DSC and Adiabatic Calorimetry.

System	$\Delta Cp\Delta T$	ΔH_{xs} (Karasz et al.)	ΔH_{xs} (DSC)
PS	19.95 J/gm	22.30	26.56
90/10	21.04	25.36	35.57
70/30	24.45	32.15	48.38
50/50	27.52	40.00	61.53
30/70	31.85	48.98	61.38
PPO	40.31	64.59	30.31

Table 5.8. Hess's Law Application to ΔH_{xs}.

Blend	$\Delta Cp\Delta T$	ΔH_{xs} (Karasz et al.)	ΔH_{xs} (DSC)
90/10	.95 J/gm	1.17	-8.64
70/30	1.61	2.84	-20.70
50/50	2.61	3.45	-33.10
30/70	2.35	2.92	-32.20

Each of the values in Table 5.8 needed to be added to the values de-
rived from the Hess's law application to the experimental heat of solu-
tion. The comparison between $\Delta Cp \Delta T$ and that derived from adiabatic
calorimetry was quite good. The DSC results were very scattered and
not useful. However, in the comparison with the adiabatic calorimetry
results, $\Delta Cp \Delta T$ appeared to be a very good approximation to the excess
glass enthalpy particularly when used for calculating the heats of mix-
ing below Tg.

Figure 5.7 illustrates the dependence of $\Delta H_m / w_1 w_2$ as a function
of composition, where w_i is weight fraction. As pointed out in Chapter
II, the quantity $\Delta H_m / w_1 w_2$ is a van Laar energy term indicative of the
polymer interaction energy. Figure 5.7 shows that the polymer interac-
tion energy was fairly constant as a function of composition. This con-
clusion was consistent with the established compatibility of all PS/PPO
blend compositions. A slightly larger negative value of $\Delta H_m / w_1 w_2$
might have been expected for the edges of composition due to the shape
of the phase boundary at higher temperatures due to the existence of
an LCST. For PS/PPO, it can be estimated by extrapolation from copoly-
mers that the LCST, if it indeed existed, would be approximately 600°C.
The shape of the phase boundary at higher temperatures is curved up-
ward. This means that at the experimental temperature, the middle com-
position blends were nearer the phase boundary than the higher composi-
tion mixtures. Therefore, one might expect the interaction energy to
be larger at the extremes of composition. However, since the LCST for
PS/PPO would be very high, the dependence of the interaction energy on
composition would be slight, well within experimental error.
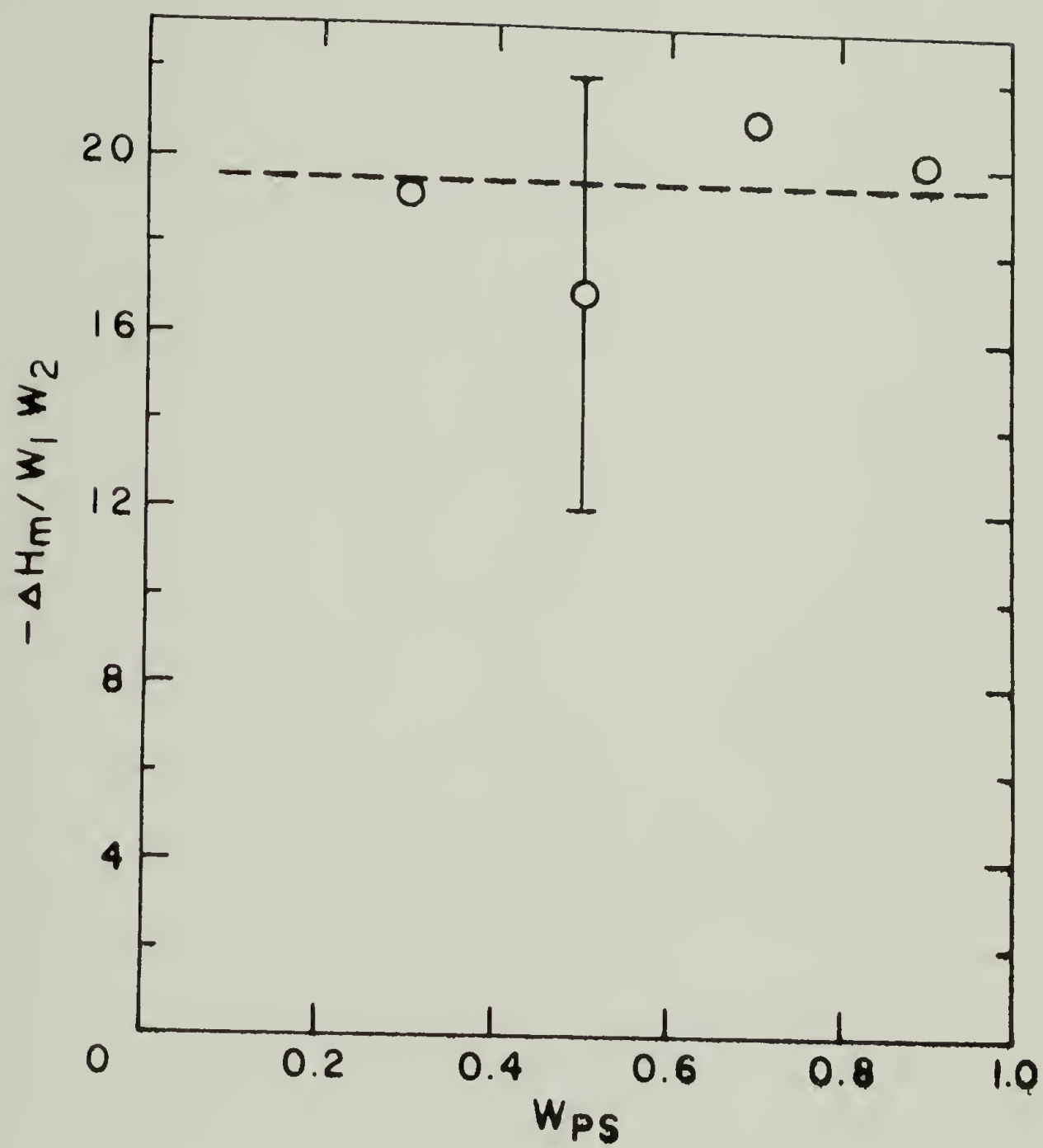
Figure 5.7. $\Delta H_m/W_1W_2$ vs. composition for PS/PPO blends.

C. Poly(4-chlorostyrene)-polystyrene Blends

Polystyrene blends with poly(4-chlorostyrene) exhibited two distinct Tg's by DSC and therefore deemed incompatible. The heat of mixing of incompatible blends is identically zero, i.e., no mixing occurs. Figure 5.8 shows the heats involved in the determination of ΔH_m for this pair. The experimental values for the heats of solutions of the polymer blends fell on a straight line between the pure component ΔH_s. Zero values of ΔH_m were not a sufficient condition for incompatibility. Compatible polymer blends could conceivably have such small heats of mixing as to be immeasurable. However, the zero heat of mixing was consistent with incompatibility as established by DSC.

In the Hess's law approach, an assumption was made concerning the heat of mixing a solution of polymer A with a solution of polymer B (see Chapter II). The assumption that the heat of mixing the two polymer solutions was zero is substantiated here. If the heat of mixing solutions was significant, a deviation from linearity would have been noticeable in Figure 5.8.

D. Poly(4-chlorostyrene-co-styrene)-PPO Blends

Blends of p(4-ClS-co-S) with PPO have been studied by Fried,[12,13] Shultz and Beach,[14] Tkacik,[15] and Alexandrovich.[16] Polystyrene is well known to be compatible with PPO. However, p(4-ClS) has been shown to be incompatible with PPO. Shultz and Beach, and Fried found that a sharp transition from compatibility to incompatibility occurred with copolymer composition for blends of PPO with
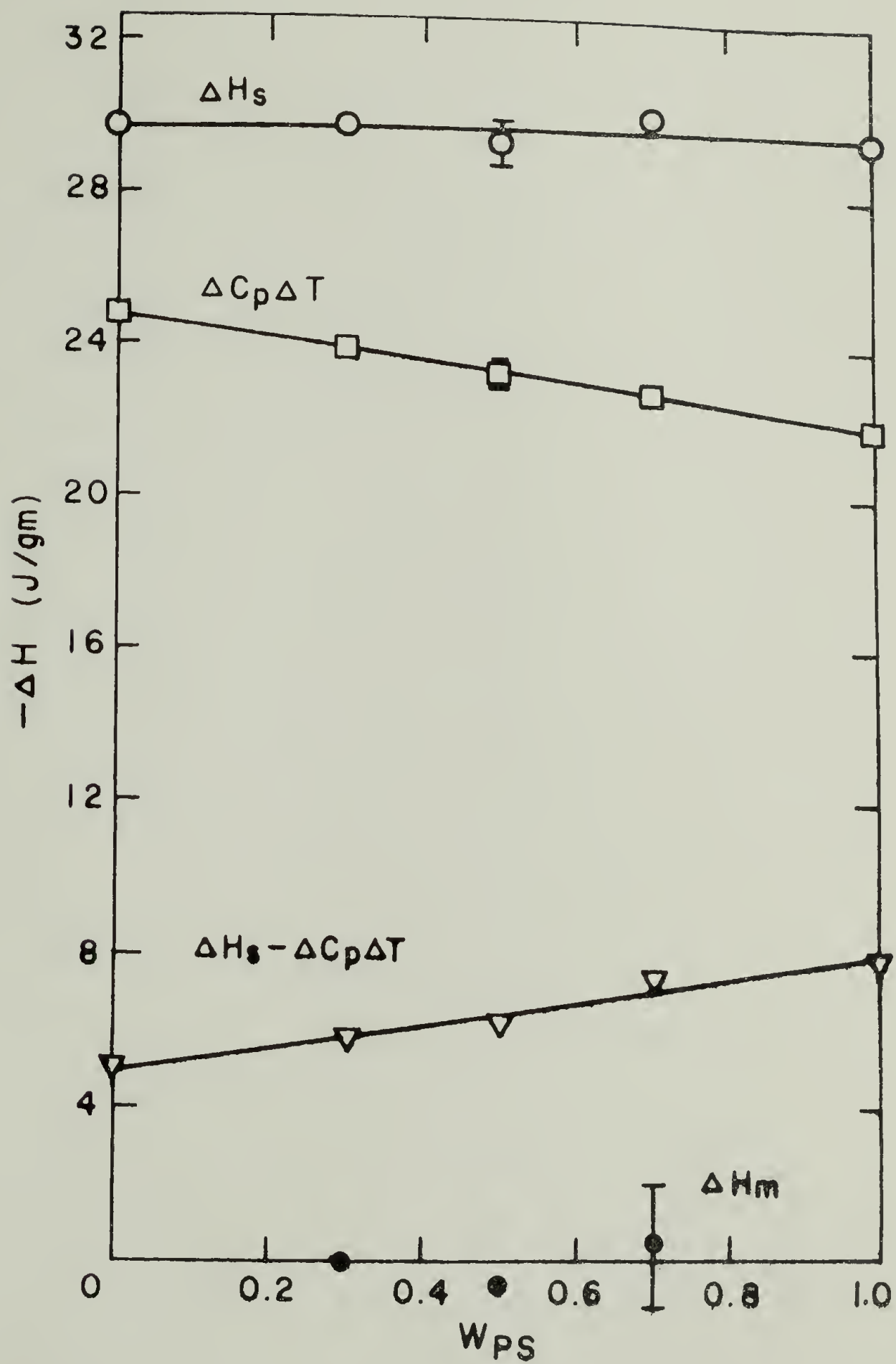
Figure 5.8.   -ΔH vs. W_PS for PS/p(4-ClS) blends.

p(4-ClS-co-S). Fried maintained that at or below 67.1 mole % 4-ClS, the copolymers were compatible with PPO. Alexandrovich took the temperature variable into account and defined a "transition zone" for compatibility of the copolymers with PPO. Figure 5.9 illustrates the findings of Alexandrovich for the copolymers blended 50/50 with PPO. The temperature for phase separation dropped over 100°C in a 16% co-polymer composition interval. Phase separation was also found to be reversible. An initially one phase material could be held above the phase separation temperature, forming two phases as evidenced by two Tg's. The two phase system could then be held just below the phase separation temperature to reform the one phase system displaying one Tg.

The purpose of the present work was to follow the behavior of the heat of mixing as the phase boundary was approached. This system gave a unique opportunity to study ΔH_m as a function of the lower critical solution temperature since the LCST was lowered with increasing 4-ClS in the copolymer. All blends were mixed 50/50 by weight. Appendix II lists the values for the heats involved in the calculation of ΔH_m.

Figure 5.10 shows the dependence of ΔH_m on copolymer composition at the experimental temperature, 34.8°C. The negative values for ΔH_m were a necessary condition for compatibility. As the phase boundary was approached, the magnitude of ΔH_m dropped quickly towards zero. For completely immiscible systems, ΔH_m is identically zero. However, for partially miscible systems, ΔH_m was not necessarily zero. A very large negative heat of mixing was found for the 50/50 blend
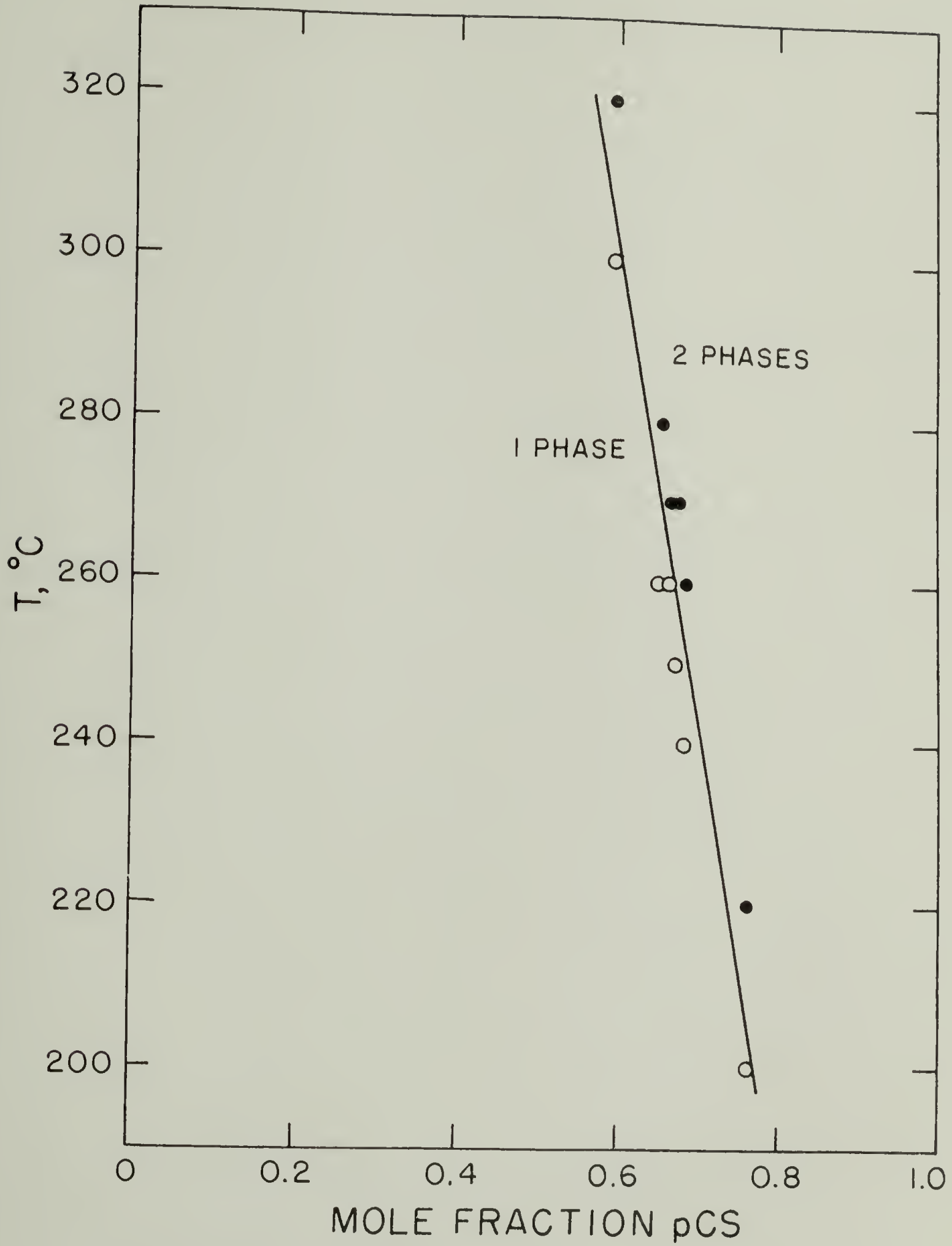
Figure 5.9. Compatibility of p(4-ClS-co-S) with PPO as a function of copolymer composition.
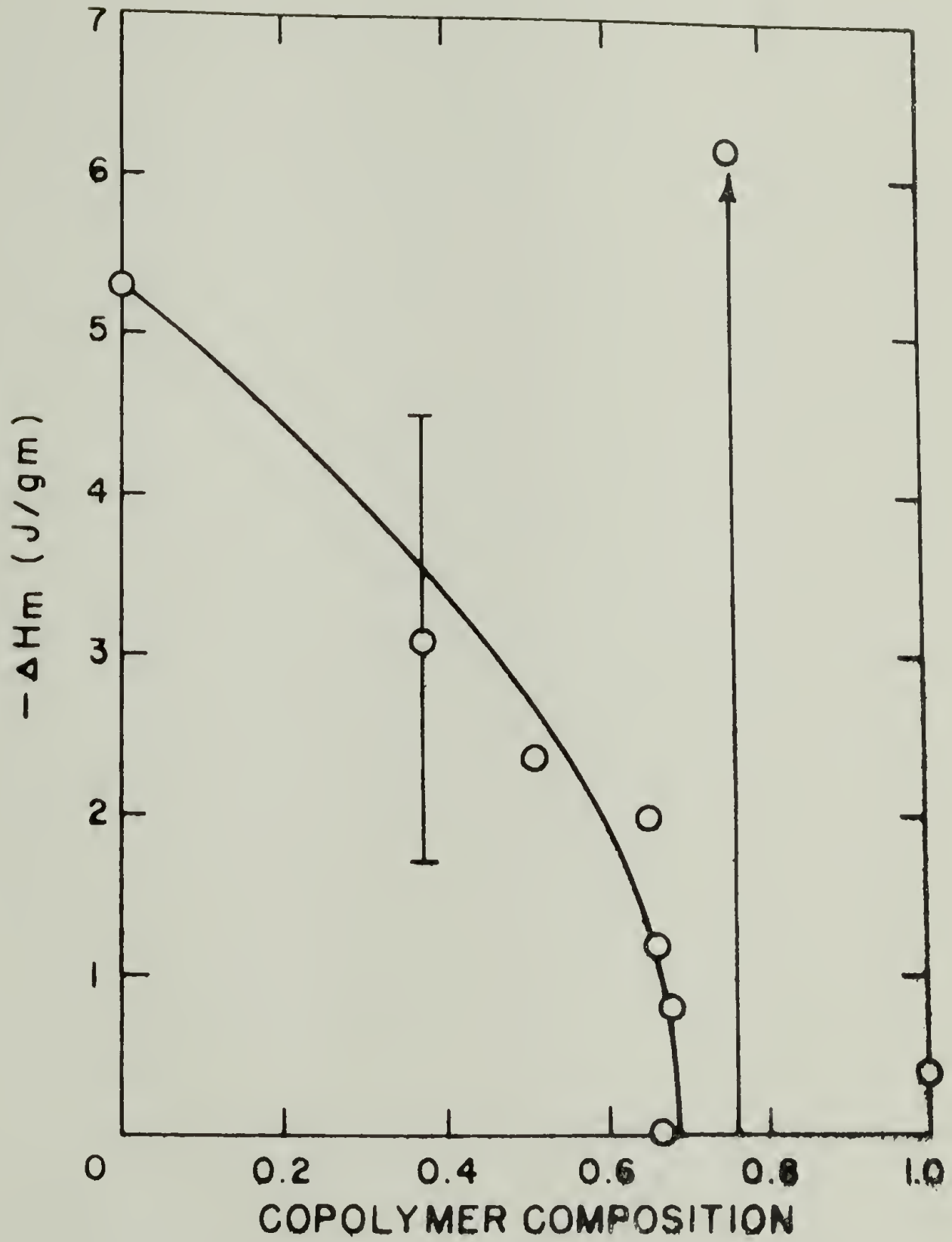
Figure 5.10. ΔH_m vs. copolymer composition for p(4-ClS-co-S)/PPO blends 50/50.

p(4-ClS(.759)-S)/PPO. This point was not anomalous in that it was the result of numerous determinations of ΔH_m. An explanation for this behavior could be shown by postulating the effect of the phase diagram on ΔH_m. Figure 5.11 illustrates the following explanation. As the percent 4-ClS in the copolymer was increased, the LCST of the blend with PPO decreased as shown in Figure 5.9. Therefore, the difference between the experimental temperature and the phase separation temperature narrowed with increasing 4-ClS content in the copolymer. It was previously pointed out that the magnitude of ΔH_m depended on the number and the strength of interpolymeric contacts. As the LCST was approached, the strength of polymeric 1-2 contacts diminished with respect to polymeric 1-1 and 2-2 interactions. Therefore, ΔH_m was expected to diminish towards zero, and in the extreme case of no polymer 1-2 contacts, i.e., complete immiscibility, ΔH_m became identically zero. The behavior of ΔH_m with copolymer composition did indeed diminish in magnitude as the LCST was lowered. However, the large negative value for p(4-ClS(.759)-S)/PPO initially was surprising. DSC showed that the p(4-ClS(.759)-S)/PPO blend was only partially miscible. Two Tg's were evident by DSC with each Tg being displaced towards the pure component Tg. Instead of a compatible 50/50 blend, the material was two incompatible phases where each phase was composed of a compatible mixture, i.e., a mixture of 30/70 with 70/30 (points A and B in Figure 5.11). Therefore, measurements of ΔH_m reflected the summation of the heats of mixing of the two compatible phases, each of which would be negative. However, the magnitude of ΔH_m for the p(4-ClS(.759)-S)/PPO blend was quite large. The following explanation could be used in an
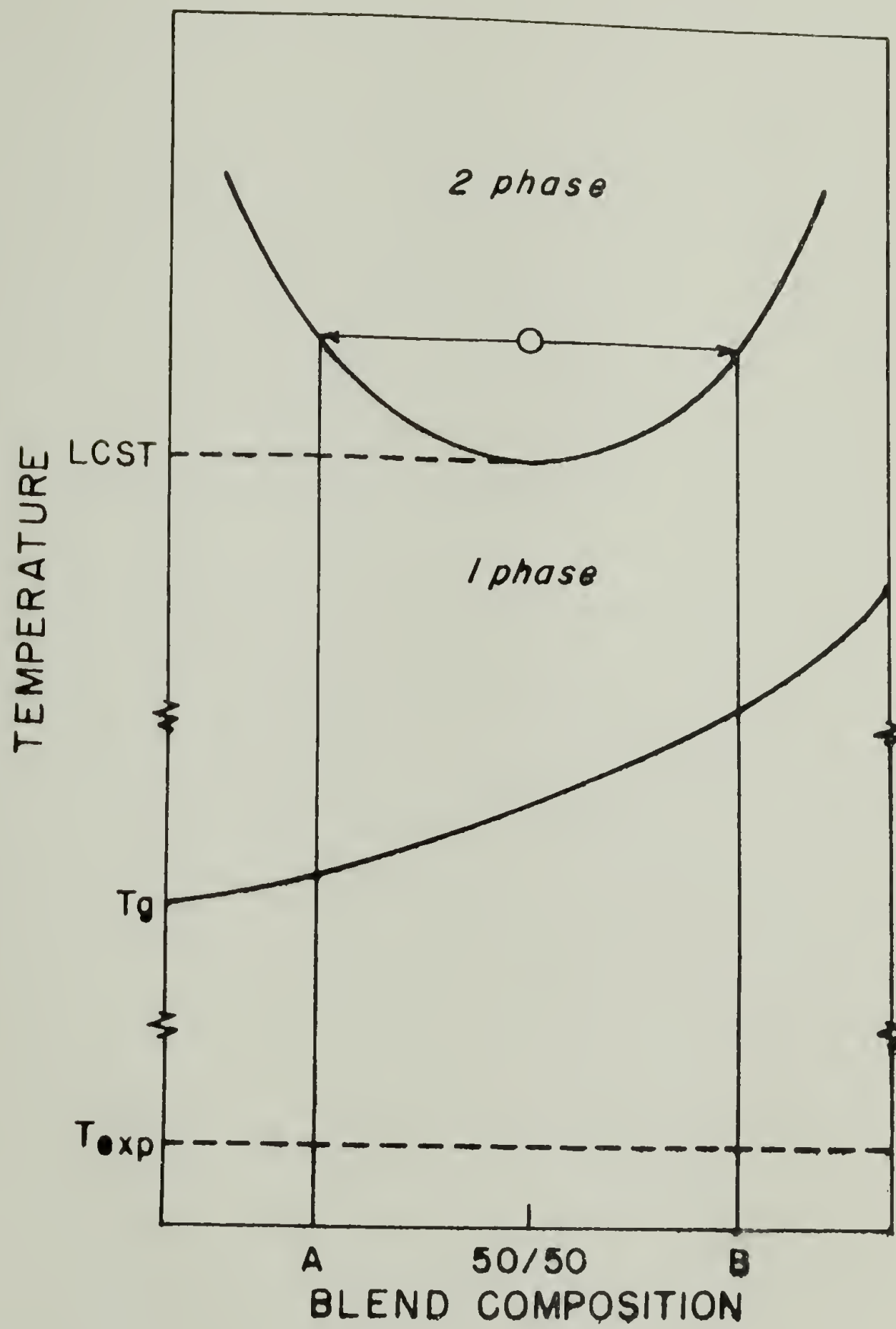
Figure 5.11. Effect of phase diagram on ΔH_m.

attempt to explain the large value of ΔH_m found for that blend. Actually, the hypothesis explained why ΔH_m for the copolymers in the 60-70% range were so small. A negative heat of mixing is a necessary, although not sufficient condition, for polymer-polymer compatibility. A negative value of ΔH_m could be found for a system that phase separates at the experimental temperature. A polymer-polymer system that phase separates upon a lowering of temperature is indicative of the occurrence of an upper critical solution temperature. Polymer-polymer UCST's have been postulated by theory but rarely found (see the next section for a more complete review on UCST's).

Figure 5.9 illustrates the dependence of the phase separation temperature on copolymer composition. The behavior of an UCST would follow the same pattern although the UCST would increase whereas the LCST decreased with increasing 4-ClS in the copolymer. The UCST could become higher than the experimental temperature as the copolymer composition changes. Figure 5.12 illustrates the effect of the phase diagram on ΔH_m. The polymer blend could be annealed at some temperature to yield a one-phase system. Should the lower phase diagram be absent, i.e., no UCST, the free energy of mixing, approximated by the heat of mixing since the entropy is zero, would change with composition as shown by curve 1. This was the case found for PS/PPO. However, should the experimental temperature fall below the UCST, polymer demixing would occur, adding a positive contribution to the heat of mixing. The value of ΔH_m would be less negative than expected for a completely miscible system (curve 2). In the extreme case, ΔH_m would become positive (curve 2a), which was found for some other systems (see next
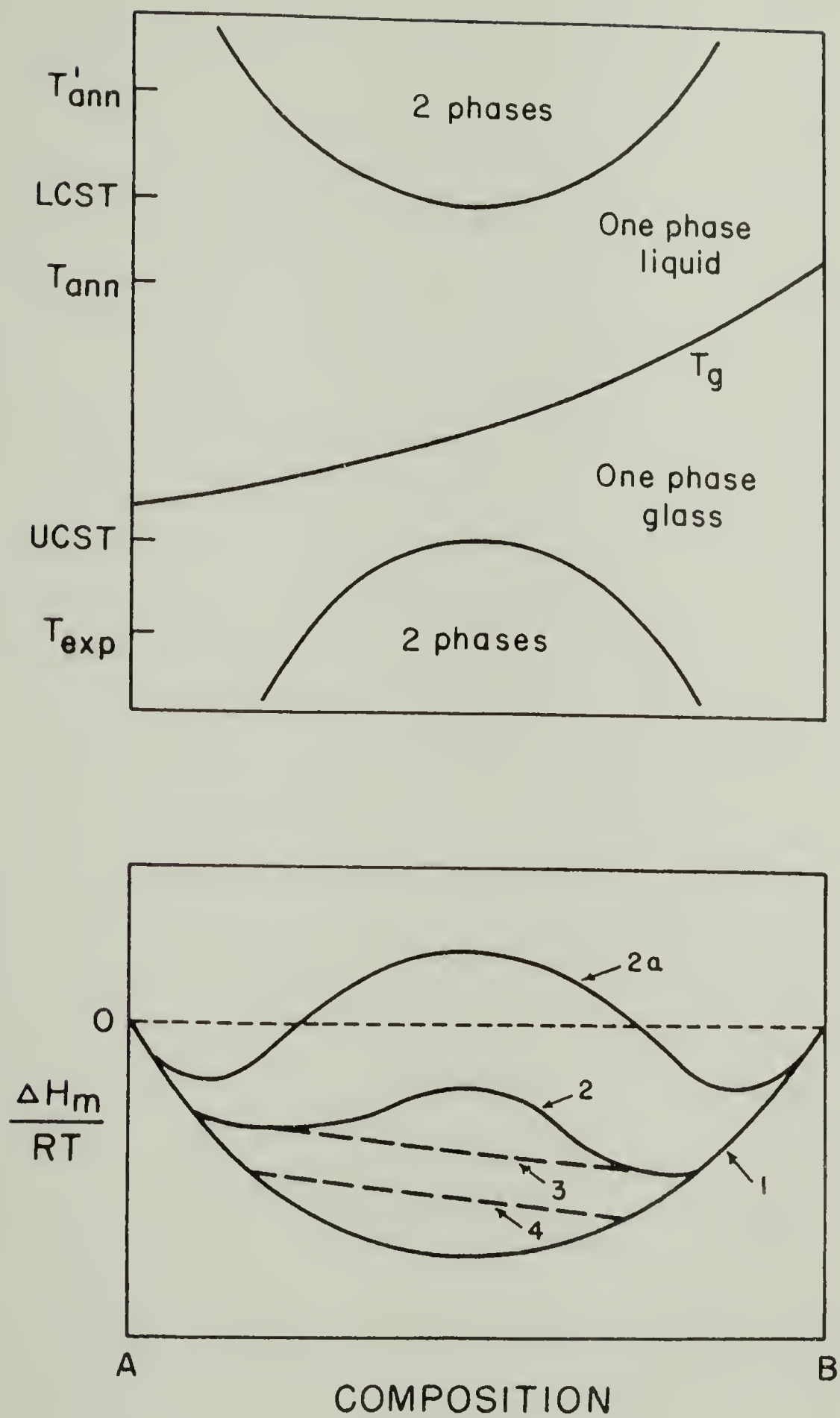
Figure 5.12.   Effect of phase stability on ΔH_m.

section).

The drop in the magnitude of ΔH_m for the copolymers between 60% and 70% 4-ClS could be explained as due to the degree the experimental temperature was below the UCST. The further below the UCST, the less negative, or more positive, would be ΔH_m.

The large negative value for the PPO blend with the .759 copolymer also follows from the above explanation. The two phases produced by annealing the blend above the LCST (T'_{ann}) might not fall inside the two phase region at the experimental temperature. Therefore, the ΔH_m would be more negative since there would be no further demixing of the phases when compared to the blends represented by curve 2 in Figure 5.12. The apparent heat of mixing would be an average of the values of ΔH_m for the two coexistent one-phase systems such as shown as point 3 or 4 in the figure. Therefore, the existence of a polymer-polymer UCST could be used to explain the results. Although this was very indirect evidence for an UCST, further studies in other systems (next two sections) have unequivocally established the existence of the lower phase diagram.

E.   Heats of Mixing Different Molecular Weights of Polystyrene with Poly(2-chlorostyrene)

The purpose of this study was to study the effect of polystyrene molecular weight on the heat of mixing polystyrene with poly(2-chlorostyrene). Alexandrovich[16] used DSC and dielectrics to ascertain the phase diagram of PS/p(2-ClS). Arrhenius plots, as determined by dielectric measurements, indicated that phase separation

occurred perhaps as low as 140°C. The Tg for p(2-ClS) was 133°C. The mobility of the polymer molecules at temperatures near Tg was severely restricted. Alexandrovich postulated that although the thermodynamic driving force would favor phase separation, the low degree of mobility near Tg would not allow complete phase separation in reasonable time periods. Gilmore[17] measured the diffusion constant for PS(20.4)/p(2-ClS) at 150°C by following the chlorine concentration profile using scanning electron microscopy with an energy dispersive analysis of x-ray fluorescence. Films of PS(20) and p(2-ClS) were placed in contact with each other, held above the Tg and allowed to diffuse for a period of approximately one month. The diffusion coefficient thus calculated was of the order of 10^{-14} cm^2/sec. Such a small diffusion coefficient illustrated the severe mobility restriction at temperatures slightly higher than Tg.

Russell[18,19] used small angle neutron scattering to determine the radius of gyration of deuterated polystyrene in a p(2-ClS) matrix. The radius of gyration was found to be larger in the p(2-ClS) matrix than in a theta solvent. This indicated that the polystyrene was compatible with p(2-ClS). However, the polystyrene component was very dilute and therefore these experiments did not shed any light on the compatibility of PS/p(2-ClS) in the more concentrated regimes.

In the present study, the heats of mixing many different molecular weight polystyrenes with p(2-ClS) were measured as a function of blend composition. Figures 5.13 through 5.20 show the magnitudes of the heats involved in the calculation of ΔH_m for each system and temperature given in the figure. The magnitude of ΔH_m was small compared
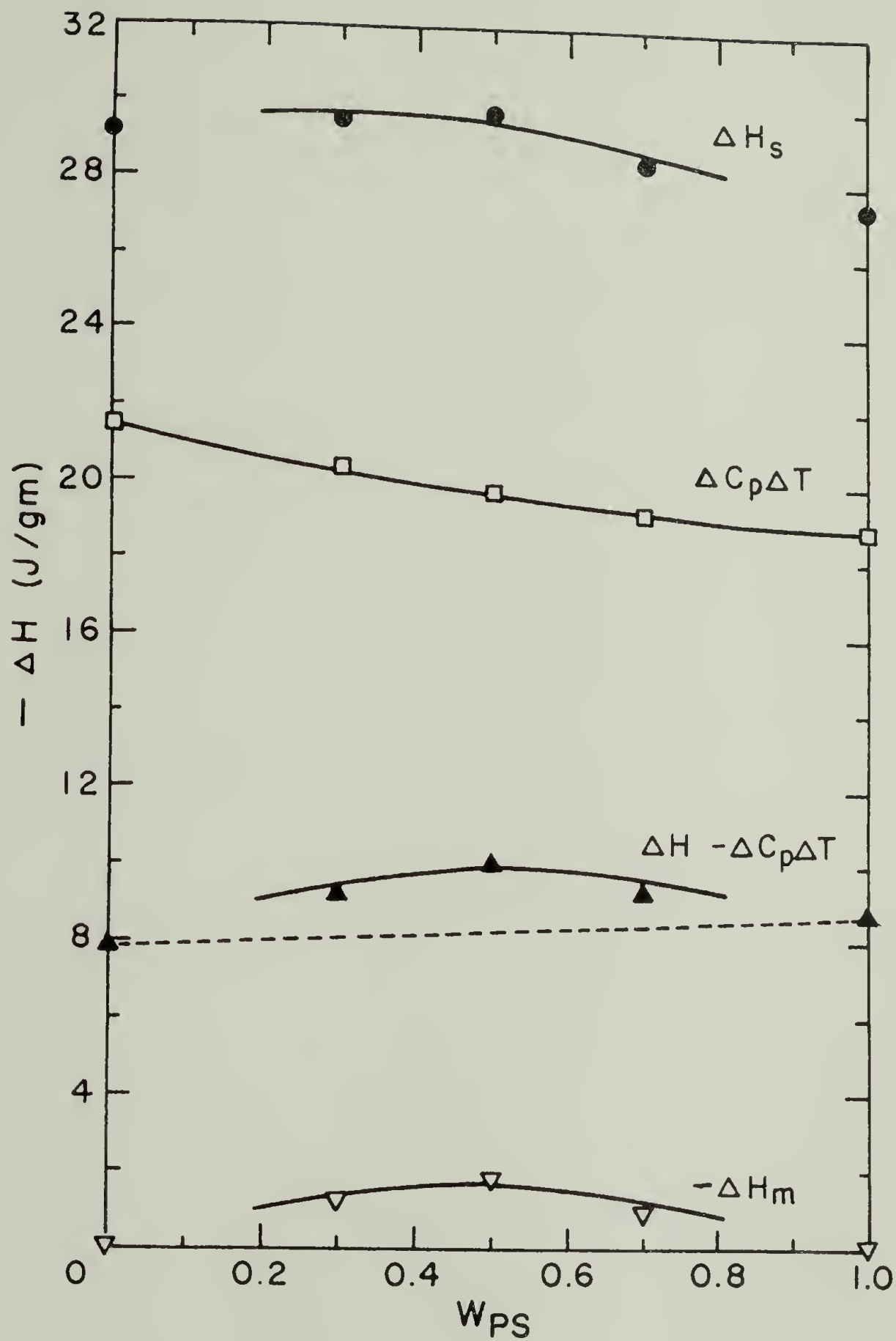
Figure 5.13. $-\Delta H$ vs. W_{PS} for PS(50)/p(2-ClS) blends.
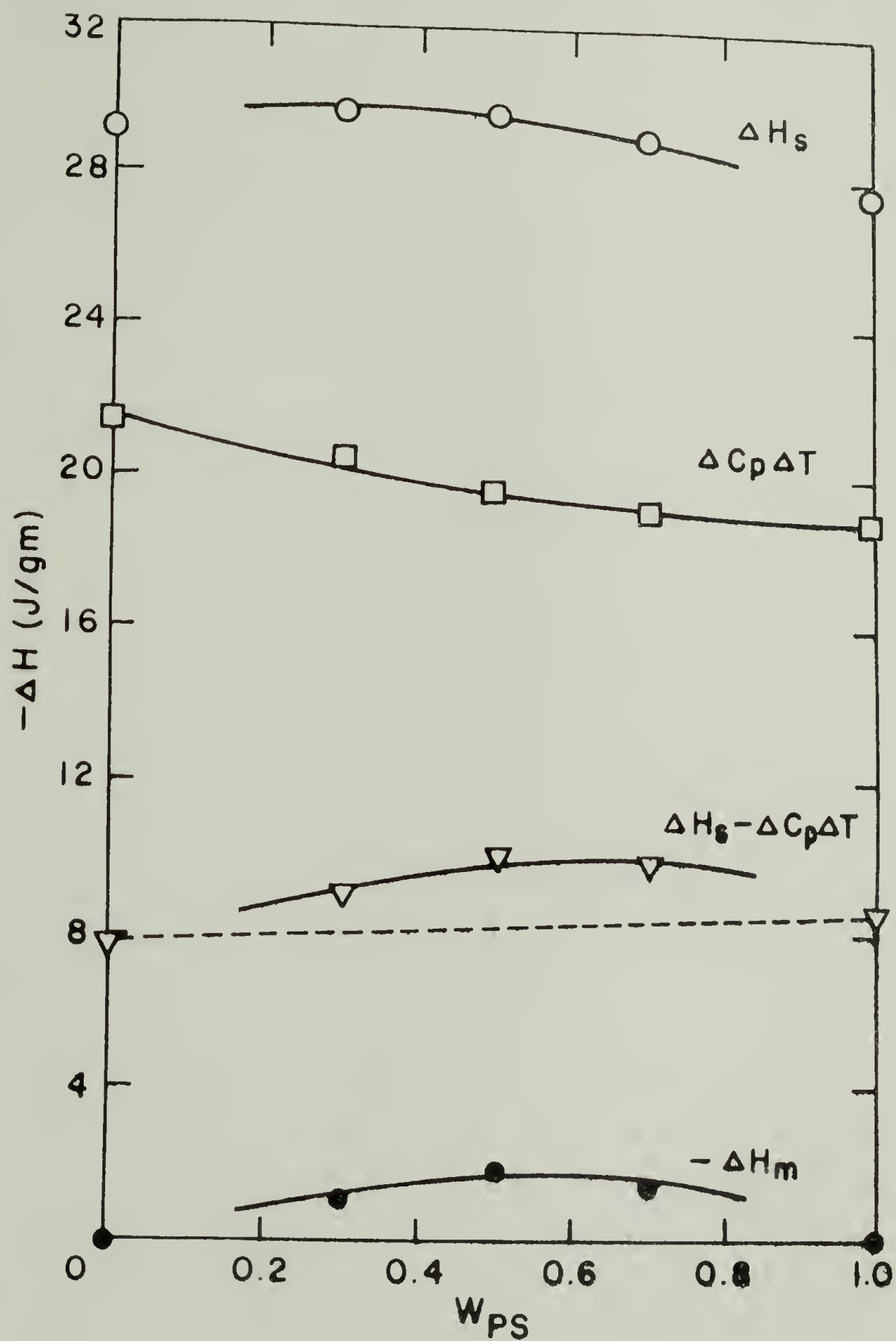
Figure 5.14. $-\Delta H$ vs. W_{PS} for PS(37)/p(2-ClS) blends.
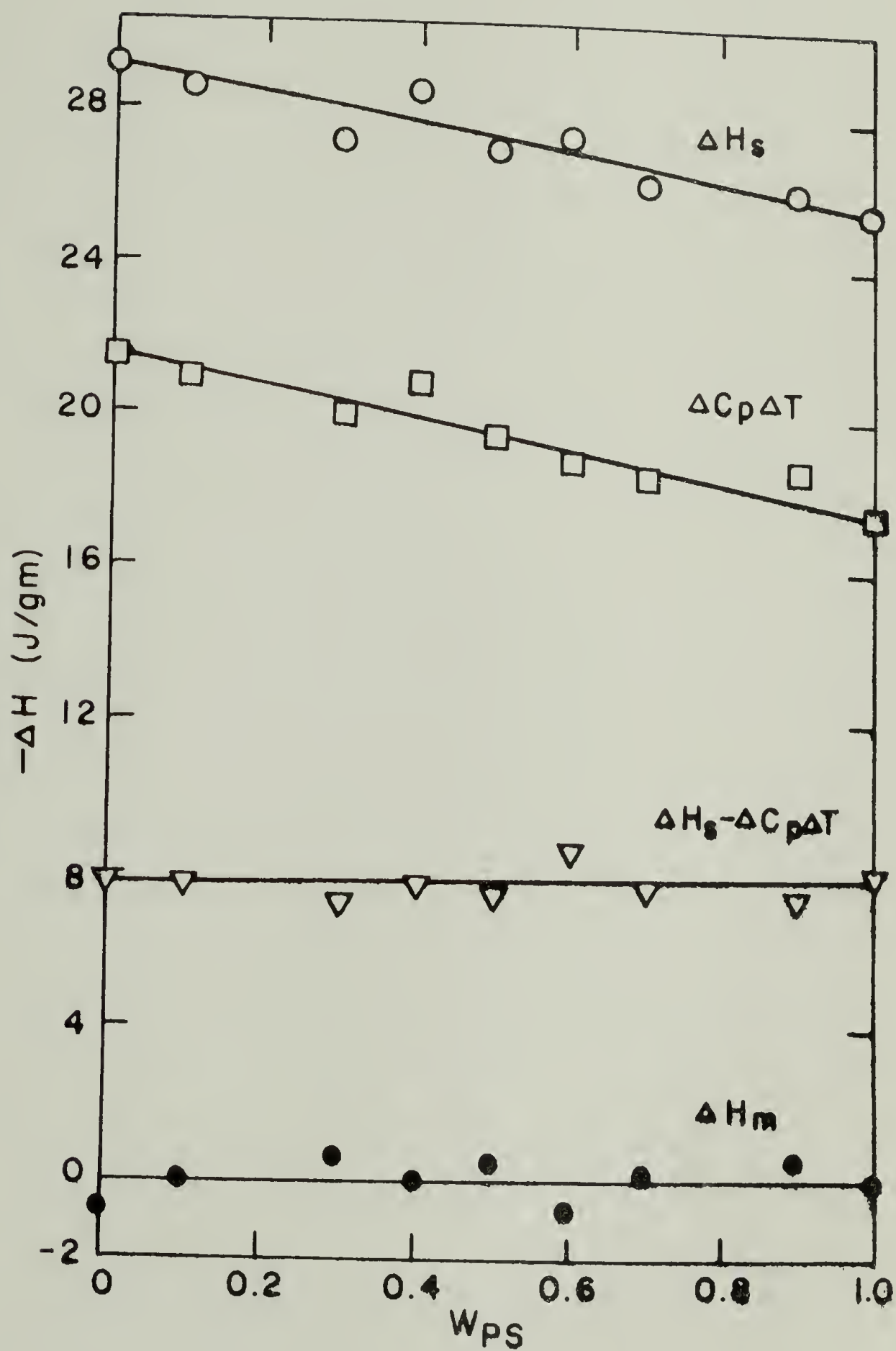
Figure 5.15.   -ΔH vs. W_{PS} for PS(32)/p(2-ClS) blends.
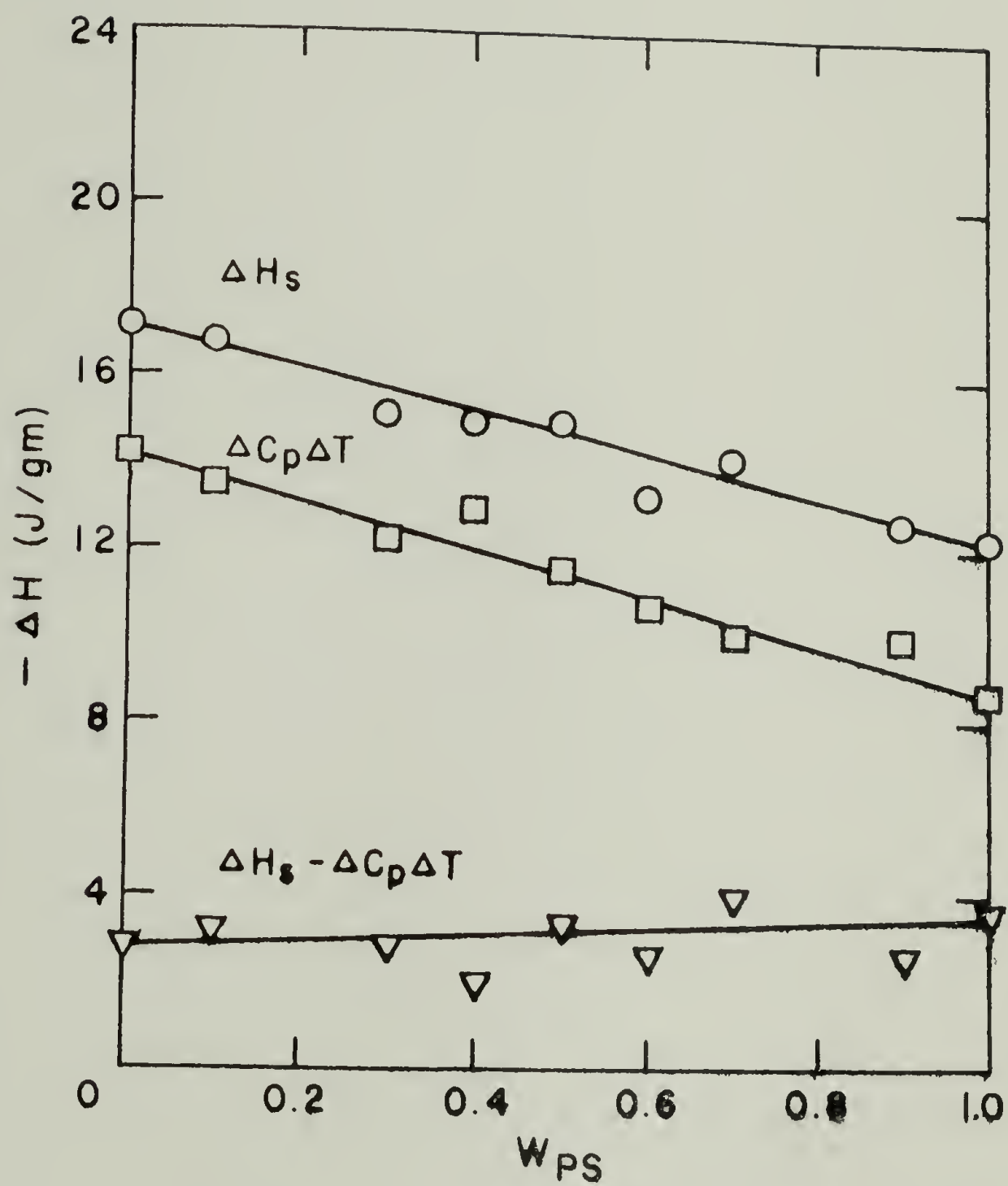
Figure 5.16. $-\Delta H$ vs. W_{PS} for PS(32)/p(2-ClS) blends (T_{exp} = 67.8°C).
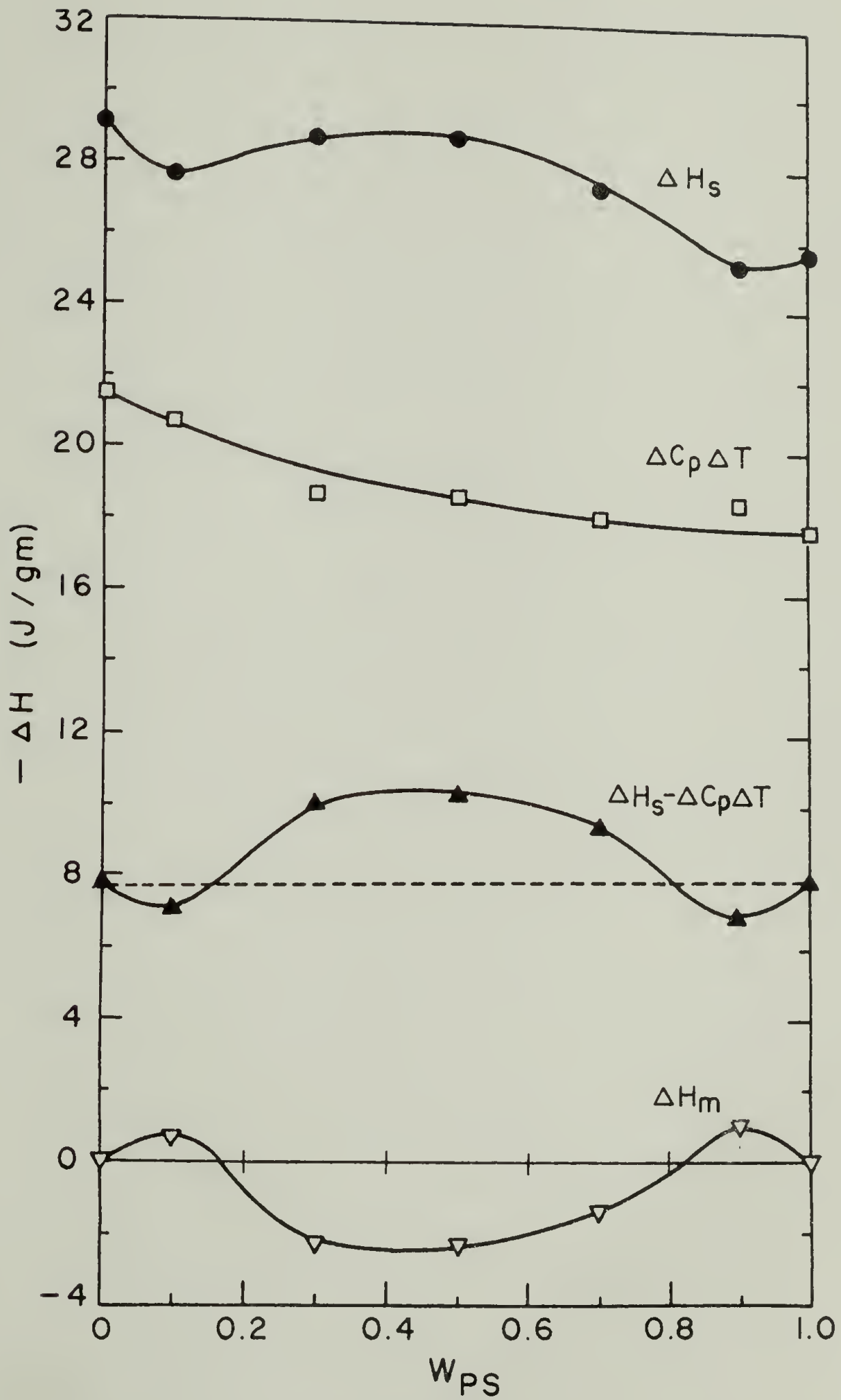
Figure 5.17. $-\Delta H$ vs. W_{PS} for PS(20.4)/p(2-ClS) blends.
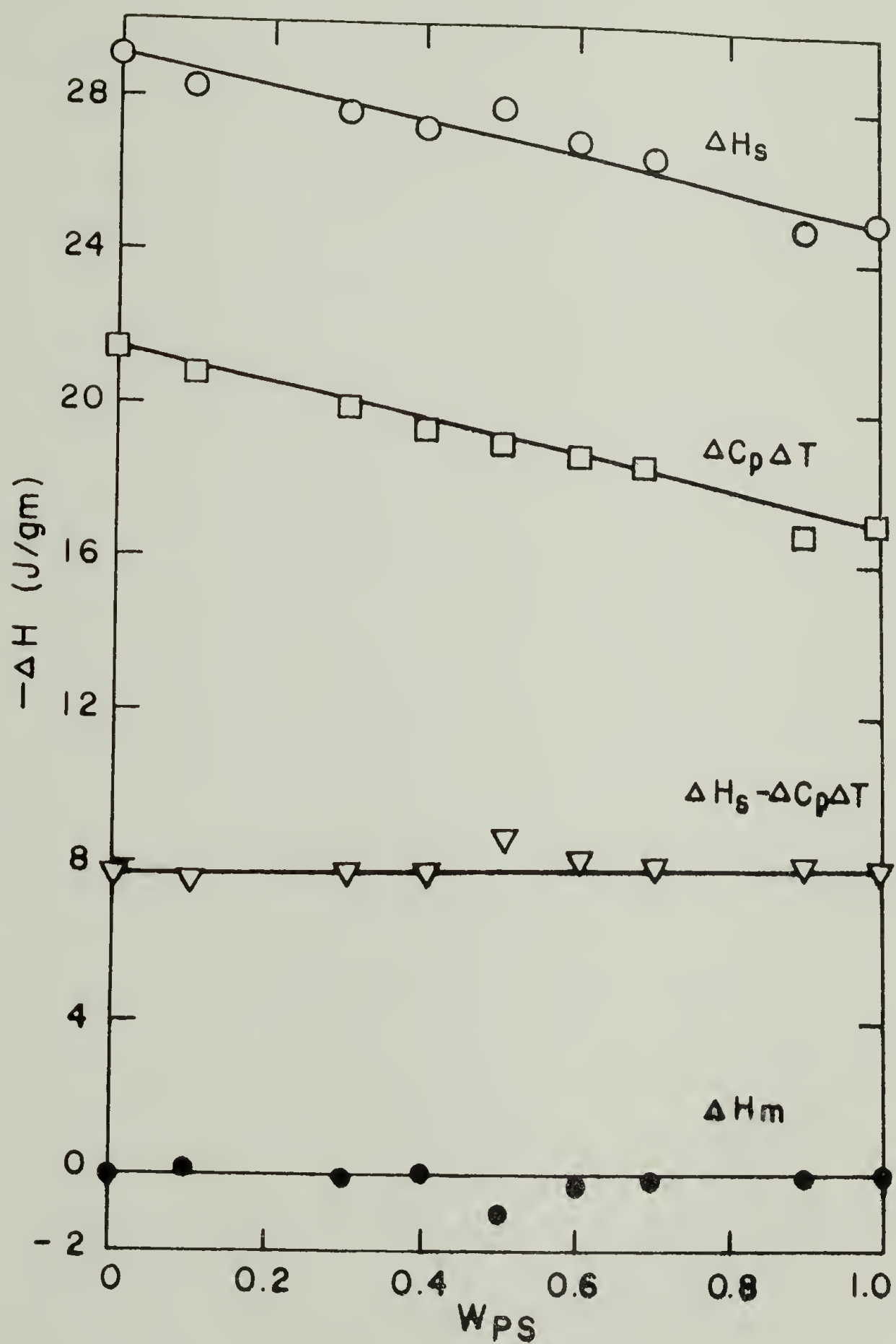
Figure 5.18. $-\Delta H$ vs. W_{PS} for PS(17.5)/p(2-ClS) blends.
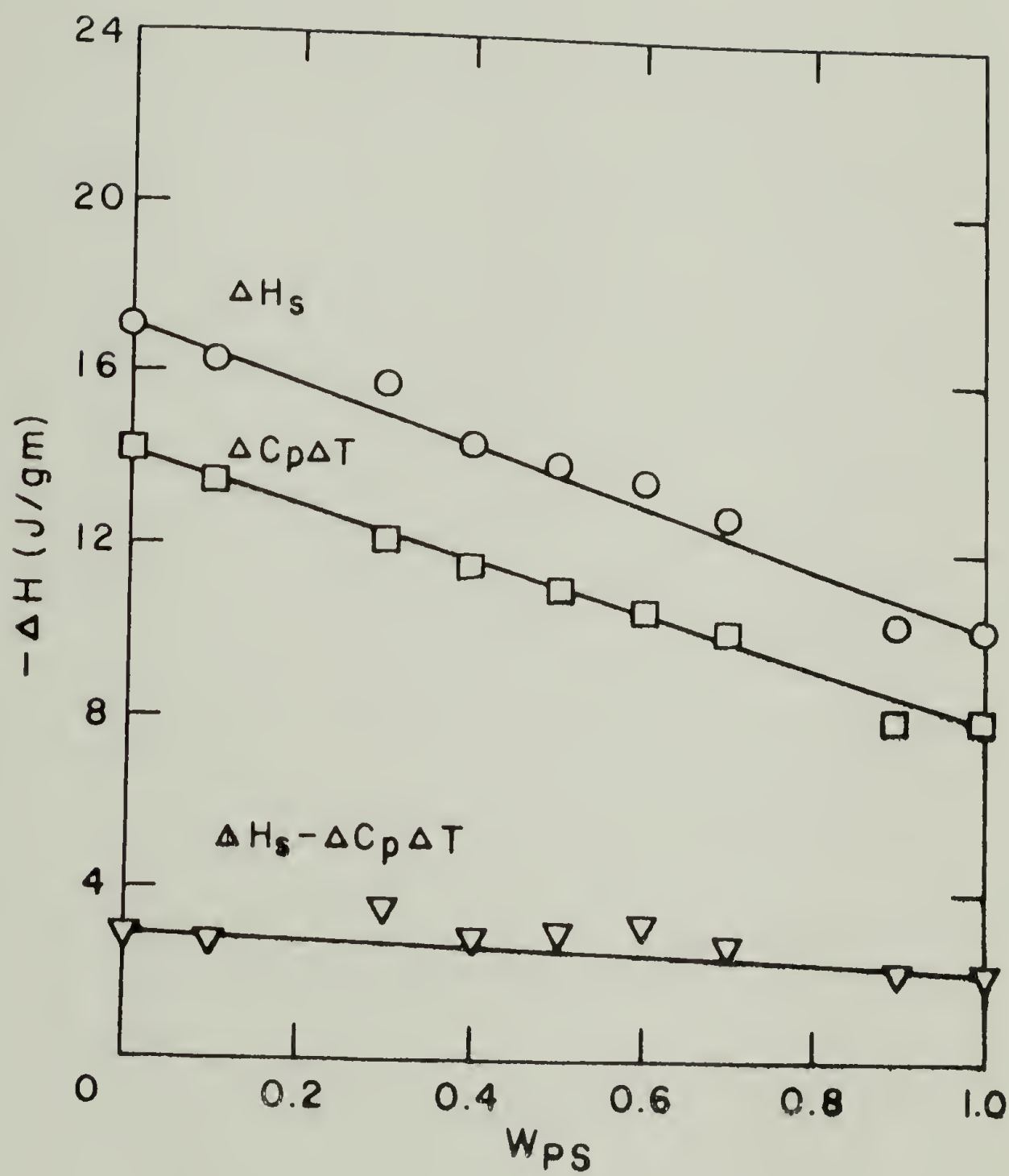
Figure 5.19. $-\Delta H$ vs. W_{PS} for PS(17.5)/p(2-ClS) blends ($T_{exp} = 67.8°C$).
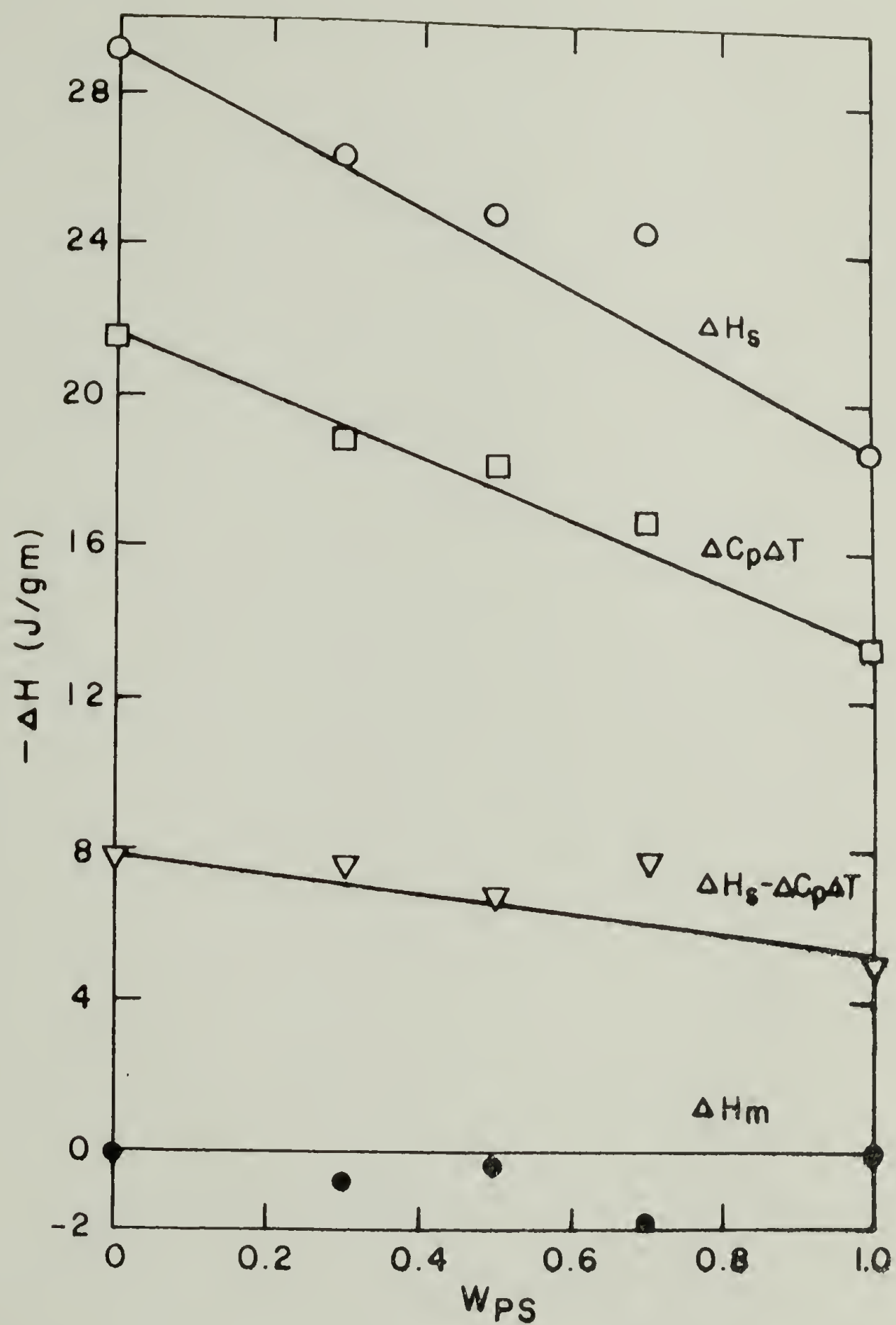
Figure 5.20.   -ΔH vs. W_{PS} for PS(9)/p(2-ClS) blends.

to ΔH_m for PS/PPO. However, a striking result was the measurement of a positive heat of mixing for each system. The explanation for the positive heat of mixing was equilibrium phase separation at the experimental temperature.[20] Measurement of the heats of solution by Tian-Calvet microcalorimetry followed by the application of Hess's law to determine ΔH_m was useful for probing the equilibrium thermodynamic state below Tg.

Polymers are unique in that they can exist for a finite amount of time in a thermodynamically unstable state. The thermodynamic driving force was unable to overcome the barrier to the severely restricted mobility below Tg. In the measurement of the heats of solution, the solvent served to first lower the Tg of the polymer, allowing sufficient chain mobility in order to quickly reach the equilibrium state at the experimental temperature. Take the case where the polymer blend was found to be compatible as evidenced by DSC measurements. Should the same polymer blend had been compatible at the experimental temperature, ΔH_m would be negative and the second derivative of the heat of mixing with respect to composition be positive. An illustration of this example would be the blend PS/PPO. However, should the initially compatible polymer blend be immiscible at the experimental temperature, ΔH_m could still be negative but the second derivative would become negative. An illustration of this case is shown for the PS(20.4)/p(2-ClS) blend. In the extreme case of incompatibility at T_{exp}, ΔH_m would become positive. What actually would be measured would not be the heat of mixing but the heat of demixing. Therefore, a positive value of ΔH_m would reflect a demixing process occurring at

the experimental temperature, indicative of phase separation at that temperature. Moreover, a positive ΔH_m would be a sufficient criterion for phase separation in polymer systems where the entropy of mixing approaches zero.

Polystyrenes with molecular weights 50,000, 37,000, 20,400, and 9,000 blended with p(2-ClS) all produced positive values of ΔH_m. The p(2-ClS) used in each case was from the same batch. The values of ΔH_m were quite small. However, the positive ΔH_m was sufficiently large to postulate the existence of phase separation at the experimental temperature. For the PS(20.4)/p(2-ClS) blend, negative values of ΔH_m were found for the composition extremes, indicative of the compatibility of the 90/10 and 10/90 blend compositions. The shape of the PS(20.4)/p(2-ClS) heat of mixing-composition curve also allowed graphical determination of the binodal and spinodal. Although more complete compositional points needed to be determined, the binodal could be determined from the common tangent of the concave sections of Figure 5.21 (dashed line, points A and B) whereas the spinodal occurred at the inflection points, C and D. PS(20.4)/p(2-ClS) was the only system that was studied in sufficient detail to enable the determination of a binodal and spinodal boundary at the single experimental temperature.

It is interesting to note that the absolute value of the normalized heats of mixing ($\Delta H_m/w_1 w_2$) for the PS(20.4)/p(2-ClS) blends were comparable (see Figure 5.21a). This would indicate that the interaction energy for each composition was equal. At the composition extremes, the interaction energy was determined from values of the
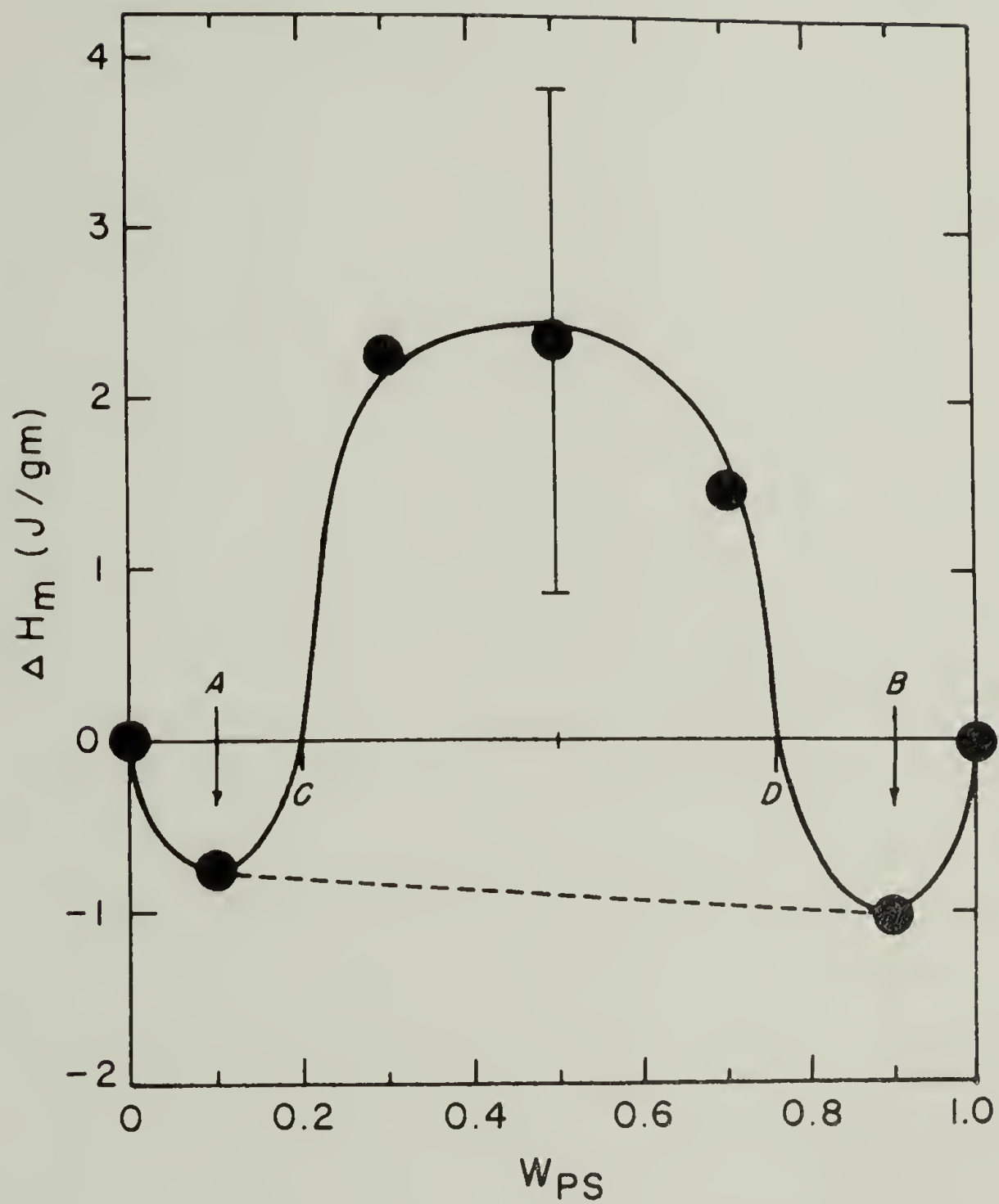
Figure 5.21. ΔH_m vs. W_{PS} for PS(20.4)/p(2-ClS) blends showing locus of binodal (A, B) and spinodal (C, D) phase boundary.
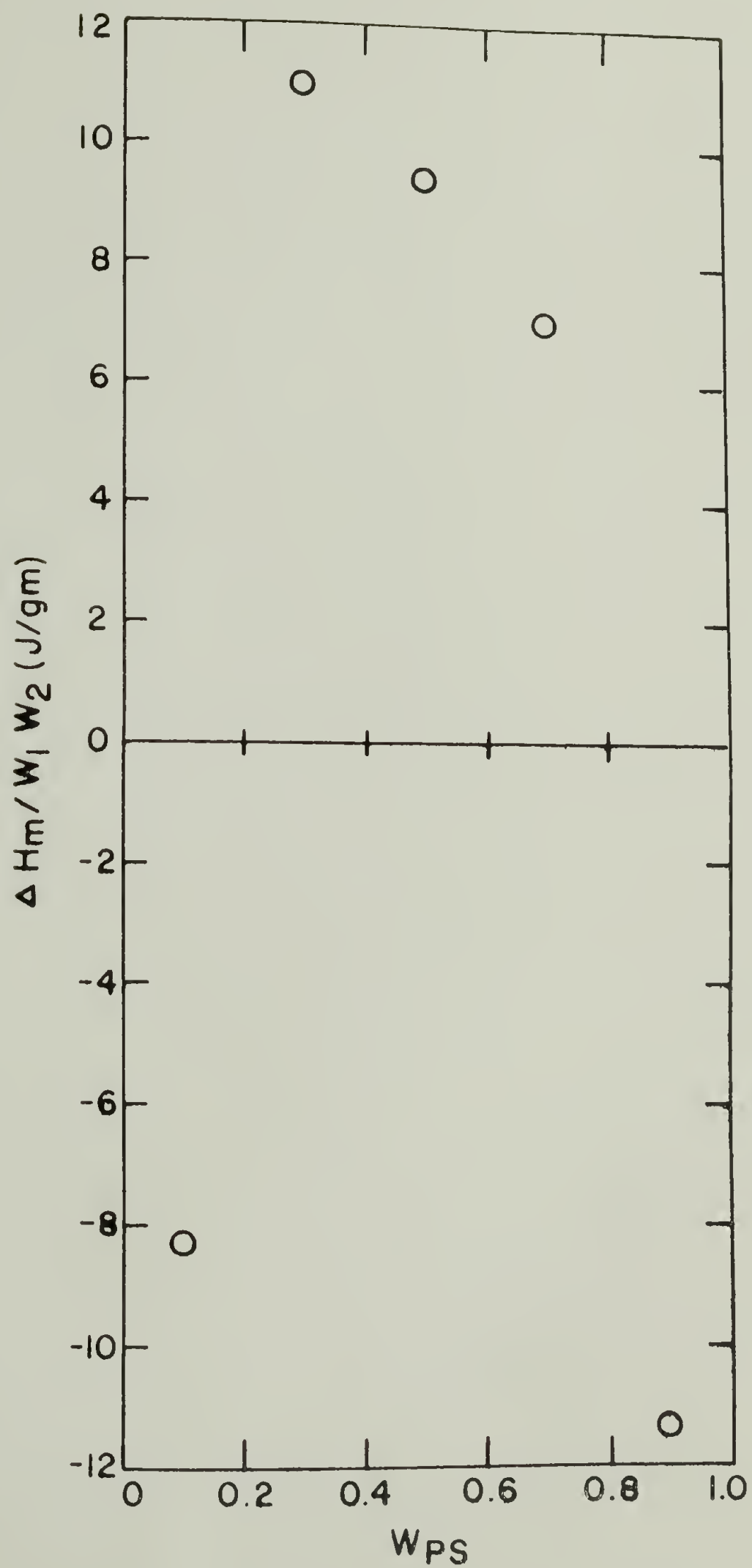
Figure 5.21a. $\Delta H_m/w_1 w_2$ vs. W_{PS} for PS(20.4)/p(2-ClS) blends.

heats of mixing whereas in the mid-composition region, the interaction energy was reflected from the measurement of the heat of demixing; the opposite process, therefore, the opposite sign.

The p(2-ClS) blends with PS(32.4) and PS(17.5) were blended with a different batch of p(2-ClS). The molecular weight and polydispersity of the p(2-ClS) was different from that used for the previous molecular weight polystyrenes. There was also a scarcity of the original batches of polystyrene with molecular weights 50,000, 37,000, 20,400, and 9,000. Therefore, the effect of the different batches of p(2-ClS) on the ΔH_m could not be performed due to lack of the appropriate materials.

The behavior of ΔH_m for blends of PS(32.4) and PS(17.5) with p(2-ClS) was different from the other molecular weight blends. Values of ΔH_m were zero, within experimental error, for each blend composition at experimental temperatures of 34.8°C and 67.6°C. Whereas blends of PS(17.5)/p(2-ClS) exhibited small positive heats of mixing as a function of composition, blends of PS(32.4)/p(2-ClS) gave scattered values of ΔH_m. Therefore, the existence of positive ΔH_m could not be ascertained for these two blend systems. The original thrust of this study was to determine ΔH_m as a function of experimental temperature in an attempt to define the existence of a phase boundary. Unfortunately, the systems with enough sample needed for such a study gave the most unsatisfying results.

The conclusions reached from measurements of ΔH_m were that the midcomposition range blends were incompatible at 34.8°C. The results of DSC also lent credence to that conclusion. Blends of

PS/p(2-ClS) were initially compatible; freeze-dried blends exhibited a single Tg intermediate the pure component Tg's. However, depending on the polystyrene molecular weight, the polymer blends could be phase separated. This was manifested by the appearance of two Tg's. Figure 5.23 shows the appearance of two Tg's from DSC annealing experiments. Polymer blends of p(2-ClS) with PS(50), PS(37) and PS(32.4) could be phase separated using annealing experiments. The phase separation was not reversible, however, as was found for the p(4-ClS-co-S)/PPO blends. Blends of p(2-ClS) with PS(20.4), PS(17.5) and PS(9) could not be phase separated even when annealed near decomposition temperatures.

The LCST for these systems was very sensitive to molecular weight, increasing at least 200°C with a decrease in polystyrene molecular weight of only 12,000. Since monodispersed polystyrenes of intermediate molecular weights could not be obtained, mixtures of two different molecular weight polystyrenes were blended with p(2-ClS). The ratio of PS(MW1):PS(MW2) was varied to give polystyrene average molecular weights in the range of interest. A mixture of PS(37) with PS(19.8) was used to give $\overline{M}_n$ values of 23,200, 26,700, 30,400 and 33,600. Blends of p(2-ClS) with PS(23.2) or PS(26.7) could not be phase separated even at degradation temperatures. Figure 5.22 shows the result of DSC annealing experiments for PS(26.7)/p(2-ClS). The initial run is shown as curve A. Only one Tg is present, indicative of compatibility. Curve D was the result of annealing at 400°C, above the degradation temperature of both polymers. Although the Tg of the blend was lower, only a single transition was evident. The lowering of Tg was due to a sharp decrease in molecular weight resulting from
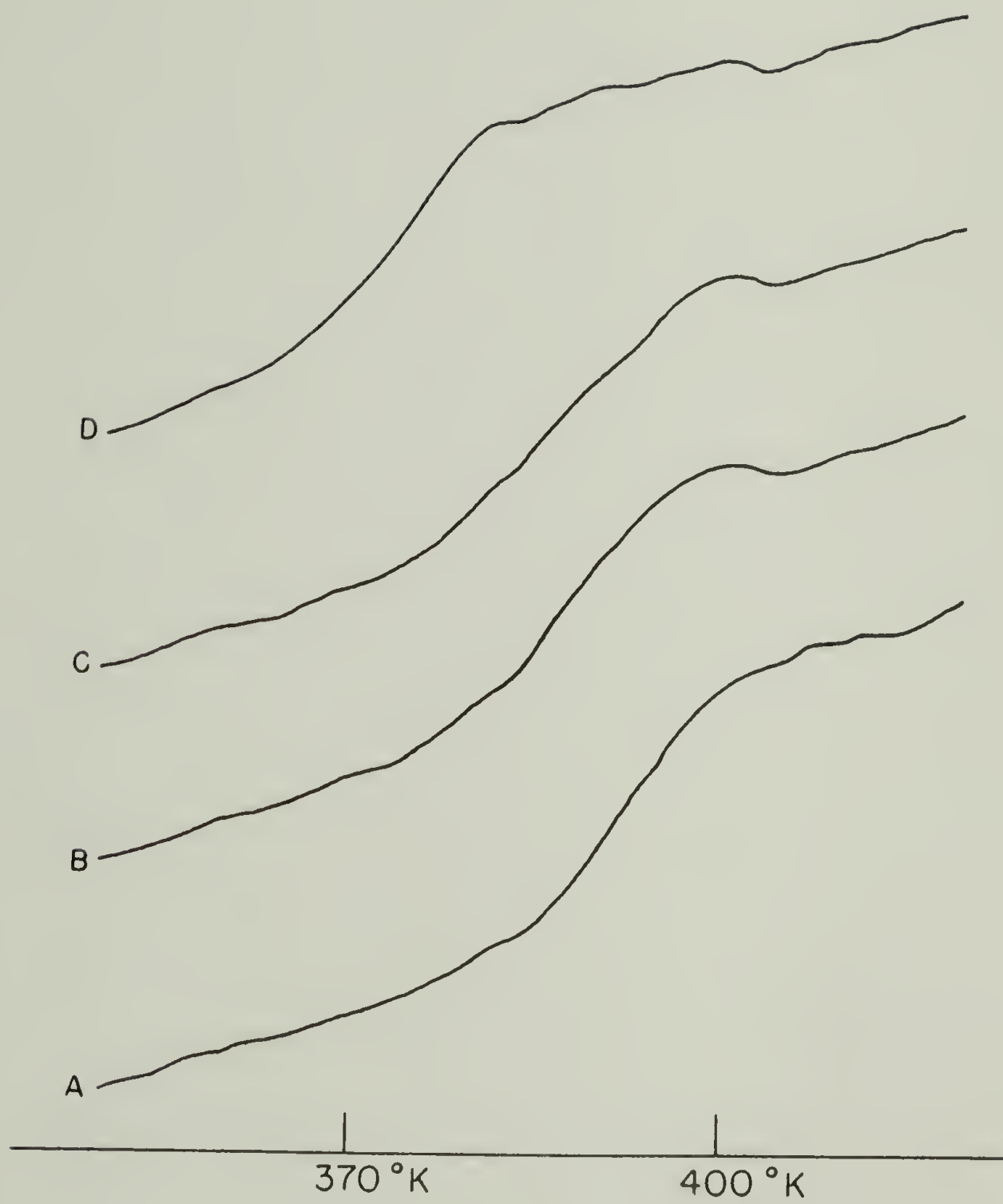
Figure 5.22.   DSC thermograms for PS(26.7)/p(2-ClS) blends 50/50.
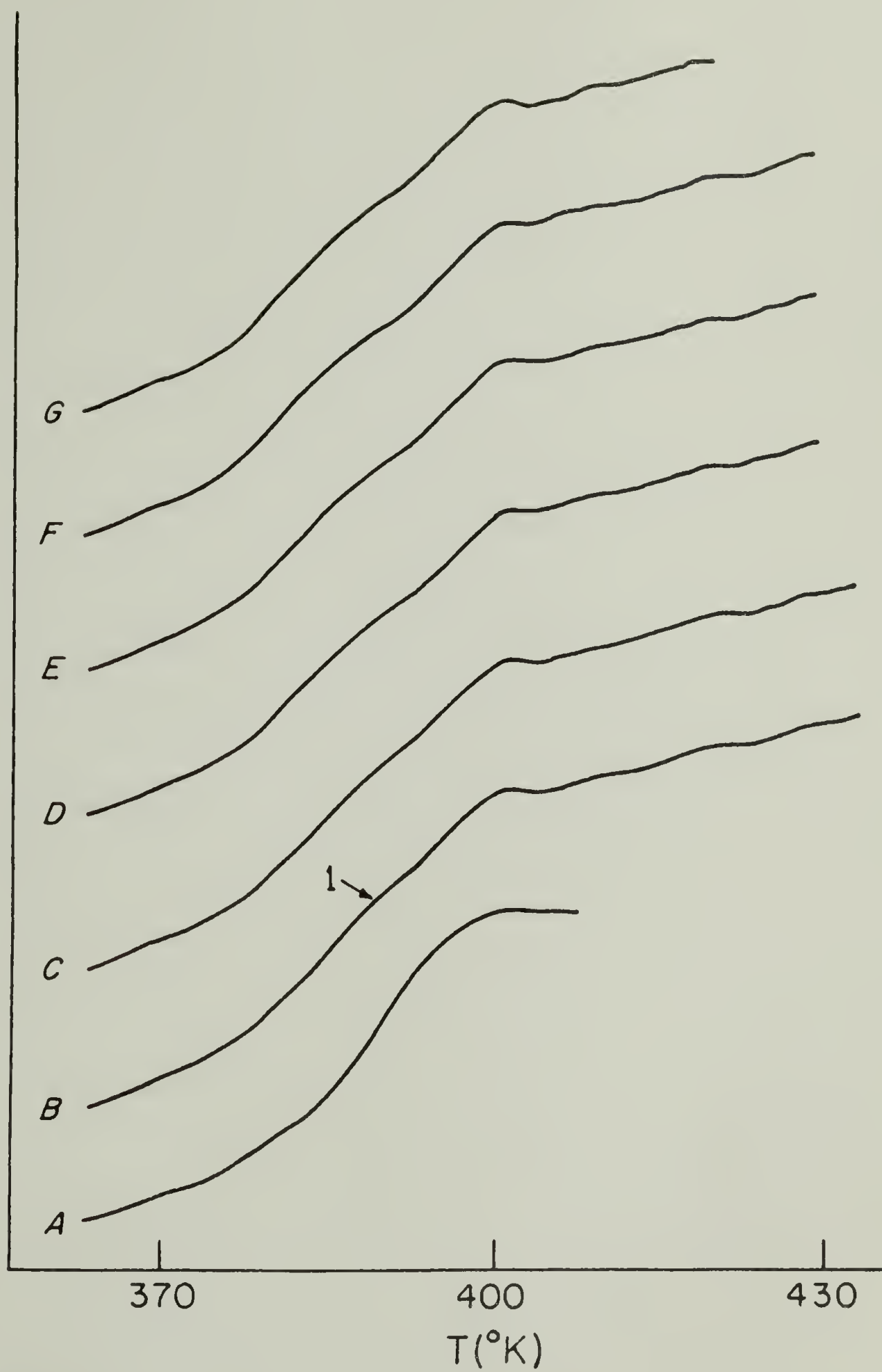
Figure 5.23.   DSC thermograms for PS(30.4)/p(2-C1S).

chain scission.

Figure 5.23 illustrates the phase separation behavior of PS(30.4)/p(2-ClS). Curve A reflects the compatibility of the original pressed blend. After being held for 2 hours at 160°C (curve B), the polymer blend hints at phase separation. The transition range broadens considerably and a second transition appeared to be formed (point 1). As the annealing temperature was increased, 170°C (curve C), 180°C (D), 190°C (E), 200°C (F), the appearance of a second Tg became much more evident. However, the phase separation was not reversible. When the polymer blend sample was held at 160°C after being phase separated (curve G), annealing for 12 hours did not show any trend back towards a one phase system.

The aforementioned experiments showed that the LCST of the PS/p(2-ClS) system dropped over 250°C with an increase of molecular weight of only 3700. Sanchez,[21-24] using lattice fluid theory, does predict a sharp lowering of the polymer-polymer LCST with an increase in molecular weight of one of the components. Sanchez predicted that an increase in molecular weight of 6000 of one component would result in a decrease of only 40-50°C for the LCST.[31] McMaster[32] utilized Flory's equation of state approach to calculate the effect of molecular weight on the binodal and spinodal curves. He found that an increase in molecular weight of 20,000 produced a decrease in the LCST of approximately 150°C. Nowhere was there predicted the LCST would drop 250°C with an increase in molecular weight of only 3600. Therefore, the evidence points to the existence of an UCST and an LCST centered around some temperature above Tg.

For polymer-solvent systems exhibiting both an upper and lower critical solution temperature, a change in polymer molecular weight produced the predicted change in the UCST and the LCST. The mid-point temperature of the LCST and UCST was not found to change substantially. Kuwahara et al.[33] studied the polystyrene-cyclohexane system as a function of polystyrene molecular weight. As the molecular weight was increased, the UCST increased and the LCST decreased. For example, the LCST for the PS(2700) solution was about 430°K whereas the UCST appeared at 290°K. When the polystyrene molecular weight was decreased to 37,000, the LCST was 455°K and the UCST 265°K. The temperature midpoint between the UCST and the LCST was 360°K for both systems. The weight fraction where the LCST and the UCST occurred, however, did shift as a function of molecular weight. This shifting of the CST's was not large for small differences in molecular weight. Other studies on polymer-solvent systems have yielded similar results.[34-39]

Coupling the findings of the polymer-solvent system along with the theoretical predictions of the molecular weight dependence of the CST's, the PS/p(2-ClS) blend system exhibited an hourglass-type phase diagram for the higher molecular weight polystyrenes. At a certain critical MW, the LCST and the UCST separate to form two separate regions of phase instability. For the p(2-ClS) blends studied above, this critical molecular weight lies somewhere between 26,700 and 30,400. However, these figures could change depending on the physical properties of the p(2-ClS).

Many factors confirm the existence of an hourglass-shaped diagram for the higher MW blends. Once the polymer was phase

separated, lengthy annealing times near the Tg of p(2-ClS) did not begin to show the reversible progress towards the one-phase system. Moreover, this was true for each PS molecular weight blend with p(2-ClS) that exhibited phase separation. One would expect that the PS(32.4) blend would not phase separate at 150°C if the LCST for the PS(50) blend was about 150°C. Again theoretical predictions showed an increase in the LCST of 150°C with a decrease in MW of 20,000.

An argument that could be used to explain the DSC results was that the LCST was located well below the Tg for PS(50)/p(2-ClS), lay slightly below Tg for PS(32.4)/p(2-ClS) and was very high for PS(20.4)/p(2-ClS). Positive values of ΔH_m for the higher MW systems, which were sufficient evidence for incompatibility at the experimental temperature, lent some credence to the existence of solely an LCST. However, positive ΔH_m values were also found for the lower MW blends. Neither of these blends could be phase separated at elevated temperatures. However, positive ΔH_m indicated incompatibility at 35°C. Therefore, 35°C would be below the UCST for the lower MW blends.

The approach used to explain the experimental results was as follows. Blends of p(2-ClS) with PS(50) and PS(37) possessed an hourglass-type phase diagram centered around the midcomposition range. Figure 5.24 is the phase diagram for PS(50)/p(2-ClS) as determined by DSC. The diagram was formulated by annealing at a certain temperature, quenching and measuring the Tg(s). From plots of Tg vs. blend composition, the composition of the phase separated regions could be determined within 5-10% from the Tg's. The phase diagram for PS(37)/p(2-ClS) was similar to Figure 5.24 although the two-phase
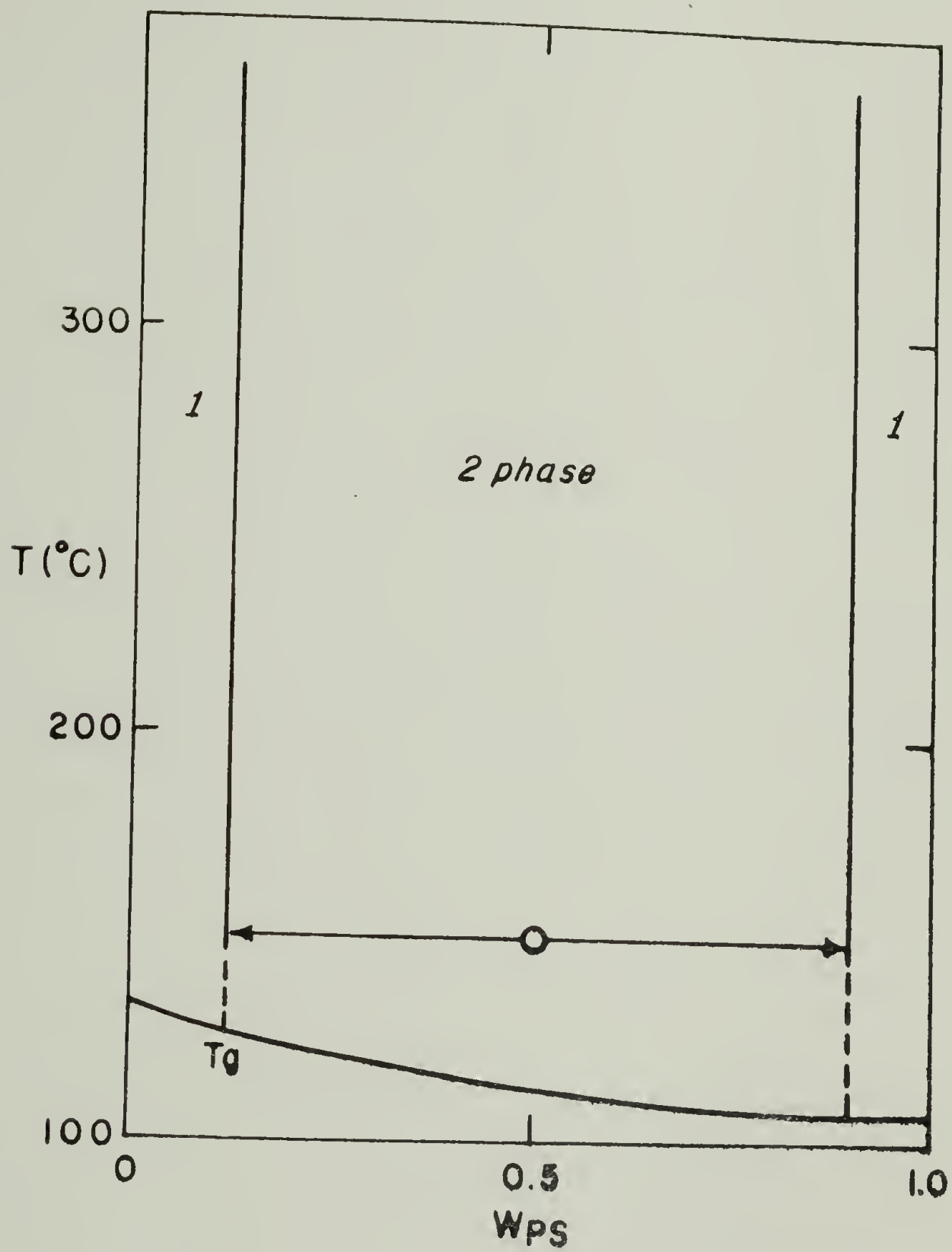
Figure 5.24. Phase diagram for PS(50)/p(2-ClS) above Tg.

region was narrowed. Therefore for p(2-ClS) blends with PS, molecular weight over 32,000, the LCST was less than the UCST, i.e., an hourglass phase diagram.

The LCST then became higher than the UCST at MW below about 32,000. However, the detection by DSC of the one-phase region between the UCST and the LCST was difficult. If it was postulated that the CST's started to diverge at around 280°C, both DSC and ΔH_m results could be explained. Should the blend be compatible at 280°C, but immiscible at 270°C, DSC results could be very misleading. Annealing at 280°C would produce a one-phase system. However, upon quenching in the DSC, the blend passes through the UCST into the two-phase region at temperatures well above the Tg. The mobility would be sufficient to allow phase separation. When rescanned, two Tg's would be evident, mistakenly assumed to reflect the equilibrium state at 280°C. In spite of numerous attempts at mixing different molecular weight polystyrene and blending with p(2-ClS), the UCST could not be lowered enough to allow its unequivocal determination. Blends rich in one component that might allow easier study of the lower phase boundary due to the shape of the phase diagram were not studied because of a scarcity of sample.

Following the above postulation on the relationship of the CST's, blends of PS(20.4)/p(2-ClS) would possess a UCST slightly below the Tg, whereas the LCST would then be above degradation temperatures. Assume T_{avg} (= ½(LCST + UCST)) equaled 280°C. If the UCST appeared at 110°C, the LCST would lie near 450°C, well above degradation temperatures. Positive ΔH_m for PS(20.4)/p(2-ClS) blends in the midcomposition

region again pointed to immiscibility at 35°C, below the supposed UCST. The ΔH_m values at the composition edges for this blend were negative. This indicated that the phase boundary for the PS(20.4)/p(2-ClS) system ran somewhere between 90/10 and 70/30 on one side and 30/70 and 10/90 on the other at 35°C. This finding was consistent with the existence of the UCST between 35°C and Tg.

For the PS(9)/p(2-ClS) blends, the UCST would be lower than for the PS(20.4) blend. However, since ΔH_m was found to be positive, the UCST would still be above 35°C. Blends of PS(9)/p(2-ClS) were very brittle and difficult to handle and were not studied extensively.

The above explanation of the experimental findings relied on the existence of an UCST and an LCST centered around a temperature of near 280°C. This was postulated in order to reflect the MW dependence of the CST's along with the consistent findings of ΔH_m greater than zero. It was assumed that the locus of the CST's was near the mid-compositional ranges for each blend and did not shift substantially with MW. This had been found for polymer-solvent systems exhibiting both critical temperatures. Another assumption was that T_{avg} did not change with polystyrene MW over the range studied. Polymer-solvent systems supported this assumption also.

The question then encountered is why the unstable blends were initially one-phase. Both freeze-drying and solvent casting techniques produced compatible polymer blends. Blends cast from benzene at both room temperature and 80°C yielded one-phase systems. The only explanation was that since the thermodynamically unstable blend was nearly stable, the blending technique was such to force compatibility. Shultz

and Mankin[40] determined that freeze-drying PS/PMMA blends allowed a considerable degree of intermixing in a thermodynamically incompatible system. In a system that was only slightly incompatible, the blending technique forced total mixing of polymers.

The hypothesis on the existence of an UCST for the PS/p(2-ClS) system rested exclusively with the measurement of a positive ΔH_m. The entropy term, $T\Delta S_m$, was assumed to be dwarfed by the enthalpic term such that ΔH_m would approximate ΔG_m. The thermodynamics of blending relied on the behavior of ΔG_m with composition whereas experimentally, ΔH_m was measured. The magnitude of $T\Delta S_m$ could be computed utilizing Flory-Huggins theory. The entropy of mixing can be derived from the lattice representation by[25,41]

$$\frac{-\Delta S_m}{NR} = \frac{\phi_1}{x_1} \ln \phi_1 + \frac{\phi_2}{x_2} \ln \phi_2 \tag{5.8}$$

where ϕ_i are the volume fractions, x_i the degree of polymerization, and N the total number of lattice points. From the density data of Fried,[12] the volume fractions for each blend composition could be calculated. The degree of polymerization was determined from the molecular weights. Table 5.9 lists the values for ϕ_i for each blend composition and Table 5.10 contains the values for x_i used in Eqn. (5.8). Using the quantities given in the tables and plugging into Eqn. (5.8), values of $T\Delta S_m$ (T = 308°K) in units of J/gm were determined. Table 5.11 lists the values of $T\Delta S_m$ and Figure 5.25 plots the entropic term as a function of composition for each blend listed. Comparison of Figure 5.25 with Figures 5.13 through 5.20 shows that the $T\Delta S_m$ term

Table 5.9. Calculated Volume Fractions for PS/p(2-ClS) Blends.

Composition	ϕ_1	ϕ_2
70/30	.74	.26
50/50	.54	.46
30/70	.34	.66

Table 5.10. Degree of Polymerization, X_i.

System	X
PS(50)	480
PS(37)	356
PS(20.4)	196
PS(9)	87
p(2-ClS)	416

Table 5.11. Values of $T\Delta S_m$ for PS(MW)/p(2-ClS).

System	70/30	50/50	30/70
PS(50)	2.98×10^{-2} J/gm	3.34×10^{-2} J/gm	2.89×10^{-2} J/gm
PS(37)	3.35	4.09	3.43
PS(20.4)	4.51	5.51	5.14
PS(9)	7.76	10.09	9.91
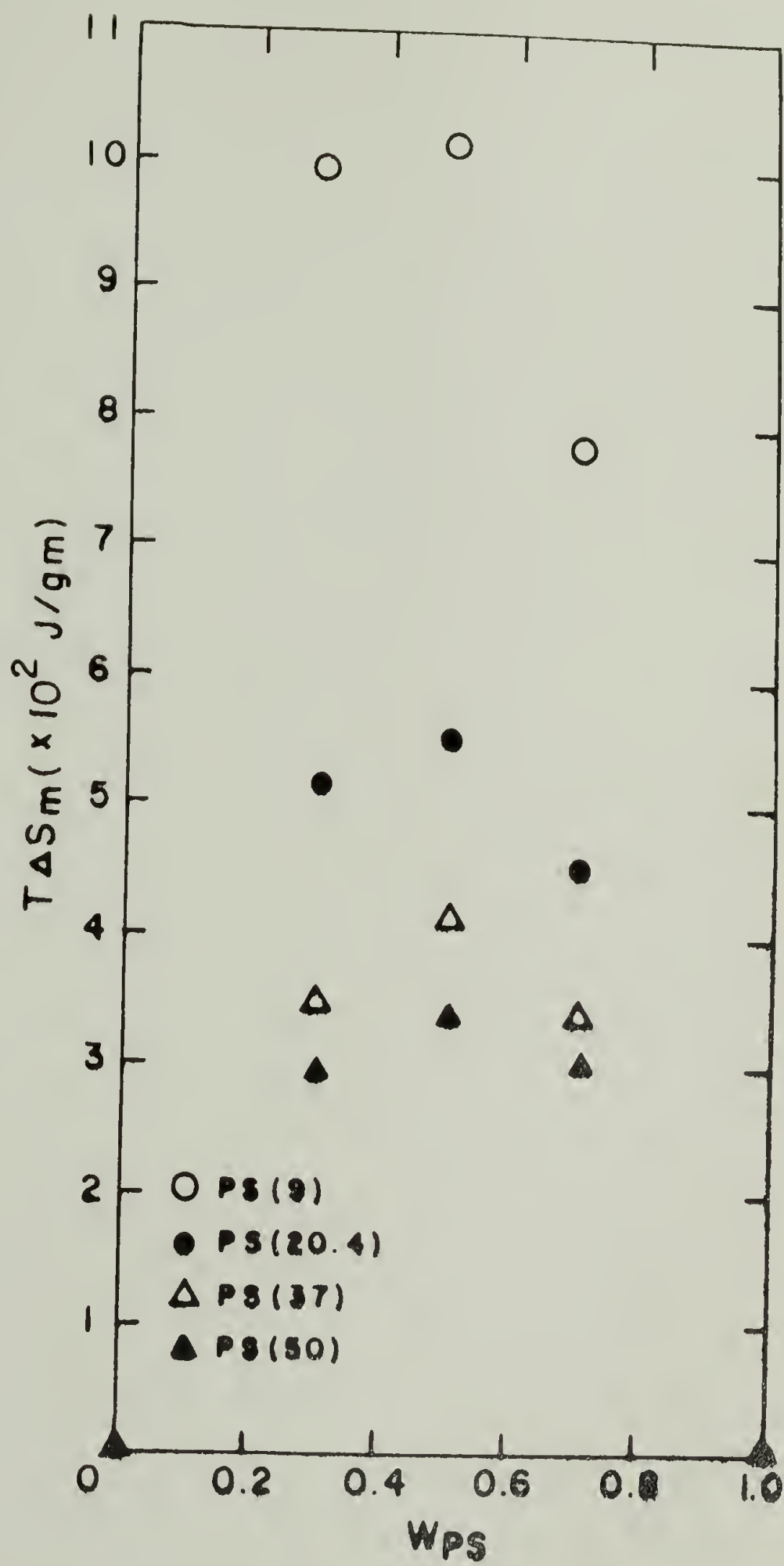
Figure 5.25. $T\Delta S_m$ vs. W_{PS} for PS/p(2-ClS) blends.

was 2-3 orders of magnitude smaller than ΔH_m even for the lower molecular weight PS blends.

The calculation of the entropy of mixing was based on classical Flory-Huggins lattice theory. Although the theory breaks down for polymer-solvent systems, qualitative results were possible for polymer-polymer systems. However, a more satisfying theoretical explanation on the phase behavior of PS/p(2-ClS) blends was based on the lattice fluid theory of Sanchez.[22-24]

According to lattice fluid theory, the condition for phase stability is given by

$$\tilde{\rho}(2\chi + \tilde{T}\psi^2 P^* \beta) < \frac{1}{r_1\phi_1} + \frac{1}{r_2\phi_2} \tag{5.9}$$

where $\tilde{\rho}$ is the reduced density, χ the enthalpic interaction parameter, $\tilde{T}$ the reduced temperature, ψ a term containing volume fractions, temperature and interaction energies, P^* the characteristic pressure, β the isothermal compressibility of the mixture, r_i the number of mers and ϕ_i the volume fractions. Since the right-hand side of Eqn. (5.9) is temperature independent, the general features of the phase diagram could be ascertained from the determination of the temperature dependence of χ and $T\psi^2 P^* \beta$. χ is either positive or negative and is inversely proportional to temperature. The term $T\psi^2 P^* \beta$ is always positive and in most cases increases monotonically with temperature. Figure 5.26 illustrates the general behavior of these terms as a function of temperature. The dashed lines are the summation of the two terms. The right-hand side of Eqn. (5.9) is much more molecular weight
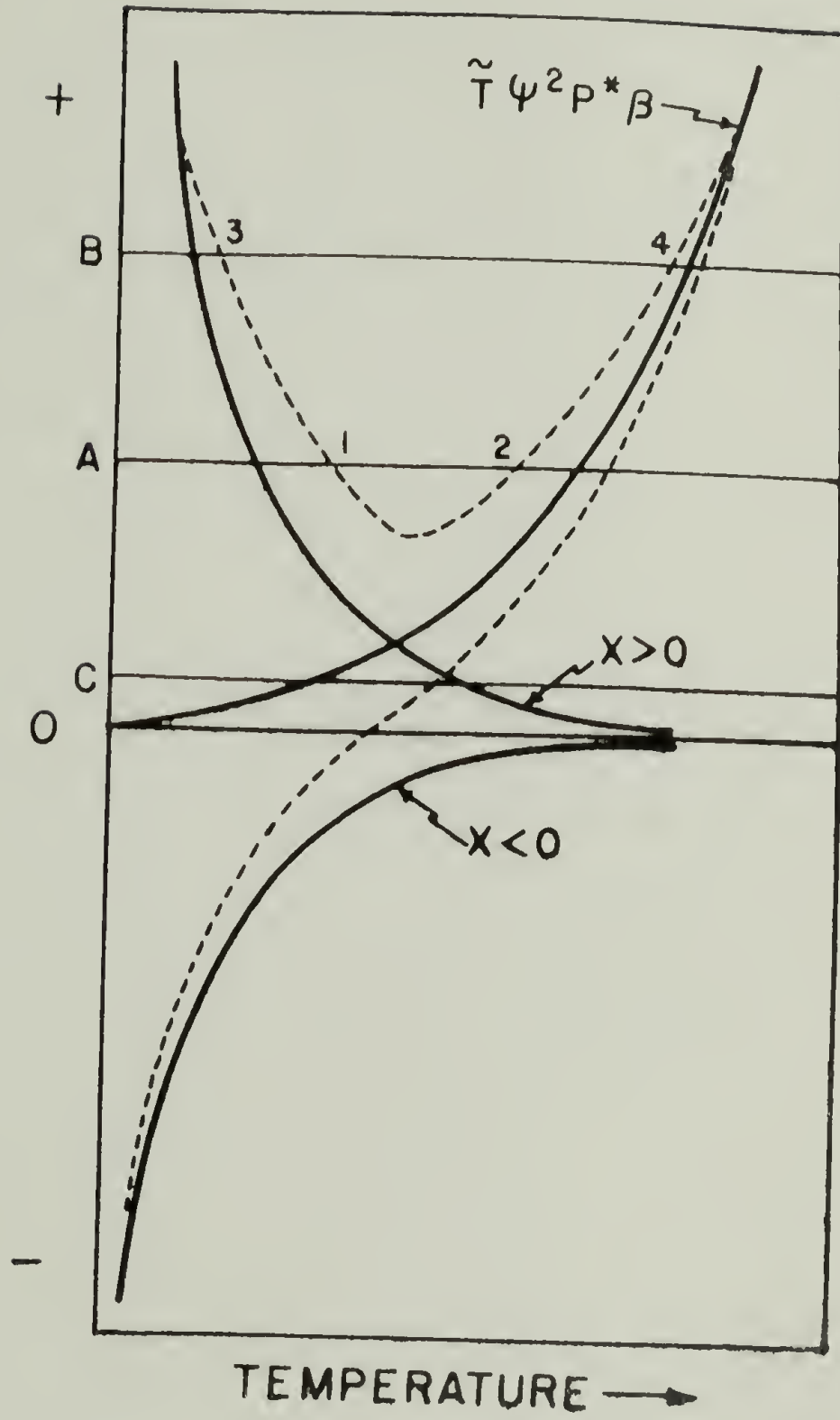
Figure 5.26. Temperature dependence of χ and $T\psi^2 P^*\beta$.

dependent than the left-hand side. As the molecular weight is increased, the RHS terms decrease, from B to A in Figure 5.26. The locus of the CST's is where the RHS of Eqn. (5.9) equals the LHS. For the higher molecular weight blends, the UCST would correspond to point 1 in the figure whereas the LCST is indicated by point 2. The region of phase stability is in the temperature range between 1 and 2. Analogously, the UCST for the lower MW blends is indicated by point 3 and the LCST by point 4. The region of phase stability is increased and the UCST decreases whereas the LCST increases for the lower molecular weights.

The experimental results indicated a large MW dependence of the CST's. Moreover, Sanchez predicted that the behavior of the critical temperature with MW was entropy controlled. The RHS of Eqn. (5.9) is entropic in nature whereas the LHS contains all the enthalpic contributions to the free energy. These enthalpic terms are not highly MW dependent. In the experimental determination of ΔH_m, the magnitude of ΔH_m did not change substantially as the MW of the PS was lowered. This is consistent with the theoretical implications of Sanchez that the mixing is entropy controlled. For the higher MW blends, the entropy is very small compared to the enthalpic terms. In Figure 5.26, the RHS of Eqn. (5.9) would lie near zero (line C). The result would be phase instability at all temperatures for that composition. As the MW of one or both of the components is decreased, the entropic contribution increases to form regions of phase stability as embodied in lines A and B. Moreover, if the LHS of Eqn. (5.9) is symmetrical with temperature, the midpoint temperature, T_{avg}, would not

change with MW.

Since the existence of a polymer-polymer UCST was not un-
equivocally found for the PS/p(2-ClS) system, the experimental results
could also be explained using the lower dashed curve in Figure 5.26.
This curve would only predict the existence of an LCST and also shows
the MW dependence of the LCST. However, since DSC results showed that
the LCST would have to increase over 250°C with a change in molecular
weight of only 3700, it was felt that the earlier based on the separa-
tion of the CST's near 280°C, was valid.

F. Heats of Mixing Poly(4-fluorostyrene-co-2-fluorostyrene) Copolymers with Polystyrene and PPO

Poly(4-fluorostyrene) and poly(2-fluorostyrene) have been found
to be incompatible with PPO.[27-29] However, certain copolymers of the
two exhibited one-phase behavior when blended with PPO. The purpose of
this section was to follow the behavior of ΔH_m as a function of copoly-
mer composition in blends, 50/50, with PPO and PS.

The Tg's of the pure components p(4-FlS) and p(2-FlS) were
found to be 383.5°K and 365.4°K, respectively, whereas PS possessed a
Tg of 378.0°K. Due to the close proximity of Tg's, the phase diagrams
of blends of PS with the homopolymers and copolymers could not be deter-
mined by DSC. A difference of at least 30°C in Tg was needed to ascer-
tain the existence of one or two Tg's for the blend. Therefore, ΔH_m
was determined for the copolymer/PS blends in the hope of elucidating
the phase behavior of these blends. Figure 5.27 is a plot of ΔH_m as a
function of copolymer composition for 50/50 blends of PS with
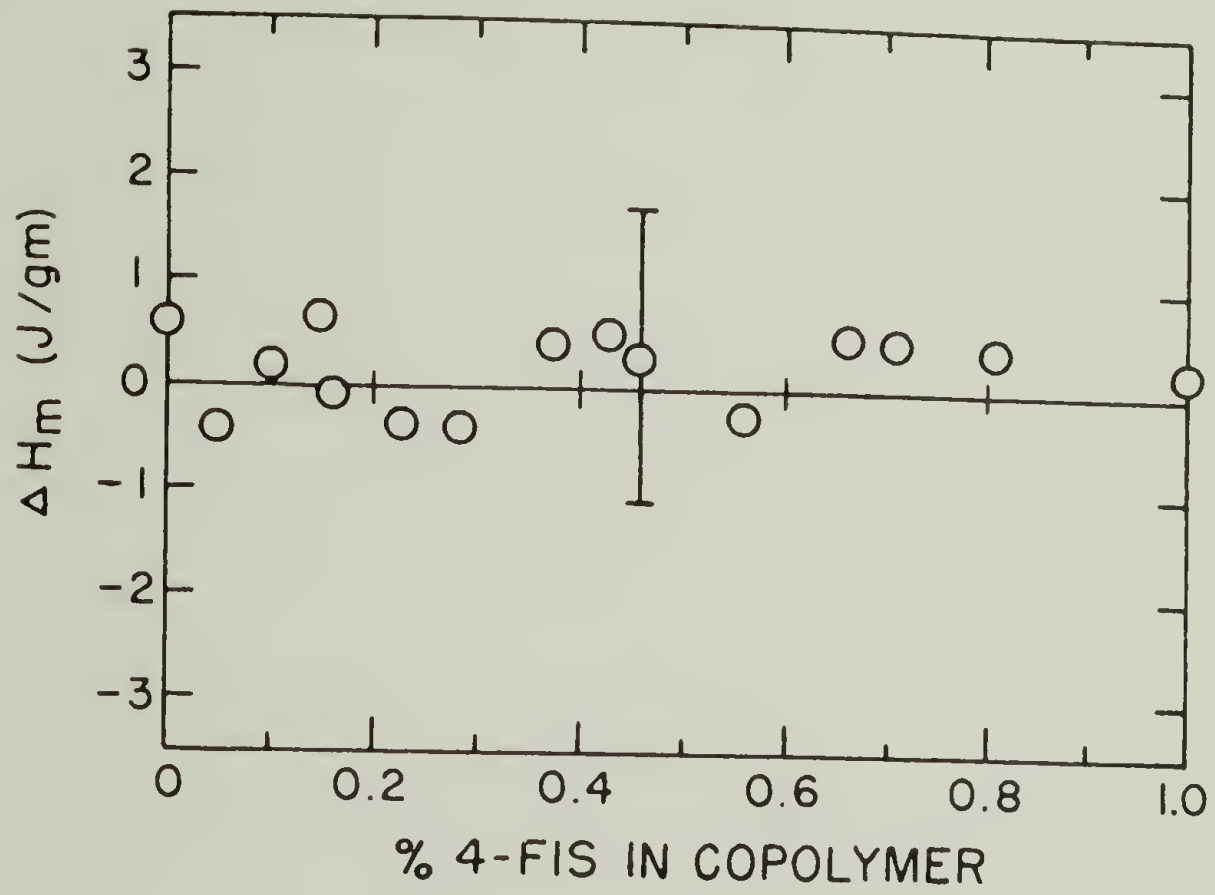
Figure 5.27. ΔH_m vs. copolymer composition (mole fraction 4-FlS) for 50/50 PS blends with p(4-FlS-co-2-FlS).

p(4-FlS-co-2-FlS) at 34.8°C. Within experimental error, each value of ΔH_m was found to be zero. Unfortunately, this finding did not serve to completely clear up the question of blend compatibility. Although $\Delta H_m = 0$ for an incompatible system, the magnitude of ΔH_m might have been so small for this compatible system as to be immeasurable. However, DSC studies appeared to have yielded two Tg's for each PS blend, although the Tg's were not separate and distinct. Therefore, DSC and ΔH_m studies seemed to conclude that copolymers of 4-FlS and 2-FlS were not compatible with PS.

Vukovic[27-29] established the compatibility of certain copolymers of the fluorinated styrenes with PPO. The existence of a polymer-polymer LCST was established from DSC annealing experiments described earlier. Figure 5.28 illustrates the dependence of the phase separation temperature of 50/50 PPO blends on the copolymer composition. Between 0 and about 5% and from about 40 to 100% 4-FlS in the copolymer, blends with PPO (50/50) were incompatible at all temperatures. Between 5 and 40%, the copolymers blended 50/50 with PPO were one-phase depending on the annealing temperature. Values of ΔH_m were thus determined in order to study the effect of phase boundary on ΔH_m. Figure 5.29 illustrates the behavior of ΔH_m as a function of copolymer composition for blends with PPO 50/50. The data for two experimental temperatures is shown. The line was drawn to help visualize the trend in ΔH_m. The behavior of ΔH_m, although at first quite puzzling, could be explained through the use of phase diagrams. Figure 5.30 shows the effect of phase diagram on ΔH_m. For incompatible polymer blends, ΔH_m was identically zero. This was found for the completely immiscible
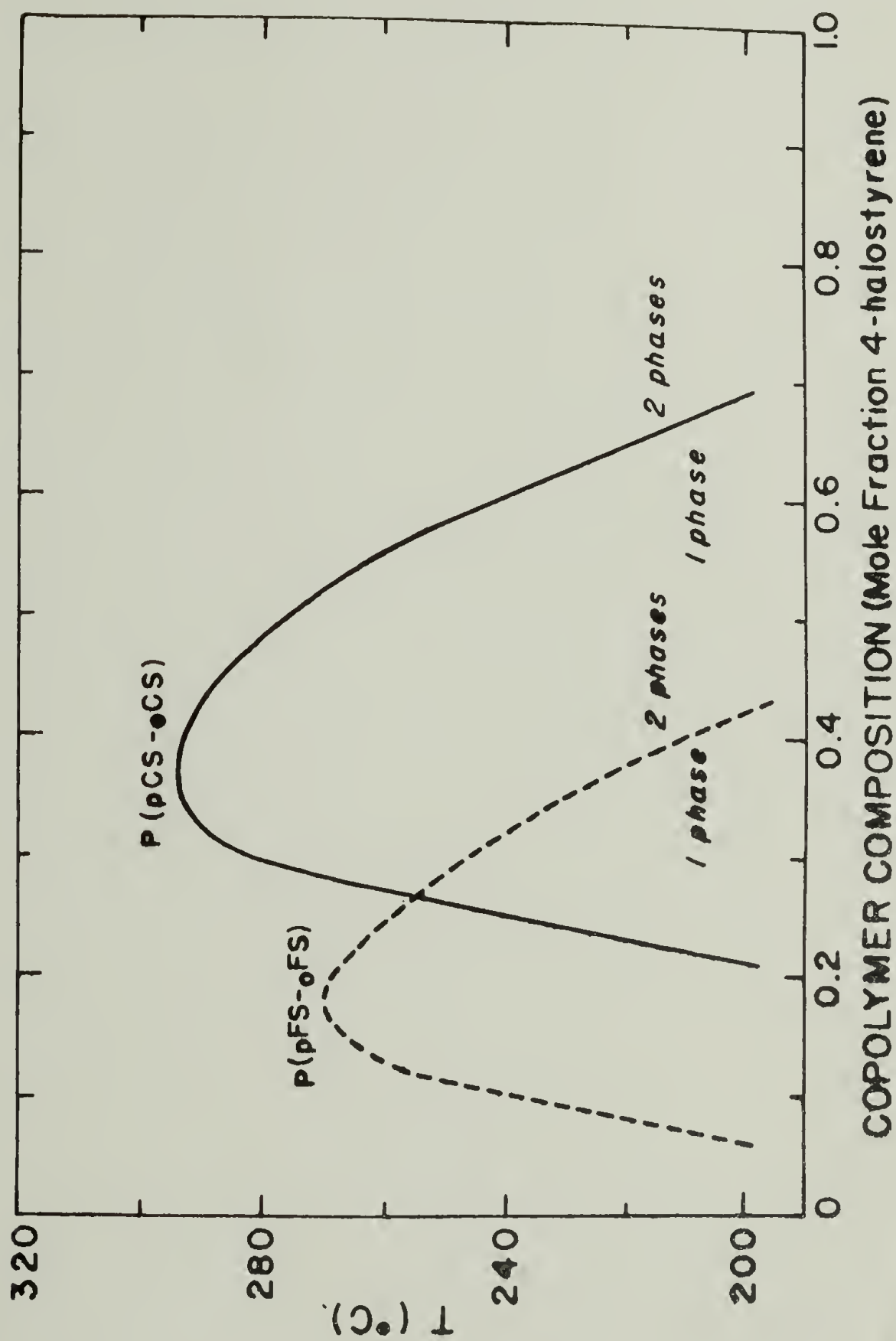
Figure 5.28. Phase separation temperature of 50/50 PPO blends with p(4-F1S-co-2-F1S) vs. copolymer composition.
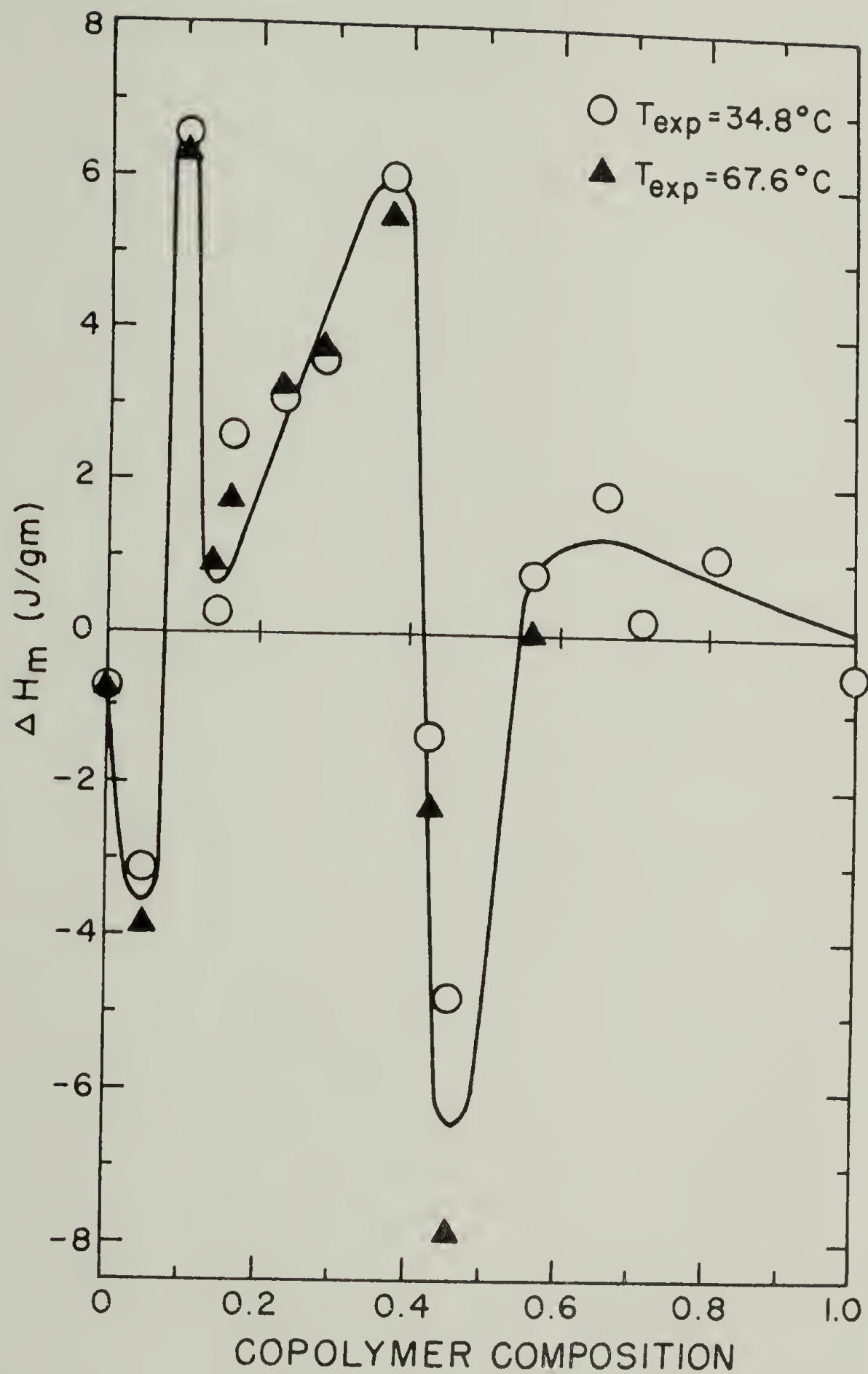
Figure 5.29. ΔH_m vs. copolymer composition (mole fraction 4-F1S) for 50/50 PPO blends with p(4-F1S-co-2-F1S).
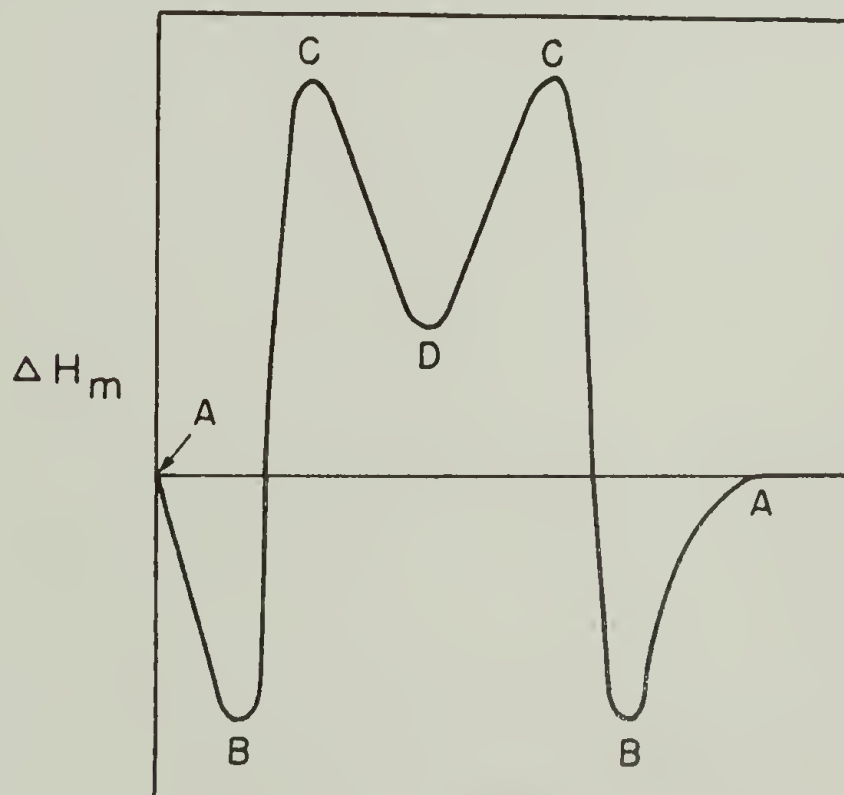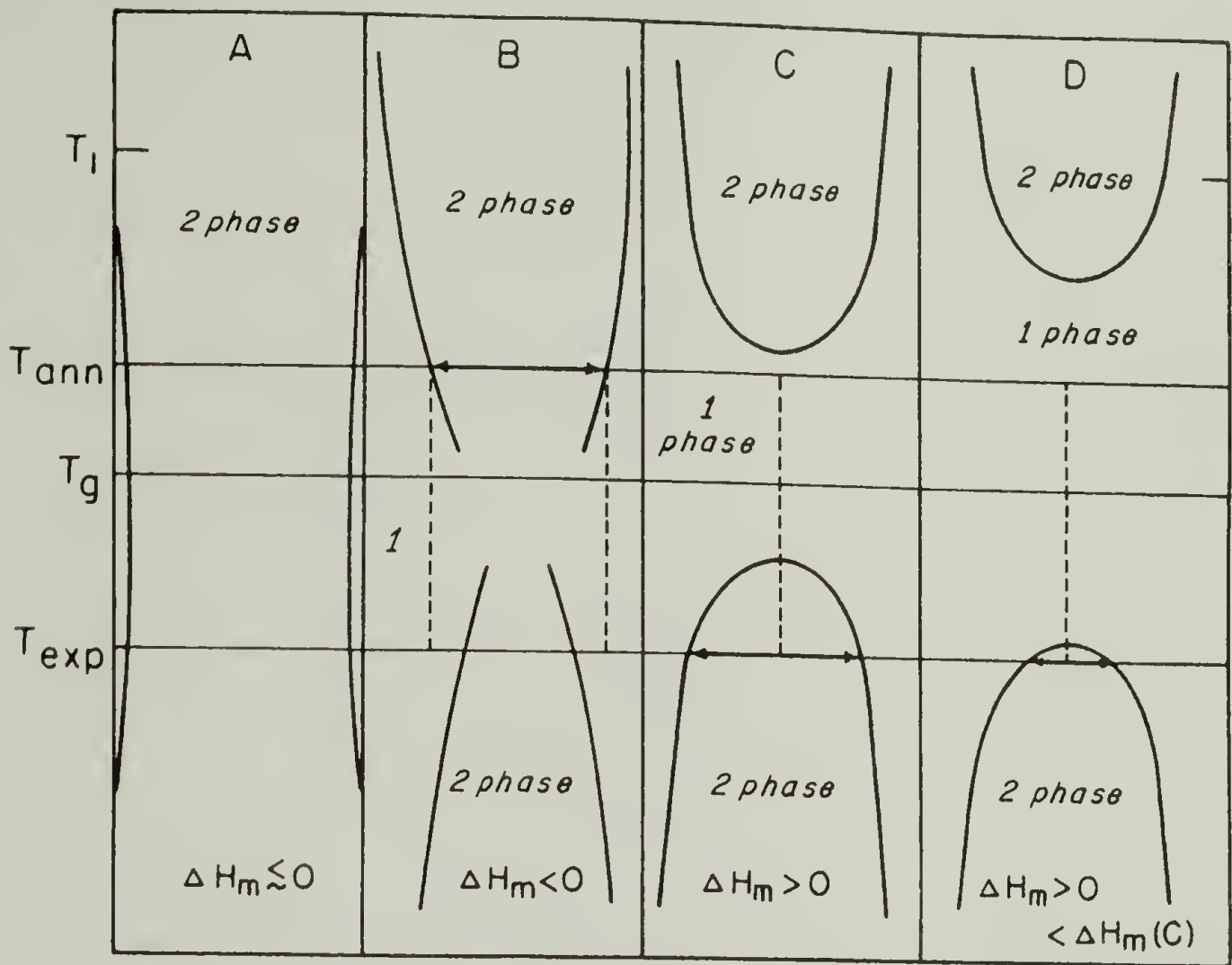
Figure 5.30. Effect of phase diagram on ΔH_m.

copolymer blends. For partially miscible polymer blends, curve B, negative values of ΔH_m would be expected. Copolymers with 5.2%, 42.3% and 45.6% 4-FlS were found by DSC to be partially miscible with PPO. Two Tg's were established for these blends, however these Tg's did not correspond to the pure component Tg's. Negative values of ΔH_m were also found for these copolymer blends.

As was established for PS/p(2-ClS) blends, positive values of ΔH_m were a sufficient condition for polymer incompatibility at the experimental temperature. Therefore, positive ΔH_m would point to the existence of a polymer-polymer UCST. Curve C illustrates the conditions needed for a positive ΔH_m. P(4-FlS(.101)-2-FlS) and p(4-FlS(.375)-2-FlS) blends with PPO gave very large (about 6 J/gm) positive values of ΔH_m. This compares to the large negative value (-5 J/gm) found for PS/PPO. Curve D shows the case for a less positive value of ΔH_m as was found for copolymer blends with PPO with 4-FlS percent equal to 14.6, 16.2, 22.8 and 23.5. The parallel between the effect of copolymer composition on ΔH_m and the LCST (Figures 5.28 and 5.29) lent credence to the above explanation.

Further experiments were performed in order to confirm the previous hypothesis. By varying the annealing temperature, ΔH_m should become more positive or negative depending on which phase diagram would be applicable. For example, if the polymer blend which possessed the phase diagram C or D in Figure 5.30 were annealed at T_1, two phases would result. The new value for ΔH_m even became negative as was the case for diagram B. Also, should the polymer blend be held at T_1 in phase diagram B, two phases would still be present. However, the two

phases would be composed of nearly pure homopolymers. Therefore, ΔH_m would approach zero.

Figure 5.31 shows the results of a series of annealing experiments. When annealed at 250°C, ΔH_m for p(4-F1S(.052)-2-F1S)/PPO changed from -3.1 to +1.2 J/gm. This was an example of the approach to $\Delta H_m = 0$ for complete phase separation. Another example was for the blend p(4-F1S(.428)-2-F1S)/PPO where ΔH_m changed from -1.4 to -0.6 J/gm upon annealing. There were also three examples of a drop from positive ΔH_m towards negative ΔH_m values. Upon annealing the samples at 250°C, values of ΔH_m at 34.8°C fell from large positive values to negative values for the PPO blends with p(4-F1S(.101)-2-F1S) and with p(4-F1S(.375)-2-F1S). These findings were also consistent with the earlier explanations on the behavior of ΔH_m with annealing temperature.

P(4-F1S(.162)-2-F1S) blends with PPO were annealed at three separate temperatures. Using annealing temperatures of 250 and 270°C, the blend was still one-phase as determined by DSC. However, ΔH_m became more positive. This finding was somewhat inconsistent. As the annealing temperature was raised, the point of phase separation was approached. Therefore, one might expect that the interpolymeric interaction energy to decrease in magnitude. Since a positive ΔH_m was actually the heat of demixing, the magnitude of ΔH_m would also be expected to decrease. This was not found however. Upon annealing above the phase separation temperature, ΔH_m did decrease drastically and actually became negative, as was found in the other annealing studies. Finally, a comparison could be made for the measurement of ΔH_m at two temperatures. Most values of ΔH_m at 34.8 and 67.6°C were the same.
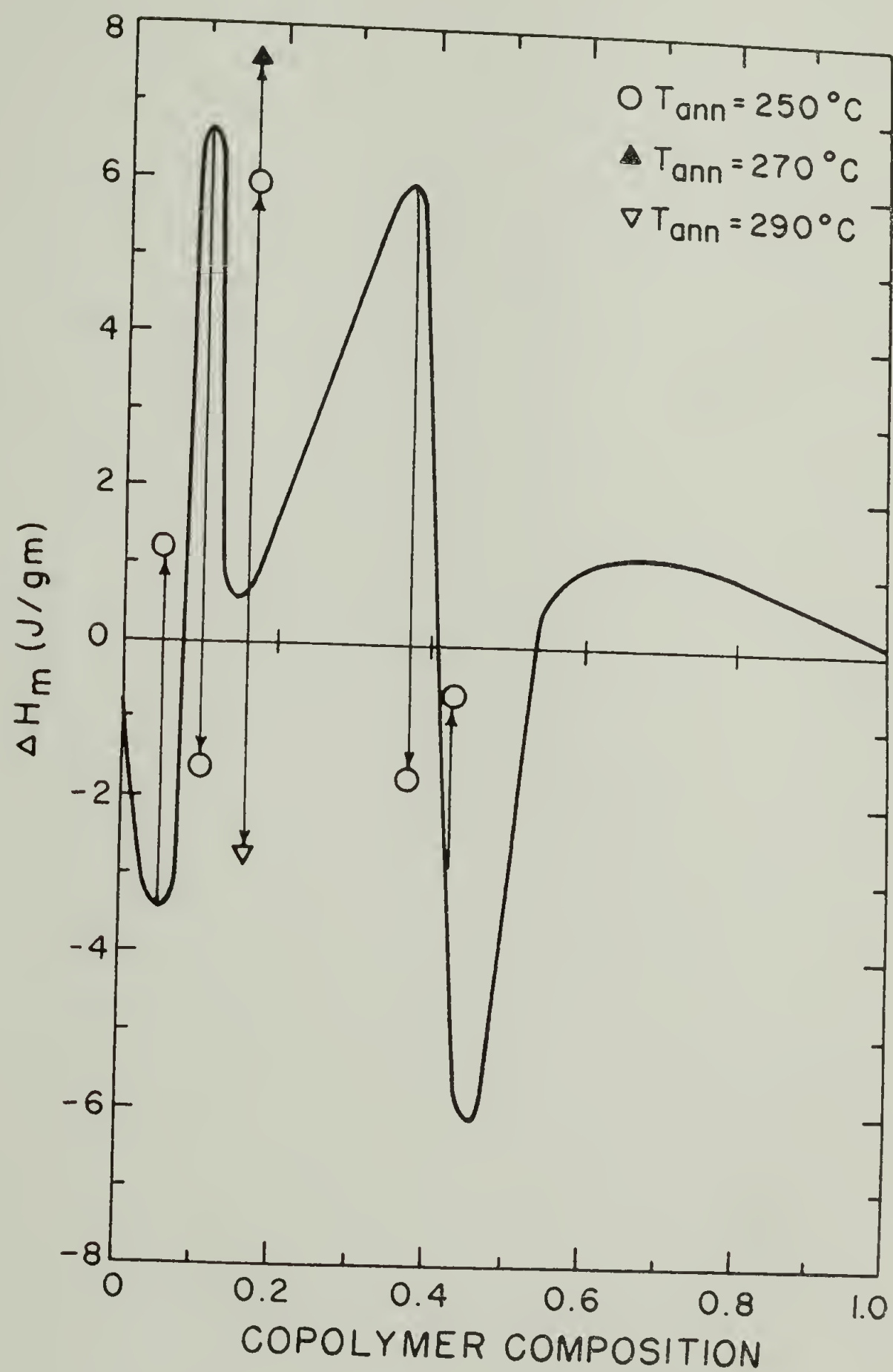
Figure 5.31.   Change in ΔH_m with annealing temperature for PPO
blends with poly(4-F1S-co-2-F1S).

However, on the periphery of the compatible copolymers, namely p(4-FlS(.052)-2-FlS) and p(4-FlS(.456)-2-FlS) blends, ΔH_m was much more negative for the higher experimental temperature. This result would be expected since in diagram B, Figure 5.30, the region of phase in-compatibility would be narrower at the higher experimental temperature. However, the temperature difference between the experimental tempera-tures was not large enough to affect the behavior of ΔH_m for the other copolymer blends.

The effect of blend composition on ΔH_m was done for blends of p(4-FlS(.285)-2-FlS)/PPO. Figure 5.32 illustrates the behavior of ΔH_m. The maximum in ΔH_m occurred near the 50/50 blend whereas all values found were positive heats of mixing. It is important to note that the copolymer study only utilized 50/50 blends with PPO. A more complete examination would also take into account different blend compositions. It was assumed in these studies that the LCST would occur at a blend composition near 50/50 for each compatible blend, i.e., a change in co-polymer composition would not greatly affect the shape of the phase diagram other than a shifting in temperature. Since the molecular weights of the copolymers were quite similar and the range of copoly-mer composition, over which compatibility was found, being small, it was felt that the above assumptions were not severe.

Whereas the positive heats of mixing were very small for the PS/p(2-ClS) system, the large ΔH_m values found for some of the copoly-mer blends pointed unequivocally to the existence of a polymer-polymer UCST. As was the case for the LCST, the existence of an UCST appeared to be more prevalent than previously believed. The problem was the
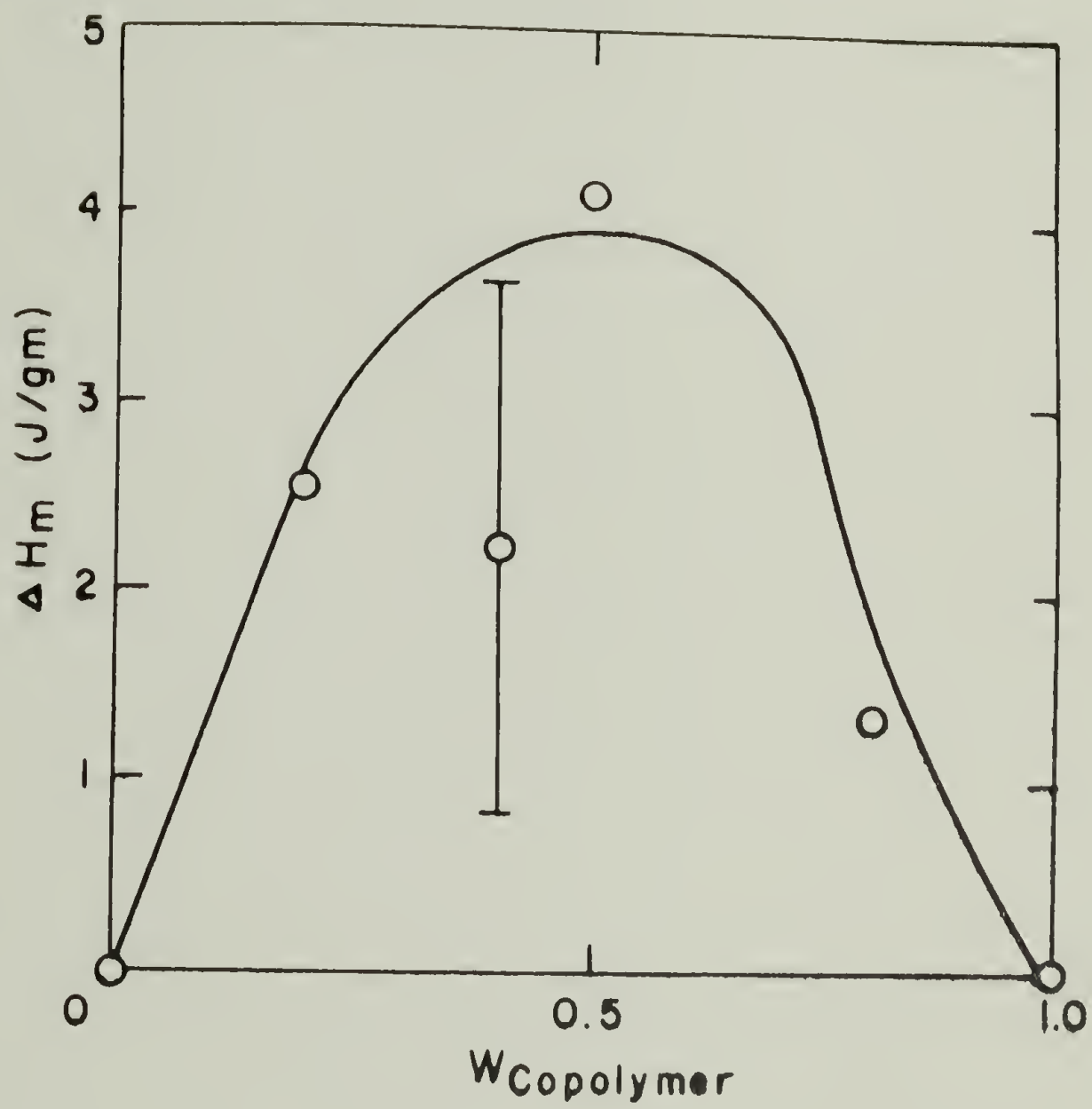
Figure 5.32. ΔH_m vs. blend composition for p(4-F1S(.285)-2-F1S)/PPO.

inability to probe equilibrium states below the Tg. The approach util-
ized in these studies allowed exploration below Tg.

G. Compatibility of Bromo-substituted Polystyrene Copolymers Blended with PPO and PS

The purpose of this study was to extend the work of Vukovic[27-29]
(fluorinated copolymers) and Alexandrovich[16,30] (chlorinated copoly-
mers) to the brominated and methylated copolymers of styrene. The be-
havior of the polymer-polymer systems could then be correlated to the
type and placement of the substituent.

Both Vukovic and Alexandrovich found that when certain amounts
of a halogen-substituted styrene were copolymerized with styrene,
blends with PPO could be either miscible or immiscible depending on
the copolymer composition and the annealing temperature. Figure 5.33
shows the phase separation temperature of blends (50/50) of PPO with
copolymers of styrene and either the 2- or 4- substituted fluorinated
or chlorinated styrenes. Whereas the 2-chlorostyrene copolymer and
the 4-chlorostyrene copolymer blends with PPO were quite similar in
phase separation behavior, more 2-FlS than 4-FlS was required in the
copolymer with styrene to produce incompatibility with PPO. Just the
opposite was found for the brominated styrene copolymer blends with PPO.
As can be seen in Figure 5.33, less 2-BrS than 4-BrS was needed in the
copolymer in order to induce incompatibility with PPO.

Poly(4-methyl styrene) was found to be compatible with PPO.
It had been expected that due to the comparable size of the methyl and
chlorine side groups, the methyl-substituted styrene copolymers would
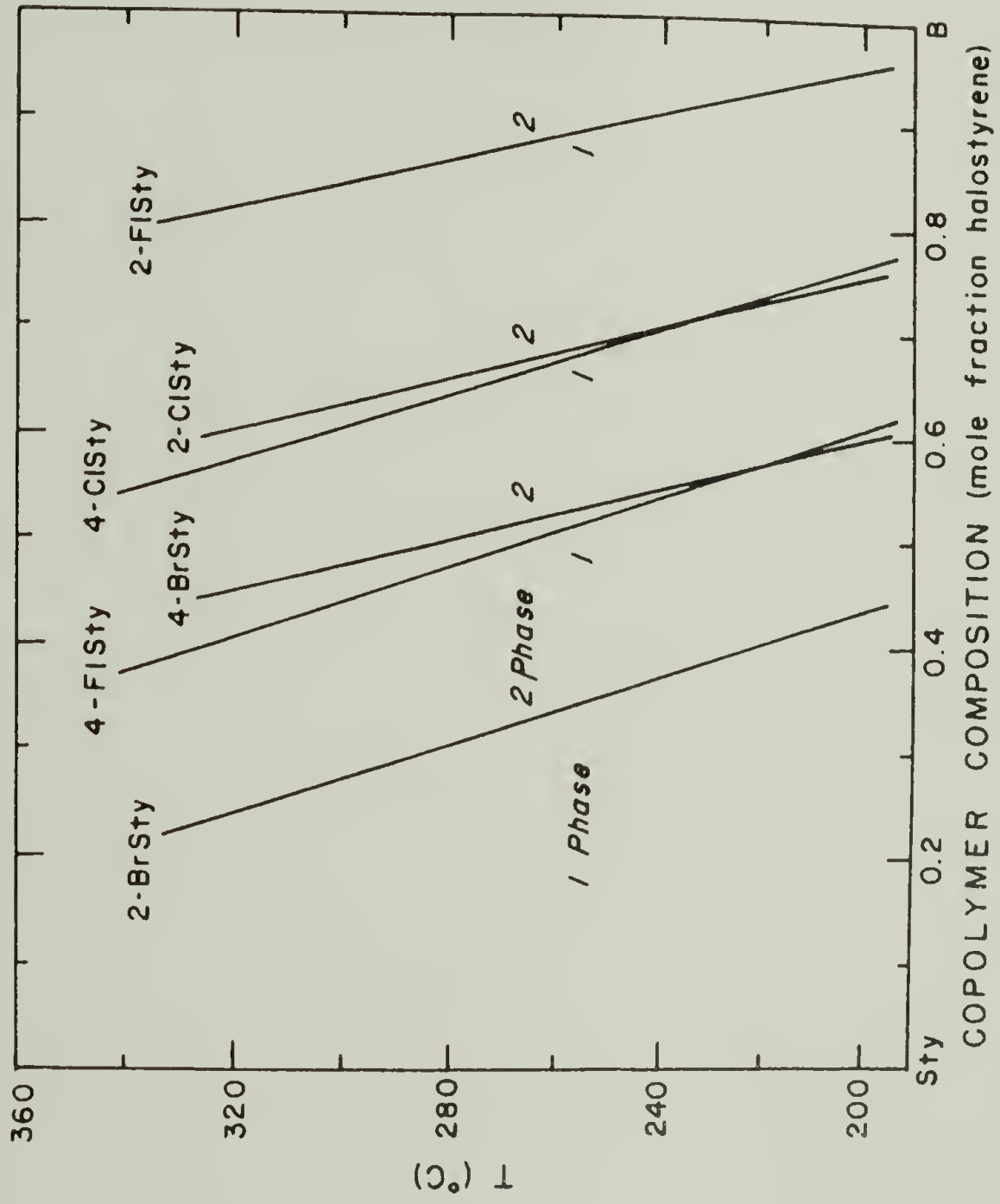
Figure 5.33. Phase separation temperatures of halogenated styrene copolymers blended 50/50 with PPO.

behave similarly to the chlorine-substituted copolymer blends with PPO. However, this was not found to be the case. From the above studies, the ability of the substituent to induce incompatibility in PS/PPO blends could be established as:

$$2\text{-Br} > 4\text{-Fl} \cong 4\text{-Br} > 4\text{-Cl} \cong 2\text{-Cl} > 2\text{-Fl} > 4\text{-Me.} \quad (5.10)$$

The ordering of the constituents and the effect on the compatibility will be discussed later.

From Figure 5.33, it can be seen that the halogenated polystyrene homopolymers were all found to be incompatible with PPO, at least within accessible molding temperatures. Vukovic and Alexandrovich found, however, that copolymers of the 2- and 4- fluorinated or chlorinated styrenes were compatible with PPO over a certain copolymer range. Figure 5.34 illustrates their findings for 50/50 blends. The behavior of the heat of mixing of the fluorinated copolymer blends was discussed in the previous section. Extension to the brominated system was the natural course of the above work. The expected result was that the brominated styrene copolymers blended with PPO would follow a simple-minded progression from the fluorine to chlorine substitution. Using such reasoning, the compatibility window of the brominated styrene blends with PPO would be larger and shifted somewhat towards higher 4-BrS content. However, experimental findings shattered this preconceived notion. It was found that none of the copolymers of 2-BrS with 4-BrS blended 50/50 with PPO were compatible. All yielded cloudy films that exhibited two Tg's corresponding to the pure components. The copolymer composition studied varied over the entire
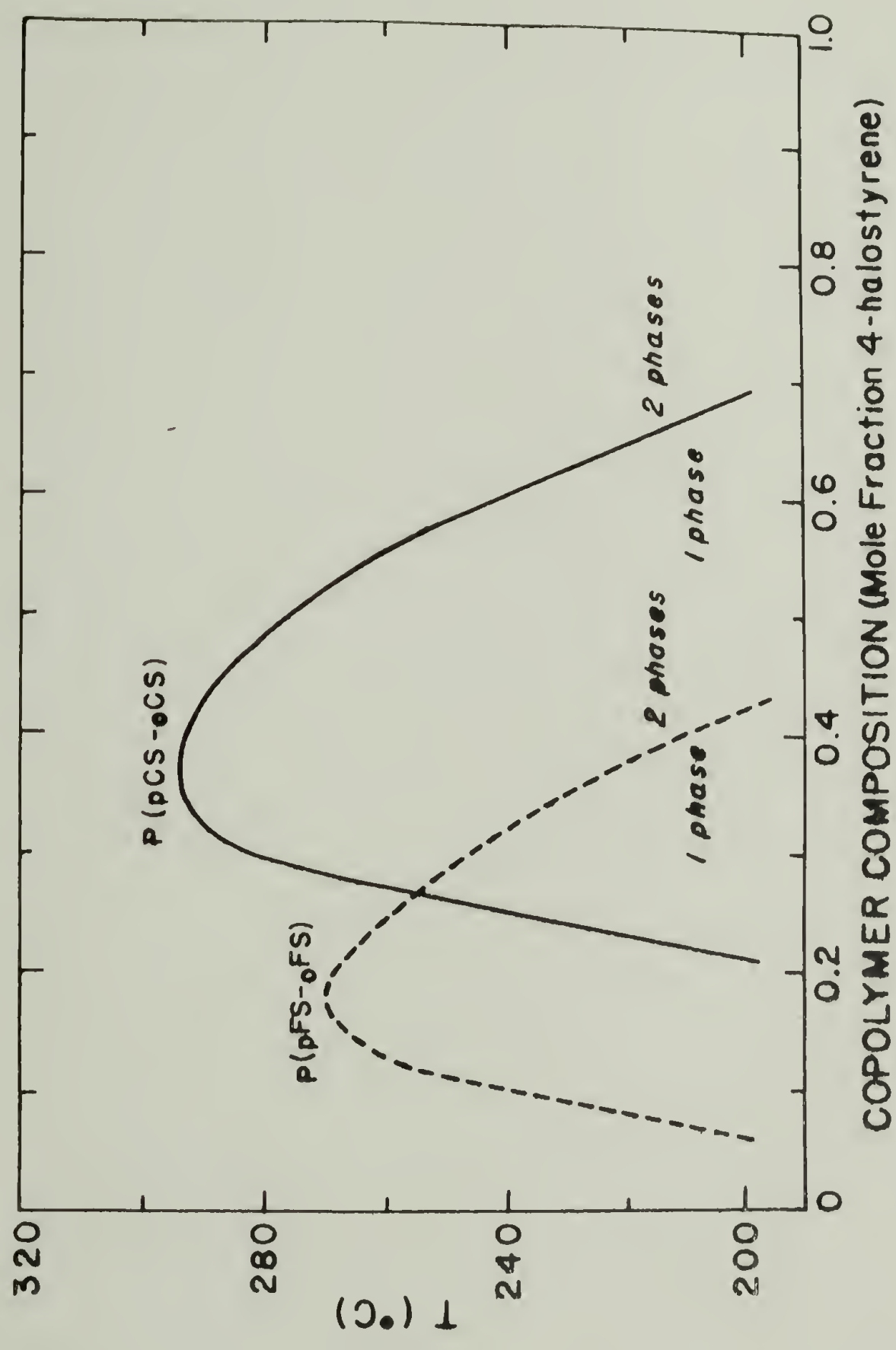
Figure 5.34. Phase separation behavior of PPO blends with p(4-FlS-co-2-FlS) and p(4-ClS-co-2-ClS) as a function of copolymer composition.

range differing from sample-to-sample by only about 10% in composition.

The brominated copolymers were also blended with PS to study the phase stability. The problem with copolymers of styrene and brominated styrene blended with polystyrene was that the higher the styrene content in the copolymer, the closer the Tg to that for pure polystyrene. Approximately a 20-30°C difference in Tg was needed to ascertain the existence of either a one phase or two phase system. However, for copolymers of 2-BrS with styrene with over 40 mole percent 2-BrS, blends with PS exhibited two distinct Tg's. The PS blend with p(2-BrS(.20)-S) appeared to exhibit a single Tg displaced from the pure component Tg's.

Copolymers of 4-BrS and styrene with 4-BrS content of over 50 mole percent 4-BrS were incompatible. Copolymer blends below 50% co-polymer composition were not prepared since this study was geared towards PPO blends. Therefore, copolymers of styrene and either 2- or 4-BrS were incompatible with PS when the brominated component was over 50 mole percent. The 2-BrS copolymers with styrene blended with PS appeared to undergo a miscible-immiscible transition somewhere between 20 and 40 mole percent 2-BrS. The same was true for the 4-BrS copolymers in the range 0-50 mole percent 4-BrS. Further work was warranted along these lines.

Analogous to what was found for the PPO blends, copolymers of 2-BrS and 4-BrS were not compatible with pure polystyrene for the accessible temperatures and compositions. The same finding was true for the fluorine-containing copolymers (see previous section). Analogous experiments had not been performed for the chlorinated styrene

copolymers.

The ordering of the effect of type and placement of the halogen substituent was given in Eqn. (5.10). The problem to be solved was why a certain halogen constituent promoted the formation of 1-1 type interactions at the expense of interpolymeric 1-2 contacts. Two effects appeared to be important. The electronegativity (polarity) of the halogen atoms decreases from F to Br. However, the bromine atom is the largest constituent of the three. Therefore, both polar and size effects were affecting the polymer-polymer compatibility.

When the halogen atom was in the 4-position, the dipole moment was perpendicular to the chain axis. Moreover, lack of steric hindrance in the para-position would promote polar modes of interactions between the 4-substituted polystyrenes. These interactions included dipole-dipole interactions and those due to London dispersion forces. Based solely on the polar intermolecular forces, one might predict that the order for inducing incompatibility of substituted polystyrene/PPO blends be 4-F > 4-Cl > 4-Br. The same reasoning could also be used for the 2-substituted polystyrene blends. However, since the direction of the dipole moment would be more along the chain axis, dipole-dipole interactions would be weaker. Steric hindrance would also limit the strength of the polar forces.

Concurrent with the intramolecular dipole-dipole interactions was the effect of substituent size. Whereas the polar effects were somewhat straightforward, size effects were much more complex. The larger halogen groups, Br and Cl, in the 2-position served to extend the unperturbed dimensions of the copolymers over the pure polystyrene.

Halogen substitution in the 4-position would have had the same effect, but not nearly as pronounced. Whereas it was difficult to ascertain the constituent size effect a priori, the ranking of the substituents showed there was a significant effect. The size effect was found to be contrary to the electronegativity effects. Whereas, polar effects were more prevalent in the fluorine-containing copolymers, the size of the bromine side group influenced the compatibility to a greater extent. Less 2-BrS comonomer was needed to induce incompatibility with PPO than 4-BrS. The chlorine substituted comonomers behaved quite similarly whereas less 4-FlS comonomer produced incompatibility with PPO than 2-FlS. The crossover between size and polarity effects occurred for the chlorinated polystyrene.

The incompatibility of all the halogenated homopolymers with PPO was evidenced by DSC. Copolymers of the 2- and 4- chlorinated and fluorinated styrene were found to be compatible with PPO over a certain copolymer composition range and temperature. None of the brominated copolymers were compatible with PPO. Alexandrovich addressed this paradox briefly in his thesis work.[16] He suggested that the thermal expansion coefficients of the copolymers might be depressed from the pure components and adequately matched to that of PPO. The linear expansion coefficients were measured using a TMS-1. Figure 5.36 shows the results of the thermal expansion coefficient as a function of temperature for the polymers indicated. The accuracy of measurement was much too limited to allow prediction of compatible polymers based on comparing the thermal expansion coefficient.

Other suggested reasoning was a matching of equation of state

parameters of certain copolymers and PPO. If the solubility parameter approach was used, perhaps the miscible copolymers had values of δ close to the δ of PPO.

Figure 5.35 puts the above speculation into a useful graphical form. The abscissa represents copolymer composition and the ordinate either solubility parameter, linear expansion coefficient or the equation of state characteristic temperature for the homopolymer. The figure would be for a single temperature only. The order of the co-monomer substituents was taken from Eqn. (5.10). A "zone of compatibility" around PPO was envisioned and represented by the gray area. Copolymers lying within the compatibility zone would mix with PPO at that temperature. The physical property of the y-axis was postulated to be depressed for the copolymers relative to the pure components. The Tg's of the copolymers were found to be depressed from linearity relative to the pure components. Since other physical properties of the copolymers were known to be depressed from linearity, a depression in one of the critical compatibility properties might also be speculated.

Several interesting features are evident in Figure 5.35. Co-polymers of 2-FlS and 4-FlS are predicted to be compatible over a small range with the copolymers rich with the 2-FlS constituent. This was found to be the case. The chlorinated copolymers also are predicted to be compatible in a certain range. However, the compatibility window would be shifted more towards the center of the composition axis. Experimentally, this was found. The initially surprising result that none of the totally brominated copolymers were compatible
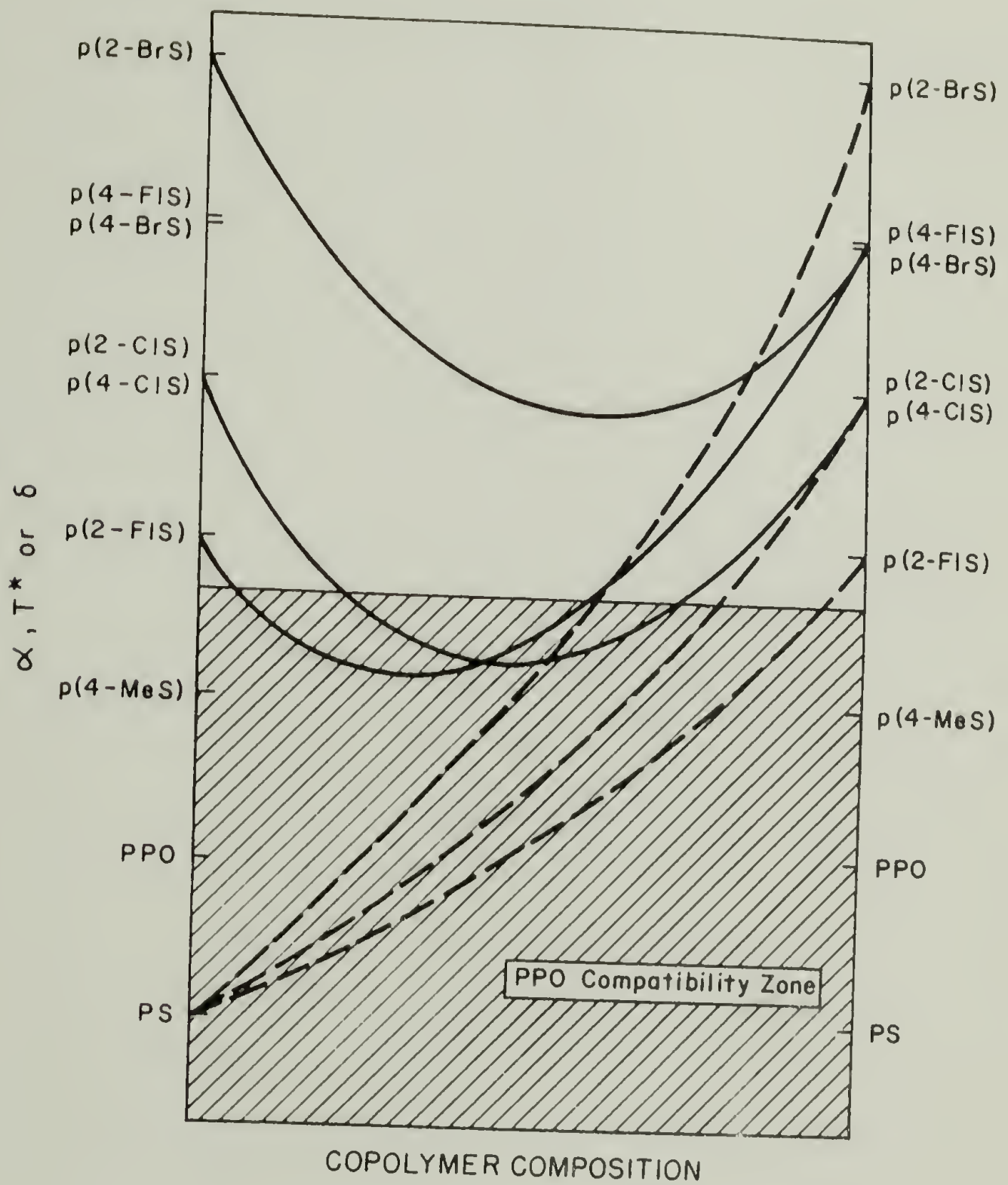
Figure 5.35. Critical compatibility property as a function of copolymer composition.
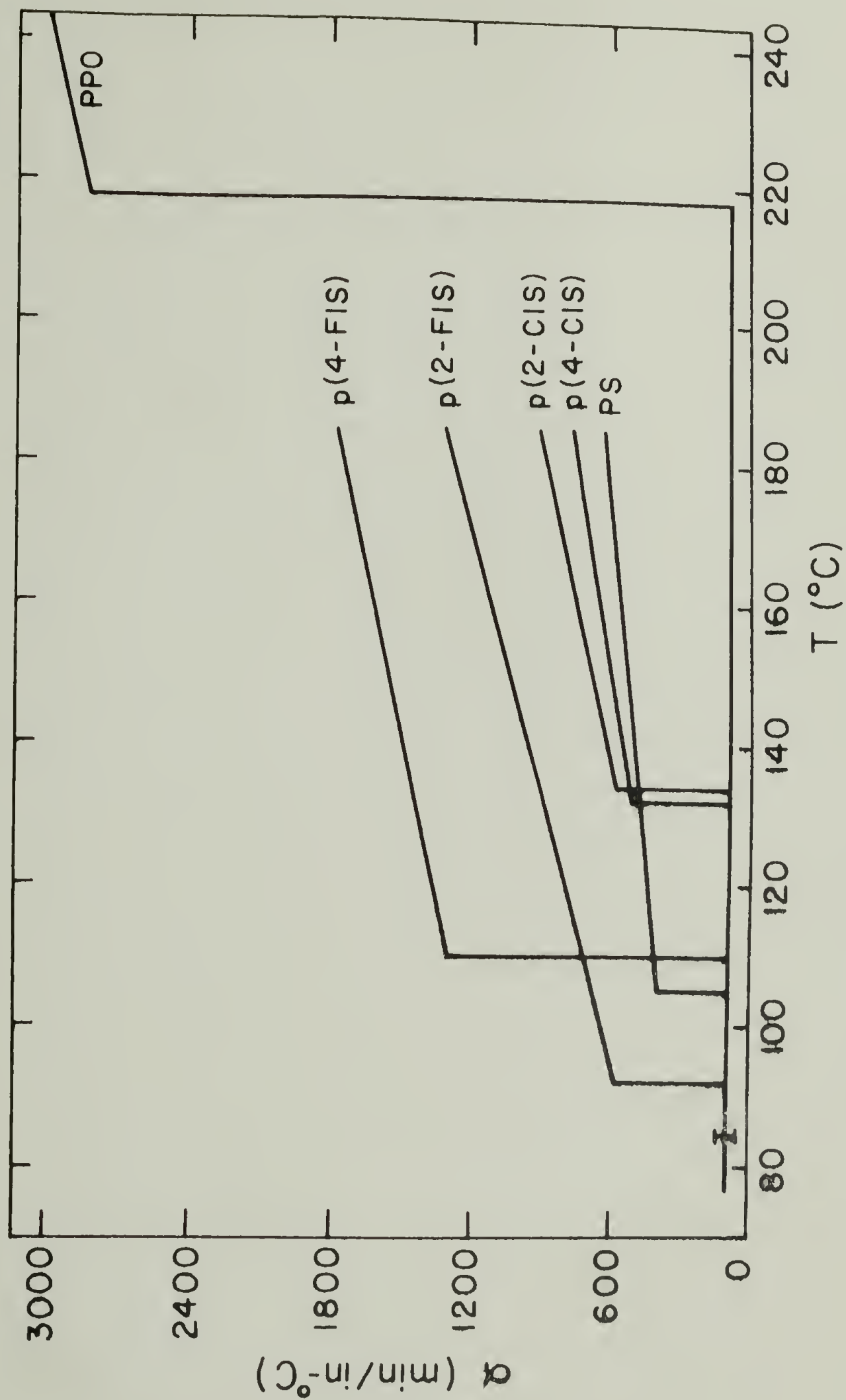
Figure 5.36. Linear expansion coefficients as a function of temperature.

with PPO could be explained by Figure 5.35. Since the properties, represented by the y-axis, of the pure brominated homopolymers are very different from PPO, the depression in those same properties of the copolymers was not significant enough to allow miscibility with PPO.

Some predictions could also be made using the schematic. If random copolymers of 2-FlS with either 2- or 4-ClS could be made, blends with PPO might also possess a compatibility window. Moreover, the probable compatible copolymers would be richer in the 2-FlS content than either of the chlorinated comonomers. Other copolymers that might contain a compatibility window with PPO are listed in Table 5.12.

Since each of the copolymer blends with PPO studied phase separated at higher temperatures, the y-axis of Figure 5.35 would expand as the temperature is increased. The compatibility zone would remain the same, however. Conversely, a decrease in temperature would serve to compress the ordinate. This would predict that even the totally brominated copolymers should be compatible with PPO at some temperature. However, evidence for the existence of a polymer-polymer UCST was presented in the previous sections. Therefore, the matching of parameters would reach a maximum at a certain temperature between the CST's and diverge from that point as the temperature is increased or decreased.

Figure 5.35 could also be used for explaining the compatibility of PS with the copolymers indicated. As drawn, PS would be compatible with copolymers of styrene and halogenated styrene, but only with slightly halogenated copolymers. The limited experimental evidence indicated this was true. None of the totally halogenated copolymers

Table 5.12. Predicted Miscible Copolymer/PPO Blends.

Comonomer 1	Comonomer 2	Prevalent Constituent in Copolymer
2-FlS	2-ClS	2-FlS
	4-ClS	2-FlS
	4-BrS	2-FlS
2-ClS	4-BrS	2-ClS
	4-FlS	2-ClS
4-ClS	4-BrS	4-ClS
	4-FlS	4-ClS
4-MeS	2-FlS	2-FlS
	2-ClS	2-ClS
	4-ClS	4-ClS
	4-BrS	mid-range
	4-FlS	mid-range
	2-BrS	4-MeS

were found to be compatible with PS. Figure 5.35 would indicate that the copolymer characteristic properties would not fall within the compatibility zone around PS. However, there might be a chance that the chlorinated copolymers would be compatible with PS especially in the midcomposition copolymer range.

Figure 5.35 is actually a simplified 2-dimensional version of a 4-dimensional diagram. One additional variable already discussed would be temperature. Another variable would be the blend composition. Figure 5.35 was based on experimental results for 50/50 blends. However, different blend compositions would yield different results. Figure 5.35 also allows comment on the compatibility of PS/p(2-ClS) blends. Using the empirical diagram, the prediction would be reached that PS would not be miscible with p(2-ClS). However, Figure 5.35 was based on PPO blends and temperatures above the PPO Tg (218°C). Since the scale would be compressed with lowering of temperature, PS/p(2-ClS) might be expected to be compatible between 140° and 220°C. However, the conclusion reached in the previous section that the UCST of the PS/p(2-ClS) could be quite high, would invalidate any conclusions based on Figure 5.35.

Since PS was compatible with p(2-ClS) at some PS MW's, Figure 5.35 would predict that those same MW PS would also be miscible with p(2-FlS) and possibly p(4-ClS). Although not studied as a function of MW of PS, blends of PS with both p(2-FlS) and p(4-ClS) have been found to be two phase.

REFERENCES

1. A.S. Marshall, S.E.B. Petrie, J. Appl. Phys. $\underline{46}$(10), 4223 (1975).

2. R. Straff, D.R. Uhlmann, J. Polym. Sci.: Polym. Phys. Ed. $\underline{14}$, 1087 (1976).

3. R.J. Roe, S.K. Lo, R.P. Chartoff, Polymer Preprints $\underline{17}$(2), 167 (1976).

4. C.R. Foltz, P.V. McKinney, J. Appl. Polym. Sci. $\underline{13}$, 2235 (1969).

5. S.E.B. Petrie, J. Polym. Sci.: A-2 $\underline{10}$, 1255 (1972).

6. M.J. Richardson, N.G. Savill, Polymer $\underline{18}$, 413 (1977).

7. M.J. Richardson, N.G. Savill, Polymer $\underline{16}$, 753 (1975).

8. N.E. Weeks, F.E. Karasz, W.J. MacKnight, J. Appl. Phys. $\underline{48}$(10), 4068 (1977).

9. L.W. Kleiner, Ph.D. Dissertation, University of Massachusetts, 1978.

10. F.E. Karasz, H.E. Bair, J.M. O'Reilly, J. Polym. Sci.: A-2 $\underline{6}$, 1141 (1968).

11. F.E. Karasz, H.E. Bair, J.M. O'Reilly, J. Phys. Chem. $\underline{69}$, 2657 (1965).

12. J.R. Fried, Ph.D. Dissertation, University of Massachusetts, 1976.

13. J.R. Fried, F.E. Karasz, W.J. MacKnight, Macrom. $\underline{11}$, 150 (1978).

14. A.R. Shultz, B.M. Beach, Macrom. $\underline{7}$, 902 (1974).

15. J.J. Tkacik, Ph.D. Dissertation, University of Massachusetts, 1976.

16. P.R. Alexandrovich, Ph.D. Dissertation, University of Massachusetts, 1978.

17. P.T. Gilmore, Ph.D. Dissertation, University of Massachusetts, 1978.

18. T.P. Russell, Ph.D. Dissertation, University of Massachusetts, 1979.

19. T.P. Russell, R.S. Stein, Polymer Preprints 20(1), 24 (1979).

20. C.L. Ryan, F.E. Karasz, W.J. MacKnight, Bull. Amer. Phys. Soc. 24(3), 290 (1979).

21. I.C. Sanchez, R.H. Lacombe, Nature (London) 252, 381 (1974).

22. I.C. Sanchez, R.H. Lacombe, J. Phys. Chem. 80, 2352 (1976).

23. R.H. Lacombe, I.C. Sanchez, J. Phys. Chem. 80, 2568 (1976).

24. I.C. Sanchez, in Polymer Blends, Vol. I, D.R. Paul, ed., Academic Press, N.Y., 1978.

25. P.J. Flory, Principles of Polymer Chemistry, Cornell University Press, Ithaca, N.Y., 1953.

26. T.K. Kwei, T.T. Wang, in Polymer Blends, Vol. I, D.R. Paul, ed., Academic Press, N.Y., 1978.

27. R. Vukovic, F.E. Karasz, W.J. MacKnight, in press.

28. R. Vukovic, F.E. Karasz, W.J. MacKnight, in press.

29. R. Vukovic, F.E. Karasz, W.J. MacKnight, in press.

30. P.R. Alexandrovich, F.E. Karasz, W.J. MacKnight, Polymer 18, 1022 (1977).

31. I.C. Sanchez, private communication.

32. L.P. McMaster, Macrom. 6(5), 760 (1973).

33. S. Saeki, N. Kuwahara, S. Konno, M. Kaneko, Macrom. 6(4), 589 (1973).

34. S. Saeki, S. Konno, N. Kuwahara, M. Nakata, M. Kaneko, Macrom. 7(4), 521 (1974).

35. S. Saeki, N. Kuwahara, M. Kaneko, Macrom. 9(1), 101 (1976).

36. S. Saeki, N. Kuwahara, S. Konno, M. Kaneko, Macrom. 6(2), 246 (1973).

37. S. Konno, S. Saeki, N. Kuwahara, M. Nakata, M. Kaneko, Macrom. 8(6), 799 (1975).

38. K.S. Siow, G. Delmas, D. Patterson, Macrom. 5(1), 29 (1972).

39. J.M.G. Cowie, I.J. McEwen, Macrom. 7(3), 291 (1974).

40. A.R. Shultz, G.I. Mankin, J. Polym. Sci.: Symp. #54, 341 (1976).

41. R. Koningsveld, L.A. Kleintjens, H.M. Schoffeleers, Pure & Appl.
    Chem. $\underline{39}$(10), 1 (1974).

CHAPTER VI

SUMMARY AND CONCLUSIONS

The purpose of this chapter is to summarize the results of this work and the conclusions reached on the compatibility of polymer-polymer blends.

A. Equilibrium States below Tg

The most significant finding was the ability to probe equilibrium thermodynamic glassy states using Tian-Calvet microcalorimetry. Polymers are unique in their ability to exist for finite time periods in a thermodynamically unstable state. Below the Tg, the severely restricted mobility of the polymer molecule is such that kinetic effects overpower the thermodynamic driving forces. Therefore, a polymer-polymer system can exist inside the spinodal for long periods of time.

Heats of solution of the homopolymers and blends were measured by Tian-Calvet microcalorimetry. Since $T\Delta S_m = 0$ for high MW polymer blends, ΔH_m accurately reflects ΔG_m. Hess's law was then used to determine the heats of mixing of polymer blends at the experimental temperature. The solution process was broken down into two processes. The first step was a lowering of the polymer of blend Tg to below the experimental temperature. This process usually accounted for the majority of the heat evolved and involved the "melting" of the glassy state to the liquid state. Once the polymer or blend was above the

175

solvent-induced Tg, the kinetic effects could be overcome by the thermo-dynamic driving forces. Therefore, if the blend was below the UCST, or in a two-phase region, demixing of the polymers would result in an exothermic process. The amount of heat evolved from demixing would depend on how deep inside the spinodal the blend was at the experimental temperature. The final step in solution was then the normal dissolution process resulting in a dilute polymer solution. The heat evolved in this final step was minimal, perhaps 5% of the total heat of solution.

The exothermic heat evolved due to demixing of the one-phase polymer blend resulted in a positive contribution to the overall heat of mixing. Figure 6.1 illustrates the effect. Prior to point A and after point B, there is no contribution to ΔH_m due to a demixing process. Points A and B are the loci of the binodal as explained in Chapter I. Between the compositions A and B, the polymer blend exists in either a metastable or unstable state. Once allowed the mobility, the blend would phase separate to compositions on the binodal. The heat evolved would be the difference, at that composition, between points on curves 1 and 2. Following this logic, the entire contours of curve 1 could be explored for polymer-polymer systems below Tg. This situation is unique to polymer blends. Mixtures of low MW compounds would inevitably follow curve 2 in Figure 6.1 since unstable states could not be frozen in. Theoretically, mixtures of low MW materials would follow curve 1, but experimentally only curve 2 could be determined. Polymer blends, however, can exist in the glassy state inside the binodal and spinodal. The experimental determination of ΔH_m
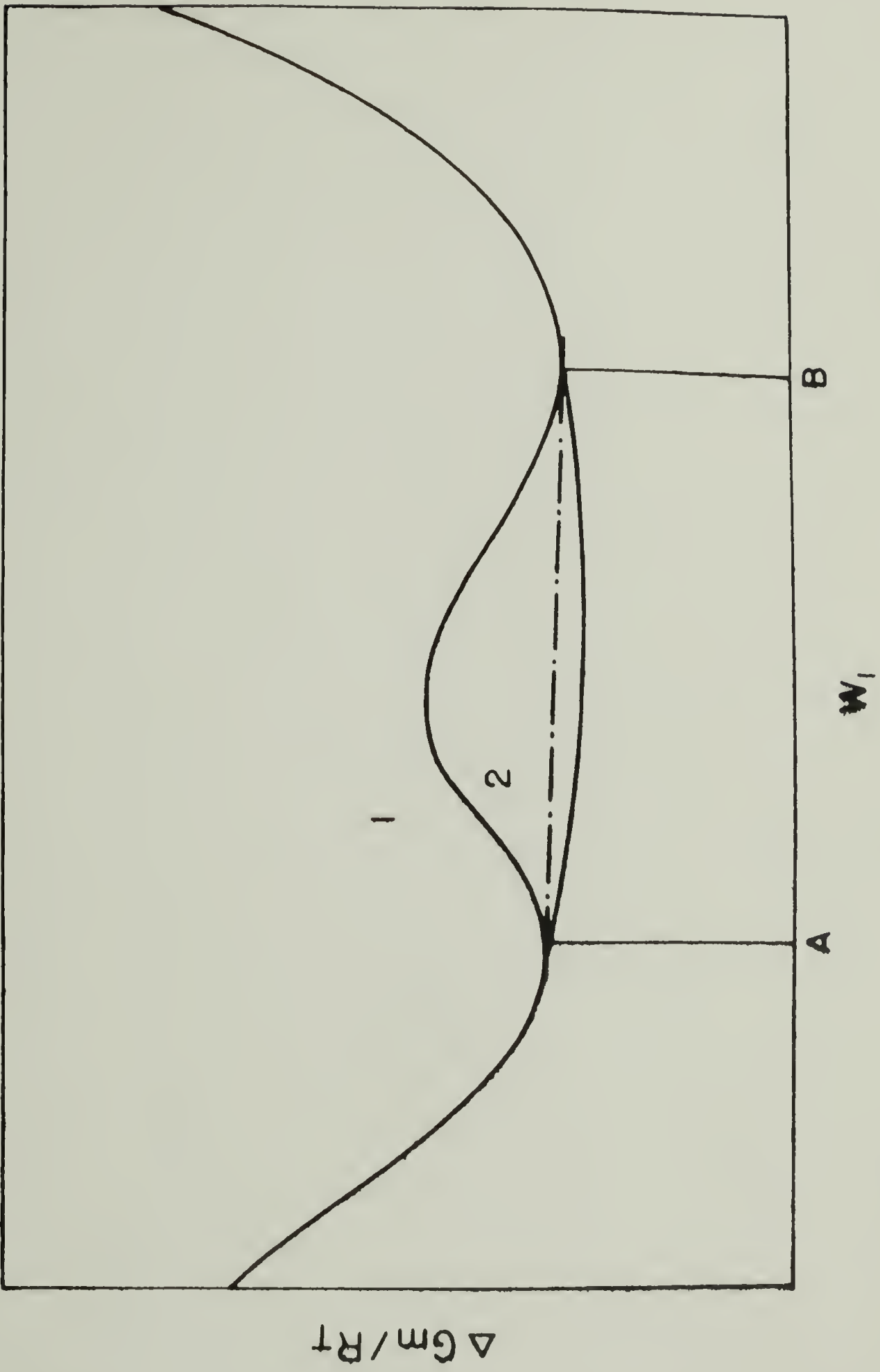
Figure 6.1. Free energy vs. composition diagram.

using the techniques described in this work makes it experimentally possible to follow the contours of curve 1. It is believed this is the first instance when this has been done for any multicomponent system. Above the glass transition temperature, polymer-polymer systems would have sufficient mobility so that the experimentally determined ΔH_m would vary with composition in the same manner as the low molecular weight materials.

The binodal and spinodal phase boundary could then be determined below Tg by performing ΔH_m measurements at many compositions and temperatures. Since $\Delta H_m \cong \Delta G_m$ for high polymer systems, the entire phase boundary below Tg is experimentally accessible.

B. Summary of Blend Systems Studied

Many different polymer blends were studied in this work. All were based on the model systems PS/PPO and included extensions of the work of Tkacik,[1] Fried,[2,3] and Alexandrovich.[4,5] The compatibility of the system was based on DSC determinations of Tg and measurementsof ΔH_m from Tian-Calvet microcalorimetry. Table 6.1 is a summary of the miscible/immiscible blends studied. Listed under the miscible blend category are those systems which are compatible at some blend composition and temperature, i.e., partially miscible systems or in the terminology of Krause,[6,7] almost compatible blends.

Polymer-polymer LCST was found for many of the above miscible systems by Alexandrovich[4,5] and Vukovic.[8-10] In addition to their findings, LCST's were found for the miscible brominated polystyrene/PPO blends. A new frontier in polymer-polymer blend behavior was the

Table 6.1. Summary of Systems Studied.

Miscible Systems	
PS/PPO	
p(4-ClS(x)-2-ClS)/PPO	x < .759
PS/p(2-ClS)	
p(4-FlS(x)-2-FlS)/PPO	0 < x ≤ .456
p(4-BrS(x)-S)/PPO	x < .6
p(4-BrS(x)-S)/PS	x < .5
p(2-BrS(x)-S)/PPO	x < .4
p(2-BrS(x)-S)/PS	x < .4
p(4-MeS)/PPO	

Immiscible Systems
PS/p(4-ClS)
p(4-FlS-co-2-FlS)/PS
p(4-BrS-co-2-BrS)/PPO
p(4-BrS-co-2-BrS)/PS

discovery of the existence of an UCST for several polymer blend systems. The existence of a lower phase diagram was unequivocally established for PPO blends with p(4-FlS(x)-2-FlS), .05 ≤ x ≤ .456. An UCST was also found to exist in the PS/p(2-ClS) system along with the p(4-ClS-co-S)/PPO blends. A major contribution of this work was the establishment of polymer-polymer UCST's.

C. PS/p(2-ClS) Blends

Blends of PS with p(2-ClS) were found to phase separate at higher temperatures as well as at temperatures below Tg depending on composition, temperature and molecular weight of the PS. For higher MW PS blends, the LCST was below the UCST to form the hourglass type phase diagram. At a critical MW between 26,700 and 30,400, the CST's were equal (somewhere near 280°C) while for lower MW PS blends, the LCST was greater than the UCST. Moreover, the UCST was below the Tg.

Utilizing the lattice fluid theory of Sanchez,[11-14] the phase stability of the low MW PS/p(2-ClS) blends was due to the entropic contributions to the free energy of mixing. The heats of mixing were found to be fairly independent of MW as predicted by Sanchez whereas the phase diagram changed substantially with MW. These findings were consistent with the results predicted by lattice fluid theory.

D. p(4-ClS-co-S)/PPO Blends

Blends of PPO with copolymers of styrene and 4-ClS were previously studied by Fried,[2,3] Alexandrovich[4] and Shultz.[15] Copolymers with less than 75 mole percent 4-ClS were miscible with PPO at some

composition and temperature. The heats of mixing 50/50 blends of PPO with the copolymer initially dropped toward zero from negative values as the phase separation temperature decreased. However, blends of PPO with p(4-ClS(.759)-S) exhibited an anomalously large negative ΔH_m. Explanation of this behavior as a function of copolymer composition did not center on the single large ΔH_m found, but instead the decrease in ΔH_m for blends of PPO with copolymers with 60-68 mole percent 4-ClS. The behavior of ΔH_m could be explained by postulating the existence of an UCST. The low values of ΔH_m were due to a positive contribution to ΔH_m resulting from a demixing exotherm at the experimental temperature. As the copolymer composition was increased, the UCST increased such that T_{exp} lay inside the binodal region. The further inside the binodal, the larger the exotherm due to demixing and therefore the less negative the experimental ΔH_m. The partially phase separated p(4-ClS(.759)-S)/PPO blend included separate one-phase regions that were not inside the binodal at T_{exp}. Therefore, there was no positive contribution to ΔH_m due to demixing and a larger measured ΔH_m.

E. p(4-FlS-co-2-FlS) Blends with PPO and PS

Vukovic[8-10] had determined that although the homopolymers p(4-FlS) and p(2-FlS) were incompatible with PPO, copolymers of the two fluorinated styrenes were compatible with PPO over a certain co-polymer composition range. Moreover, the PPO blends reversibly phase separated at higher temperatures. The temperature at which phase separation occurred was highest for the p(4-FlS(.285)-2-FlS)/PPO blend and fell on either side of that copolymer composition. Experimentally,

only copolymers with between 5 and 45% 4-FlS were miscible with PPO.

The heat of mixing followed a complicated pattern as a function of copolymer composition in blends 50/50 with PPO. Moreover, large positive values of ΔH_m were found for some of the copolymer blends. The dependence of ΔH_m with changing copolymer composition was explained postulating the existence of an UCST. The behavior of the UCST was anti-parallel to the LCST; as the LCST rose, the UCST decreased to its lowest temperature for PPO blended with p(4-FlS(.285)-2-FlS). The temperature midpoint between the CST's was assumed constant as a function of copolymer composition.

Whereas the existence of an UCST might have been questionable for the systems PS/p(2-ClS) and p(4-ClS-co-S)/PPO, the large positive ΔH_m coupled with the behavior of ΔH_m with copolymer composition pointed unequivocally to the existence of an UCST for this system.

Blends of p(4-FlS-co-2-FlS) with PS were probably immiscible. Values of ΔH_m were zero which indicated an incompatible system. However, the values for ΔH_m for a compatible system might have been so small as to be immeasurable. DSC data hinted at two Tg's for many of the copolymer blends although the difference in pure component Tg's was too small to be definitive.

F. Halogen-substituted Polystyrene Blends with PPO

Two halogen-substituted polystyrene blends with PPO were already discussed. The purpose of this study was to extend the fluorinated and chlorinated polystyrene blends with PPO to the brominated and methylated polystyrenes. The effect of substituent on

the compatibility was then studied.

Copolymers of 4-BrS and 2-BrS were incompatible with PPO. This was contrary to the findings for the fluorinated and chlorinated copolymer blends. Copolymers of styrene with either 4-BrS or 2-BrS were compatible with PPO depending on the copolymer composition. From analogous studies on the fluorinated and chlorinated copolymers with PS, a ranking of the constituents' ability to induce incompatibility of PS with PPO was

$$2\text{-Br} > 4\text{-Fl} \cong 4\text{-Br} > 2\text{-Cl} \cong 4\text{-Cl} > 2\text{-Fl} > 4\text{-Me}. \quad (6.1)$$

The ordering of Eqn. (6.1) means that it took less 2-BrS in the copolymer with styrene to produce immiscible blends with PPO than for copolymers of 2-FlS and styrene. In fact, the homopolymer p(4-MeS) was compatible with PPO.

The arrangement of Eqn. (6.1) was difficult to interpret. Two effects were opposed to each other. The polar effects favored the fluorinated systems over the brominated whereas size effects were overwhelming for the brominated systems and negligible for the fluorinated copolymers. The chlorinated systems were intermediate in both size and polar effects.

The polar forces were strongest in copolymers of 4-FlS with styrene since the dipoles were aligned perpendicular to the chain axis. Therefore, the formation of interactions between the 4-FlS groups on different polymer chains would be at the expense of polymer miscibility. The polar interactions between the 2-substituted fluorine copolymers were not as strong since the dipole was oriented more along

the chain axis. Therefore, more 2-FlS was needed than 4-FlS in the copolymer to induce immiscibility with PPO.

The size effects appeared to produce the opposite results, although the reasoning was not clear. The crossover between size and polarity effects occurred for the chlorinated copolymer blends with PPO.

The order of Eqn. (6.1) was used to explain the apparent paradox of compatible copolymers of 2- and 4-halogenated polystyrenes with PPO. Certain completely fluorinated and chlorinated styrene copolymers were miscible with PPO whereas none of the brominated copolymers mixed with PPO. The explanation used was that a critical physical property, e.g., characteristic temperature, T^*, thermal expansion coefficient or solubility parameter, of the copolymers was not a linear function of copolymer composition. Instead, there was a depression from linearity postulated, similar to the depression of Tg or density found experimentally. The depression resulted in a fortuitous matching of these parameters with PPO, enabling the formation of miscible polymer pairs. The characteristic physical properties for the brominated copolymers were too different from PPO in order for the property depression to be sufficient for blending.

An empirical diagram was constructed based on the above conclusions. From this diagram, many more copolymers were postulated to form compatible blends with PPO.

G. Suggestions for Future Work

Figure 5.35 predicted many more copolymers that would be miscible with PPO. The copolymer composition range was even predicted. It might prove interesting to explore some of these mixed halogen copolymers in order to test the predictions. Of course, extension of the copolymers to include meta-substitution unveils an entire new area of exploration. However, polar effects in the meta-position are much different than either the ortho- or para-position. Experiments with the 3-halogenated copolymers might shed some light on the effect of substituent size and polarity on the compatibility with PPO.

The compatibility of the halogenated copolymers with PPO postulated a depression from linearity of a characteristic copolymer property. McMaster[16] maintained that the critical property was the thermal expansion coefficient. Careful measurements of the thermal expansion coefficient might help clarify the above speculation. Sanchez[11-14] predicted that compatibility occurred when the characteristic temperatures were within 200°C. However, equation of state parameters are very difficult to measure with the required precision.

Polymers have also been shown to dissolve in a mixture of two non-solvents.[17] The above explanation about a matching of critical properties could also be applicable to these type systems. One possibility would be that the solubility parameters, for example, would bracket the solubility parameter of the polymer. Mixtures of the two non-solvents would then include areas of matching parameters. Cowie,[17] however, has found systems where the two non-solvents have solubility

parameters which do not bracket the polymer but still can dissolve the polymer. Analogous to the completely halogenated copolymer blends with PPO, an explanation might be a synergistic effect on the critical property of the mixed solvents relative to the pure solvent properties. Bearing these results in mind, a ternary blend system of PPO/p(2-FlS)/p(4-FlS), or the corresponding chlorinated case, might be interesting to investigate the phase behavior.

Polymer-polymer UCST was shown to be prevalent for many of the systems. Although perhaps questionable for PS/p(2-ClS), the search for a UCST by changing the MW of the PS would be worthwhile. In each of the previous studies, polydispersed p(2-ClS) was used. However, blends of monodispersed PS with monodispersed p(2-ClS) would allow easier study of the phase diagram. Along these same lines, heats of mixing studies of PS with p(2-FlS) would probably prove interesting. Although the Tg's of the pure components are too close to be studied by DSC, ΔH_m should behave similar to PS/p(2-ClS). In fact, the compatibility window should be more experimentally accessible.

Now that a high pressure DTA is available, studies on the effect of pressure on the polymer-polymer phase diagram would be worthwhile. Prime candidates for study would be PPO blends with either the completely chlorinated or fluorinated polystyrenes. The LCST's for these systems are experimentally accessible. High pressure work might also clarify the phase diagram for PS/p(2-ClS) and the postulated existence of a merged CST which diverge as a function of MW

Work needs to be perfected on the high temperature (over 70°C) operation of the Tian-Calvet microcalorimeter. By extending the

experimental temperatures to higher levels, the correction for the excess glass enthalpy would be minimized. Moreover, in cases where the UCST was postulated to occur below Tg, the temperature variable would be useful to study the effect of ΔH_m as a phase boundary is approached for a constant system.

Finally, many of the studies in this work involved only 50/50 blends. The phase behavior not only changes as a function of temperature, but also as a function of blend composition. It was postulated that the p(4-ClS-co-S)/PPO blend was incompatible at 35°C. A more complete check on this system would be useful. Measurement of ΔH_m as a function of blend composition would make it possible to pinpoint the spinodal and binodal boundaries. The critical points could be obtained for a variety of copolymer compositions and temperatures to more completely document the dependence of copolymer composition on phase stability.

REFERENCES

1. J.J. Tkacik, Ph.D. Dissertation, University of Massachusetts, 1976.

2. J.R. Fried, Ph.D. Dissertation, University of Massachusetts, 1976.

3. J.R. Fried, F.E. Karasz, W.J. MacKnight, Macrom. $\underline{11}$, 150 (1978).

4. P.R. Alexandrovich, Ph.D. Dissertation, University of Massachusetts, 1978.

5. P.R. Alexandrovich, F.E. Karasz, W.J. MacKnight, Polymer $\underline{18}$, 1022 (1977).

6. S. Krause, J. Macrom. Sci.--Revs. Macrom. Chem. $\underline{C7}$(2), 251 (1972).

7. S. Krause, in _Polymer Blends_, Vol. I, D.R. Paul, ed., Academic Press, N.Y., 1978.

8. R. Vukovic, F.E. Karasz, W.J. MacKnight, to be published.

9. R. Vukovic, F.E. Karasz, W.J. MacKnight, to be published.

10. R. Vukovic, F.E. Karasz, W.J. MacKnight, to be published.

11. I.C. Sanchez, R.H. Lacombe, Nature (London) $\underline{252}$, 381 (1974).

12. I.C. Sanchez, R.H. Lacombe, J. Phys. Chem. $\underline{80}$, 2352 (1976).

13. R.H. Lacombe, I.C. Sanchez, J. Phys. Chem. $\underline{80}$, 2568 (1976).

14. I.C. Sanchez, in _Polymer Blends_, Vol. I, D.R. Paul, ed., Academic Press, N.Y., 1978.

15. A.R. Shultz, B.M. Beach, Macromol. $\underline{7}$(6), 902 (1974).

16. L.P. McMaster, Macrom. $\underline{6}$(5), 760 (1973).

17. I. Cowie, private communication.

A P P E N D I X   I

ERROR ANALYSIS OF THE HEATS OF MIXING

As in the case of any new phenomenon that might be controversial, a detailed error analysis is required to quell some opposition. It is the purpose of this appendix to calculate the maximum errors associated with the heats of mixing of each of the polymer-polymer systems studied.

There are two equivalent methods for calculating the heats of mixing for experimental temperatures below the glass transition temperature of each of the components in the Hess's law approach. The method used throughout each of the studies involved applying Hess's to the heat of solution corrected by subtracting out the glassy excess heats,

$$\Delta H_s(\text{corrected}) = \Delta H_s(\text{experimental}) - \Delta Cp\Delta T \qquad (A1.1)$$

where $\Delta Cp\Delta T$ was explained earlier. Heats of mixing of polymer-polymer systems could also be calculated by applying Hess's law to the right-hand terms of Eqn. (A1.1) and adding together.

$$\Delta H_m(\text{soln}) = a\Delta H_s^1 + b\Delta H_s^2 - \Delta H_s^{bl}$$

$$\Delta H_m(\text{excess}) = a\Delta H_{xs}^1 + b\Delta H_{xs}^2 - \Delta H_{xs}^{bl} \qquad (A1.2)$$

$$\Delta H_m(\text{actual}) = \Delta H_m(\text{soln}) + \Delta H_m(\text{excess}) .$$

189

It is very important to keep the sign of individual quantities in Eqn. (A1.2) consistent. In the convention employed in Eqn. (A1.2), ΔH_m(soln) could either be positive or negative while ΔH_m(excess) was always positive when the Tg of the blend was depressed from linear additivity of pure component Tg's, and zero for incompatible polymers. It is significant to note that the heat of mixing term derived from the excess glassy heats is always unfavorable to the overall heat of mixing since it is always endothermic. One assumption used to reach this conclusion was ΔCp for the blends is a linear function of the pure components, i.e., $\Delta Cp^{bl} = a\Delta Cp^1 + b\Delta Cp^2$. Differential scanning calorimetry appears to verify this assumption. In either case ΔCp for the blends is not concave upward as a function of composition which would be necessary to explain the positive heats of mixing as being solely a glassy phenomenon. The actual magnitude of a ΔCp inflation from linearity to account for all observed positive heats will be explored later.

Graphical procedures can be used to show equivalence between approaches to ΔH_m utilizing either Eqn. (A1.1) or (A1.2). Figure A1.1 shows the general shapes and magnitudes of the heats involved. Equivalence of Eqn. (A1.1) and (A1.2) means that:

$$\overline{EF} = \overline{AB} - \overline{CD} = \Delta H_m . \tag{A1.3}$$

Since point E = A - C and F = B - D, simple subtraction of one from the other gives

$$\Delta H_m = (A - C) - (B - D) = (E - F) \tag{A1.4}$$
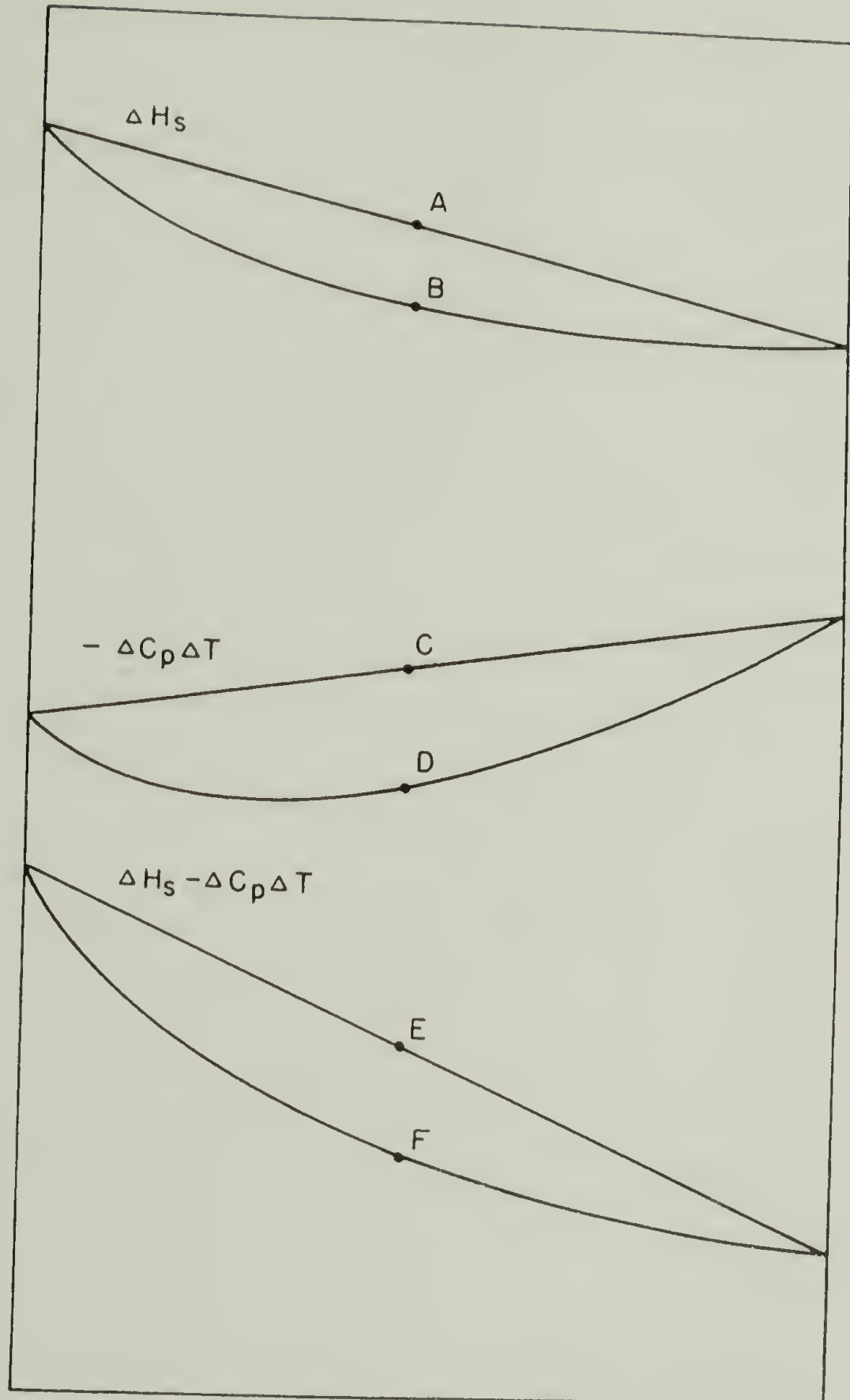
Figure A1.1. General behavior of -ΔH vs. composition.

which is equivalent to Eqn. (A1.3).

For purposes of error analysis and propagation, it is more straightforward to utilize the approach of Eqn. (A1.2). The excess heat was shown previously to be approximated as:

$$\Delta H(excess) = a\Delta C\overset{1}{p}(Tg_1 - T_{exp}) + b\Delta C\overset{2}{p}(Tg_2 - T_{exp})$$
$$- \Delta C\overset{bl}{p}(Tg_{bl} - T_{exp}) \qquad (A1.5)$$

where the subscripts 1, 2 and bl refer to the pure components and the blend while a and b are the corresponding composition fractions. If one assumes linear additivity of the specific heat changes at Tg, Eqn. (A1.5) simplifies, with appropriate substitutions, to:

$$\Delta H_m(excess) = a\Delta Cp_1(Tg_1 - Tg_{bl}) + b\Delta Cp_2(Tg_2 - Tg_{bl}) . \qquad (A1.6)$$

The actual heat of mixing at T_{exp} is therefore given as

$$\Delta H_m(actual) = a\Delta H_{s_1} + b\Delta H_{s_2} - \Delta H_{s_{bl}} + a\Delta Cp_1\Delta Tg_1 + b\Delta Cp_2\Delta Tg_2$$
$$(A1.7)$$

where $\Delta Tg_i = Tg_i - Tg_{bl}$. Error analysis of Eqn. (A1.7) is now quite straightforward. For each of the experimental values of the heats of solution, the probable error was rarely above 0.63 Joules/gram for all measurements. Glass transition temperatures are estimated to be good to $\pm 2°K$ whereas ΔCp is in error of upwards to 12%. If one estimates the error in specific heat as determined by DSC to be 1%, the error in ΔCp is as high as 12% for polystyrene. Therefore, ΔCp measurements

might involve errors as much as ±0.03 J/°K-gm. Propagation of errors as outlined by Lyon[1] would then produce an error in measurement of the actual ΔH_m of

$$\Delta H_m(error) = a(.63) + b(.63) + (.63) + a(.03)(4°K) + b(.03)(4°K)$$

$$= 1.38 \text{ Joules/gram.}$$

This analysis shows that the error in ΔH_m is independent of the magnitude of Tg or the value of the experimental temperature as long as the experimental temperature is below the glass transition temperature of all components. Moreover, since the ΔCp's of all the polymers in this work are of the same magnitude, i.e., errors in ΔCp are approximately the same, all computed values for the heats of mixing are subject to a gross estimate of error of approximately 1.4 J/gm regardless of component Tg or experimental temperature.

One argument against this interpretation of the positive heats of mixing is that the positive heat is due entirely to the glassy heats and a breakdown in the approximation that the change in specific heats at Tg of the blends is a linear function of the pure component ΔCp. For the PS(20.4)/p(2-ClS) 50/50 blend, the experimental value for ΔH_m at 35°C is +2.3 J/gm. In order to account for such a large positive heat of mixing, ΔCp for this blend would need to be .277 J/°K-gm since $\Delta T = 75.6°$. This compares with the least squares experimental value of .246 J/°K-gm. Moreover, determination of ΔCp by DSC of the polymer blends shows no trend towards curvature as a function of composition. This conclusion is consistent with the find-

ings of Fried.[2] Therefore, the positive heats of mixing found for the PS/p(2-ClS) blends are not experimental artifacts, but a consequence of incompatibility at experimental temperatures. The case for blends of poly(4-fluorostyrene-co-2-fluorostyrene) with PPO is much stronger since the positive heats of mixing are very large.

REFERENCES

1. A.J. Lyon, <u>Dealing with Data</u>, Pergamon Press, N.Y., 1970.

2. J.R. Fried, Ph.D. Dissertation, University of Massachusetts, 1976.

A P P E N D I X   I I

DATA TABULATION

Table A2.1 lists all values for Cp, Tg, and ΔCp for each poly-
mer and blend studied. Values for Cp above and below Tg are least
squares fits. In many cases, ΔCp and least squares Cp lines were de-
termined twice. One method used the facilities of Bell Laboratories.
A DSC-2 was interfaced with a Tektronic calculator to convert all
points to J/°-gm. The other method utilized the point-by-point sub-
traction outlined in Chapter III. The Tg's determined Bell Labs were
consistently high whereas the point-by-point subtraction gave consis-
tently low Tg's. Reasons for this were postulated in Chapter IV. The
next-to-last column in Table A2.1 gives the Tg's determined at the
time the Cp's were calculated. The last column gives the values for
Tg's used in all calculations.

Table A2.2 lists the heats measured and calculated in the deter-
mination of the heats of mixing of the polymers.

Table A2.1. Tg, Cp, ΔCp Data for all Polymers Studied.

System		Below Tg		Above Tg		ΔCp	Tg	Tg
		Slope x 10^3	Intercept	Slope x 10^3	Intercept	(J/°-gm)	(°K)	(°K)
PS(HH101)		4.575	-.1301	2.618	.9092	.290	383.0	378.0
		2.7845	.3773	1.055	1.2742	.245	377.0	
PS(50)		4.790	-.2063	2.253	1.0816	.322	380.7	377.0
		2.741	.3669	.8914	1.3269	.267	374.5	
PS(37)		4.848	-.2184	2.906	.8125	.293	380.1	377.3
		3.811	.0386	3.662	.3554	.261	376.0	
PS(32)		4.762	-.2577	2.828	.8100	.333	379.7	372.5
		5.111	-.3862	3.064	.6249	.245	370.0	
PS(20.4)		4.814	-.2473	2.675	.8527	.294	377.0	373.2
		4.607	-.2270	3.174	.5583	.255	369.8	
PS(17.5)		4.562	-.1377	3.305	.6096	.275	375.4	370.5
PS(9)		4.605	-.1862	3.127	.6113	.266	360.0	357.5
		7.636	-1.167	3.837	.4014	.227	353.0	
p(2-ClS)		3.390	.0414	1.790	.9330	.239	408.0	406.0
		3.730	-.1218	1.818	.8848	.232	405.0	
PS(50)/p(2-ClS)	70/30	4.1486	-.0548	2.0372	1.0569	.298	385.4	382.7
		4.619	-.3270	2.5951	.6824	.238	381.0	
	50/50	3.9577	-.0343	1.507	1.1958	.268	392.5	388.3
		4.7606	-.3936	2.595	.6561	.213	386.5	
	30/70	3.6564	.0243	1.678	1.0745	.261	399.0	394.7
		5.428	-.6597	3.026	.4980	.213	393.5	

Table A2.1--Continued.

System		Below Tg		Above Tg		ΔCp	Tg	Tg
		Slope × 10³	Intercept	Slope × 10³	Intercept	(J/°-gm)	(°K)	(°K)
PS(37)/p(2-ClS)	70/30	4.804	-.363	2.686	.6816	.242	379.0	382.3
	50/50	4.874	-.415	2.647	.6743	.230	386.0	387.5
	30/70	4.389	-.308	2.159	.7994	.231	393.2	395.0
PS(32)/p(2-ClS)	90/10	3.586	.2046	2.231	1.0276	.308	380.2	378.0
		4.718	-.4259	2.895	.5203	.261	376.0	
	70/30	4.008	.0418	2.458	.9330	.299	382.0	380.0
		5.155	-.4752	3.041	.5589	.235	378.0	
	60/40	4.120	-.0473	2.764	.7401	.266	384.4	383.0
		5.119	-.5106	2.150	.8537	.235	380.5	
	50/50	3.998	-.0314	2.696	.7443	.268	389.8	387.5
		4.738	-.3642	3.604	.3027	.232	384.0	
	40/60	3.455	.0075	3.602	.1485	.199	396.0	395.0
	30/70	3.682	.0146	1.970	.9615	.269	396.3	393.0
		4.174	-.2509	2.012	.8195	.223	392.0	
	10/90	4.967	-.4807	1.299	1.2042	.200	404.7	401.2
		4.483	-.3371	2.597	.6550	.240	399.0	
PS(20.4)/p(2-ClS)	90/10	3.854	.0887	3.553	.4569	.254	379.0	376.8
		5.737	-.5732	3.762	.3911	.228	372.7	
	70/30	3.769	.0933	2.949	.6845	.278	381.5	378.2
		5.136	-.4852	2.230	.8659	.257	376.5	
	50/50	3.581	.0992	1.6934	1.1104	.279	387.7	383.5
		4.919	-.4552	2.8479	.5706	.227	385.5	
	30/70	3.193	.2008	1.648	1.0878	.285	389.5	387.5
		4.757	-.3770	2.863	.5788	.215	391.0	
	10/90	3.443	.0444	2.037	.8368	.226	403.0	400.2
		4.005	-.2163	2.406	.6610	.240	398.5	

Table A2.1--Continued.

System		Below Tg		Above Tg		ΔCp	Tg	Tg
		Slope $\times 10^3$	Intercept	Slope $\times 10^3$	Intercept	(J/°-gm)	(°K)	(°K)
PS(17.5)/p(2-ClS)	90/10							371.0
	70/30							380.2
	60/40							382.5
	50/50							385.3
	40/60							383.7
	30/70							392.5
	10/90							400.8
PS(9)/p(2-ClS)	70/30	7.3756	-1.2544	2.6460	.7129	.213	371.0	373.5
	50/50	5.380	-.6030	2.688	.6473	.231	378.5	382.0
	30/70	5.191	-.5724	3.028	.4596	.198	385.5	387.7
p(2-ClS(.35)-S)		4.628	-.4100	2.414	.6602	.207	390.0	391.5
p(2-ClS(.49)-S)		4.246	-.2344	2.483	.6736	.231	384.0	385.5
p(2-ClS(.724)-S)		4.566	-.2860	3.258	.4651	.254	380.0	383.2
p(4-ClS(.379)-S)		4.000	-.0623	3.566	.3406	.283	397.5	388.7
		4.348	-.2036	2.731	.6593	.235	388.0	
	/PPO 50/50	3.781	.0169	2.195	.9287	.237	425.7	425.0
p(4-ClS(.511)-S)		3.385	.1301	3.241	.4364	.249	395.0	390.5
		3.992	-.1302	2.371	.7419	.240	390.0	
	/PPO 50/50	3.538	.1098	2.758	.6745	.230	429.0	429.0
p(4-ClS(.652)-S)		3.523	.0711	2.494	.7134	.235	395.3	394.5
		4.245	-.2154	2.607	.6580	.229	393.5	
	/PPO 50/50	3.211	.2041	2.701	.6322	.209	430.0	429.5

Table A2.1--Continued.

System	Below Tg		Above Tg		ΔCp	Tg	Tg
	Slope x 10³	Intercept	Slope x 10³	Intercept	(J/°-gm)	(°K)	(°K)
p(4-ClS(.661)-S)	3.467	.0678	1.931	.9125	.237	396.0	394.5
	3.166	.1337	2.465	.6711	.260	395.0	
/PPO 50/50	3.061	.2913	2.851	.5973	.215	431.0	429.0
p(4-ClS(.670)-S)	3.432	.0858	1.709	1.0502	.277	399.0	395.8
	3.974	-.1420	2.593	.6635	.231	395.0	
/PPO 50/50	2.980	.2840	3.339	.3228	.194	431.5	431.6
p(4-ClS(.679)-S)	3.918	-.1020	1.797	.9878	.246	397.5	394.7
	3.883	-.1134	2.408	.7000	.232	394.0	
/PPO 50/50	2.523	.4620	2.557	.6659	.219	430.0	433.0
p(4-ClS(.759)-S)	2.096	.4280	1.263	.9862	.222	403.5	396.0
	3.671	-.0771	2.640	.5461	.215	395.5	
/PPO 50/50							2 Tg
p(4-ClS)	3.084	.1594	1.418	1.0845	.245	408.5	405.0
	3.811	.1555	2.351	.6490	.214	404.3	
/PPO 50/50							2 Tg
PPO	3.010	.3247	1.472	1.3075	.222	494.8	488.2
	4.056	-.1387	3.173	.5271	.232	491.5	
p(2-FlS)	3.263	.2222	3.667	.2983	.226	369.5	365.4
	3.153	.1686		.1461	.153	374.0	
p(4-FlS(.052)-2-FlS)	4.623	-.1979	2.340	.8590	.214	369.5	366.0
	3.325	.1331	1.053	1.1557	.194	364.5	

Table A2.1--Continued.

System	Below Tg		Above Tg		ΔCp	Tg	Tg
	Slope x 10³	Intercept	Slope x 10³	Intercept	(J/°-gm)	(°K)	(°K)
p(4-F1S(.101)-2-F1S)	4.361	-.1494	2.587	.7309	.222	371.0	369.2
	3.709	.0014	1.113	1.1448	.192	366.5	388.3
/PPO 50/50							
p(4-F1S(.146)-2-F1S)	4.097	-.0992	1.610	1.0372	.222	367.5	364.5
	3.958	-.0711	1.852	.8593	.170	361.0	404.8
/PPO 50/50							
p(4-F1S(.162)-2-F1S)	4.255	-.1443	4.634	.4786	.216	374.4	370.0
	3.668	.0136	1.132	1.1311	.183	368.5	410.7
/PPO 50/50							
p(4-F1S(.228)-2-F1S)	4.4204	-.1925	3.232	.4619	.209	374.9	371.5
	3.735	.0097	1.500	1.0295	.190	369.8	409.8
/PPO 50/50							
p(4-F1S(.295)-2-F1S)	2.502	.3798	3.004	1.3806	.183	371.5	372.5
/PPO 80/20							379.7
/PPO 60/40							398.6
/PPO 50/50	3.481	.1778	3.043	.5448	.189	406.6	405.0
/PPO 40/60							414.0
/PPO 20/80							440.0
p(4-F1S(.375)-2-F1S)	4.115	-.0460	2.540	.7757	.231	375.3	373.5
	3.565	.0500	.849	1.2648	.204	372.3	398.2
/PPO 50/50							
p(4-F1S(.428)-2-F1S)	4.430	-.1644	3.407	.4142	.193	376.5	374.5
	3.247	.1439	1.528	.9946	.211	372.5	
/PPO 50/50							2 phases

Table A2.1--Continued.

System	Below Tg		Above Tg		ΔCp	Tg	Tg
	Slope x 10^3	Intercept	Slope x 10^3	Intercept	(J/°-gm)	(°K)	(°K)
p(4-FlS(.456)-2-FlS)	4.219	-.0895	2.593	.7602	.232	379.8	375.2
	3.210	.1645	1.266	.2356	.198	374.2	
/PPO 50/50							2 phases
p(4-FlS(.562)-2-FlS)	4.191	-.1088	3.229	.4745	.216	381.5	377.2
	3.307	.1331	1.427	1.0522	.212	376.0	
/PPO 50/50							2 phases
p(4-FlS(.662)-2-FlS)	3.671	.0816	3.241	.4042	.227	383.0	379.0
	2.952	.2408	1.166	1.1286	.214	377.0	
/PPO 50/50							2 phases
p(4-FlS(.710)-2-FlS)	4.445	-.1966	3.013	.5690	.215	384.6	381.5
	2.467	.3856	1.003	1.1564	.215	380.0	
/PPO 50/50							2 phases
p(4-FlS(.811)-2-FlS)	3.460	.1402	3.874	.1816	.200	383.2	379.5
	2.775	.3149	1.829	.8983	.226	378.0	
/PPO 50/50							2 phases
p(4-FlS)	4.213	-.0724	3.346	.4464	.184	386.2	383.5
	4.844	-.3600	2.709	.6827	.231	380.0	
/PPO							2 phases

Table A2.1.

System	Tg (°K)	PS Blend Tg (°K)	PPO Blend Tg (°K)
p(4-MeS)	384.3	---	419.0
p(4-BrS)	414.5	---	415.0, 478.0
p(4-BrS(.373)-S)	395.0	---	438.3
p(4-BrS(.357)-S)	398.5	---	434.5
p(4-BrS(.446)-S)	400.0	382.5, 411.0	438.0
p(4-BrS(.520)-S)	399.5	380.0, 408.5	434.0
p(4-BrS(.576)-S)	402.0	378.0, 410.0	410.0, 476.0
p(4-BrS(.622)-S)	412.8	---	412.8, 485.8
p(4-BrS(.675)-S)	413.5	---	412.2, 485.5
p(4-BrS(.663)-S)	409.0	---	412.2, 486.0
p(2-BrS)	410.7	---	411.0, 487.0
p(2-BrS(.125)-S)	382.5	379.0	417.8
p(2-BrS(.313)-S)	385.0	370.5, 386.8	431.5
p(2-BrS(.297)-S)	393.0	372.0, 389.0	430.5
p(2-BrS(.405)-S)	399.5	372.1, 395.0	410.2, 481.0
p(2-BrS(.482)-S)	409.2	381.0, 407.5	410.0, 481.0
p(2-BrS(.530)-S)	405.8	377.6, 408.0	410.2, 485.5
p(2-BrS(.774)-S)	421.0	375.8, 415.7	417.5, 485.0
p(4-BrS(.135)-2-BrS)	428.0	369.0, 413.5	425.0, 487.7
p(4-BrS(.217)-2-BrS)	419.7	380.0, 418.5	421.0, 489.0
p(4-BrS(.302)-2-BrS)	417.5	379.0, 417.7	419.0, 486.5
p(4-BrS(.371)-2-BrS)	417.0	379.5, 417.5	418.8, 487.3
p(4-BrS(.453)-2-BrS)	416.5	379.0, 415.5	417.5, 488.0
p(4-BrS(.542)-2-BrS)	411.5	379.2, 416.0	416.3, 487.5
p(4-BrS(.631)-2-BrS)	415.0	379.7, 416.3	417.2, 487.2
p(4-BrS(.714)-2-BrS)	414.2	380.0, 415.6	416.0, 488.0
p(4-BrS(.838)-2-BrS)	415.5	380.0, 416.0	415.0, 488.4

Table A2.2. Values of ΔH Determined for all Polymers Studied.

System	$-\Delta H_s$ (J/gm)	$\Delta Cp\Delta T$ (J/gm)	$-(\Delta H_s - \Delta Cp\Delta T)$	ΔH_m	$\Delta H_m/w_1w_2$
PS/PPO blends T_{exp} = 34.77°C					
PS(HH101)	26.82	19.95	6.87	---	---
90/10	27.03	21.04	5.99	-1.82	-20.21
70/30	29.71	24.45	5.26	-4.43	-21.08
50/50	34.81	27.52	7.29	-4.28	-17.10
30/70	41.25	31.85	9.40	-4.04	-19.25
PPO	56.57	40.31	16.26	---	---
PS/p(4-ClS) blends T_{exp} = 34.77°C					
PS(HH101)	29.71	19.13	10.58	---	---
70/30	30.17	19.94	10.23	.48	2.28
50/50	29.37	20.49	8.89	-.31	-1.24
30/70	29.71	21.03	8.68	.03	.15
p(4-ClS)	29.66	21.84	7.82	---	---
p(4-ClS(.xxx)-S)/PPO blends (50/50) T_{exp} = 34.77°C					
PS(HH101)	28.21	19.48	8.73	---	---
/PPO	34.83	27.09	7.74	-5.31	-21.25
p(4-ClS(.379)-S)	28.22	20.52	7.70	---	---
/PPO	37.66	28.21	9.45	-3.09	-12.36
p(4-ClS(.511)-S)	27.97	20.40	7.58	---	---
/PPO	38.92	28.82	10.10	-2.37	-9.49
p(4-ClS(.652)-S)	28.23	20.78	7.45	---	---
/PPO	38.87	28.45	10.42	-1.99	-7.96
p(4-ClS(.661)-S)	28.37	20.78	7.60	---	---
/PPO	39.62	28.33	11.29	-1.20	-4.78
p(4-ClS(.670)-S)	28.54	21.00	7.54	---	---
/PPO	41.36	28.94	12.42	-.04	-.15
p(4-ClS(.679)-S)	27.92	20.74	7.18	---	---
/PPO	40.73	29.27	11.46	-.82	-3.27
p(4-ClS(.759)-S)	27.57	20.70	6.87	---	---
/PPO	36.75	30.81	5.94	-6.18	-24.71
p(4-ClS)	29.07	21.84	7.23	---	---
/PPO	44.18	31.46	12.72	.42	1.68
PPO	58.47	41.10	17.37	---	---

Table A2.2--Continued.

System		$-\Delta H_s$ (J/gm)	$\Delta Cp\Delta T$ (J/gm)	$-(\Delta H_s - \Delta Cp\Delta T)$	ΔH_m	$\Delta H_m / w_1 w_2$
p(2-ClS) blends	T_{exp} = 34.77°C					
PS(50)		27.48	18.86	8.63	---	---
	70/30	28.51	19.22	9.29	.93	4.41
	50/50	29.85	19.77	10.07	1.88	7.54
	30/70	29.64	20.39	9.25	1.23	5.86
PS(37)		27.58	18.94	8.65	---	---
	70/30	28.88	19.11	9.77	1.39	6.62
	50/50	29.58	19.57	10.00	1.80	7.20
	30/70	29.52	20.46	9.06	1.04	4.93
PS(32)		25.62	17.63	7.99	---	---
	90/10	26.11	18.78	7.33	-.64	-7.13
	70/30	26.16	18.52	7.64	-.28	-1.34
	60/40	27.43	18.84	8.58	.69	2.86
	50/50	26.93	19.57	7.36	-.52	-2.06
	40/60	28.62	20.90	7.72	-.13	-.52
	30/70	27.16	20.00	7.17	-.65	-3.11
	10/90	28.55	20.89	7.65	-.13	-1.38
PS(20.4)		25.69	17.82	7.87	---	---
	90/10	25.29	18.46	6.84	-1.02	-11.34
	70/30	27.38	18.06	9.32	1.49	7.08
	50/50	28.76	18.59	10.17	2.36	9.42
	30/70	28.80	18.70	10.10	2.31	10.99
	10/90	27.69	20.67	7.02	-.75	-8.32
PS(17.5)		25.11	17.08	8.03	---	---
	90/10	24.96	16.90	8.06	.06	.67
	70/30	26.68	18.57	8.11	.16	.78
	60/40	27.06	18.72	8.34	.43	1.77
	50/50	27.91	19.03	8.88	.99	3.96
	40/60	27.31	19.39	7.93	.07	.27
	30/70	27.73	19.87	7.86	.02	.11
	10/90	28.37	20.80	7.57	-.22	-2.41
PS(9)		18.65	13.53	5.12	---	---
	70/30	24.55	16.85	7.70	1.79	8.52
	50/50	24.95	18.22	6.73	.30	1.18
	30/70	26.36	18.75	7.61	.65	3.10
p(2-ClS)		29.23	21.48	7.76	---	---
p(2-ClS(.65)-S)		27.28	19.89	7.89	---	---
p(2-ClS(.51)-S)		26.73	19.01	7.73	---	---
p(2-ClS(.27)-S)		26.94	19.42	7.52	---	---

Table A2.2--Continued.

System	$-\Delta H_s$ (J/gm)	$\Delta Cp\Delta T$ (J/gm)	$-(\Delta H_s - \Delta Cp\Delta T)$	ΔH_m	$\Delta H_m/w_1 w_2$
T_{exp} = 67.6°C					
PS(32)	12.30	8.67	3.64	---	---
90/10	12.64	9.98	2.65	-.91	-10.15
70/30	14.14	10.09	4.06	.65	3.10
60/40	13.18	10.60	2.58	-.75	-3.13
50/50	14.90	11.50	3.40	.15	.58
40/60	14.94	13.02	1.92	-1.26	-5.23
30/70	15.10	12.28	2.83	-.27	-1.28
10/90	16.86	13.54	3.32	.38	4.22
PS(17.5)	10.25	8.12	2.13	---	---
90/10	10.29	8.10	2.19	-.02	-.18
70/30	12.85	10.14	2.71	.36	1.70
60/40	13.64	10.48	3.16	.74	3.07
50/50	13.93	10.96	2.98	.48	1.91
40/60	14.39	11.51	2.89	.32	1.31
30/70	15.82	12.16	3.66	1.01	4.81
10/90	16.28	13.45	2.83	.03	.38
p(2-ClS)	17.15	14.29	2.87	---	---
Fluorinated styrene blends with PPO and PS [all blends 50/50 unless otherwise indicated T_{exp} = 34.77°C					
p(2-FlS)	16.29	11.38	4.91	---	---
/PS	22.88	15.25	7.63	.63	2.53
/PPO	36.67	26.24	10.43	-.71	-2.84
p(4-FlS(.025)-2-FlS)	16.75	11.56	5.20	---	---
/PS	22.04	15.34	6.70	-.44	-1.78
/PPO	34.51	26.33	8.18	-3.10	12.40
p(4-FlS(.101)-2-FlS)	16.60	12.25	4.35	---	---
/PS	22.59	15.69	6.90	.18	.72
/PPO	34.65	17.20	17.45	6.59	26.35
p(4-FlS(.146)-2-FlS)	15.34	11.37	3.97	---	---
/PS	23.12	15.25	7.87	.63	2.50
/PPO	31.77	29.83	10.95	.28	1.10
p(4-FlS(.162)-2-FlS)	17.68	12.48	5.21	---	---
/PS	22.86	15.80	7.05	-.09	-.36
/PPO	35.94	22.09	13.85	2.56	10.22
p(4-FlS(.228)-2-FlS)	17.67	12.91	4.77	---	---
/PS	22.57	16.08	6.55	-.38	-1.51
/PPO	36.17	22.00	14.16	3.09	12.37

Table A2.2--Continued.

System	$-\Delta H_s$ (J/gm)	$\Delta Cp\Delta T$ (J/gm)	$-(\Delta H_s - \Delta Cp\Delta T)$	ΔH_m	$\Delta H_m / w_1 w_2$
p(4-F1S(.285)-2-F1S)	19.59	13.17	6.42	---	---
/PS	23.54	16.15	7.39	-.36	-1.45
/PPO	36.42	20.97	15.45	3.56	14.23
p(4-F1S(.375)-2-F1S)	19.22	13.51	5.72	---	---
/PS	24.13	16.32	7.82	.42	1.67
/PPO	37.14	19.59	17.56	6.01	24.04
p(4-F1S(.428)-2-F1S)	20.05	13.78	6.27	---	---
/PS	24.68	16.46	8.22	.54	2.19
/PPO	37.91	27.44	10.47	-1.35	-5.40
p(4-F1S(.456)-2-F1S)	20.41	13.93	6.48	---	---
/PS	24.63	16.53	8.10	.32	1.28
/PPO	34.62	27.51	7.10	-4.82	-19.30
p(4-F1S(.562)-2-F1S)	20.69	14.55	6.14	---	---
/PS	24.17	16.84	7.33	-.28	-1.12
/PPO	40.33	27.83	12.51	.75	3.00
p(4-F1S(.662)-2-F1S)	21.78	15.07	6.71	---	---
/PS	25.51	17.10	8.41	.51	2.05
/PPO	41.98	28.09	13.90	1.86	7.42
p(4-F1S(.710)-2-F1S)	21.94	15.67	6.27	---	---
/PS	25.58	17.40	8.18	.51	2.02
/PPO	40.41	28.39	12.02	.20	.80
p(4-F1S(.811)-2-F1S)	21.81	15.39	6.42	---	---
/PS	25.43	17.26	8.17	.42	1.67
/PPO	41.19	28.25	12.91	1.04	4.18
p(4-F1S)	22.51	16.47	6.03	---	---
/PS	25.61	17.80	7.81	.26	1.02
/PPO	39.98	28.79	11.19	-.52	-2.06
PS(HH101)	28.21	19.13	9.08	---	---
PPO	58.47	41.10	17.37	---	---
p(4-F1S(.285)-2-F1S)					
/PPO 80/20	25.17	15.14	10.03	1.42	8.88
60/40	30.51	19.33	11.17	.38	1.58
50/50	37.09	21.06	16.03	4.14	16.56
40/60	38.50	23.26	15.24	2.25	9.38
20/80	47.41	29.57	17.84	2.66	16.63
p(4-F1S(.052)-2-F1S)					
/PPO T_{ann} = 250°C	38.83	26.33	12.50	1.22	4.88
p(4-F1S(.101)-2-F1S)					
/PPO T_{ann} = 250°C	37.79	28.57	9.21	-1.64	-6.56

Table A2.2--Continued.

System	$-\Delta H_s$ (J/gm)	$\Delta Cp\Delta T$ (J/gm)	$-(\Delta H_s - \Delta Cp\Delta T)$	ΔH_m	$\Delta H_m / w_1 w_2$
p(4-F1S(.162)-2-F1S)					
/PPO T_{ann} = 250°C	38.98	22.10	16.89	5.60	22.40
T_{ann} = 270°C	39.03	20.21	18.82	7.53	30.12
T_{ann} = 290°C	37.57	29.02	8.55	-2.74	-10.96
p(4-F1S(.375)-2-F1S)					
/PPO T_{ann} = 250°C	39.34	29.51	9.83	-1.71	-6.84
p(4-F1S(.428)-2-F1S)					
/PPO T_{ann} = 250°C	40.14	28.93	11.21	-.61	-2.44

T_{exp} = 67.6°C

System	$-\Delta H_s$ (J/gm)	$\Delta Cp\Delta T$ (J/gm)	$-(\Delta H_s - \Delta Cp\Delta T)$	ΔH_m	$\Delta H_m / w_1 w_2$
p(2-F1S)	5.15	4.88	.27	---	---
/PPO	26.11	19.62	6.49	-.68	-2.71
p(4-F1S(.052)-2-F1S)	4.77	5.02	-.25	---	---
/PPO	22.89	19.84	3.04	-3.86	-15.45
p(4-F1S(.101)-2-F1S)	5.15	5.69	-.54	---	---
/PPO	23.35	10.17	13.17	6.41	25.65
p(4-F1S(.146)-2-F1S)	3.77	4.77	-1.00	---	---
/PPO	21.21	13.77	7.44	.92	3.66
p(4-F1S(.162)-2-F1S)	6.95	5.88	1.07	---	---
/PPO	24.35	15.04	9.31	1.75	6.99
p(4-F1S(.228)-2-F1S)	7.41	6.24	1.17	---	---
/PPO	25.77	14.91	10.75	3.25	12.98
p(4-F1S(.285)-2-F1S)	7.28	6.48	.81	---	---
/PPO	25.06	13.88	11.19	3.75	15.01
p(4-F1S(.375)-2-F1S)	7.53	6.74	.79	---	---
/PPO	25.40	12.46	12.93	5.51	22.03
p(4-F1S(.428)-2-F1S)	7.99	6.98	1.01	---	---
/PPO	25.77	20.51	5.26	-2.28	-9.11
p(4-F1S(.456)-2-F1S)	8.24	7.13	1.11	---	---
/PPO	21.00	21.27	-.26	-7.85	-31.40
p(4-F1S(.562)-2-F1S)	8.91	7.65	1.26	---	---
/PPO	28.66	21.00	7.66	-.00	-.01
PPO	45.36	31.29	14.06	---	---